Josip Juraj Strossmayer University of Osijek
University of Dubrovnik
Ruđer Bošković Institute, Zagreb

University Postgraduate Interdisciplinary Doctoral Study
Molecular Biosciences

Marta Popović

IDENTIFICATION, CHARACTERIZATION AND ECOTOXICOLOGICAL RELEVANCE OF MEMBRANE TRANSPORT PROTEIN FAMILIES SLC21 AND SLC22 IN ZEBRAFISH (*DANIO RERIO* Hamilton, 1822)

DOCTORAL THESIS

Zagreb, 2014.

TEMELJNA DOKUMENTACIJSKA KARTICA

Sveučilište Josipa Jurja Strossmayera u Osijeku **Doktorski rad**
Sveučilište u Dubrovniku
Institut Ruđer Bošković
Sveučilišni poslijediplomski interdisciplinarni
doktorski studij Molekularne bioznanosti

Znanstveno područje: Prirodne znanosti
Znanstveno polje: Biologija

Identifikacija, karakterizacija i ekotoksikološka važnost membranskih transportnih proteina obitelji SLC21 i SLC22 zebrice (*Danio rerio* Hamilton, 1822)

Marta Popović

Rad je izrađen u: Institut Ruđer Bošković, Zagreb

Mentor: dr.sc. Tvrtko Smital, znanstveni savjetnik

Kratki sažetak doktorskog rada:

Polispecifični SLC21 i SLC22 (*Solute carriers*) membranski transporteri odgovorni su za unos širokog spectra endo- i ksenobiotika u stanicu. Unatoč iznimnoj važnosti u toksikološkom odgovoru organizma, njihov ekotoksikološki značaj do sada nije bio istraživan. U ovom istraživanju identificirali smo ukupno 14 *Slc21* gena i 14 *Slc22* gena kod ribe zebrice (*Danio rerio*). Rezultati filogenetske i tkivno-ekspresijske analize ukazali su na potencijalnu važnost transportera Oatp1d1, Oatp2b1, Oat3, Oat2c-e i Oct1 za transport ksenobiotika kod riba. Pokazali smo da je Oatp1d1 funkcionalni ortolog ljudskih transportera OATP1A2, 1B1 i 1B3, te da ima važnu ulogu u transportu konjugata steroidnih hormona kod zebrice, kao I u eliminaciji mnogobrojnih okolišnih zagađivala putem jetre.

Broj stranica: 171
Broj slika: 51
Broj tablica: 20
Broj literaturnih navoda: 206
Jezik izvornika: engleski
Ključne riječi: SLC transporteri, *Danio rerio*, filogenetska analiza, ekspresija, funkcija, ADME

Datum obrane: 13.2.2014.

Stručno povjerenstvo za obranu:
1. Andreja Ambriović Ristov, dr.sc. viša znanstvena suradnica, Institut Ruđer Bošković, predsjednik
2. Tvrtko Smital, dr.sc. znanstveni savjetnik, Institut Ruđer Bošković, mentor i član
3. Vera Cesar, dr.sc. redovita profesorica, Odjel za Biologiju, Sveučilište J.J Strossmayer u Osijeku, član
4.
5.
6. Đurđica Ugarković, dr.sc. znanstvena savjetnica, Institut Ruđer Bošković, Zagreb, zamjena člana

Rad je pohranjen u: Nacionalnoj i sveučilišnoj knjižnici Zagreb, Ul. Hrvatske bratske zajednice 4, Zagreb; Gradskoj i sveučilišnoj knjižnici Osijek, Europska avenija 24, Osijek; Sveučilištu Josipa Jurja Strossmayera u Osijeku, Trg sv. Trojstva 3, Osijek

BASIC DOCUMENTATION CARD

Josip Juraj Strossmayer University of Osijek **PhD thesis**
University of Dubrovnik
Ruđer Bošković Institute
University Postgraduate Interdisciplinary Doctoral Study of
Molecular biosciences

Scientific Area: Natural sciences
Scientific Field: Biology

Identification, characterization and ecotoxicological relevance of membrane transport protein families SLC21 and SLC22 in zebrafish (*Danio rerio* Hamilton, 1822)

Marta Popović

Thesis performed at: Institut Ruđer Bošković, Zagreb

Supervisor: PhD, Tvrtko Smital, Senior Researcher

Short abstract:

Polyspecific SLC21 and SLC22 (*Solute carriers*) membrane transporters are responsible for the uptake of various endo- and xenobiotics into the cell. Despite their crucial role in toxicological response of organisms, their ecotoxicological relevance has not been studied so far. We have identified 14 *Slc21* and 14 *Slc22* genes in zebrafish (*Danio rerio*). Phylogenetic and tissue distribution analysis suggest that Oatp1d1, Oatp2b1, Oat3, Oat2c-e and Oct1 could be important for xenobiotic transport in fish. We have found that Oatp1d1 is a functional ortholog of human OATP1A2, 1B1 and 1B3 and is crucial for the transport of conjugated steroid hormones in zebrafish, as well as for the elimination of numerous environmental contaminants through liver.

Number of pages: 171
Number of figures: 51
Number of tables: 20
Number of references: 206
Original in: English
Key words: SLC transporters, *Danio rerio*, phylogenetic analysis, expression, function, ADME

Date of the thesis defense: 13.02.2014.

Reviewers:
1. Andreja Ambriović Ristov, PhD, Senior Associated Researcher, Ruđer Bošković Institute, Zagreb
2. Tvrtko Smital, PhD, Senior Researcher, Ruđer Bošković Institute, Zagreb
3. Professor Vera Cesar, PhD, Josip Juraj Strossmayer University of Osijek
4.
5.
6. Đurđica Ugarković, Senior Researcher, Ruđer Bošković Institute, Zagreb

Thesis deposited in: National and University Library in Zagreb, Ul. Hrvatske bratske zajednice 4, Zagreb; City and University Library of Osijek, Europska avenija 24, Osijek; Josip Juraj Strossmayer University of Osijek, Trg sv. Trojstva 3, Osijek

Research for this PhD thesis was performed in the Laboratory for Molecular Ecotoxicology, Division of Marine and Environmental Research, Ruđer Bošković Institute, Zagreb, under the supervision of dr. sc. Tvrtko Smital. This work was supported by the Ministry of Science, Education and Sport of the Republic of Croatia [Project 098-0982934-2745]. Experiments with radioactively labeled compounds were performed at the laboratory of dr.sc Karl Fent at the University for Applied Sciences, Basel, Switzerland during Marta Popović 5 months stay in 2010 supported by the SCOPES joint research project [Swiss National Science Foundation (SNSF) Grant SCOPES-IZ73ZO_128025/1.]

Acknowledgments

For the freedom in my research and all the support, I thank my supervisor Tvrtko. I thank Roko for teaching me all the methods he knew and much more. Also, a big part of this would not be possible without our collaborator from Basel, Karl: thank you for the immensely generous opportunity to stay in your lab and for all your expert advice and help.

Big thanks to Jovica and Ivan, in the LME lab, for all the support and occasional cell seeding on weekends…

I thank my parents for their unconditional and selfless support, my brother and grandmas. I thank all of my friends for their patience when I missed a lot of important stuff during the last years because of the endless weekend experiments, and finally to Roko for all the advice, knowledge and patience.

Table of Contents

1. Introduction

1.1. Absorption, Distribution, Metabolism and Elimination (ADME) at the cellular level

The central paradigm in toxicology encompasses (1) source of contamination, (2) absorption, distribution, metabolism and elimination (ADME) of chemicals, and (3) effects of contaminants (Stegeman *et al*. 2010). Recently, a new, wider terminology has been introduced; the so called, chemical defensome (Goldstone, 2006). Chemical defensome comprises all protein classes that protect the cell through their coordinate action. Thus, defensome genes include transcription factors that sense toxicant or cellular damage, membrane transporters that mediate uptake or efflux of xenobiotics and their metabolites across the cell membrane, enzymes that are involved in the metabolism of xenobiotics in the cytosol, and antioxidant enzymes that protect the cell against reactive oxygen species (ROS) and other radicals (Stegeman *et al*. 2010). A big portion of the defensome involves ADME processes that usually comprise four phases: (1) uptake phase that includes polyspecific uptake transporters that mediate entrance of compounds into the cell, (2) phase I that comprises cytochrome P450 superfamily of monooxygenases (CYP) and flavin-containing monooxygenases (FMO) responsible for the oxidative and reductive transformation of compounds upon entrance, (3) phase II that encompass conjugating enzymes from glutathione S-transferase (GST), uridine 5'-diphospho-glucuronosyltransferase (UDP-glucuronosyltransferase, UGT) and sulfotransferase (SULT) superfamilies which add different functional groups to xenobiotics thus forming more soluble metabolites, and finally, (4) efflux transporters from ATP-binding Cassette superfamily (ABC) and Multidrug and Toxic compound Extrusion (MATE) family that mediate efflux of compounds and their metabolites out of the cell (Fig. 1.1).

Membrane transporters are crucial part of the ADME and are recognized as key determinants of toxicological response to various xenobiotics (Klaassen and Lu, 2008). It has traditionally been considered that compounds (especially lipophilic) enter the cell by passive diffusion. In the past decades, however, uptake transporters have been characterized and recognized as key players in mediating the entrance of metabolites and foreign compounds into the cell by the means of facilitated diffusion. Together with the efflux transporters from the ATP binding cassette (ABC) and Multidrug and toxin extrusion (MATE) families, uptake transporters from the Organic anion transporting polypeptide (OATP/Oatp) family (gene name *SLC21*, synonym *SLCO*) and SLC22/Slc22 family determine cellular concentrations and effects of xenobiotics (Klaassen and Lu, 2008; Zair *et al*.; 2008; Koepsell, 2013).

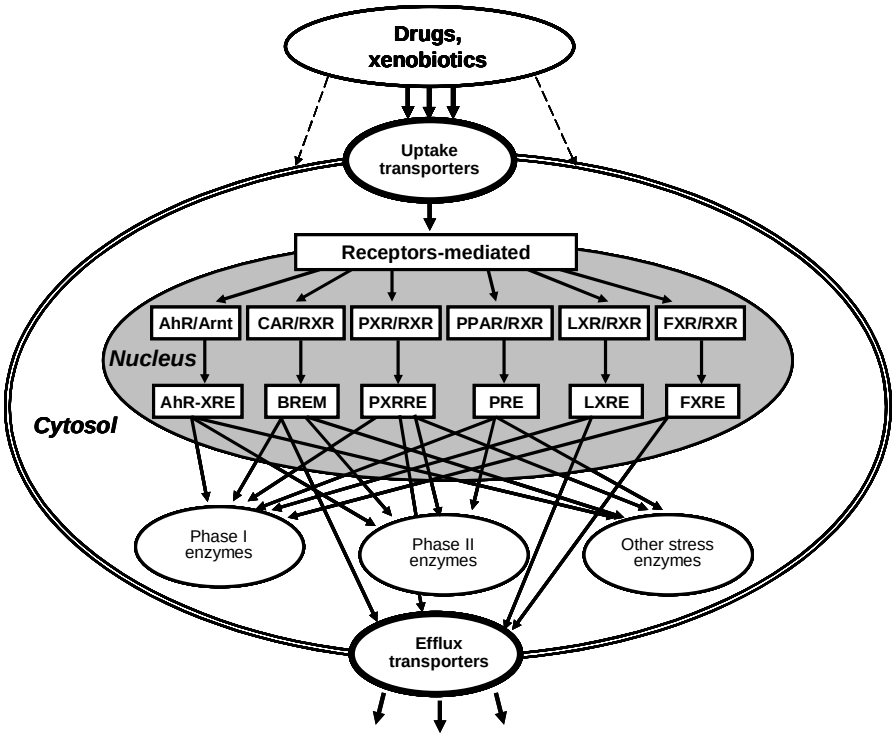

Figure 1.1. Schematic representation of cell stress response leading to the activation of specific uptake transporters, receptor-mediated gene expression of phase I and II drug metabolizing enzymes, other stress enzymes, and efflux transporters. Modified from Xu *et al*. (2005).

1.2. Absorption, Distribution, Metabolism and Elimination (ADME) at the level of organism

Primary routes of xenobiotic entry into fish organism are through skin, gills and gut, out of which the dermal uptake may contribute up to 50% of the total uptake of hydrophobic compounds (Sukardi *et al*., 2010). Therefore, skin, gills and gut represent the first contact of fish with xenobiotics present in the aquatic environment. Some hydrophobic compounds can enter the body by passive diffusion through the cell membranes of epithelial, gill cells or enterocytes, but most xenobiotics require specific carriers. These carriers are membrane proteins which enable uptake of xenobiotics through the skin and gills directly from the aquatic environment and through the brush-border membrane of enterocytes after digestion (Zair *et al*., 2008). The compounds afterwards enter the circulation, through the action of membrane transporters, thus enabling their distribution into the tissues where

they primarily exert their effects, or into the main excretory organs, intestine, liver and kidney which enables their excretion out of the body (Hilgendorf *et al*., 2007).

In order to enter target tissue from the circulation, the action of membrane transporters is required in most cases. After ingestion, majority of compounds is transported from the intestinal lumen accross the brush-border membrane of enterocytes through the carrier-mediated uptake. Alternatively, some can enter through the paracellular and/or transcellular diffusion. From the enterocytes, compounds enter the portal blood circulation across the basolateral membrane of enterocytes through the action of efflux transporters. Some are transported from the portal blood circulation across the basolateral membrane of hepatocyes into the liver by the action of SLC21 and/or SLC22 transporters. The principal place of xenobiotic metabolism is liver, which through enzymatic processes mediated by the phase I and/or phase II enzymes catalyze modifications of original compounds. These modifications can be favorable: e.g., conjugation of glutathione to xenobiotic compounds by GST enzymes makes an original compound less damaging to the cell, as well as more soluble and more favorable substrate for the ABC efflux proteins that can then successfully eliminate given xenobiotic metabolite into the bile. Conversely, a xenobiotic can be metabolized by CYP enzymes into oxidative forms that are more damaging to the cells than the original compound. If these metabolites are not subsequently processed by phase II enzymes, the effect can be damaging to the cell. In the end, non-metabolized (native) compounds or their metabolites are excreted from the hepatocytes through the basolateral membrane back into the circulation or through the apical membrane into the bile primarily through the action of efflux transporters (Fig. 1.2) (Zair *et al*., 2008). Apart from liver, major excretory routes in fich include kidney and gills. In the kidney, on the basolateral membrane of renal epithelial cells, compounds enter from the circulation with the action of uptake transporters, and are excreted through the apical membrane by the action of efflux transporters (Fig 1.2). In gills, xenobiotic membrane transporters including SLC21 and SLC22 have not been characterized before this study. However, metabolic processes of CYP enzymes have been observed (Abrahamson *et al*., 2007), suggesting the importance of gills in the metabolism of xenobiotics. Apart from enterohepatic and renal membrane barriers, transporters are important at the blood-brain and blood-testes barrier where they have protective role in preventing entry of xenobiotics into the brain and testes (Zair *et al*., 2008).

In summary, primary routes of xenobiotic excretion in fish are intestine, liver, kidney and gills. In each of these tissues, on the basolateral side of the cells (i.e., facing the circulation), polyspecific uptake transporters from the OATP and SLC22 families are responsible for the transport of xenobiotics into the tissue, which is a first step toward their elimination from the organism. On the apical side of the cell layer facing the lumen of intestine, kidney, liver and presumably gills, efflux

transporters (ABCs and MATEs) enable the excretion of xenobiotics and their metabolites into the feces, urine, bile or the surrounding water (Fig 1.2).

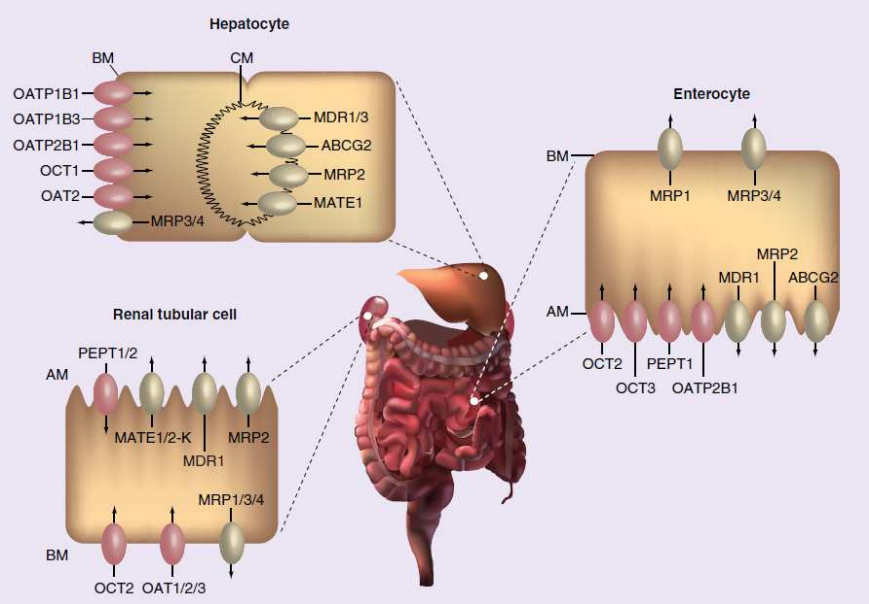

Figure 1.2. Scheme of major human excretory organs: liver, kidney and intestine with the uptake (SLC21 and SLC22) and efflux transporters (ABCs and MATEs) located on basolateral membrane (BM), or apical membrane (AM) (in hepatocytes apical membrane is also reffered to as canalicular membrane (CM) (Zair *et al*., 2008).

1.3. OATP family

Organic anion transporting polypeptides (OATPs in humans, Oatps in all other species; gene symbol *SLC21/Slc21,* synonym *SLCO/Slco*) are polyspecific transporters that mediate transport of large amphipathic molecules across cell membranes of eukaryotes. OATP family (SLC21 or SLCO family) belongs to the SLC superfamily (SoLute Carrier), the second largest superfamily of membrane proteins which includes 52 families and 386 proteins found in humans (Schlessinger *et al*., 2013). SLC21 family is also a part of Major Facilitator Superfamily (MFS) clan which holds SLCs and other groups of membrane proteins (Höglund *et al*., 2011). The family will be futher on be reffered to according to its protein name, namely OATP family. OATPs transport a wide range of endogenous compounds (steroid hormones, bile salts, prostaglandins etc.) and exogenous compounds (pharmaceuticals, natural toxins). More than 160 OATPs /Oatps have been identified on the genome

level in at least 25 animal species. Based on phylogenetic analysis, all so far identified OATPs/Oatps have been classified into six subfamilies (OATP1-6) (Hagenbuch and Meier, 2004) and species dependent number of transporters within each subfamily which will be from now on reffered as groups (e.g. OATP1 subfamily includes 3 groups in humans: OATP1A, B and C). OATP family is not present in plants, yeast and bacteria (Höglund *et al*., 2011).

A typical Oatp transporter is a 643-722 amino acids long with molecular mass between 80 and 90 kDa. Based on the high-resolution crystal structure for several bacterial SLC transporters and computational prediction algorithms, it has been suggested that OATPs/Oatps share a similar structure, with 12 transmembrane domains (TMDs) and a large extracellular loop 9 (LP9) between TMD 9 and 10 (Hagenbuch and Gui, 2008) (Fig 1.3). In the case of rat Oatp1a1, it was experimentally proven that protein consists of 12 TMDs (Wang *et al*., 2008). Conserved structural features of the OATP family include 13 amino acids long signature on the border of the LP5 (extracellular) and TMD6 and a large extracellular LP9 with 10 conserved cysteine (C) residues. Role of the highly conserved signature sequence is not known. On the contrary, 10 highly conserved cysteines within the LP9 are involved in the formation of disulfide bonds and are important for the membrane localization of OATPs (Hanggi *et al*., 2006) (Fig 1.3).

Homology model for OATP1B1 and OATP2B1 based on the crystal structures of distantly related major facilitator superfamily (MFS) members in bacteria, glycerol-3-phosphate transporter and lactose permease, suggests that TMDs form positively charged pore through which substrates are translocated in a rocker switch type of mechanism (Maier-Abt *et al*., 2005, Roth *et al*., 2012) (Fig. 1.3). The transport mechanism of OATPs/Oatps has not been elucidated conclusively, although the anion antiport has been suggested as a presumable driving force. The majority of human OATPs, including OATP1A2, OATP1B1 and OATP1B3, function as [HCO_3^-] antiporters (Satlin *et al*., 1997; Kobayashi *et al*., 2003; Leuthold *et al*., 2009; Martinez-Becerra *et al*., 2011). However, some rat transporters, namely Oatp1a1 and Oatp1a4 use glutathione for the antiport (Li *et al*., 1998; Li *et al*., 2000). Considering the number of substrate binding sites, several human OATPs were studied. It has been shown that OATP1A2 has one substrate binding site, whereas OATP1B1, and probably OATP1B3, have two substrate binding sites (for estrone-3-sulfate (E3S)) (Tamai *et al*., 2000; Hirano *et al*., 2006; Noe *et al*., 2007; Roth *et al*, 2011). Biphasic transport kinetics was also suggested for the transport of estradiol-17β-glucuronide and T4 by OATP1C1 (Kindla *et al*., 2011; Roth *et al*., 2011).

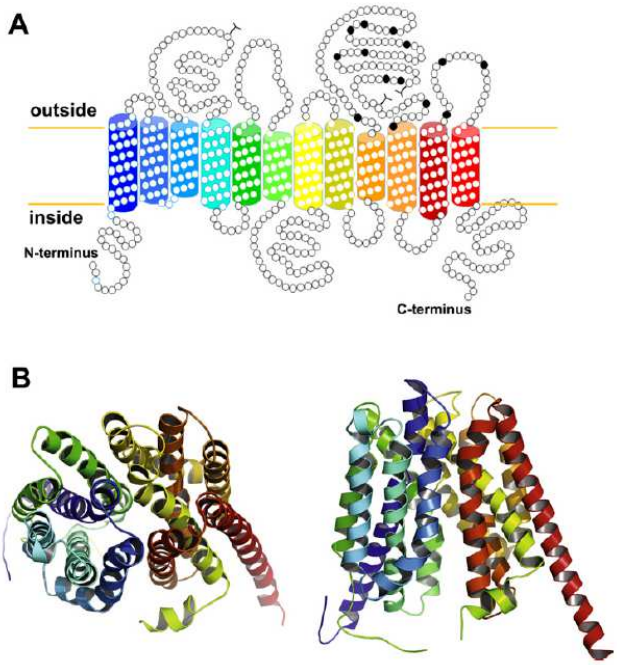

Figure 1.3. (**A**) Topology prediction for human OATP1B1 shows 12 transmembrane domains (TMDs), and large extracellular loop 9 (LP9) between TMD 9 and 10 that carries conserved cysteine residues (black dots); (**B**) Homology model of OATP1B1 which shows the protein from the extracellular side (left) and within the lipid bilayer (right) (Roth *et al*., 2012). Colors of the TMDs in the topology model (A) match colors in the homology model (B) (Hagenbuch and Stieger, 2013).

OATP family encompasses six subfamilies in mammals: OATP/Oatp1-6, with overall 11 transporters in human, 15 transporters in mouse and 16 in rat. There is a substantial difference within the OATP1/Oatp1 and OATP6/Oatp6 subfamilies among human and rodents, whereas in the OATP2-5 subfamilies, clear one-to-one orthology relationship is present (Table 1.1). OATP1/Oatp1 subfamily has been most extensively studied because of the link to human diseases and cancer treatement, thus knock-out animal models were so far only generated for the members of this subfamily (Hagenbuch and Stieger, 2013).

OATP1 subfamily includes four proteins in humans: OATP1A2, OATP1B1, OATP1B3 and OATP1C1 (Hagenbuch and Maier, 2004); six transporters in mouse (Oatp1a1, Oatp1a4-6, Oatp1b2, Oatp1c1) and seven transporters in rat (Table 1.1). Ubiquitously expressed OATP1A2 mediates transport of physiologically important compounds such as conjugates of steroid hormones (estrone-3-sulfate (E3S), dehydroepiandrostenedione sulfate (DHEAS) and estradiol-17β-glucuronide); thyroid hormones (thyroxin (T4) and triiodothyronine (T3)), bilirubin, bile salts (cholate (CH), taurocholate (TC)), taurochenodeoxycholate (TCDC)) and prostaglandin E2 (PGE2). The substrate specificity of rodent Oatp1a proteins overlaps with human OATP1A2 (Hagenbuch and Stieger, 2013). Along with

the role in the balance of hormones and bile salts, OATP1A2 has been shown to transport various pharmaceuticals. Given its ubiquitous distribution, along with the role in the transport of endogenous compounds, it is probably important for the tissue-specific disposition, pharmacokinetics and toxicity of xenobiotics (Badagnani *et al*., 2006).

Unlike ubiquitously expressed OATP1A2 transporter, OATP1B1 and OATP1B3, as well as rodent Oatp1b2, are liver specific proteins (Evers and Chu, 2008). The substrates of human and rodent OATP1B/1b transporters largely overlap and include conjugates of steroid hormones (E3S, DHEAS, estradiol-17β-glucuronide), bile salts (CH, TC, TCDC) and bilirubin and its conjugates. However, their affinities for the same substrates can significantly differ (Hagenbuch and Gui, 2008). OATP1B1, OATP1B3 and rodent Oatp1b2 have been extensively studied because they are largely responsible for the disposition of drugs (e.g., lipid lowering agents and chemotherapeutics) and their subsequent elimination through bile. Knock-out (KO) mice generated for Slc211b2 (Lu *et al*., 2008; Zaher *et al*., 2008; Csanaky *et al*., 2011) and Slc211a/1b (Steeg *et al*., 2010), showed elevated plasma levels of unconjugated bile salts and unconjugated and conjugated bilirubin, thus indicating the physiological importance of Oatp1a and Oatp1b transporters in the uptake and elimination of bile salts and bilirubin through liver.

Human OATP1C1 and rat and mouse Oatp1c1, unlike most OATPs/Oatps, have a narrow substrate range that principally includes thyroid hormones: thyroxine (T4), triiodothyronine (T3), reverse triiodothyronine (rT3) and their sulphated conjugates. OATP1C1 is predominantly expressed at the blood brain barrier (BBB) (Pizzagalii *et al*., 2002; Sugiyama *et al*., 2003; Roth *et al*., 2012; Hagenbuch and Stieger, 2013). Along with monocarboxylate transporters (MCT8 and MCT10), NTCP (Na-taurocholate cotransporting polypeptide) and L-amino transporters (LAT1 and LAT2), OATP1C1 has crucial role in the balance of thyroid hormones in mammals (Deure *et al*., 2010). The role of OATP1C1/Oatp1c1 has been recently confirmed *in vivo* in the Oatp1c1 KO mouse which exhibited reduced thyroxin levels and altered expression of deiodinases in the brain (Mayerl *et al*., 2012).

OATP2/Oatp2 subfamily encompasses two transporters: OATP2A1/2a1 and OATP2B1/2b1 in human, mouse and rat (Table 1.1). Human and rat OATP2A1/Oatp2a1 transporters are expressed ubiquitously across tissues and are involved in the transport of prostaglandins and other eicosanoids (Lu *et al*., 1996). Similarly, human OATP2B1 and rat Oatp2b1 are ubiquitously expressed, but the substrate range is substantially wider than the one of OATP2A1/2a1. Human OATP2B1 transports physiological substrates including steroid conjugates E3S and DHEAS, as well as bile salt taurocholate and thyroid hormone thyroxine (T4). Unlike OATP2A1, which is not implicated in the transport of drugs, OATP2B1 mediates uptake of several pharmaceuticals including statins, fexofenadine and glibenclamide (Hagenbuch and Gui, 2008; Roth *et al*., 2011).

The only member of OATP3 subfamily, OATP3A1, is suggested to play important role in the transport of neuron-active peptides, thyroid hormones and prostaglandins and is ubiquitously expressed across tissues in humans and rodents (Huber *et al*., 2007).

Two members of OATP4 subfamily differ significantly with respect to their tissue distribution and substrate specificity. The OATP4A1 is ubiquitously expressed uptake transporter involved in the transport of thyroid hormones, taurocholate and probably prostaglandins (Tamai *et al*, 2000; Fujiwara *et al*., 2001). Similar to the human ortholog, rat Oatp4a1 transports taurocholate and T3 (Fujiwara *et al*., 2000). Unlike widely expressed OATP4A1, the other member of OATP4 subfamily, OATP4C1 is a kidney-specific transporter that, beside thyroid hormones, transports cAMP and several drugs (digoxin, methotrexate, ouabain) (Mikkaichi *et al*., 2004).

Function and tissue distribution of OATP5A1 is unknown (Hagenbuch and Stieger, 2013). The single member of the OATP6 family in humans, OATP6A1, is highly expressed in tumors of testicular tissue and several cancer cell lines (Suzuki *et al*., 2003; Lee *et al*., 2004). However, similar to OATP5A1, its function remains unknown (Roth *et al*., 2012). Rat co-orthologs of OATP6A1, Oatp6b1 and 6d1 have been characterized. They are predominantly found in testes where they transport dehydroepiandrosterone (DHEA) and its sulfated conjugate, DHEAS, into the testicular tissue (Suzuki *et al*., 2003).

Table 1.1. OATP family in mammals: summary of tissue distribution and substrate specificities (BM, basolateral membrane). OATP subfamilies are divided with dotted lines (adapted from Hagenbuch and Stieger, 2013).

Mouse	Rat	Human	Tissue expression	Predominant substrates
Oatp1a1	Oatp1a1	OATP1A2	ubiquitous	Bile salts, E3S, DHEAS, prostaglandins, estradiol-17b-glucuronide, thyroid hormones, drugs
	Oatp1a3			TC, DHEAS, E3S, estradiol-17b-glucuronide, T3, T4
Oatp1a4	Oatp1a4			bile salts, DHEAS, E3S , estradiol-17b-glucuronide, T3, T4
Oatp1a5	Oatp1a5			bile salts, estradiol-17b-glucuronide, prostaglandins, T3, T4
Oatp1a6	Oatp1a6			unknown
Oatp1b2	Oatp1b2	OATP1B1	liver (BM)	Bile salts, E3S, DHEAS, estradiol-17b-glucuronide, bilirubin and its conjugates, T4, T3, drugs
		OATP1B3	liver (BM)	Bile salts, E3S, DHEAS, estradiol-17b-glucuronide, bilirubin and its conjugates, T4, T3, drugs
Oatp1c1	Oatp1c1	OATP1C1	brain	Thyroid hormones (T4, T3, rT3)
Oatp2a1	Oatp2a1	OATP2A1	ubiquitous	Prostaglandins
Oatp2b1	Oatp2b1	OATP2B1	liver, intestine, placenta, eye	E3S, DHEAS, TC, T4
Oatp3a1	Oatp3a1	OATP3A1	brain, gonads, eye	E3S, prostaglandin, T4
Oatp4a1	Oatp4a1	OATP4A1	ubiquitous	TC, T3, prostaglandins
Oatp4c1	Oatp4c1	OATP4C1	kidney (BM)	Thyroid hormones, drugs
Oatp5a1	Oatp5a1	OATP5A1	unknown	unknown
	Oatp6a1	OATP6A1	testes	unknown
Oatp6b1	Oatp6b1		testes	DHEAS, DHEA
Oatp6c1	Oatp6c1			unknown
Oatp6d1	Oatp6d1		testes	DHEAS, DHEA

1.4. SLC22 family

The SLC22 family (SLC22 in human, Slc22 in all other organisms), like SLC21, belongs to the SLC superfamily (SoLute Carrier) and a clan of Major Facilitator Superfamily (MFS) (Höglund *et al*., 2011). Similarly to the SLC21/Slc21, the SLC22/Slc22 family includes polyspecific membrane transporters that mediate uptake of a wide range of endogenous substrates (monoamine neurotransmitters, short chain fatty acids, uric acid, prostaglandine, α-ketoglutarate, carnitine etc.) and xenobiotic substrates (pharmaceuticals, natural toxins, herbicides) across the cell membranes of eukaryotes. Main difference in terms of substrate preferences is the fact that SLC22 family, as opposed to SLC21 family, transports not only anionic, but also positively charged compounds, whereas SLC21 transporters primarily transport anionic substrates. The SLC22 family encompasses three subgroups of transporters: (1) Organic anion transporters (OATs), (2) Organic cation transporters (OCTs), and (3) Organic carnitine transporters (OCTNs) (Koepsell, 2013). Considering that SLC22 family encompass three distinct subgroups, there is no unique protein name for this family, and will thus further on be reffered to as SLC22 family. Except in the animal kingdom, Slc22 family is found in plants (Torres *et al*., 2003; Lelandais-Briere *et al*., 2007; Schmidt *et al*., 2007; Kufner *et al*., 2008), but not in yeast and bacteria.

SLC22 transporters are smaller than SLC21 family members and are typically 541-594 amino acids long. The secondary structure is similar to the SLC21 in the sense that SLC21 transporter consists out of 12 α-helical TMDs. The organization of loops is substantially different in comparison to the OATPs: SLC22 transporters have large extracellular LP1 between TMDs 1 and 2, and a large intracellular loop 6 (LP6) between TMDs 6 and 7 (Fig. 1.4). Extracellular LP1 is important for the glycosylation of the protein and in some cases for its homo-oligomerization (Brast *et al*., 2011; Keller *et al*., 2011), while intracellular LP6 is involved in posttranscriptional regulation (Koepsell *et al*., 2007). Although crystal structure of SLC22/Slc22 transporters is not solved, several homology models based on the related bacterial MFS proteins suggests the structure of 12 α-helices (TMDs) (Fig. 1.4). So far, modeled structure has been proposed for human OAT1 (Perry *et al*., 2006), human OCT2 (Pelis *et al*., 2006), rat Oct1 (Popp *et al*., 2005) and rabbit Oct2 (Zhang *et al*., 2005) based on the bacterial lactose permease (LacY) transporter and/or glicerol-3-phosphate transporter (GlpT). These models have been validated by several mutagenesis studies (reviewed in Roth *et al*., 2012). Conserved motifs of SLC22/Slc22 family include the 13 amino acid long MSF superfamily signature between the TMD2 and TMD3 G(RKPATY)L(GAS)(DN)(RK)(FY)GR(RK)(RKP)(LIVGST)X(LIM), and the 11 amino acids long domain that is conserved within the OCT subgroup S(T/S)IVTE(W/F)(D/N)LVC (Wright and Dantzler, 2004).

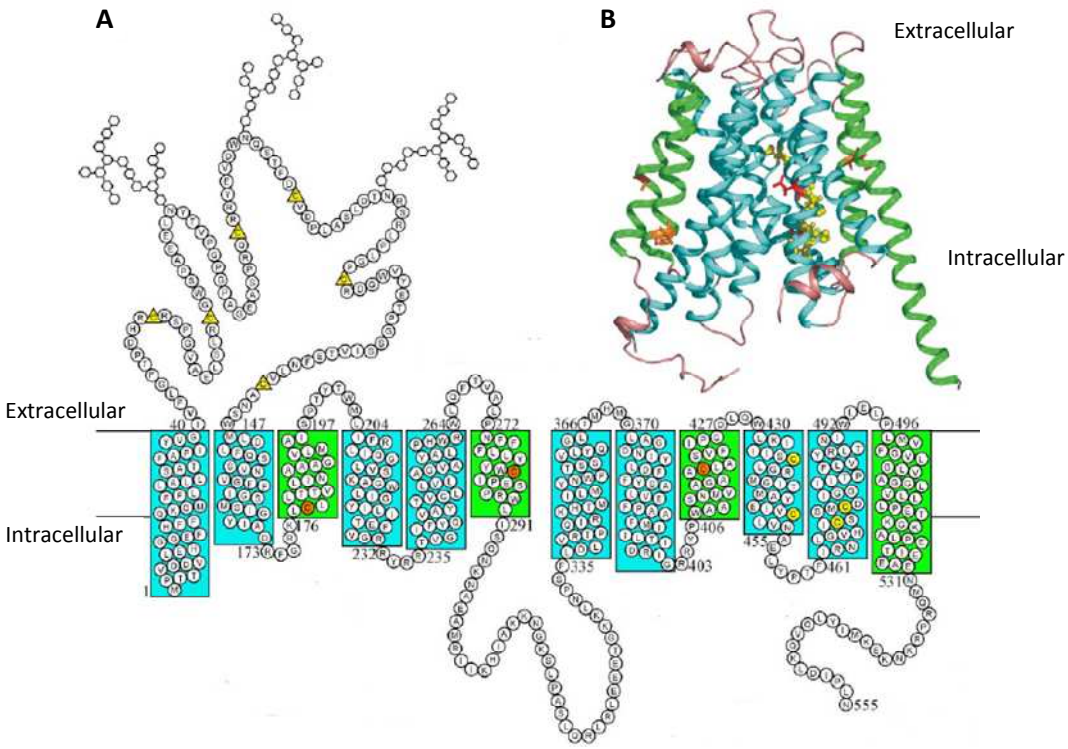

Figure 1.4. A) Prediction of the secondary structure of human OCT2 with 12 TMDs and a large extracellular LP1 bearing three glycosylation sites (hexagons) and conserved cysteines (yellow triangles), and a large intracellular loop 6 (LP6). Cysteines within TMDs are shown in yellow (pore facing) and orange circles (peripheral residues). **B)** Homology model of OCT2 based on the glicerol-3-phosphate transporter (GlpT) (Pelis *et al*., 2006).

Transport mechanism of SLC22 transporters varies among the groups. OCTs function through the sodium independent facilitated diffusion along the electrochemical gradient. OCTN1 acts as organic cation/proton exchanger, as cation exchanger, as sodium dependent transporter for zwitterions, or as sodium-independent transporter for zwitterions, while OCTN2 can function as a sodium cotransporter or as a sodium independent bidirectional cation uniporter (Koepsell *et al*., 2007; Urban *et al*., 2007). OAT1 is a sodium independent dicarboxylate exchanger where outwardly directed gradient of α-ketoglutarate drives the uptake of organic anions against the opposing force of the membrane potential (Burckhardt *et al*., 2012). The exact transport mechanism of other OATs is unknown, but there are indications which suggest sodium independent anion exchange similar to OAT1 (Koepsell, 2013). Although OCTs are traditionally regarded as uptake transporters, it was eventually discovered that OCTs can actually transport compounds in both directions across the plasma membrane (influx and efflux). This is so far proven for human OCT1 and 3, and rat Oct1, 2 and 3 (Busch *et al*., 1996; Budiman *et al*., 2000; Koepsell *et al*., 2003).

Typical OAT substrates are monovalent anions of less than 400 g/mol molar weight (e.g., p-amiohippurate (pAH)), and polyvalent, larger anions with more than 500 g/mol molar weight (e.g., estradiol-17β-glucuronide). Typical OCTs substrates include small monovalent cations of less than 400 g/mol molar weight (e.g., tetraethylammonium (TEA)). Although OATs and OCTs predominantly transport anions and cations, respectively, certain non-charged compounds can also be transported (Wright and Dantzler, 2004; Koepsell, 2013). In the case of OCTs, some neutral compounds, including for example corticosterone and estradiol, and some anions including probenecid and α-ketoglutarate, can inhibit OCTs activity, but are themselves not transported (Ahn and Nigam, 2009). Extensive mutagenesis studies were conducted on numerous SLC22 transporters mainly from OCT and OAT subgroups in order to identify amino acids involved in the substrate binding (reviewed in Koepsell *et al*., 2007 and Burckhardt *et al*., 2012). In summary, the TMDs are forming the pore, a substrate binding region where charged amino acid residues determine binding of anionic versus cation substrates. More specifically, two conserved amino acids with positive charge, arginine 454 (R) and lysine 370 (K) are involved in the binding of anions, whereas changing these amino acids into aspartate (D) and alanine (A), respectively, shifts the specificity towards cation binding (Feng *et al*., 2001).

In humans, 16 members of SLC22 family were identified (Table 1.2). Recently, 7 novel SLC22 transporters have been predicted on the genome level (SLC22A15, 17, 18, 23-25, 31), but considering that they have not characterized (Koepsell, 2013), those were omitted from the Table 1.2. Unlike OATP family, SLC22/Slc22 family has clear one-to-one orthologs in mouse and rat, with the exception of an additional OCTN/Octn member, rodent Octn3 (Koepsel, 2013) and OAT4, 5 and 7 which are specific for humans. OATs and OCTs have been extensively studied because of their role in the transport of a wide range of pharmaceuticals.

The three subgroups of SLC22 family include: (1) Organic anion transporters (OATs) with OAT1-7, OAT10 (gene names *SLC22A6, 7, 8, 11, 10, 16, 9 and 13*), URAT1 (*SLC22A12*) and ORCTL3 (*SLC22A13*), (2) Organic cation transporters (OCTs) with three members, OCT1, OCT2 and OCT3, encoded by *SLC22A1-3*, and (3) Organic carnitine transporters (OCTNs): OCTN1 (*SLC22A4*) and OCTN2 (*SLC22A5*) and OCT6 (*SLC22A16*) (Koepsell, 2013).

Within the OAT subgroup, most extensively studied are OAT1 and 3 given their crucial role in the uptake of drugs at the basolateral membrane of renal cells, and OAT2, which is the major SLC22 transporter at the basolateral membrane of hepatocytes, where, similar to previously described OATP1 transporters (section 1.3), it is responsible for the entry of substances from the circulation into the liver, thus enabling their subsequent metabolism and excretion.

OAT1 is primarily expressed in the kidney where it mediates uptake of numerous endogenous compounds including medium chain fatty acids, α-ketoglutarate, citrulline (key intermediate in the

urea cycle) (Nakakariya *et al*., 2009), cAMP and cGMP (Cropp *et al*., 2008), prostaglandins E2 and F2, urate, and acidic neurotransmitter metabolites such as vanilmandelic acid (Rizwan and Burckhardt, 2007) (Table 1.2). Numerous drugs are transported into kidneys through OAT1, including antiviral drugs, NSAIDs (ibuprofen, indomethacin), diuretics (furosemide, bumetanide) and antibiotic tetracycline. Except in kidneys, OAT1 is expressed in the brain and choroid plexus. Its primary physiological role is (1) uptake of urate into the kidneys, thus representing the first step in urate excretion, (2) renal reapsorption of various organic anions from the circulation, and (3), transport of organic anions in human placenta (Koepsell, 2013).

Human OAT2 is primarily expressed on the basolateral membrane of liver (Simonson *et al*., 1994), followed by kidney, testes and intestine. Localization in kidneys differs among mammals: in humans OAT2 is localized to the basolateral membrane of proximal tubule, whereas in rodents it is found on the apical membrane of proximal tubule cells (Ljubojevic *et al*., 2007; Rizwan and Burckhardt, 2007). Gender differences in expression pattern are observed in rats: in males, Oat2 is highly expressed in liver and weakly expressed in kidneys, as opposed to the high kidney expression and low liver expression in females (Nishimura and Naito, 2005; Hilgendorf *et al*., 2007). OAT2 transports wide range of endogenous compounds including glutamate, glutarate (Kobayashi *et al*., 2005b), urate (Sato *et al*., 2010), L-ascorbate, orotic acid, trigonelline, a wide range of purine and pyrimidine nucleobases, nucleosides and nucleotides, hypoxanthine, GMP, GDP, GTP, cGMP (Cropp *et al*., 2008), cAMP, prostaglandins E2 and F2, E3S, allopurinol, and probably also DHEAS and α-ketoglutarate (Rizwan and Burckhardt, 2007; Srimaroeng *et al*., 2008). In addition to the transport of important physiological compunds, OAT2 transports various xenobiotics including drugs salicylate, antibiotics (erythromycin, tetracycline) and methothrexate, and natural toxins like mycotoxin and aflatoxin B1 (Koepsell, 2013).

Human OAT3 is primarily expressed in kidney at the basolateral membrane of proximal tubule cells (Motohashi *et al*., 2002), followed by low expression in brain, choroid plexus and liver. Substrates of OAT3 largely overlap with OAT1 and partly with OAT2. Endogenous substrates include cAMP, cortisol, prostaglandins, conjugates of steroid hormones (DHEAS, ES and estradiol-17β-glucuronide), bile salts (taurocholate and cholate, indoxyl sulphate, glucuronide conjugates of flavonoids (Wong *et al*., 2011), vanilmandelic acid (Alebouyeh *et al*., 2003), and urate (Rizwan and Burckhardt, 2007; Vanwert *et al*., 2010). OAT3 transports similar range of pharmaceuticals as do OAT1 and OAT2 (Koepsell, 2013). The main physiological role of OAT3 is similar to OAT1, i.e., the first step in the elimination of urate and numerous anionic drugs through kidneys (Eraly *et al*., 2008). OAT3 is distinct from OAT1 in the sense that it eliminates uremic toxin indoxyl-suplhate through the kidney. In the brain, it is proposed to be involved in the removal of neurotransmitter metabolites and drugs (Ose *et al*., 2009; Vanwert *et al*., 2010). In comparison to other OATs in human kidney, OAT3 is

dominant, with 3-fold higher expression than OAT1, and over ten times higher expression than OAT2 and OAT4. Direct rodent orthologs of human OAT1, 2 and 3, Oat1,2 and 3 have similar tissue distribution and substrate specificities to their human counterparts (Ahn and Nigam, 2009). In addition to *in vitro* studies, *in vivo* insights into physiological role of mouse Oat1, 2 and 3 obtained form the KO mouse models suggest that (1) Oat1 is important for the uptake of pAH, benzoate, 3-hydroxybutirate, N-acetylaspartate and urate from circulation into the renal proximal tubule cells, and their subsequent elimination through kidney (Eraly *et al*., 2006; Vallon *et al*., 2009) (2) Oat2 is responsible for the transport of propionate and cGMP into the liver and kidney, and thus indirectly involved in the metabolism regulation and intracellular signaling, and finally, (3) Oat3 is involved in the elimination of tymidine on the basolateral side of renal proximal tubule cells which indirectly effects blood pressure as well as in the uptake of pAH, E3S and TC (Sweet *et al*., 2002; Eraly *et al*., 2008; Vallon *et al*., 2009).

OAT4 is primarily expressed in the kidney at the apical side of proximal tubule cells and in human placenta where it transports E3S, urate, prostaglandins and DHEAS (Rizwan and Burckhardt, 2007). Its proposed physiological role is the reapsorption of urate, prostaglandins, anionic drugs and xenobiotics in human renal proximal tubules from the lumen, and the removal of toxic anionic metabolites from fetal circulation through the placenta (Ugele *et al*., 2003; Zhou *et al*., 2006).

OAT7 is liver specific transporter which mediates uptake of E3S, DHEAS and butyrate from the circulation into the hepatocytes (through the basolateral membrane). It has been suggested that OAT7 can influence the metabolism of short-chain fatty acids in the liver through the regulation of butyrate uptake (Ahn and Nigam, 2009).

Human OAT10, previously known as ORCTL3, is primarily found in kidneys on the apical membranes of proximal tubules, where it is suggested to play a role in the urate reabsorption (along with OAT4) and uptake of the vitamin nicotinate in renal proximal tubule cells (and small intestine) (Bahn *et al*., 2008).

URAT1 is dominantly expressed at the apical membrane of renal proximal tubules, where it is a primary transporter responsible for the urate uptake from the renal lumen. In addition to the renal expression, URAT1 is found in small intestine, liver, heart, skeletal muscle, prostate, adrenal and pituitary gland (Nishimura and Naito, 2005; Bleasby *et al*., 2006).

OCT1, 2 and 3 have largely overlapping substrate range, as well as tissue distribution pattern. However, OCT1 is primarily expressed in the liver, OCT2 in kidney, whereas OCT3 is ubiquitously expressed (Table 1.2). OCT2 and 3 are important for the transport of neurotransmitters and neuromodulators in the brain, whereas OCT1 does not transport neurotransmitters (but does neuromodulators) (Koepsell, 2013). In general, physiological substrates of OCTs are scarce (Table 1.2). However, OCTs transport a wide variety of pharmaceuticals, and few environmental toxins.

Functional studies of OCTs are mainly performed with model cation substrates: radioactively labeled tetraethylammonium (TEA) and 1-methyl-4-phenylpyridinium (MPP) and fluorescent dyes 4-[4-(dimthylamino)-styryl]-Nmethylpyridinium (ASP) and 40,6-diamidino-2-phenylindol (DAPI).

More specifically, human OCT1 is mainly expressed in the liver on the basolateral membranes of hepatocytes, followed by the expression in small intestine, brain, lung, heart and skeletal muscle. On the contrary, in rodents, Oct1 is highly expressed in the kidney, as opposed to low renal expression in humans. OCT1 transports physiological compounds that include neuromodulators histidyl-proline diketopiperazine (cyclo(His-Pro)) and salsolinol (Tachampa *et al*., 2008), the L-arginine metabolite agmatine, and the polyamine putrescine (Winter *et al*., 2011), as well as a variety of pharmaceuticals including: antidiabetic drug metformin, certain antiviral and antiparasitic drugs and antineoplastic drugs (e.g., oxaliplatin) (Koepsell *et al*., 2007; Lovejoy *et al*., 2008; More *et al*., 2010). Considering very wide range of transported drugs, OCT1 is considered crucial for the uptake of cationic xenobiotics from the circulation across the basolateral memebrane of hepatocytes, thus representing the first step in their subsequent elimination. Another main physiological role of OCT1 is transport of compounds across the blood-brain barrier (BBB) and absorption of certain drugs into the lungs (Koepsell, 2013).

Similar to OCT1, OCT2 transports neuromodulators cyclo(His-Pro) and salsolinol, L-arginine metabolite agmatine (Winter *et al*., 2011) and putrescine. As opposed to OCT1, OCT2 also mediates transport of neurotransmitters (acetylcholine, dopamine, epinephrine, norepinephrine, serotonin, histamine) and choline (Koepsell *et al*., 2007; Nies *et al*., 2010). OCT2 is involved in the transport of various drugs that mostly overlap with OCT1. As opposed to OCT1, it is mainly expressed in the human kidney, with very low expression in the liver. OCT2 is also found in other tissues including small intestine, lung, placenta, thymus, brain and the inner ear (Ciarimboli *et al*., 2010; Koepsell *et al*., 2003). Proposed physiological roles of OCT2 are: (1) the transport of neurotransmitters from the circulation across the luminal side of BBB, thus regulating their concentration in the neurons, and (2) reapsorption of choline and neurotransmitters in the kidney. OCT2 is one of the main drug transporters in humans: it transports drugs (1) across the basolateral membrane of proximal tubules in the kidney, thus representing the first step ofrenal drug elimination, and (2) across the BBB into the brain (Koepsell, 2013).

Ubiquitously expressed OCT3 transports neurotransmitters (epinephrine, norepinephrine and histamine) and neuromodulators (agmatine, Cyclo(His-Pro) and salsolinol) across the BBB, similar to OCT2 (Nies *et al*., 2010). It is also involved in the uptake of drugs (e.g., anesthetic lidocaine, antiarrhythmic drug quinidine, metformin) into the brain, heart, and liver (basolateral membrane) (Koepsell, 2013).

OCTN transporters were at first identified to transport only L-carnitine, thus the name Organic Carnitine Transporters. L-carnitine has crucial physiological function in the transport of long-chain fatty acids into mitochondria which enables their oxidation. With the advances in functional studies as well as drug transport research, other substrates of OCTNs have been identified (Table 1.2). Both OCTN transporters, OCTN1 and OCTN2 are ubiquitously expressed, both transport L-carnitine and various pharmaceuticals (Koepsell, 2013). However, apart from carnitine physiological substrates differ among the two transporters: OCTN1 transport acetylcholine, aminoacid derivatives ergothioneine (thiourea derivative of histidine) and glycine-betaine (glycine derivative), whereas OCTN2 transports only choline (Koepsell *et al*., 2007; Urban *et al*., 2007). In respect to drug transport, there is also substrate overlap among the two OCTNs. Both OCTN1 and OCTN2 transport calcium-channel blocker verapamil, histamine H1 antagonist pyrilamin and anticholinergic drugs ipratropium and tiotropium. Although both OCTNs are ubiquitously expressed, their expression does not completely overlap: both are expressed in the kidney, intestine, heart, prostate and skeletal muscle, but OCTN1 is also found in the brain, testes, sperm, spleen and thymus, whereas OCTN2 is found in the lung, pancreas, thyroid and adrenal gland (Horvath *et al*., 2007; Meier *et al*., 2007; Gilchrist and Alcorn, 2010; Lamhonwah *et al*., 2011). The primary physiological role of OCTN1 is considered to be reabsorption of zwitterions and secretion of organic cations in the renal proximal tubules. *In vivo* evidence of mouse Octn2 function from the KO mouse model showed that (1) Octn2 mediated L-carnitine and CSF (cationic pentapeptide which activates intracellular survival and stress-signal pathways) uptake into colon is crucial for normal function of the colon (Fujiya *et al*., 2007; Shekhawat *et al*., 2007) (2) that Octn2 transports L-carnitine into adipocytes, skeletal muscle cells (Furuichi *et al*., 2010), colonic epithelial cells and neurons (Januszewicz *et al*., 2010), and (3) that it is involved in the transport of L-carnitine and acetyl-L-carnitine across the blood–retinal barrier (Koepsell *et al*., 2007; Tachikawa *et al*., 2010).

OCT6 is localized at the blood-testis barrier where it mediates uptake of L-carnitine and sperimidine which are required for maturation of spermatozoa into the testicular tissue. Apart from testes, OCT6 is found in embryonic liver, in hematopoietic cells and several cancers. In addition to mentioned physiological substrates, OCT6 transports model cation TEA and drugs doxorubicin and bleomycin A5 (Aouida *et al*., 2010; Koepsell *et al*., 2007).

Table 1.2. SLC22 family in humans - summary of tissue distribution and substrate specificities (BM, basolateral membrane; LM, luminal membrane). SLC22 subgroups are divided with dotted lines. (Adapted from Koepsell, 2013).

Human	Tissue expression	Predominant substrates
OAT1	kidney (BM), brain, placenta	fatty acids, a-ketoglutarate, citrulline, cGMP, cAMP, prostaglandins, urate, drugs and toxins
OAT2	liver (BM), kidney (BM)	glutamate, glutarate and a-ketoglutarate, urate, nucleobases, nucleosides and nucleotides, hypoxanthine, orotic acid, prostaglandins, E3S, DHEAS, drugs and toxins
OAT3	kidney (BM), brain (LM), sceletal muscle	cAMP, cortisol, prostaglandins, DHEAS, E3S, estradiol-17b-glucuronide, bile salts, urate, indoxyl-sulphate, drugs and toxins
OAT4	kidney (LM), placenta	E3S, urate, prostaglandins, DHEAS
OAT5	liver	unknown
OAT6	olfactory mucosa	odortype organic anions
OAT7	liver	E3S, DHEAS, butyrate
URAT1	kidney	urate, L-lactate, nicotinate
OCRTL3	kidney, intestine, brain, heart	urate, L-lactate, nicotinate, succinate, GSH
ORTCL4	kidney, intestine	unknown
OCT1	liver (BM), intestine, kidney, brain, lung	neuromodulators, putrescine, agmatine, drugs and toxins
OCT2	kidney (BM), intestine, brain (ubiquitous)	neurotransmitters, neuromodulators, putrescine, agmatine, choline, drugs and toxins
OCT3	ubiqitous	neurotransmitters, neuromodulators, agmatine, drugs and toxins
OCT6	testes, kidney	L-carnitine, spermidine
OCTN1	ubiqitous	acetylcholine, ergothioneine, glycine-betaine, L-carnitine
OCTN2	ubiqitous	L-carnitine, choline

1.5. Zebrafish

Zebrafish (*Danio rerio* Hamilton, 1822) is a teleost fish species that belongs to the class of Actinopterygii, a sister group to the class Sarcopterygii (both are jawed vertebrates or Gnathostomates). Zebrafish belongs to the family of Cyprinidae which comprise around 3600 fish species. Teleosts emerged around 350 million years ago and underwent 'fish specific' whole genome duplication (WGD) event after the separation of the evolutionary branches that led to actinopterygians (ray-finned fish) and to sarcopterygians (lobe-finned fish) (Amores *et al*. 1998; Taylor *et al*. 2001). After the WGD, diversification of teleosts started (Ravi and Venkatesh, 2008), which led to the occurrence of a wide variety of species that adapted to the different habitats. WGD

is considered one of the reasons that teleosts comprise more than half of all vertebrate species today (Ravi and Venkatesh, 2008). Because of the WGD, it would be expected that zebrafish and other teleosts have a duplicated number of gene pairs in comparison to tetrapod species, including mammals. However, only around 25% of duplicated genes have been retained in zebrafish, while others have been lost through the course of evolution (Ravi and Venkatesh, 2008). Nevertheless, WGD is the reason why often zebrafish has two paralogs that correspond to the single gene in other vertebrate species, including humans (Ravi and Venkatesh, 2008). Although zebrafish reproduction is different from mammals given the fact that they reproduce in the water without pregnancy; that they spawn every week with extensive production of eggs and that juvenile fish of both genders have juvenile ovaries which are developed into testes in males in the 4-12 weeks after fertilization (Biran *et al*., 2008; Clelland and Peng, 2009), zebrafish retains basic vertebrate physiology. Despite the additional round of genome duplication in fish, large portion of vertebrate genes and cellular pathways are evolutionary conserved in vertebrates, and findings on zebrafish can generally be translated to other vertebrate species. For example, endocrine system of zebrafish is similar to mammals with direct homology of hormones and receptors of zebrafish with the mammalian counterparts (Busby *et al*., 2010).

From the small aquarium fish, zebrafish has risen to the widely used model in the biomedicine, developmental biology and environmental toxicology. It is advantageous to the use of invertebrate model species, such as well known fruit fly (*Drosophila melanogaster*) and worm *Chenorabditis elegans* due the lack of similarity between organ anatomy and physiology of invertebrates and mammals. When we consider vertebrate models, mouse has been mostly used so far. However, zebrafish has numerous advantages in comparison to mouse including very high fecundity (thousands of eggs per week), short generation time (2-3 months), transparent embryos and adults (casper strain) and low maintainance costs (Fig. 1.6). For these reasons, zebrafish is today used in the study of human diseases including cancer, blood disorders and cardiovascular diseases, muscle diseases, infections and inflammation as well as for the study of vertebrate embryonic development (Xu and Zon, 2010).

In environmental toxicology, zebrafish is currently the only vertebrate model used for the medium and/or high throughput *in vivo* toxicity screening (Carvan *et al*., 2007; Stegeman *et al*., 2010), thus replacing the cell based assays and mammalian models. Through the genomics and transcriptomic studies it has provided valuable insight into the xenobiotic metabolism and biotransformation of certain environmental contaminants including pharmaceuticals and pesticides. These insights can be used to predict effects of exposure of zebrafish to the certain environmental contaminants at the relevant concentrations. However, apart from toxicity studies and large scale 'omics' approach, there is a large gap in knowledge in the study of ADME of xenobiotics in appropriate model species.

Without proper understanding of the ADME processes, however, the (eco)toxicology fails in its primary mission to understand the mechanism of action of contaminants, as well as to predict pollution effects (Sukardi, 2011). Only few defensome genes involved in the ADME processes have been fully characterized in zebrafish (gene identification, transcriptional analysis, protein expression and determination of substrate and inhibitor) specificity). Characterized defensome genes in zebrafish so far only include several phase I CYP enzymes (Stegeman *et al*., 2010), some phase II enzymes of GST and UGT familes (Huan and Wu, 2010), and one transporter gene, a member of ABC family, Abcb4 (Fischer *et al*., 2013).

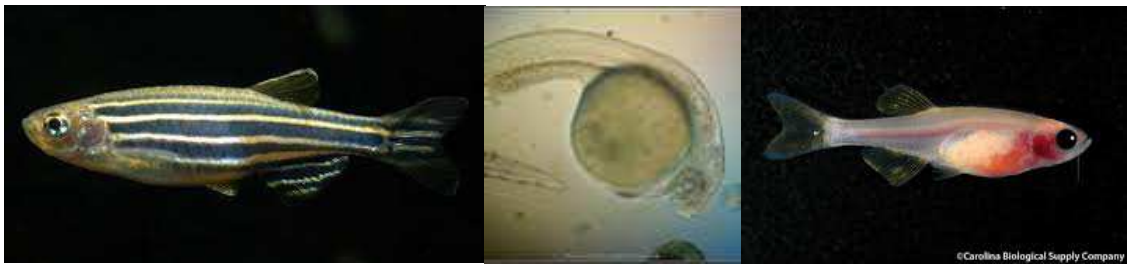

Figure 1.6. Adult zebrafish, transparent zebrafish embryos 72 hours post fertilization, and zebrafish transparent adult strain (the so-called casper strain) (in the order from left to right) (Adapted from: http://www.carolina.com/teacher-resources/Interactive/casper-fish-genetics/tr22624.tr).

1.6. Current knowledge about uptake transporters in non-mammalian species

Despite their physiological importance and role in cellular detoxification, the knowledge about uptake transporters in non-mammalian species is modest.

Within the OATP family, few *SLC21* genes have been identified on the genome level in non-mammalian organisms including: six genes in chicken (*Gallus gallus*), five genes in frog *Xenopus tropicalis*, four genes in zebrafish and 13 invertebrate *Slc21* genes (Meier-Abt *et al*, 2005). So far, only a few studies focused on the analysis of non-mammalian Oatps on the functional level that includes characterization of Oatps in birds and insects (Nakao *et al*., 2006; Mulenga *et al*., 2008). In fish, mainly within the toxicologically driven research, uptake of various compounds into fish liver has been studied (Boyer *et al*., 1976; Reed *et al*., 1982; Fricker *et al*., 1987; Hugentobler, 1987; Boyer *et al*., 1993; Fricker *et al*., 1994; Rabergh *et al*., 1994; Smith *et al*., 2005), but without the understanding the mode of transport. Only liver specific Oatp1 transporter in little skate (*Leucoraja erinacea*) has

been partly characterized (Cai *et al*., 2002; Meier-Abt *et al*., 2007). Skate Oatp1 transporter was shown to mediate transport of several substartes including E3S, anionic dye bromosulfophthalein (BSP), drug ouabain and toxin phalloidin. Because of the phalloidin transport, it was suggested that Oatp1 transporter is responsible for the elimination of xenobiotics in skate liver (Meier-Abt *et al*., 2007). Apart from the Oatp1 in skate, Oatp1-like transporter has been identified in the liver of rainbow trout (*Oncorhynchus mykiss*) (Boaru *et al*., 2006) without the determination of its substrate specificity.

Similar to the OATP family, SLC22/Slc22 transporter family has mainly been studied in mammals including human, mouse, rat, rabbit and pig. However, SLC22 is very diverse and even in humans, function of several transporters still remains unknown (Table 1.2). Overall, Slc22 transporters in non-mammalian species have been studied more than OATPs, but the number of studies still remains scarce. Among invertebrate Slc22 transporters, Octs have been identified on the genome level in fruit fly (*Drosophila melanogaster*) and *C. elegans* (Eraly *et al*., 2004). The authors have reported 9 Octs in fruit fly and 4 Octs in *C. elegans*, and performed phylogentic analysis of the OCT subgroup. In respect to functional analysis, two transporters have been functionally characterized in *C. elegans*: CeOat1 (George *et al*., 1999) and CeOct1 (Wu *et al*., 1999). CeOct1 transports wide range of organic cations including model cation TEA and many pharmaceuticals and neurotoxins, thus it was proposed to play a role in the elimination of cationic xenobiotics from the organism (Wu *et al*., 1999). In the same year, another Slc22 transporter has been characterized in *C. elegans*, CeOat1 (George *et al*., 1999). CeOat1 has broad substrate specificity and is proposed to play a role in xenobiotic elimination, similar to the CeOct1. It was found that CeOct1 transports endogenous compunds pAH and folate, as well as pharmaceuticals: indomethacin, furosemide, probenecid, and benzylpenicillin, similar to the human OAT1 (George *et al*., 1999). In vertebrates, three studies on SLC22/Slc22 transporters have been reported: Lennard *et al*. (2006) analyzed Octs in teleost species on the genome level (gene structure and phylogenetic analysis), Levavasseur *et al*. (1998) reported tha presence of Oct6 in zebrafish, and finally, Oat1 from winter flounder (*Pseudopleuronectes americanus*) have been partly functionally characterized by Ashlamkan *et al*. (2006) and Wolff *et al*. (2001). Ashlamkan *et al*. (2006) report that fOat1 transports E3S, dichlorophenoxyacetic acid and adefovir and propose that it is a fish counterpart of the two mammalian OATs/Oats, OAT1/Oat1 and OAT3/Oat3. Based on the *in vivo* inhibition of fluorescein uptake into the renal proximal tubules, they suggest that fOat is the primary renal basolateral Oat in teleosts. They also report one Oat gene sequence in zebrafish and one gene in pufferfish (*Takifugu rubripes)* that are similar to the fOat. The other study by Wolff *et al*. (2001) examined the influence of several fOat1 mutants on pAH uptake and found that K394 and R478 are crucial for protein activity.

1.7. Summary and aims

In summary, the uptake phase of ADME has seldom been considered in the context of environmental toxicology, and uptake transporters in zebrafish were not characterized before our study. We aimed to bridge this gap in knowledge and provide a comprehensive overview of uptake transporters involved in the cellular ADME in zebrafish as a valuable toxicological model. More specific goals of our study were:

1. To perform a complete phylogenetic analysis of OATP and SLC22 families in zebrafish which would enabled us to:

    a) determine the number of genes within each group,
    b) position zebrafish genes against their co-orthologs of other vertebrate species, and
    c) assign protein names to the unannotated zebrafish transporters.

2. To obtain the tissue expression profile of *Slc21* and *Slc22* genes in zebrafish, leading to:

    a) determination of the mRNA expression in liver, kidney, intestine, gills, brain and gonads of zebrafish,
    b) determination of gender differences in expression patterns, and
    c) identification of dominantly expressed genes in tissues that are key determinants of xenobiotic elimination (intestine, liver, kidney and gills).

3. To perform:

    a) functional characterization of selected OATP and SLC22 transporters,
    b) molecular characterization of a selected SLC transporter that would enable insights into the evolution of structural properties and transport mechanism, and
    c) determine interaction of selected SLC transporter/s with environmental contaminants that would enable better understanding of their role in the cellular ADME in zebrafish.

2. Materials and Methods

2.1. Materials

[^{3}H]estrone-3-sulfate ([^{3}H]E3S; 50 Ci/mmol) and [^{3}H]p-aminohippurate ([^{3}H]pAH; 4.1 Ci/mmol) were purchased from PerkinElmer (Waltham, MA, USA). Unlabeled E3S, p-aminohippurate (pAH), Lucifer yellow (LY) and other fluorescent probes as well as all other chemicals were purchased from Sigma-Aldrich (Taufkirchen, Germany) or Carl Roth GMBH (Karlsruhe, Germany).

Plasmids used in this study are listed in Table 2.1, enzymes are shown in Table 2.2, commercial kits in Table 2.3 and antibodies used for Western blotting analysis and immunocytochemistry in Table 2.4. Primers used for the quantitative PCR analysis and for cloning of full length amplicons/genes are shown in Table 2.5 and 2.6, respectively.

Table 2.1. Plasmids

Vector	Characteristics	Source
pGEM - T	Amp^R, AT cloning, E.colli expression	Promega
pJET 1.2	Amp^R, blunt cloning, E.colli expression	Invitrogen
pcDNA3.1(+)	Amp^R, CMV promoter, mammalian cells expression	Invitrogen
pcDNA3.1-His(+)	Amp^R, CMV promoter, mammalian cells expression	Invitrogen
pEGFP-N	Kan/Neo^R, SV40 promoter, mammalian cells expression, green fluorescence	Clonetech
pEGFP-C	Kan/Neo^R, SV40 promoter, mammalian cells expression, green fluorescence	Clonetech
pCS2+8NmCherry*	Amp^R, SV40 promoter, mammalian cells expression, red fluorescence	A. Hamdoun (gift)
pCS2+8NmCitrine*	Amp^R, SV40 promoter, mammalian cells expression, green fluorescence	A. Hamdoun (gift)

* also available from Addgene database

Table 2.2. Enzymes

Enzyme	Source
Taq DNA polymerase	Fermentas
Phusion proof reading polymerase	Thermoscientific
Reverse transcriptase	Applied Biosystems
Restriction enzymes: EcoRI, KpnI, NotI, SacI, XbaI, XhoI	Fermentas
Dnase I	Applied Biosystems
T4 DNA ligase	Fermentas

Table 2.3. Commercial kits

Kit	Source
Rneasy Mini Kit	Qiagen
MinElute Gel Extraction Kit	Qiagen
QIAquick PCR Purification Kit	Qiagen
QIAprep Spin Miniprep Kit	Qiagen
Plasmid midi kit	Qiagen
High Capacity cDNA Reverse Transcription Kit with Rnase Inhibitor	Applied Biosystems
pGEM-T Vector System I	Promega
DC Protein assay Kit	BioRad

Table 2.4. Antibodies

Antibody	Source
6XHis tag primary antibody, anti-mouse	Santa Cruz Biotechnology
Xpress tag primary antibody, anti-mouse	Life technologies
Na,K-ATPase primary antibody, anti-mouse	Santa Cruz Biotechnology
Goat anti-mouse IgG-HRP (secondary ab)	Bio-Rad Laboratories
Goat anti-mouse IgG-FITC (secondary ab)	Santa Cruz Biotechnology
Cy3-conjugated anti-mouse IgG-HRP (secondary ab)	Santa Cruz Biotechnology

Table 2.5. Primers used in the quantitative Real time PCR (qRT-PCR).

Protein name		Primer sequence 5' -> 3'	T_a	Final conc. (nM)	Efficiency (%)
Oatp1d1	F	ACGCCCTGTACAGCTCATCCT	60	300	93
	R	ACTGGTCCTTTAGCGCTTGCT	59	300	
Oatp1d2	F	TGCAAATGAGACTGTCGTTATAGCT	58	300	91
	R	TGGTATTATCGATGTGCTGTATTGAG	58	300	
Oatp1f2	F	ACAGCTGCCACCCACACTAAT	58	300	95
	R	GGCATCCAGAAAAAGGCTGTT	59	900	
Oatp2a1	F	GACTCATTGCAAGCCTGACACA	60	300	99
	R	AGCAAAAACTGGATCCCTATGG	58	300	
Oatp2b1	F	ACGCAGACTGGGTTTGACTGT	58	300	87
	R	GCAGCCAATAAAAAGAAGTGGAA	58	300	
Oatp3a1	F	TGTGGATGCTTTGTTCATCGA	59	900	100
	R	GGCACCGCAGATGAGGAAT	60	300	
Oatp3a2	F	GTGCGCTTGCAGCATGAT	58	50	80
	R	TCAGCTCTGGGCTCACAGTTC	59	300	
Oatp5a1	F	ATCGTGGGCTGTGAAAGCA	59	300	81
	R	CGTCAGGTTTCTGTGGGTCAA	60	300	
Oat1	F	TGCTGTTCTGATCTTGGACGA	62	300	92
	R	TGCTATTAAACCAGCGATGAC	60	300	
Oat3	F	GGGTCAGCATTTACCTCATCCA	60	300	105
	R	GATGGCCGTCGTCCTAACAT	58	300	
Oat2a	F	TCGCCATTGCAAGAACCTTAT	58	300	92
	R	AAGGTGCGATGCTTAACATCTG	58	300	
Oat2b	F	GATTGTAAGTGTTCCAGCACAAGAA	58	300	101
	R	TGAGCTGCTGGACGAGTTTATC	58	300	
Oat2c	F	GCACTTTGATAACAGCACCTTCAT	58	300	95
	R	GAAGAAGATGGTGGTTGTCAATTTC	59	300	
Oat2d	F	ACAGTATGGCATGGGCTGTT	60	300	100
	R	AAGGTGAAGTGACAGCCACT	60	300	
Oat2e	F	GGTGTTATGAtCAGTTTGGATT	60	300	95
	R	TTGGAGCAGTTACTGTGAGG	58	300	
Oct1	F	GAGTCACAGGGATTCTGGT	58	300	99
	R	ACCATCCAACCGCCCTTCA	60	300	
Oct2	F	TGGCCTTGGAGTCTCTGG	60	300	99
	R	TGGCGGTCCATGCTCCTTT	60	300	
Octn1	F	GCTCTGGAATCGGGCAGAT	60	300	100
	R	GGCCAGTGAGGGCGTTTG	60	300	
Octn2	F	CACCGCCTCACTGGCCAACC	60	300	112
	R	ATCTCTTCCTGGAAAGCTT	60	300	
Oct6	F	GCTGTAGGGAGTGGTAGTAT	60	300	96
	R	CGATGAGCTGCGGCAGATA	60	900	
Orctl3	F	ACCTCGTGTCCCAGTTCATT	60	300	100
	R	TGCATATGATCTCTGGGCGA	60	300	
Orctl4	F	TCACCGCCTTCCACATGTT	59	300	96
	R	TTGGAGCCTGTCGGAGGAT	59	300	
Ef1α	F	CCTGGGAGTGAAACAGCTGATC	60	300	96
	R	GCTGACTTCCTTGGTGATTTCC	60	300	

Table 2.6. Primers used for cloning of selected *Slc21* and *Slc22* genes. Part of the primer sequences that were introduced for digestion with specific restriction enzymes are shown in blue.

Protein name		Primer sequence 5' -> 3'
Oatp1d1	F	TTAGCGGCCGCATGAGTACGGAGAAGAAGAAG
	R	TTAGGTACCTCTAGACTTCAGATGGTGGTCTCCTG
Oat3	F	TTAGCGGCCGCAAGCTTTCATGGCGTTCTCCGACCTGT
	R	GGTACCCTCGAGAACAGACTCTTTCAGGAGGA
Oat2c	F	TTAGCGGCCGCAAGCTTTCATGAGATTTGAAGATCTGCTCT
	R	TTAGGTACCTCTAGACTAGTGTTCTGCACAATTAAATTA
Oat2d	F	GAATTCATGAAGTTTGAAGATCTAATTAC
	R	GCGGCCGCGGTACCCTGGGGTTCATTCATTGCAA

For the purpose of gene cloning, DH5α E.coli competent cells were used (Invitrogen, CA, USA). All transfection experiments were performed with the HEK293 cells (Human Embryonic Kidney cells) (ATCC, CRL-1573), which are routinely used in cell biology due to their low duplication time (<24h) and high transfection efficiency (Tom *et al*., 2008). HEK293 cells were grown in the complete growth medium that consisted of DMEM high glucose (Dulbecco's modified Eagle medium) (Life technologies, CA, US) and 10% fetal bovine serum (FBS) (Invitrogen, CA, USA).) in the 5% CO_2 incubator at 37 °C.

2.2. Methods

2.2.1. Phylogenetic analysis and membrane topology

Protein sequences were retrieved from following databases: NCBI (http://www.ncbi.nlm.nih.gov/), ENSEMBL (http://www.ensembl.org/index.html) using blastx algorithm. Following species were included in the phylogenetic analysis: mammals: human (*Homo sapiens*) and mouse (*Mus musculus*); bird: chicken (*Gallus gallus*); reptile: anole lizard (*Anolis carolinensis*), amphibian: frog *Xenopus tropicalis* and *X. laevis*; actinopterygian or ray-finned fishes: zebrafish (*Danio rerio*), pufferfishes: Japanese pufferfish (*Takifugu rubripes*) and green spotted pufferfish (*Tetraodon nigroviridis*), Atlantic cod (Gadus morhua), stickleback (*Gastrosteus aculeatus*) and medaka (*Oryzas latipes*); sarcopterygian or lobe-finned fish: West Indian Ocean coelacanth *Latimeria chalumnae* and tunicate sea squirt (*Ciona intestinalis*).

Sequences were considered to be part of the OATP/Oatp family if they complied to three criteria: blastx hit with threshold value of e = 10^{-3}, presence of the Oatp conserved domain with threshold value of e = 10^{-6}, and presence of the family signature (D-X-RW-(I,V)-GAWW-XG-(F,L)-L) on the border of extracellular LP3 and TMD6 (Marchler-Bauer *et al.*, 2005). In the case of SLC22/Slc22 family, all hits below the threshold value of e = 10^{-3} were considered, and false positives were excluded based on

the phylogenetic analysis. Sequences were aligned with MUSCLE algorithm (Edgar, 2004) and phylogenetic tree was constructed using Maximum Likelihood method in PhyML 3.0.1 software (Guindon and Gascuel, 2003). Confidence of nodes was estimated by approximate likelihood ratio test (aLRT) (Anisimova and Gascuel, 2006). Based on the phylogenetic relationships, all previously unclassified genes were provisionally annotated. Names were given in accordance with the new nomenclature adopted by the HUGO Gene Nomenclature Committee (Hagenbuch and Meier, 2004).

TMDs were predicted using HMMTOP algorithm version 2.0. (Tusnady and Simon, 2001), followed by prediction correction according to the multiple alignments with human OATPs and/or SLC22 proteins. BioEdit Software version 7.0. was used for sequence editing and alignment display (Hall, 1999), while sequence identities were calculated in DNAstar Software (version 7.0.0). Potential N-glycosilation sites were predicted using the NetNGlyc 1.0 server (http://www.cbs.dtu.dk/services/NetNGlyc/).

2.2.2. Tissue-specific gene expression analysis: RNA isolation, reverse transcription and qRT-PCR

Fish were purchased from a local fish supplier and sacrificed by decapitation for the collection of tissues. Tissues (brain, gills, liver, kidney, intestine and gonads from five specimens were pooled together in order to get substantial amount of material for RNA isolation. Three independent pools were collected. In order to get enough tissue for RNA isolation from kidney, 13 individuals had to be sacrificed. Tissues were stored in RNA later (Qiagen, Hilden, Germany) and afterwards homogenized for 20 seconds using rotor-stator homogenizer at 10,000 rpm. Total RNA isolation was carried out using Rneasy Mini Kit (Qiagen, Hilden, Germany). Genomic DNA digestion was carried out using Rnase-free DNase Set (Qiagen, Hilden, Germany). Total RNA was quantified using Agilent 2100 Bioanalyzer (Agilent Technologies, Palo Alto, CA, USA) followed by reverse transcription (1 µg of total RNA using High Capacity cDNA Reverse Transcription Kit with Rnase Inhibitor (Applied Biosystems, Foster City, CA, USA).

For the purpose of quantitative Real time PCR (qRT-PCR), specific primers were designed in the Primer express 3.0 Software (Applied Biosystems, CA, USA), adjusted manually if necessary and purchased from Invitrogen (Carlsbad, CA, USA) (Table 2.6). Target amplicons of 90-100 bp were cloned using pGEM-T Vector System I (Promega, Madison, WI, USA). Plasmids were purified by QIAprep Spin Miniprep Kit (Qiagen, Hilden, Germany) and amplicons were verified by sequencing at the Rudjer Boskovic Institute DNA Service (Zagreb, Croatia). Primer efficiencies were determined using the recombinant pGEM-T as a template, for each primer pair. Primer concentrations were

optimized combining three primer concentrations: 300, 600 and 900 nM. Primer concentrations resulting in the highest fluorescence signal at lowest Ct number were chosen as optimal. Primer sequences, optimal concentrations and primer efficiency of target gene sequences are given in Table 2.5, while accession numbers of target genes are given in the Table S1 and S2. For the purposes of inter-gene comparison throughout one tissue, relative quantification was used as method of choice. Target genes were normalized to the housekeeping gene (HKG) using Q-Gene application (http://www.qgene.org/) for the processing of qRT-PCR data (described in detail by Muller et al. (2002) and Simon (2003) according to equation:

$$MNE = ((E_{ref}) \hat{} Ct_{ref,mean}) / ((E_{target}) \hat{} Ct_{target,\ mean})$$

where, MNE stands for mean normalized expression; E_{ref} is housekeeping gene efficiency; E_{target} is target gene efficiency; $Ct_{ref,\ mean}$ is mean Ct value for the housekeeping gene; and finally, $Ct_{target,\ mean}$ stands for mean Ct value of the target gene. Data are presented as gene of interest expression relative to the housekeeping gene expression multiplied by the factor of 10,000. Elongation factor (EF1α) was chosen as a housekeeping gene given the fact that its expression was similar across all analysed tissues. Expression was considered to be high for MNE > $600*10^5$ (C_t > 22), moderate for MNE $20*10^5$ - $600*10^5$ (C_t = 23-26) and low for MNE < $20*10^5$ (C_t >27).

qRT-PCR was performed using the ABI PRISM 7000 Sequence Detection System using Power SYBR Green PCR Master Mix (Applied Biosystems, Foster City, CA, USA). qRT-PCR reaction mix was prepared to a final volume of 10 µl containing: 5 µl of SYBER Green master mix, 0.5 µl of each primer (of adequate concentration), 1 µl of template (10 ng/well) and 3 µl of Ultrapure Dnase/Rnase free distilled water (Molecular Bioproducts, San Diego, CA, USA). After the denaturation at 95˚C for 10 min, 40 cycles of amplification were carried out with denaturation at 95˚C for 15 sec, annealing and elongation at 60˚C for 1 min altogether followed by the melting curve analysis. Data were analysed with ABI PRISM Sequence Detection Software 1.4 (Applied Biosystems, Foster City, CA, USA) and GraphPad Prism Software version 5.00.

2.2.3. Cloning of full-length zebrafish genes

Full-length zebrafish genes, Oatp1d1, Oat3, Oat2c and Oat2d were amplified from the zebrafish liver, kidney and intestine, respectively using primer pairs listed in the Table 2.6 with high fidelity Phusion DNA polymerase (Finnzymes, Vantaa, Finland). Accession codes for each gene is given in the Table S1 and S2. Genes were cloned according to the standard procedure (Sambrook, 1989) as follows: (1) amplification of target gene by PCR from the cDNA of a given tissues, (2) separation of

DNA fragements on the agarose gel electrophoresis, (3) purification of desired DNA bands from the agarose gel using the commercialy available kit (Table 2.3), (4) blunt-end ligation of purified DNA fragments with the previously prepared pJET 2.0 vector (Table 2.1), (5) transformation of competent bacterial cells dH5α, (6) PCR colony screening of transformants with target DNA insert, (7) purification of recombinant plasmid carrying target gene from the selected clones using the plasmid isolation kit (Table 2.3), and (8) verification of gene sequence by DNA sequencing at the VBC-Biotech Services GmbH (Vienna, Austria). For each gene, three clones were sequenced, and compared to the the gene sequence from the NBCI database. If one sequence differed from the other two in respect to one or more base pairs, one of the two identical clones were chosen. In most cases all clones were also identical to the predicted gene sequence from NCBI.

Each gene was subcloned into the pcDNA3.1 and pcDNA3.1/His vectors suitable for the heterologous expression in the mammalian cells, as well as in the plasmids containing coding sequences for the expression of fluorescent proteins (Table 2.1). Subcloning from the pJET vector was possible due to the introduced sites for digestion with specific restriction enzymes into the initial primers (Table 2.6). Subcloning was performed as follows: (1) digestion of pJET recombinant plasmid carrying target gene by restriction enzymes (Table 2.2), (2) separation of DNA fragment mixture on the agarose gel and purification of desired bands by gel extraction kit (Table 2.3), (3) sticky-end ligation with T4 DNA ligase (Table 2.2), (4) PCR colony screening of transformants with target DNA insert, (5) purification of recombinant plasmid carrying target gene from the selected clones using the plasmid isolation kit (Table 2.3).

2.2.4. Heterologous expression in HEK293 cells

HEK293 cells were transiently transfected using the PEI (polyethyleneimine) reagent in 24-well plates for the E3S uptake assay and in 48-well plates for the LY uptake assay. The method was performed as previously described (Tom *et al*., 2008) with some modifications. HEK293 cells were seeded 48h before the transfection into the 24-well or 48-well plates at 1,8 $*10^5$ cells/ml cell density (0.5ml/well in the 24-well plates, and 0.25ml/well in 48 well plates). The transfection mixture consisted of recombinant plasmid carrying target gene and PEI reagens in the 1:1 ratio with the final concentration of 0,75 μg/well of each constituent for 24-well plate and 0,375 μg/well for 48-well plate. Both, PEI and DNA were diluted in the phosphate buffer saline (PBS), previously warmed to 37 °C, followed by the mixing of DNA and PEI solutions, brief vortexing (3 X 3min), and incubation of the mixture for 15min at room temperature. The complete growth medium was removed from the assay plates in which HEK293 cells were grown for 48 hours, and 0.45ml of medium without sera was added in each well in the 24-well plates. The 50 μl of DNA/PEI mixture was added in each well,

followed by 24h incubation period at 37 °C (5% CO_2 incubator). After 24h incubation, medium was exchanged for the complete growth medium, and cells were grown for another 24h after which transport assays were performed when transfection efficiency was above 70%. Reactions were appropriately scaled-down for the 48-well plates. Branched PEI is used as a transfection reagens on the basis of its ability to encapsulate DNA into the positively charged particles, which bind to anionic cell surface residues and enter the cell through endocytosis (Boussif *et al*., 1995).

To evaluate transfection efficiency, cells were in parallel transfected with pcDNA3.1/His/LacZ plasmid and transfection efficiency was evaluated 24 h after transfection with the LacZ staining protocol (Sambrook and Russell, 1989). The assay is based on the ability of enzyme β-galactosidase (gene LacZ) to catalyze X-gal (5-bromo-4-chloro-3-indolyl-β-D-galactopyranoside) into the an intensely blue product 5,5'-dibromo-4,4'-dichloro-indigo. Adherent HEK293 cells transfected with pcDNA3.1/His/LacZ were washed twice with PBS, followed by fixation in 0.5% glutaraldehyde (in PBS), and 24h incubation (at 37° C) in the X-gal solution (1mM X-gal, 40mM ferricyanide, 40mM ferrocyanide, 2mM $MgCl_2$ in PBS).

2.2.5. Transport measurements

For the purpose of the transport assay, HEK293 cells overexpressing Oatp1d1 were preincubated in the transport medium (145 mM NaCl, 3 mM KCl, 1 mM $CaCl_2$, 0.5 mM $MgCl_2$, 5 mM D-glucose and 5 mM hydroxyethyl piperazineethanesulfonic acid (HEPES), pH 7.4) for 10 min at 37°C. To assess transport, the medium was removed and the same medium containing the substrate was added. After incubation, the cells were rapidly washed three times with ice-cold phosphate-buffered saline (PBS), lysed in 500 µl of 0.1% sodium dodecyl sulphate (SDS) for 30 min, transferred to scintillation vials, and measured by a liquid scintillation counter (Tri-carb 2800 TR, PerkinElmer, Waltham, MA, USA) in the case of [^{3}H]E3S and [^{3}H]pAH or transferred to the 96 well black plates (Sigma-Aldrich, Taufkirchen, Germany) and measured using the microplate reader (Infinite 2000, Tecan, Salzburg, Austria) for the fluorescently labeled substartes. Calibration curves for E3S and LY were generated in the 0.1% SDS and in the cell matrix dissolved in the 0.1% SDS. In the case of both substrates, linear calibration curves were the same in the SDS and in the dissolved cell matrix. Using the calibration curves, uptake of E3S and LY was expressed as nM of substrates per mg of protein. Total cell protein content was determined according to manufacturer instructions using the DC protein assay kit (Bio-Rad Laboratories, CA, USA).

In the inhibition experiments, the cells were preincubated for 20 seconds with test compounds, followed by 5 min incubation with [^{3}H]E3S (5 nM) or 30 minutes with LY (5 µM). For the interactors that showed uptake inhibition above 50%, K_i values were determined. Compounds with K_i values in

nanomolar range (<1 μM) were considered to be very strong interactors, compounds with K_i of 1 - 20 μM were designated as strong interactors, whereas K_i of 20 – 100 μM indicated moderate interaction and K_i above 100 μM, weak interaction.

For the purpose of distinguishing the type of interaction with chosen compounds, shift in K_m and V_{max} values for LY was determined in the presence of a target compound (at the concentration equal to the K_i value of a compound), at varying LY concentrations (8 points) and after 15 min of incubation, which was within the linear range of the LY transport rate. To determine shift in K_m and V_{max} values for LY more accurately, all of the competition type experiments were performed within a single transfection experiment (repeated at least 3 times) in order to eliminate inter experiment differences due to the transient transfection system. The uptake into vector-transfected HEK293 cells (mock cells) was subtracted to obtain the transporter-specific uptake.

2.2.6. pH manipulations

To determine if Oatp1d1 activity is pH dependent, transport assays were performed in transport buffers of varying pH similar as described previously (Kobayashi *et al*., 2003). Uptake medium contained: 145 mM NaCl, 3 mM KCl, 1 mM $CaCl_2$, 0.5 mM $MgCl_2$, 5 mM D-glucose and 25 mM 2- (N morpholino) ethanesulfonic acid (MES) in the case of pH 5.5 medium; 5 mM HEPES for the pH 7.4 uptake medium; and 25 mM Tris for pH 8 medium. By exchanging extracellular media of pH 7.4 to pH 5.5, i.e.lowering extracellular pH, an inwardly directed [H^+] gradient was achieved. Outwardly directed [H^+] gradient was created by acidifying intracellular space with NH_4Cl (30 minutes incubation at 37°C in 30 mM NH_4Cl in the presence of 0.5 mM amiloride) or with alkalizing extracellular pH by exchanging extracellular media of pH 7.4 to pH 8 similarly as previously described (Bendayan *et al*., 1994; Hong *et al*., 2001). When cells are exposed to the 30 mM NH_4Cl, intracellular alkalinization occurs due to the rapid influx of NH_3 (dissociated from the [NH_4^+]) which binds intracellular [H^+]. However, when extracellular NH_4Cl solution is removed (and replaced by regular HEPES based incubation media of pH 7.4), intracellular pH (pH_i) rapidly falls due to the dissociation of intracellular [NH_4^+] which rapidly leaves the cell to NH_3 and [H^+] which is trapped inside the cell and casues the acidification (Boron and De Weer, 1976).

Acidification of intracellular space was verified using BCECF method (2',7'-bis-(2-carboxyethyl)-5-(and-6)-carboxyfluorescein) (Ozkan and Mutharasan, 2002), while calibration was performed *in vitro* with BCECF free acid (Boyarsky *et al*., 1996). Lipophilic acetoxymethyl (AM) ester form of the fluorescent dye BCECF (BCECF-AM) (2',7'-bis-(2-carboxyethyl)-5-(and-6)-carboxyfluorescein acetoxymethyl ester) enters the cell by the menas of passive diffusion where esterases hydrolyse it, releasing the charged membrane impermeant BCECF whose fluorescence spectra is pH sensitive. For

the pH_i measurements of HEK293 cells after the NH_4Cl treatement, cells were preloaded with 5µM BCECF-AM (45min at 37 °C), washed 2 times in IM to remove BCECF-AM that did not enter the cells and subsequently treated with NH_4Cl solution as described above. At each point of interest, BCECF fluorescence was measured on the intact cell layer at two excitation wavelengths 490nm and 440nm and emission at 535 nm. The pH_i was calculated from the 490/535nm and 440/535 nm fluorescence ratio according to the formula

pH_i= logEC50-log((max-y)/(y-min))/H,

where y is 490/535nm and 440/535 nm fluorescence ratio, while EC50, min, max and H (Hill slope) are parameters from the calibration curve of the BCECF free acid (Boyarsky *et al*., 1996).

2.2.7. Glycosylation inhibition

To determine if N-glycosylation is involved in post-translational processing of Oatp1d1, tunicamycin, a general N-glycosylation inhibitor, was added in varying concentrations during the 24 h post-transfection period. After 24 h, cells were briefly incubated in medium without tunicamycin and [^{3}H]E3S and LY uptake was determined as described above and compared to the non-treated transfected cells. HEK293 mock cells (vector-transfected cells) were assayed as well, with and without tunicamycin treatment.

2.2.8. Site directed mutagenesis

Site directed mutagenesis was performed with asymmetric overlap extension method (Xiao *et al*., 2007). For site-directed mutagenesis, two mutant fragments of the same gene are amplified in the first round of PCR and then annealed and extended in the second round of PCR (Fig. 2.1). Proof reading Phusion polymerase was used. In the first PCR round PCR mixture I. included amplification of the first part of the gene with the introduced site mutation in the mutagenesis forward primer (MPF), while PCR mixture II. included amplification of the second part of the gene with the introduced site mutation in the mutagenesis reverse primer (MPR).

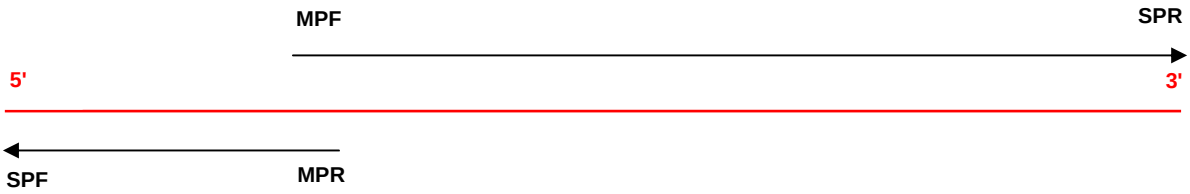

Figure 2.1 Schematic representation of the asymmetric overlap extension method for site directed mutagenesis (MPF, mutagenic forward primer; MPR, mutagenic reverse primer; SPF, specific F primer; SPR, specific R primer). Target gene is shown in red.

After the denaturation at 90˚C for 10 min, 30 cycles of amplification were carried out with denaturation at 90˚C for 10 sec, annealing and elongation at 60˚C for 1 min. All PCR reactions were performed in the 50 µl reaction volume, with final primer concentration of 500 nM for specific primers, and 50 nM for mutagenesis primers and 10 ng of template. Finally, without purification steps 25 µl of PCR mixtures I. and II. were mixed and incubated at 60 °C for 1 min (annealing) and at 72 °C for 10 min (extension).

2.2.9. Western blotting and immunocytochemistry

Cells were collected from 25 cm^2 culture flasks 24 h after transfection, lysed in RIPA buffer (NaCl 150 mM, EDTA 1 mM, Tris 25 mM, NP-40 0.8%) with protease inhibitors cocktail AEBSF (Sigma-Aldrich, Taufkirchen, Germany) for 30 min on ice, subjected through 3 freeze/thaw cycles, briefly sonicated and centrifuged at 1,000 *g* for 10 min at 4°C. Protein concentration in total cell lysate (TCL) was measured according to the manufacturer instructions using the DC protein assay kit (Bio-Rad Laboratories, CA, USA). Twenty micrograms of protein per lane was separated by electrophoresis in 1% sodium dodecyl sulphate polyacrylamide gel. The proteins were then transferred to the polyvinylidene difluoride membrane (Millipore, MA, US) by semidry blotting. Blocking was performed in blocking solution, containing 5% low fat milk, 50 mM Tris, 150 mM NaCl and 0.05% Tween 20. Subsequently, membranes were washed and incubated for 1 h with anti-Xpress (Life technologies, CA, USA), or 2 h with anti-His antibody (Santa Cruz Biotechnology, CA, USA). Goat anti-mouse IgG-HRP was used as secondary antibody (Bio-Rad Laboratories, CA, USA). The proteins were visualized by chemiluminescence (Abcam, Cambridge, UK). Protein size was estimated by use of protein marker (ThermoFischer Scientific, MA, USA).

For immunofluorescence detection, HEK293 cells were grown on glass coverslips in 24-well culture plates. Twenty four hours after transfection, cells were fixated with 4% paraformaldehyde in

PBS during 30 min, washed three times in 100 mM glycin/PBS, permeabilized for 15 min in methanol and blocked in 5% low fat milk for 30 min with gentle agitation. Subsequently, coverslips were transferred on microscope slides and incubated with Xpress antibody (1:100) in blocking solution for 1 h at 37°C in humidity chamber, washed and then incubated with secondary FITC antibody (fluorescein isothyocyanate) (1:100) in blocking solution for 1 h at 37°C. When double staining was performed after incubation with FITC, blocking was done in 5% low fat milk for 30 min with gentle agitation, followed by incubation with Na,K-ATPase anti-mouse primary antibody (Santa Cruz Biotechnology, CA, USA) for 2 hours (1:150), washing, and 1 hour incubation with Cy3-conjugated anti-mouse IgG-HRP (Cyanine3) as a secondary antibody (1:200) (Santa Cruz Biotechnology, CA, USA). Nuclei were stained with DAPI for 45 min at 37°C in 300 nM DAPI/PBS. After mounting the samples in Fluoromount medium (Sigma-Aldrich, Taufkirchen, Germany), immunofluorescence was detected using confocal microscope Leica TCS SP2 AOBS (Leica Microsystems, Wetzlar, Germany).

2.2.10. Cell surface biotinylation

Surface biotinylation of Oatp1d1 at the plasma membrane was performed as described previously (Yao *et al*., 2012) with some modifications. Transiently transfected cells (with pcDNA3.1/His vector alone or with pcDNA3.1/His - Oatp1d1) were washed three times with PBS, and surface proteins were biotinylated with Sulfo-NHS-LC-LC-biotin (Pierce, 1 mg/ml) in PBS for 2 h at 4°C. Subsequently, cells were washed three times with ice-cold PBS containing 100 mM glycine, lysed as described above and centrifuged at 10,000 *g* for 10 min at 4°C to pellet insoluble fraction. Total cell lysates were incubated with hydrophilic streptavidin magnetic beads (New England Biolabs, MA, US) overnight on ice with gentle agitation. Bound proteins were washed and eluted according to the manufacturer instructions and analyzed using Western blotting with anti-His primary antibody (1:3000) and visualized by chemiluminescence. Binding of streptavidin and biotin molecules is the strongest noncovalent biological interaction known with the dissociation constant, K(d), in the order of 4x10 (-14) M, thus making it widely used procedure in the protein purification via its biotinylation and binding to the streptavidin coated beads (Holmberg *et al*., 2005)

2.2.11. Data analysis

All assays were performed in 2 - 4 independent experiments run in triplicates. Data represents mean $\pm$ standard errors (SE) or standard deviations (SD). All calculations were performed using GraphPad Prism 5 for Windows as described below. The kinetic parameters, K_m and V_{max} values were calculated using the Michaelis-Menten equation,

$$V = \frac{V_m \text{ x } [S]}{S + K_m}$$

where *V* is velocity (nanomoles of substrate per milligram of proteins per minute), V_{max} is maximal velocity, [*S*] is substrate concentration and K_m is the Michaelis Menten constant. The uptake into vector-transfected HEK293 cells was subtracted to obtain transporter-specific uptake. Hill coefficient (*h*) estimating the degree of cooperativity was determined from Hill plot (X = log [S], Y = log (V / V_{max} - V). For the purpose of K_i calculations data were fitted to the sigmoidal four parameters dose–response model (variable slope):

$$V = V_{min} + \frac{(V_{max} - V_{min})}{1 + 10^{((\log Ki - A)h))}}$$

where *V* is response, V_{min} represents minimum of response, V_{max} represents maximum of response, *h* is Hill slope parameter, K_i is the concentration of inhibitor that corresponds to 50% of maximal effect and *A* is concentration of tested compound.

3. Results

3.1. Phylogenetic analysis

3.1.1. OATP family

We have identified fourteen SLC21 genes in zebrafish. Unlike in mammals, where six families are found (OATP1-6), 5 subfamilies are present in zebrafish: (1) Oatp1 with 7 genes: Oatp1c1, 1d1, 1d2, and 1f1-1f4; (2) Oatp2 subfamily that includes Oatp2a1 and 2b1; (3) Oatp3 with Oatp3a1 and 3a2; (4) Oatp4 with a single member, Oatp4a1; and (5) Oatp5 with Oatp5a1 and 5a2. Oatp6 subfamily is specific for mammals, and is not present in other analyzed vertebrate species, including zebrafish (Fig. 3.1, Table 3.1). Out of the 14 zebrafish genes, six have not been annotated so far. We have classified these newly identified Oatps within 2 groups: Oatp1d and Oatp1f (Fig. 3.1, Table 3.1). These two groups are specific for teleost fish and are not present in tetrapods (Table 3.1). All OATP/Oatp protein sequence accession numbers and annotations are given in the Supplemental material (Table S1).

Within the Oatp1 subfamily cluster, we report the first finding of OATP/Oatp in a primitive chordate, tunicate sea squirt (*Ciona intestinalis*). The gene, provisionally named Oatp1-like, belongs to the OATP1/Oatp1 subfamily, within which it positions outside of the vertebrate OATP1/Oatp1 clusters (Fig. 3.1). This newly identified OATP/Oatp could represent a gene sequence most similar to the ancestral sequences of the OATP1/Oatp1 subfamily. Within the vertebrate cluster, OATP1A/Oatp1a and OATP1B/Oatp1b are found in all tetrapod representatives, including West Indian Ocean coelacanth *Latimeria chalumnae*. However, they are not present in teleost fish (Fig. 3.1, Table 3.1). The OATP1C/Oatp1c cluster is conserved throughout vertebrate subphylum, including teleosts and the cartilaginous fish little skate (*Leucoraja erinacea*). Herewith we reassign the annotation of the skate Oatp gene that was previously annotated as Oatp1d1 (Cai *et al*., 2002; Maier-Abt *et al*., 2007). According to our revised phylogeny (with more fully sequenced genomes available), the skate *Slc21* gene is an OATP1C1/Oatp1c1 ortholog.

The Oatp1d is a teleost specific group which forms a distinct cluster with a high node confidence (alRT = 0.99) between OATP1B/Oatp1b and OATP1A/1C (Oatp1a/1c). Apart from zebrafish, Oatp1d1 and 1d2 orthologs are present in other analyzed teleost species: pufferfishes (*Tetraodon nigroviridis* and *Takifugu rubripes*), stickleback (*Gastrosteus aculeatus*) and Atlantic cod (*Gadus morhua*) (Fig. 3.1). In terms of amino acid sequence identity of zebrafish Oatp1d1 and Oatp1d2, both proteins show similar differences to all mammalian Oatp1 groups (39-48% and 36-45%, respectively). Oatp1d proteins (1d1 and 1d2 orthologs in teleosts) are equally similar to the Oatp1a members in vertebrates (39-47% amino acid identity), and to the Oatp1b (39-50 %), whereas slightly higher sequence identity is found with Oatp1c group (44-50%). Within the Oatp1d group, Oatp1d1 orthologs

in fish share 61-78% amino acid identity within Oatp1d1 group and 42-54% amino acid identity with Oatp1d2 group. Oatp1d1 group is 48-50% identical to the newly identified Oatp1c1 from little skate, while Oatp1d2 group shows 40-48% amino acid sequence identity with LeOatp1c1.

Oatp1f cluster is present only in zebrafish, and absent from all other teleost species. It forms a distinct gene cluster with high amino acid sequence identity amongst each other (70-87%). Oatp1f proteins are most similar to Oatp1c and 1d members (40-46% amino acid identity) in other fish species. Similarly to the Oatp1d, Oatp1f group is equally similar to the Oatp1a members in other vertebrates (42-54%) as well as to the Oatp1b members (37-46%), whereas it shows slightly higher sequence identity with Oatp1c members (42-47%).

Single Oatp2a and 2b members are found in genomes of all analyzed vertebrate species, including fish (Fig. 3.1, Table 3.1). As expected, zebrafish Oatp2a1 is most similar to Oatp2a1 orthologs in other fish (55-59 % amino acid sequence identity), followed by 50-52% sequence identity with OATP2A/Oatp2a members in other vertebrates. Similar pattern is observed in the case of zebrafish Oatp2b1 which shares 53-54% amino acid sequence identity with Oatp2b orthologs in fish and 42-49% sequence identity with OATP/Oatp2b members in other vertebrates.

Within Oatp3a group, two members are found in teleosts including zebrafish (Fig. 3.1, Table 3.1). On the contrary, only one Oatp3a co-ortholog is present in all other vertebrates. Oatp3 subfamily in fish shows high amino acid sequence identity within the subfamily (76-77%) as well as in comparison to orthologs in other vertebrate species (71-75%).

OATP4A/Oatp4a proteins are highly conserved from sea squirt to mammals, with one ortholog present in vertebrates, including zebrafish, and three genes present in sea squirt. Amino acid sequence identity among all Oatp4a1 orthologs is 59-67%. Oatp4c group clusters more closely to the mammalian specific Oatp6 subfamily. The Oatp4c group contains one gene, and is conserved within tetrapods including *Latimeria chalumna*e. However, this group is not found in teleosts. In terms of amino acid identity, OATP4C/Oatp4c is closer to OATP4A/Oatp4a (32-39%), than to OATP6/Oatp6 subfamily (23-38%).

Two members are found within OATP5/Oatp5 subfamily in teleosts, including zebrafish, whereas a single member is present in other vertebrates (Table 3.1, Fig.3.1). OATP5A1/Oatp5a1 group contains highly similar sequences, with 68-90% amino acid sequence identity within co-orthologs of all vertebrate species analyzed. Within the teleost specific Oatp5a2 group, the sequence identity is substantially lower, with 50-53% amino acid identity among the co-orthologs. The similarity amongst the OATP5A1/Oatp5a1 and Oatp5a2 group is 50-69% amino acid identity.

Accession codes and annotations of protein sequences for chordate OATP family members are given in the Supplemental material (Table S1).

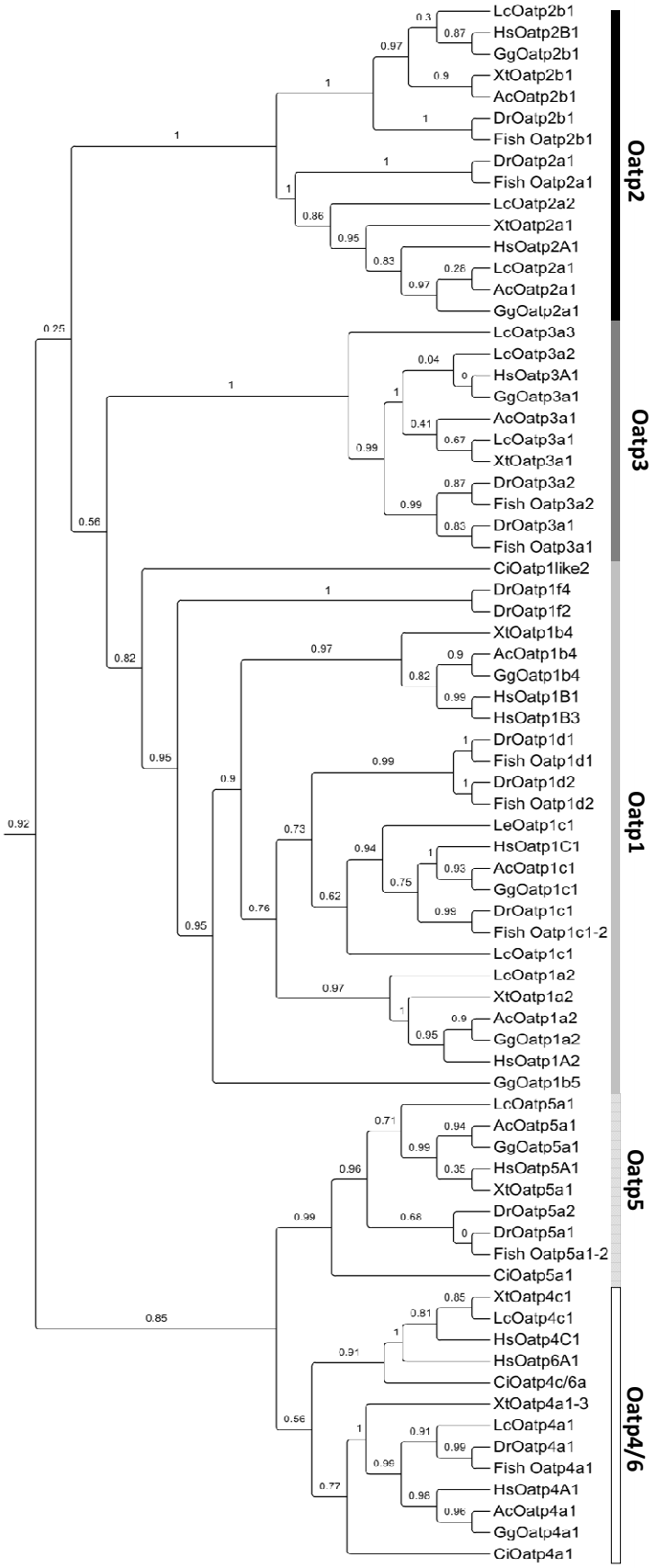

Figure 3.1. Phylogenetic tree of the OATP/Oatp family (Organic anion transporting polypeptide family) in vertebrates. The tree is a part of a larger phylogenetic tree shown in Figure S1. Due to the

space constraint, in this tree, subcluster of all fish species except zebrafish was merged together for illustration purposes. Species abbreviations: Hs, *Homo sapiens*; Gg, *Gallus gallus*; Ac, *Anolis carolinensis*; Xt*, Xenopus tropicalis;* Dr*, Danio rerio;* Lc*, Latimeria chalumnae;* Le*, Leucoraja erinacea;* Ci, *Ciona intestinalis*.

Table 3.1. Number of transporters present within Oatp subfamilies in chordates.

	Oatp1					Oatp2		Oatp3	Oatp4		Oatp5	Oatp6
Species	1a	1b	1c	1d	1f	2a	2b	3a	4a	4c	5a	6a-d
H. sapiens	1	2	1	-	-	1	1	1	1	1	1	1
M. musculus	4	1	1	-	-	1	1	1	1	1	1	3
G. gallus	1	1	1	-	-	1	1	1	1	-	1	-
A. carolinensis	1	1	1	-	-	1	1	1	1	-	1	-
X. tropicalis	1	1	1	-	-	1	1	1	1	1	1	-
D. rerio	-	-	1	2	4	1	1	2	1	-	2	-
G. morhua	-	-	1	2	-	1	1	2	1	-	2	-
T. rubripes	-	-	2	2	-	1	1	2	1	-	1	-
T. nigroviridis	-	-	2	2	-	1	1	2	-	-	2	-
G. aculeatus	-	-	1	1	-	1	1	3	1	-	2	-
O. latipes	-	-	2	1	-	1	1	2	1	-	1	-
L. chalumnae	1	-	1	-	-	2	1	3	1	1	1	-
C. intestinalis			2*			-	-	-	3	1**	1	1**

* Two Oatps belong to Oatp1 subfamily, but none of the known groups (Oatp1a-f).

** One Oatp is ancestral to Oatp4 and Oatp6 subfamilies, i.e. does not belong to neither of them.

3.1.2. SLC22 family

We have identified fourteen *Slc22* genes in zebrafish. Within the subgroup of Organic Anion Transporters (OATs), 7 genes were found: (1) 5 co-orthologs of mammalian OAT2/Oat2 (Organic anion transporter 2) annotated as Oat2a-e; and (2) co-orthologs of mammalian OAT1/Oat1 (Organic anion transporter 1) and OAT3/Oat3 (Organic anion transporter 3), provisionally annotated as zebrafish Oat1 and Oat3. Phylogenetic analysis showed that OAT2 is conserved within the vertebrate lineage with orthologs present in chicken (*Gallus gallus*), anole lizard (*Anolis carolinensis*) and teleost fish including pufferfishes, zebrafish and stickleback (*Gastrosteus aculeatus*). Tetrapods have only one OAT2 ortholog, whereas multiple orthologs are present in all analyzed teleost species: 5 in zebrafish, 4 in *Tetraodon nigroviridis*, 3 in *Takifugu rubripes* and 2 in stickleback (Table 3.2) which indicates that radiation of this subfamily occurred in teleosts after the separation from the vertebrate tree axis. In teleost species, orthologs that clearly cluster with OAT2/Oat2 in tetrapods were annotated as Oat2a, while other co-orthologs were named Oat2b-2e (Fig. 3.2). Amino acid sequence identity among OAT2/Oat2 co-orthologs in vertebrates is 40-54%, while somewhat higher sequence identity is found amongst Oat2 proteins within the teleost group (43-62% amino acid identity).

Within the OAT1/OAT3 cluster, two genes are present in each tetrapod species, as well as in each teleost species analyzed. However, teleost subcluster is distinct from the tetrapod cluster, thus direct orthologs of human OAT1 and OAT3 in fish species cannot be distinguished among each other. That is the reason why all teleost transporters are provisionally annotated as Oat1 and/or Oat3 in the order of appearance within the phylogenetic tree (Fig. 3.2). The third cluster of OATs includes OAT4-7 and URAT1 genes. These genes are found only in mammals and do not have orthologs in other vertebrates. The exception is one gene found in anole lizard and annotated as Organic anion transporter like 1 (Oatl1) (Fig. 3.2, Table 3.2). Amino acid sequence identity among OAT1 and OAT3 co-orthologs in vertebrates is 46-56%, similar as when we compare each cluster separately: OAT1/Oat1 co-orthologs share 46-56 % amino acid sequence identity, while OAT3/Oat3 co-orthologs share 46-56 % amino acid sequence identity. However, Oat1 and Oat3 proteins from teleosts share higher sequence identity between each other (52-70%). OAT1/OAT3 cluster differs substantially from the OAT2 protein cluster (28-30%).

The SLC22 cluster that encompasses two genes in humans*: SLC22A13*, also known as Organic Cation Transporter-Like 3 (ORCTL3) or OAT10 and *SLC22A14*, known as Organic Cation Transporter-Like 4 (ORCTL4), together with the co-orthologs in other vertebrates forms a distinct cluster that is closer to the OATs, than to the group of Organic Cation transporters (OCTs) and Organic Carnitine Transporters (OCTNs) (Fig. 3.2). Thus, our results suggest that phylogenetically, this group of transporters is actually closer to the OATs than to the OCTs (Fig. 3.2). Within the ORCTL3/4 cluster, clear orthologs are present in human and mouse, whereas two co-orthologs are found in chicken, one in the anole lizard, none in frog *Xenopus laevis*, two in zebrafish, *T. nigroviridis* and medaka, and three in the other pufferfish *T. rubripes*. In summary, zebrafish Orctl3/4 group includes 2 transporters provisionally annotated as DrOcrtl3 and DrOrctl4. Despite the conservation of ORCTL3/4 cluster in vertebrates, protein sequences are more dissimilar within the cluster, in comparison to OAT1, 2 and 3 clusters: amino acid sequence identity among ORCTL3/4 co-orthologs in vertebrates is 33-53%, whereas within teleost Orctl3/4 cluster is 38-61 %. Two Orctl proteins from *C. intestinalis* share 19-23% amino acid identity with the ORCTL3/Orctl3 and ORCTL4/Orctl4 co-orthologs in vertebrates.

Organic cation and carnitine transporters (OCTs and OCTNs, respectively) include: (1) OCT1, 2 and 3 co-orthologs; (2) OCTN co-orthologs, and (3) OCT6 co-orthologs (Fig. 3.2, Table 3.2). Within the group of OCTs/Oct-s, OCT1/Oct1 and OCT2/Oct2 are conserved from fish to mammals with two genes present in each tetrapod species (with the exception of one ortholog in *X. laevis*). On the contrary, orthologs of human and mouse OCT3/Oct3 are present in higher vertebrates, but absent from amphibian *X. laevis* and all analyzed teleost species, including zebrafish (Table 3.2). Amino acid sequence identity among vertebrate OCT group is 42-53 %, whereas protein sequences share slightly higher identity among fish OCT proteins (43-72%).

OCTN/Octn group is well conserved from fish to mammals with two members in each tetrapod species: OCTN1/Octn1 and OCTN2/Octn2. Two co-orthologs of these human genes are found in all vertebrates, including zebrafish. The exception is the third member in *T. nigroviridis* (Fig. S2B). OCT6/Oct6 co-orthologs are found in all vertebrate species analyzed (Fig. 3.2; Table 3.2). All together, zebrafish OCT/OCTN group includes 5 transporters provisionally annotated as DrOct1, DrOct2, DrOctn1, DrOctn2 and DrOct6. Amino acid sequence identity within OCTN group is 44-52 %, whereas OCT6/Oct6 orthologs share 39-59 % identity among vertebrates, and 70-74 % among fish proteins. Two Oct6 proteins from *C. intestinalis* are 23-32 % identical to vertebrate OCT6/Oct6 proteins.

Accession codes and annotations of protein sequences for chordate SLC22/Slc22 family members are given in the Supplemental material (Table S2).

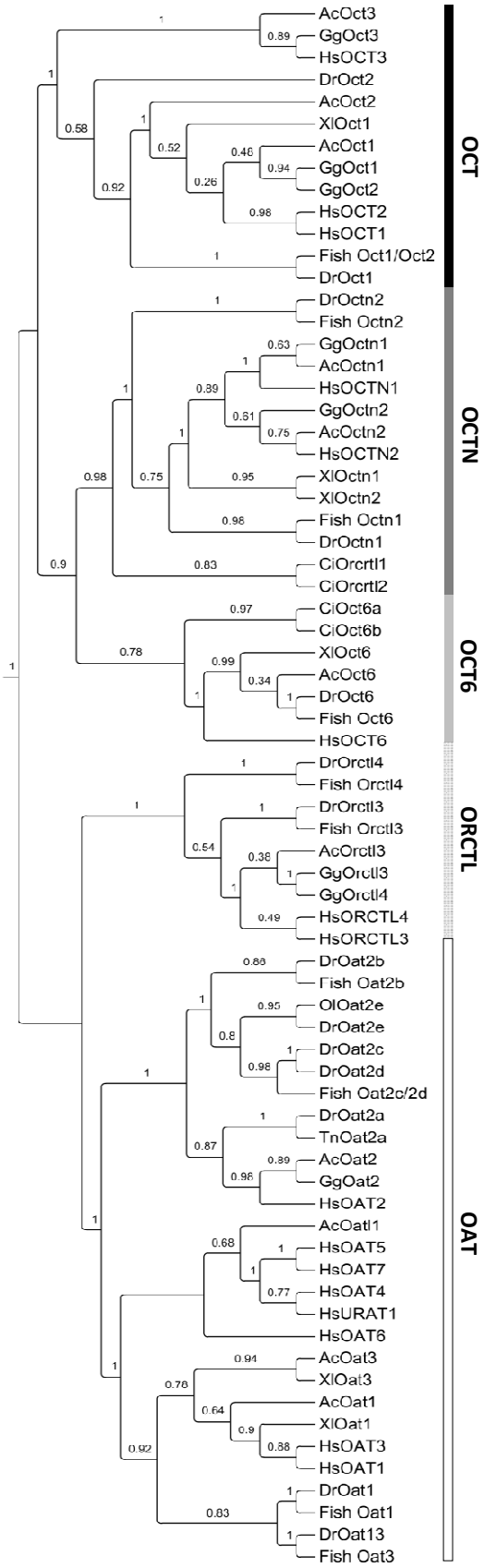

Figure 3.2. Phylogenetic analysis of the SLC22 family in vertebrates. The tree is a part of a larger phylogenetic tree shown in Figure S2. Due to the space constraint, in this tree, subcluster of all fish

species except zebrafish was merged together for illustration purposes. Species abbreviations: Hs, *Homo sapiens*; Gg, *Gallus gallus*; Ac, *Anolis carolinensis*; Xl*, Xenopus laevis;* Dr*, Danio rerio*.

Table 3.2. Number of transporters present within SLC22 family in chordates.

	Oat								Oct			Octn			Oct6	Orctl	
Species	1	2	3	4	5	6	7	Urat	1	2	3	1	2	3		3	4
H. sapiens	1	1	1	1	1	1	1	1	1	1	1	1	1	-	1	1	1
M. musculus	1	1	1	-	-	1	-	1	1	1	1	1	1	1	1	1	1
G. gallus	-	1	-	-	-	-	-	-	1	1	1	1	1	-	-	1	1
A. carolinensis	1	1	1	-	-	-	-	-	1	1	1	1	1	-	1	1	-
X. laevis	1	-	1	-	-	-	-	-	1	-	-	1	1	-	1	-	-
D. rerio	1	5	1	-	-	-	-	-	1	1	-	1	1	-	1	1	1
G. morhua	1	2	1	-	-	-	-	-	1	1	-	1	1	-	1	-	-
T. rubripes	1	2	1	-	-	-	-	-	1	-	-	1	1	-	1	1	-
T. nigroviridis	1	4	-	-	-	-	-	-	1	1	-	2	-	-	1	3	1
G. aculeatus	1	2	1	-	-	-	-	-	1	1	-	1	1	-	1	-	-
O. latipes	1	1	1	-	-	-	-	-	-	-	-	1	1	-	1	1	1
C. intestinalis	-	-	-	-	-	-	-	-	-	-	-		1		2	-	-

3.2. Conserved motifs and membrane topology

3.2.1. OATP family

Zebrafish Oatp tranporters are 548-725 amino acid long, similar to the human OATPs (643-722). Only transporters from the OATP5/Oatp5 subfamily are slightly longer: human OATP5A1 is 848 amino acids long, similar to zebrafish Oatp5a2 (859 amino acids). Predicted topologies of all zebrafish Oatps include 12 TMDs. Some uncertainties were present in the topology prediction of zebrafish Oatp1c1 and Oatp2a1, so membrane topologies of mentioned transporters were adjusted according to the multiple sequence alignment with the homology model of OATP1B3 (Meier Abt *et al*., 2005). Three conserved motifs were identified in the zebrafish Oatp members: the OATP family signature, the large extracellular LP9 and the Kazal SLC21 domain. We confirmed that family signature (D-X-RW-(I,V)-GAWW-XG-(F,L)-L) is highly conserved within vertebrate OATPs/Oatps. Analysis of TMDs and LPs confirmed that all zebrafish Oatps have a large extracellular LP9 between TMD9 and TMD10 that contains 10 conserved cysteines present in all analyzed vertebrate OATPs/Oatps. Within the LP9, the Kazal SLC21 domain is found, a domain similar to the Kazal-type serine protease inhibitor domain. This motif is 49 amino acids long ($CX_3CXCX_6PVC\ X_6YXSXCXAGC\ X_{11}Y\ X_2CXCV$) and encompasses first eight conserved cysteines within the LP9 (Fig. 3.3). Overall, membrane topology comparison of all

analyzed vertebrate OATP/Oatps revealed that lengths and arrangements of TMDs and LPs are very similar within the vertebrate lineage.

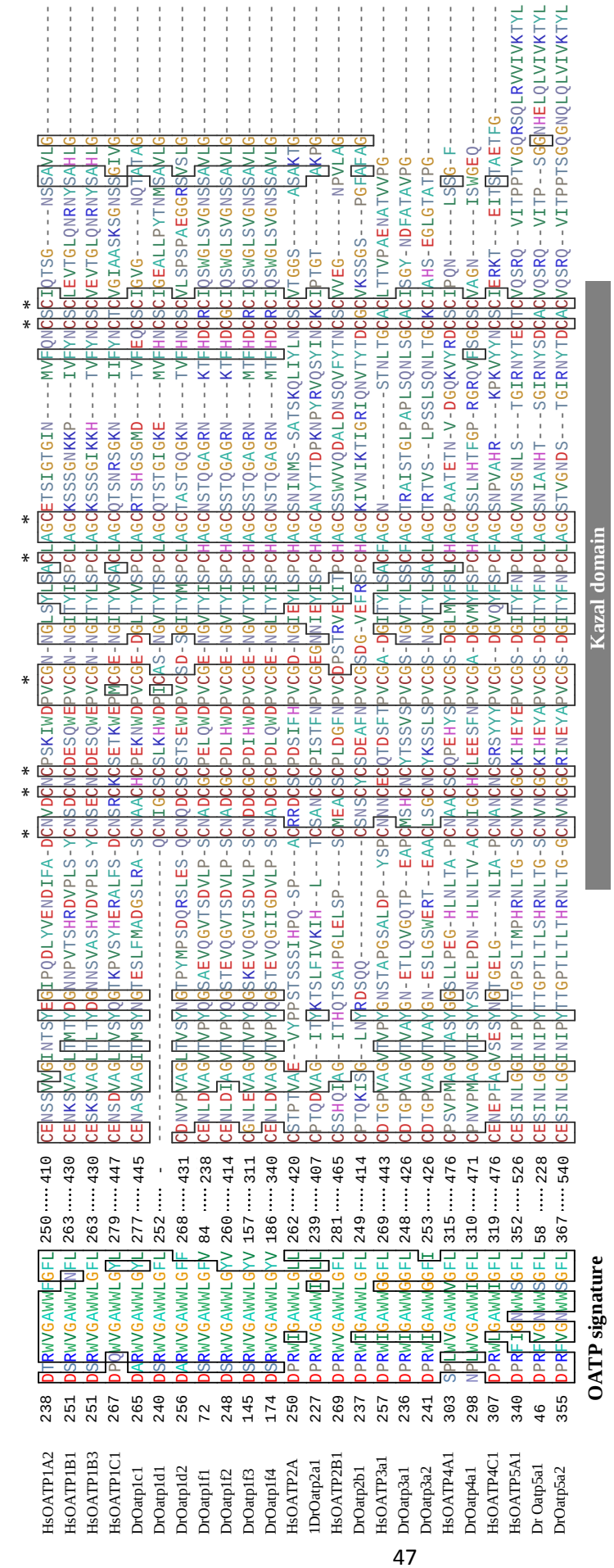

Figure 3.3. Extract from the multiple alignment of zebrafish and human OATP/Oatp family showing family signature, extracellular loop 9 (LP9) with 10 conserved cysteine residues denoted with asterisk (*) and the Kazal SLC21 domain.

3.2.2. SLC22 family

Zebrafish SLC22 transporter family comprises proteins of 542-567 amino acids in length, similar to the length of human SLC22 transporters (541-594 amino acids). The exception is human and mouse specific OAT6/Oat6 that is slightly shorter (483 amino acids). All zebrafish Slc22 transporters have 13 amino acids long, major facilitator family signature (MFS), G(RKPATY)L(GAS)(DN)(RK)(FY)GR(RK)(RKP)(LIVGST)(LIM) between the TMD2 and TMD3 (Fig. 3.4), similar to human SLC22 transporters. Another conserved domain is found within zebrafish Slc22 family: the so-called amphiphilic solute facilitator (ASF) domain located before TMD2. This motif is also present in all three groups of human SLC22 family (OCTs, OCTNs and OATs) (Fig. 3.4). The predicted topologies, along with the alignment with homology models of human OAT1 and human OCT1, show 12TMDs, with intracellular orientation of C and N termini, a large extracellular LP1 between TMD 1 and TMD2, and a large intracellular LP6 between TMDs 6 and 7.

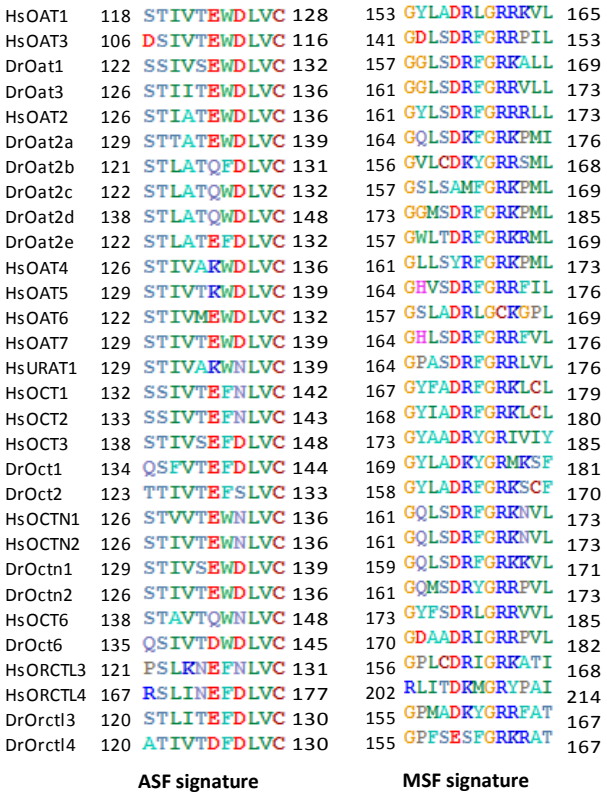

Figure 3.4. Extract from the multiple alignment of zebrafish and human SLC22/Slc22 proteins showing the multifacilitator superfamily (MSF) signature and the amphiphilic solute facilitator (ASF) domain.

3.3. Tissue expression analysis

In zebrafish liver we observed dominant expression of Oatp1d1, Oct1 and Oatp2b1 followed by Oct2 in both sexes and Oatp2a1 in males (Fig. 3.5A). Oatp1d1 shows very high expression in males and high expression in females, while Oct1 shows very high expression in males and moderate expression in females. The expression of Oatp2b1 and Oct2 in both sexes, as well as Oatp2a1 in the liver of males is moderate. All other *SLC21* and *SLC22* genes show low expression in zebrafish liver. The description of low, moderate, high and very high level of expression is given in the methods section. Most pronounced gender differences are observed in Oatp1d1, Oct1 and Oatp2a1 expression pattern which show 10-, 9- and 5-fold higher expression in males, respectively.

In kidney, more complex expression pattern is found in comparison to liver. In females, dominant genes are Oct1, Oat3 and Oatp1f2 with the very high expression, followed by (1) high expression of Oatp2b1, Oat2c, Oat2e, Octn2 and Ortcl3; (2) moderate expression of Oatp5a1, Oct2, Oct6, Oatp2a1, Oatp3a1, and finally Oatp1d1 and Oat2d (Fig. 3.5B). In males, the expression pattern differs to some extent. The dominant genes are Oct1 and Oatp1f2 that show very high expression, similar to the expression in the kidney of females. However, these expressions are followed by high expression of Oat2e, as opposed to very high expression of Oat3 in females. The high expression of Oat2e is followed by high expression of Oatp2b1, Oat2c, Oct2, Octn2, Orctl4 and finally Oat3. Moderately expressed genes in male kidney are Oatp1d1, Oatp3a1, Oatp5a1, Oat2d and Oatp2a1 (Fig. 3.5B), similar to expression pattern in female kidney. Most pronounced gender differences in Slc22 expression are observed for Oct6, Oat3 and Oatp2a1 which are 22-, 8- and 6-fold more expressed in females, respectively; and for Oatp1d1 which is on the contrary 5 times higher expressed in males (Fig. 3.5B).

In the intestine, the levels of expression of *SLC21* and *SLC22* genes are not as high as in liver and kidney (Fig. 3.5C). Dominant genes found in intestine are Oatp2b1 and Oat2d present at high expression levels in both sexes. These are followed by moderate expression of Oatp1d1, Oatp3a1, Oat3, Oct2, Octn2 and Orctl4 in both genders. In addition, in females, moderately expressed are Oct6 and Orctl4 that show low expression in male intestine (6- and 7-fold lower than in females, respectively) (Fig. 3.5C). Apart from the mentioned Oct6 and Orctl4, most pronounced gender expression difference is observed for Octn2 that is 3 times higher expressed in males.

In zebrafish gills, *Slc21* and *Slc22* genes are generally lower expressed in comparison to other tissues with pronounced dominance of Slc21 family (Fig. 3.5D). Dominant gene is Oatp2b1 found at very high expression level, followed by moderate expression of Oatp1d1 and Oatp3a1, Oatp3a, Oatp2a1 and Oct2 in both genders. Additionally, in males, Oatp1f2, Oct1 and Oct6 show moderate expression, as opposed to low expression in females (Fig. 3.5D).

In the brain, similar to gills, there is a pronounced dominance of *Slc21* over *Slc22* genes (Fig. 3.5E). In females and males, Oatp3a2 shows very high expression and high expression, respectively, followed by high expression of Oatp2b1 and Oatp1d1 in both genders, high expression of Oatp3a1 and Oatp5a1 in females, and moderate expression of Oatp3a1 and 5a1 in males. In brain, high number of *Slc21* and *Slc22* genes are expressed at moderate levels, including Oatp1d2, Oatp2a1, Oat1 and 3, Oat2a-b, Oat2e, Oct 1 and 2. In addition, Oat2d and Octn2 are found at moderate expression levels in males, and Oat2c in females, as opposed to low expression in the other gender (Fig. 3.5E). Very high expression difference among genders is observed for Oat1 which is 30 times higher expressed in males, and for Oat2d which shows 25 times higher expression in females. Less pronounced, but still substantial gender differences are observed for Oatp3a2 and 5a1 which show 4 and 5 times higher expression in females, respectively, and for Oct1 that is 5-fold higher expressed in males (Fig. 3.5E).

In the gonads, expression pattern of *SLC21* and *SLC22* genes is very different among genders (Fig. 3.5F). In ovaries, majority of genes show negligible or low expression. Only 6 genes are expressed, overall at moderate expression levels including Oatp2b1 and Oatp5a1, followed by Oatp3a1, Oat2c, Oat2e and Oct6 (Fig. 5.3F). On the contrary, in testes, majority of *SLC21* and *SLC22* genes show moderate to high expression (Fig. 5.3F). Actually, only Octn1, Orctl3 and 4 are weakly expressed. Oat2a shows the highest expression, followed by high expression of Oatp1d1, Oatp2b1, Oatp3a2, Oat1, Oat2b-e, Oct1 and 2 and Octn2. Genes expressed at moderate levels include Oatp1d2, Oatp1f2 and Oat3, followed by Oatp2a1, oatp3a1, Oatp5a1 and Oct6 (Fig. 5.3F).

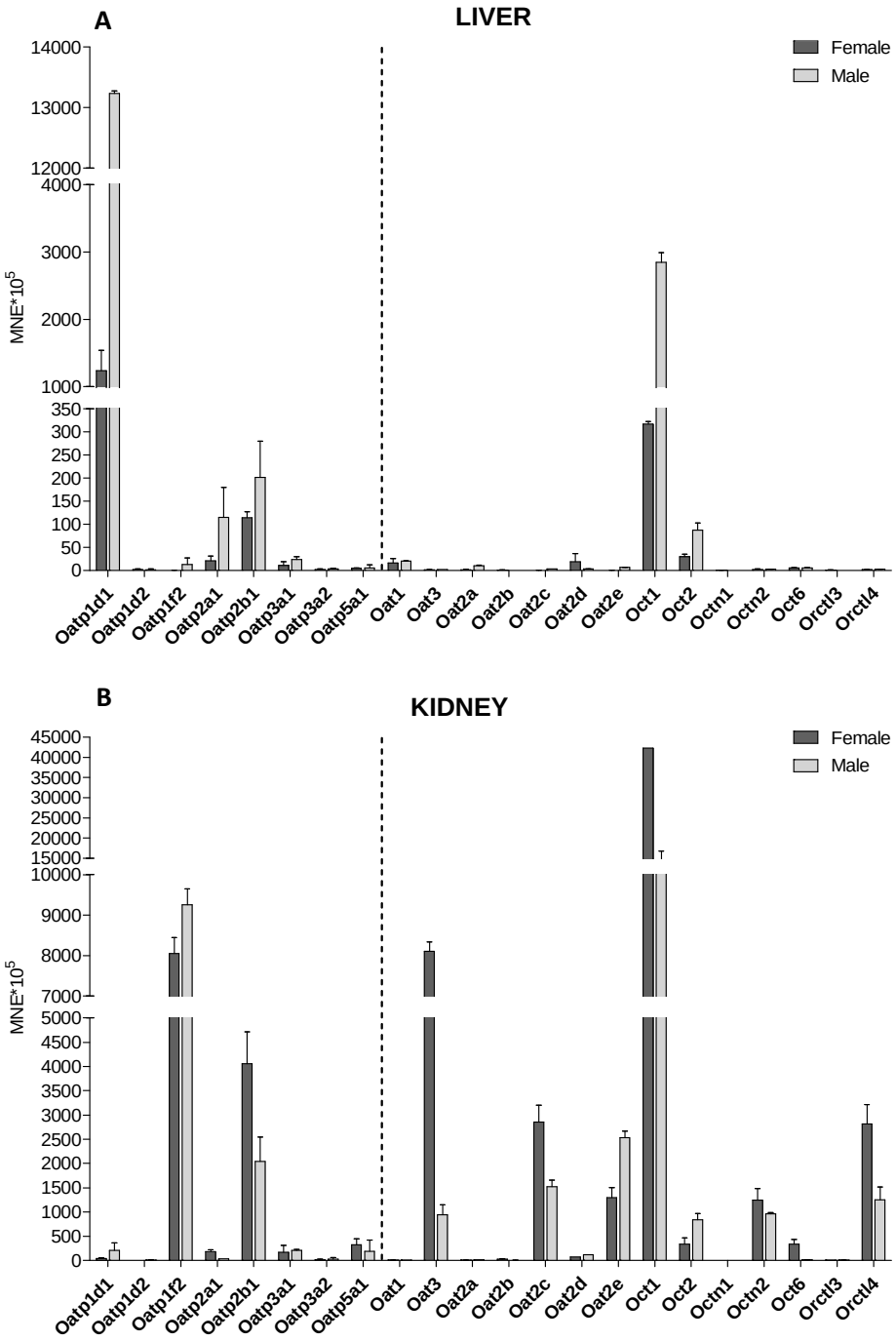
A
LIVER
Female
Male
MNE*10^5
14000
13000
12000
4000
3000
2000
1000
350
300
250
200
150
100
50
0
Oatp1d1
Oatp1d2
Oatp1f2
Oatp2a1
Oatp2b1
Oatp3a1
Oatp3a2
Oatp5a1
Oat1
Oat3
Oat2a
Oat2b
Oat2c
Oat2d
Oat2e
Oct1
Oct2
Octn1
Octn2
Oct6
Orctl3
Orctl4
B
KIDNEY
Female
Male
MNE*10^5
45000
40000
35000
30000
25000
20000
15000
10000
9000
8000
7000
5000
4500
4000
3500
3000
2500
2000
1500
1000
500
0
Oatp1d1
Oatp1d2
Oatp1f2
Oatp2a1
Oatp2b1
Oatp3a1
Oatp3a2
Oatp5a1
Oat1
Oat3
Oat2a
Oat2b
Oat2c
Oat2d
Oat2e
Oct1
Oct2
Octn1
Octn2
Oct6
Orctl3
Orctl4

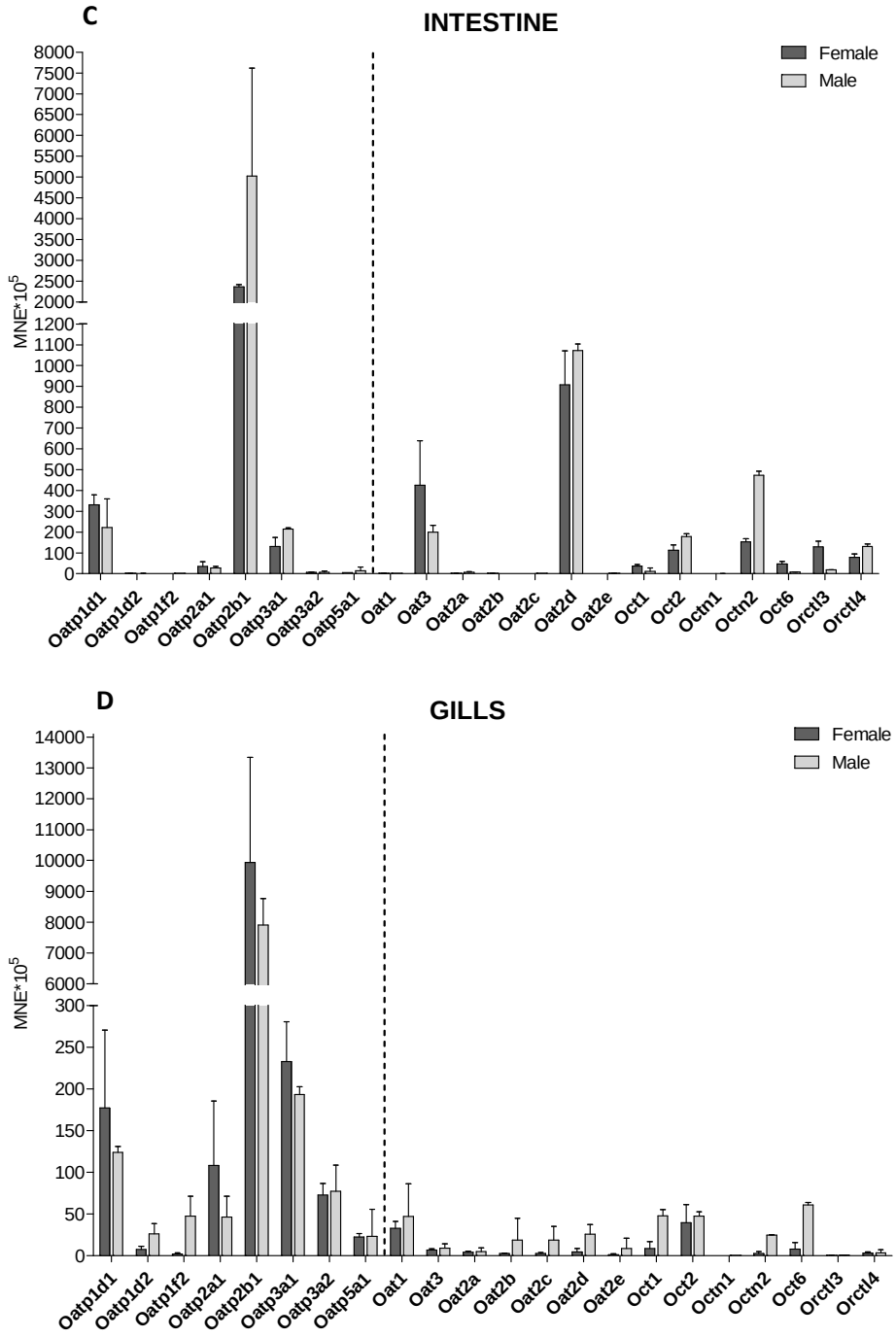
C
INTESTINE
Female
Male
MNE*10^5
8000
7500
7000
6500
6000
5500
5000
4500
4000
3500
3000
2500
2000
1200
1100
1000
900
800
700
600
500
400
300
200
100
0
Oatp1d1
Oatp1d2
Oatp1f2
Oatp2a1
Oatp2b1
Oatp3a1
Oatp3a2
Oatp5a1
Oat1
Oat3
Oat2a
Oat2b
Oat2c
Oat2d
Oat2e
Oct1
Oct2
Octn1
Octn2
Oct6
Orctl3
Orctl4
D
GILLS
Female
Male
MNE*10^5
14000
13000
12000
11000
10000
9000
8000
7000
6000
300
250
200
150
100
50
0
Oatp1d1
Oatp1d2
Oatp1f2
Oatp2a1
Oatp2b1
Oatp3a1
Oatp3a2
Oatp5a1
Oat1
Oat3
Oat2a
Oat2b
Oat2c
Oat2d
Oat2e
Oct1
Oct2
Octn1
Octn2
Oct6
Orctl3
Orctl4

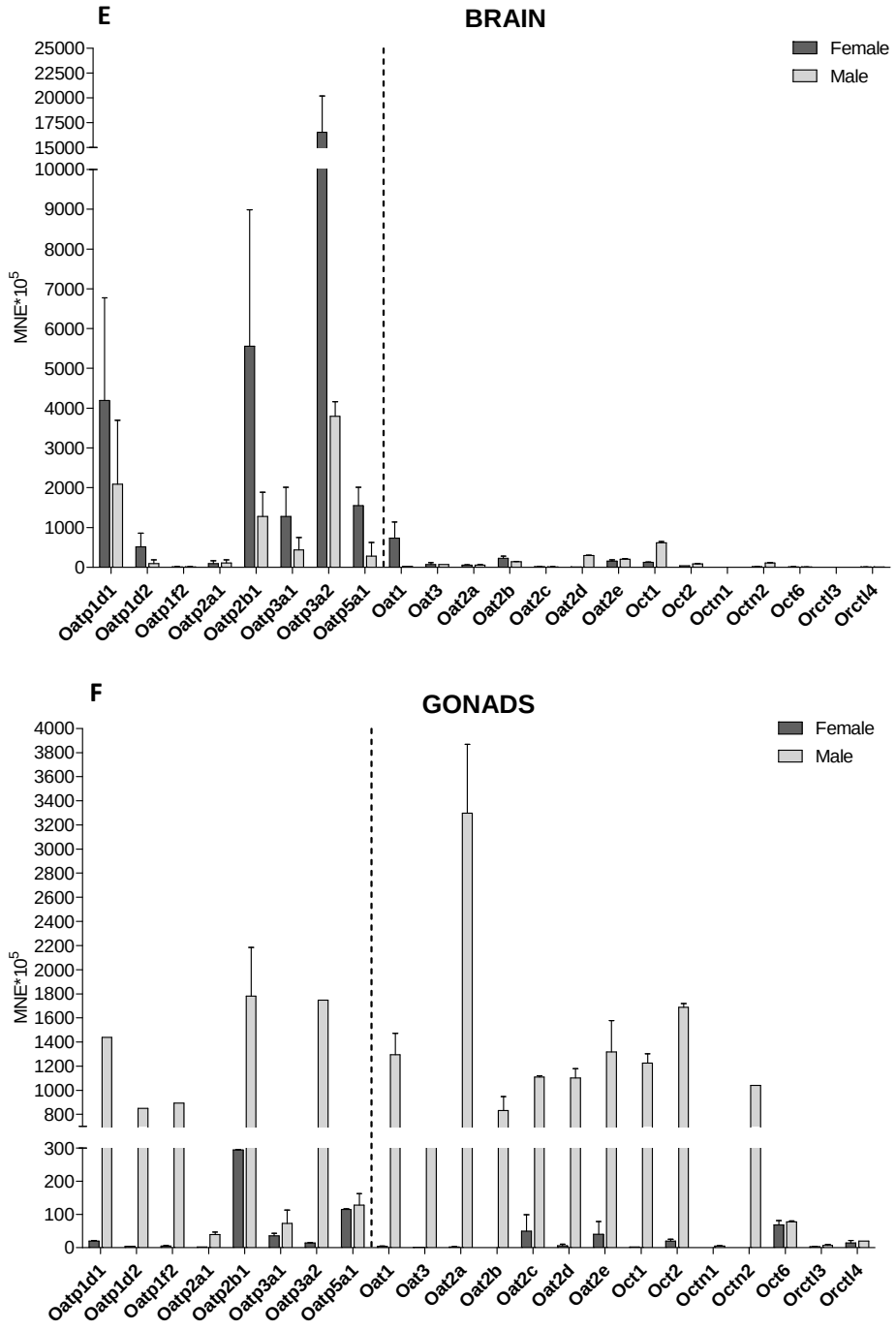

Figure 3.5. Tissue expression pattern of *SLC21* and *SLC22* genes in male and female zebrafish in the following tissues: **A)** liver, **B)** kidney, **C)** intestine, **D)** gills, **E)** brain, and **F)** gonads. Data represent MNE (mean normalized expression) ± SD normalized to the Ef1α.

3.4. Molecular characterization of Oatp1d1

3.4.1. Tissue expression pattern and sex differences in Oatp1d1 expression

Oatp1d1 shows ubiquitous tissue expression pattern with the highest expression in liver, brain and testes, followed by intestine, kidney, gills and skeletal muscle (Fig. 3.6). Sex differences in Oatp1d1 expression pattern are most pronounced in testes where Oatp1d1 expression is 50 times higher than in ovaries. Differential mRNA expression is also present in zebrafish liver where Oatp1d1 is 10 times higher expressed in males, followed by smaller difference of 2.5-fold higher expression in the male kidney. In brain, gills and intestine Oatp1d1 is similarly expressed in both genders.

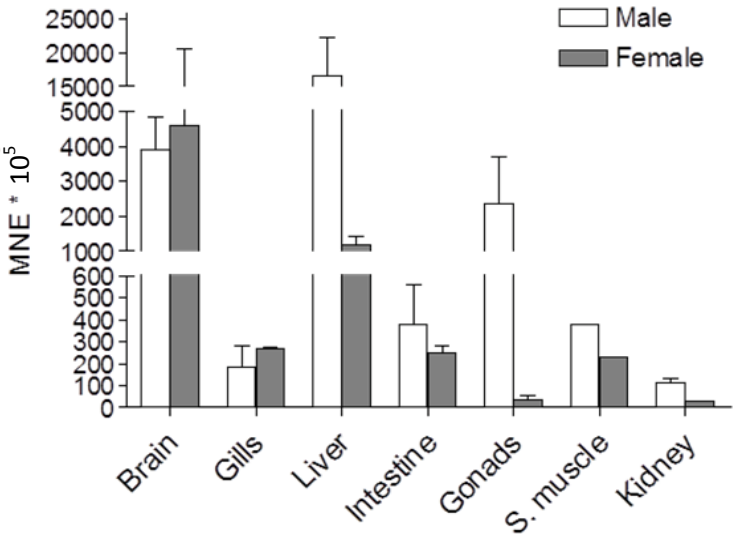

Figure 3.6. Tissue expression pattern of *Slco1d1* in male and female zebrafish. (S. muscle denotes skeletal muscle). Data represent MNE (mean normalized expression) ± SE normalized to the Ef1α.

3.4.2. Functional characterization of Oatp1d1

The transport of two substrates, E3S and the anionic dye Lucifer yellow (LY) follows the classical Michaelis-Menten kinetics with saturable uptake of E3S after 2 min (Fig. 3.7A) and LY after 10 min (Fig. 3.5C), respectively. Oatp1d1 shows high affinity for E3S with K_m 1.75 ± 0.12 µM (Fig. 3.5B) and moderate affinity for LY with K_m 41.7 ± 10.1 µM (Fig. 3.5D). V_{max} for E3S is 6.02 ± 0.17 nmol E3S/mg protein/min, while V_{max} for LY is 57.5 ± 6.49 nmol LY/mg protein/min. The Hill number is close to one; 1.2 for E3S and 0.78 - 1.2 for LY (4 independent experiments), which indicates a low degree of cooperativity and possibly one binding site for E3S and LY. K_i values for a set of model OATP1 substrates are similar when obtained either with the E3S or the LY inhibition assay (correlation

analysis: R^2 = 0.9218, p = 7.44 x 10^{-7}, n = 10) which indicates that LY and E3S share the same binding site.

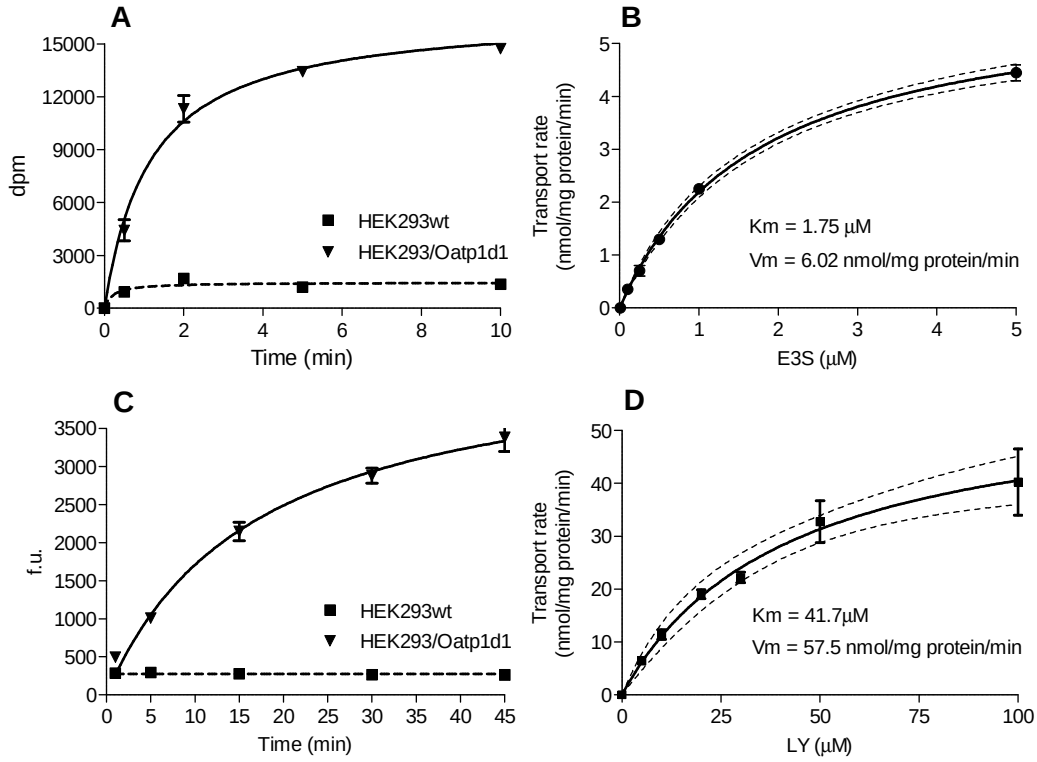

Figure 3.7. Michaelis-Menten kinetics of zebrafish Oatp1d1 mediated uptake of [^{3}H]E3S and fluorescent dye LY. **A,** time - response of Oatp1d1 [^{3}H]E3S mediated uptake expressed as change in disintegration parts per minute (dpm) over the incubation time. **B,** dose - response of Oatp1d1 [^{3}H]E3S uptake expressed as transport rate of [^{3}H]E3S (nmol/mg protein/min) over [^{3}H]E3S concentration (μM) after 5 min incubation with [^{3}H]E3S (50 Ci/mmol). **C,** time - response of LY expressed as increase in fluorescence (fluorescence units - f.u.) over time (min), and **D,** concentration dependence of LY uptake expressed as transport rate (nmol/mg protein/min) over LY concentration (μM) after 15 min incubation with LY.

In order to elucidate the physiological role of Oatp1d1 we tested a series of known OATP1/Oatp1 substrates including steroids, corticosteroids, thyroid hormones, prostaglandin E2 (PGE2), bile salts and bilirubin. In addition to endogenous compounds, we analyzed several pharmaceuticals that are known to interact with mammalian OATP1/Oatp1 members in order to gain further insight into the specificity of Oatp1d1 substrate binding site. A summary of the described inhibition assays is presented in Fig. 3.8. For the most active compounds (inhibition of LY uptake > 50%) K_i values were determined and shown in Table 3.3. Dose responses of representative model substrates and

inhibitors are given in Figs. 3.9A and 3.9B. In order to determine the type of interaction with Oatp1d1, we compared kinetic parameters of LY uptake (eight different LY concentrations) in the absence and in the presence of different interacting compounds, where their concentrations were equal to their previously calculated K_i values. The summary of these findings is presented in Table 3.4, and representative dose response curves of a typical competitive inhibitor (E3S) and non-competitive inhibitor (testosterone) are shown in Fig. 3.10. This type of analysis has been previously successfully used to determine the type of interaction for a wide range of physiological substrates and fibrates for OATP1B1 (Gui *et al*., 2009; Yamazaki *et al*., 2005), and the interaction of OATP1B1, OATP1B3 and OATP1C1 with non-steroidal anti-inflammatory drugs (NSAIDs) (Kindla *et al*., 2011, Westholm *et al*., 2009). If an interacting compound is a competitive inhibitor of LY, we can assume that it is being transported by Oatp1d1, in which case the K_i value of the interacting compound actually represents its K_m value.

The first major group of Oatp1d1 interacting compounds includes steroid and thyroid hormones. High affinity substrates of Oatp1d1 are sulphated and glucuronidated steroid conjugates, E3S (K_m = 1.75 μM), DHEAS (K_i = 0.68 μM) and estradiol-17β-glucuronide (K_i = 3.26 μM) (Tables 3.3 and 3.4). Non-conjugated steroids, estradiol (E2) (K_i = 2.83 μM), progesterone (K_i = 9.1 μM) and dihydrotestosterone (K_i = 23.35 μM) are potent uncompetitive inhibitors of LY uptake, while testosterone (K_i = 29.98 μM) and androstenedione (K_i = 3.78 μM) show moderate to strong inhibition of the noncompetitive type (Table 3.4). Interestingly, progestagen and pregnenolone show no interaction with Oatp1d1. In comparison to progestagens and androgens, corticosteroids cortisol and corticosterone show weaker interactions with Oatp1d1, with K_i values of 120 μM and 105 μM, respectively (Table 3.3). Cortisol is a substrate, whereas corticosterone is an uncompetitive inhibitor of Oatp1d1 (Table 3.4). We also wanted to determine if thyroid hormones thyroxine (T4) and triiodothyronine (T3), as prototypical OATP1C/Oatp1c substrates (Deure *et al*., 2010), interact with Oatp1d1. We found that Oatp1d1 does not interact with T4, and T3 is moderately strong uncompetitive inhibitor (K_i = 42.7 μM) of Oatp1d1 (Table 3.4). Eicosanoid PGE2, a specific OATP1B1 substrate (Gui *et al*., 2009), weakly interacts with Oatp1d1 (K_i = 227.4 μM).

The second major group of Oatp1d1 interacting compounds is bile salts. Oatp1d1 shows interaction with all four major bile salts: cholate, taurocholate (TC), deoxycholate and taurochenodeoxycholate (TCDC), with increasing potency (K_i = 141, 36.9, 9.94 and 3.39 μM, respectively). All four tested bile salts are inhibitors of LY transport: TC shows noncompetitive inhibition, whereas the other three are uncompetitive inhibitors (Table 3.4). Besides steroids, thyroids and bile salts, known physiological substrates of OATP1/Oatp1 subfamily in mammals are bilirubin and its conjugates. However, bilirubin is not transported by Oatp1d1, but rather behaves as

a potent uncompetitive inhibitor (K_i = 14.5 µM) (Table 3.4). Bilirubin conjugates were not tested due to their commercial unavailability.

After testing a wide series of physiological OATP1/Oatp1 subfamily interactors, we selected a set of known xenobiotic interactors in order to compare interaction strength and substrate specificities among zebrafish and human OATP1/Oatp1 members. Data on modulation of Oatp1d1 activity with model xenobiotics are shown in Table 3.1. Most potent interacting compounds include warfarin, cyclosporine A (CycA), BSP, gemfibrozil (Gfb), pravastatin and rifampicin. Moderately strong interactors are probenecid, bezafibrate and fenofibrate, while methotrexate, clofibrate, benzylpenicillin and erythromycin show weak interaction.

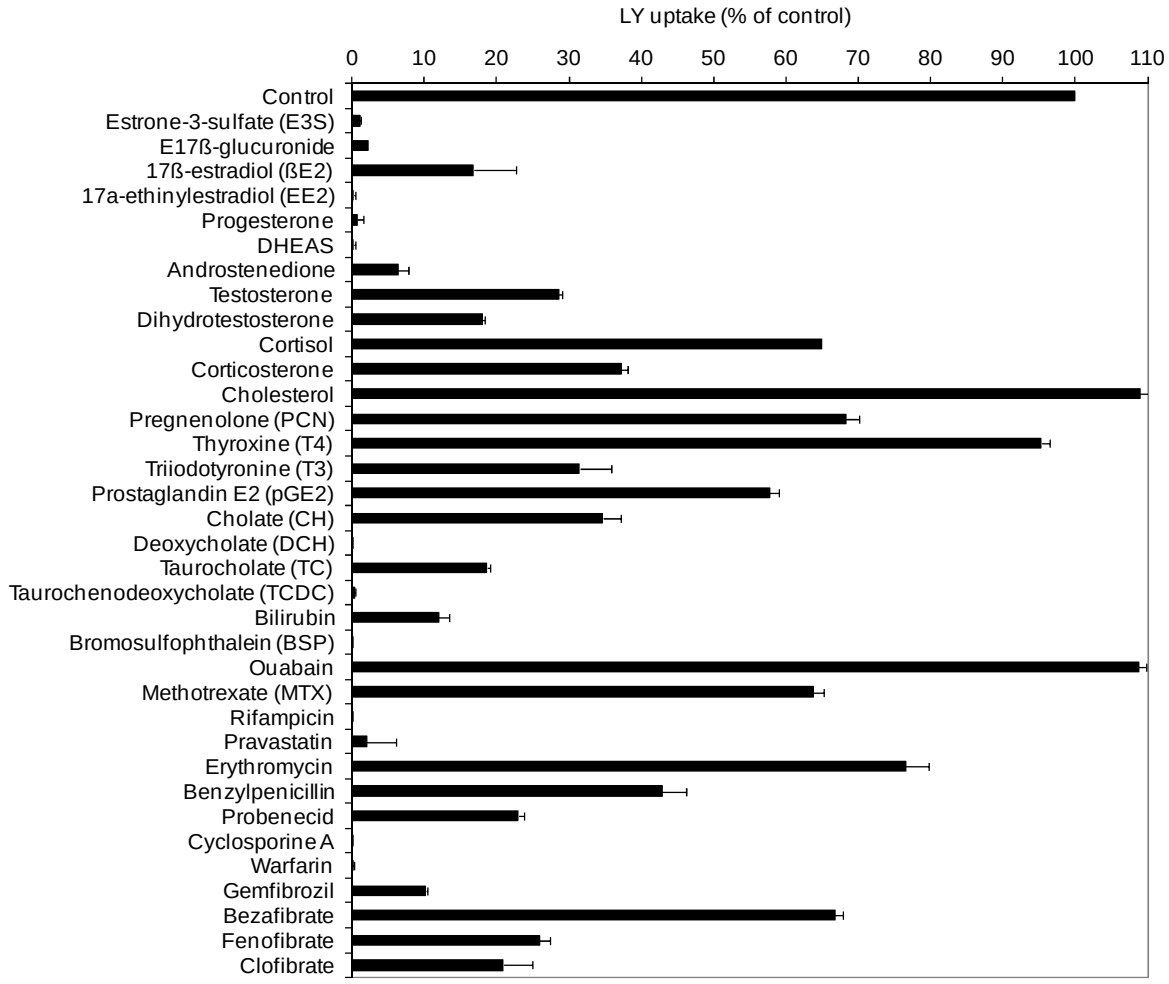

Figure 3.8. Interaction of zebrafish Oatp1d1 with known substrates and inhibitors of mammalian OATP1/Oatp1 subfamily members. Data are expressed as a percentage (%) of LY uptake after co-incubation with each interactor (100 µM) relative to LY uptake in the absence of interactor which is set to 100%.

Table 3.3. Interaction of Oatp1d1 with typical endo- and xenobiotic substrates and inhibitors of OATP1/Oatp1 subfamily. Physiological interactors are separated from xenobiotic interactors with solid line. Mean, SD and confidence intervals (c.i.) are calculated from triplicate determinations (ne - no effect; nd - not determined).

Compound	LY uptake (%) mean	SD	K_i (µM)	c.i.
Control	100	0.10	-	-
Estrone-3-sulfate (E3S)	1.04	0.20	1.01	0.75 - 1.37
E17ß-glucuronide	2.25	0.10	3.26	2.83 - 3.75
17ß-estradiol (ßE2)	16.8	5.79	2.83	2.27 - 3.51
17a-ethinylestradiol (EE2)	0.20	0.14	5.93	4.41 - 7.97
Progesterone	0.67	0.88	9.06	8.06 - 10.2
DHEAS[1]	0.21	0.15	0.68	0.46 - 0.99
Androstenedione	6.33	1.40	3.78	2.85 - 5.02
Testosterone	28.6	0.51	30.0	25.5 - 35.2
Dihydrotestosterone	18.0	0.23	23.4	18.6 - 29.3
Cortisol	65.0	0.04	120	73.8 - 194
Corticosterone	37.2	0.92	105	38.0 - 288
Cholesterol	109	2.48	ne	ne
Pregnenolone (PCN)	68.2	1.89	nd	nd
Thyroxine (T4)	95.2	1.19	ne	ne
Triiodotyronine (T3)	31.4	4.41	42.7	18.9 - 95.9
Prostaglandin E2 (pGE2)	57.7	1.30	227	98.7 - 524
Cholate (CH)	34.7	2.39	141	33.8 - 591
Deoxycholate (DCH)	0.18	0.07	9.94	6.53 - 15.1
Taurocholate (TC)	18.6	0.37	36.9	30.2 - 45.1
Taurochenodeoxycholate (TCDC)	0.28	0.09	3.40	2.66 - 4.33
Bilirubin	12.0	1.41	14.5	12.8 - 16.5
Bromosulfophthalein (BSP)	0.11	0.01	2.99	2.19 - 4.06
Ouabain	109	1.16	ne	ne
Methotrexate (MTX)	63.8	1.36	222	62.4 - 792
Rifampicin	0.19	0.04	12.7	9.86 - 16.2
Pravastatin	1.98	4.15	9.27	6.75 - 12.7
Erythromycin	76.5	3.06	882	640 - 1,216
Benzylpenicillin	42.8	3.41	372	271 - 510
Probenecid	23.0	0.67	26.0	14.5 - 46.6
Cyclosporine A	0.17	0.06	1.34	1.19 - 1.50
Warfarin	0.11	0.13	0.36	0.31 - 0.42
Gemfibrozil	10.2	0.20	7.44	4.37 - 12.7
Bezafibrate	66.7	1.16	40.4	22.9 - 71.4
Fenofibrate	25.9	1.48	54.4	37.8 - 78.3
Clofibrate	20.9	3.94	345	252 - 470

[1]Dehydroepiandrosterone sulfate

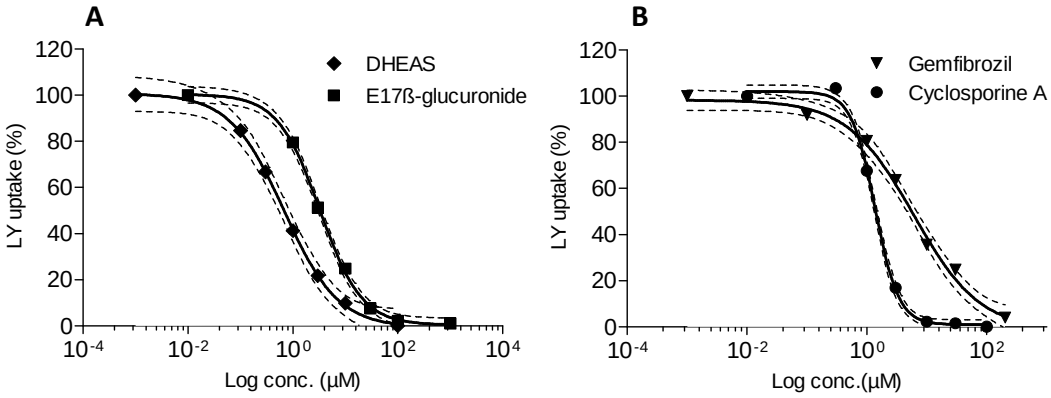

Figure 3.9. Concentration dependent inhibition of Oatp1d1 mediated LY uptake by typical interactors of OATP1/Oatp1 subfamily. Representative compounds are shown: DHEAS and estradiol-17ß-glucuronide as typical substrates (**A**); and gemfibrozil (Gfb) and cyclosporine A (CycA) as model inhibitors (**B**).

Table 3.4. Determination of substrates and inhibitors of zebrafish Oatp1d1. Kinetic parameters of LY uptake are given as apparent K_m ($K_{m\ app}$) (µM), apparent V_m ($V_{m\ app}$) (nmol LY/mg protein/min), and 95% confidence intervals (c.i.) for each. Data are mean ± SD from triplicate determinations.

Interactor	Km_{app} (LY)	c.i.	Vm_{app} (LY)	c.i.	Interaction type
Ctrl	59.3	31.4 - 87.2	50.7	43.2 - 58.1	
Estrone-3-sulfate	147	128 - 167	54.9	50.9 - 58.9	S
Estradiol-17ß-glucuronide	93.6	73.9 - 113	56.3	50.1 - 62.5	S
Estradiol	61.7	44.9 - 78.5	31.6	27.9 - 35.2	I
Testosterone	54.6	37.7 - 71.5	15.6	13.1 - 18.1	I
Dihydrotestosterone	42.4	21.8 - 63.1	24.0	18.8 - 29.1	I
DHEAS[1]	129	81.9 - 175	59.4	48.6 - 70.1	S
Androstenedione	60.1	35.9 - 84.2	40.6	36.1 - 45.2	I
Progesterone	56.2	32.8 - 79.6	20.3	16.3 - 24.3	I
Cortisol	84.3	32.7 - 136	76.6	53.4 - 99.8	S
Corticosterone	32.0	23.8 - 40.3	41.3	36.4 - 46.1	I
Triiodothyronine	22.6	12.8 - 32.4	16.8	14.3 - 19.2	I
Cholate	39.7	18.9 - 60.5	25.1	19.7 - 30.4	I
Deoxycholate	29.2	2.74 - 55.7	16.3	9.91 - 22.6	I
Taurocholate	64.1	3.06 - 125	16.9	11.5 - 22.2	I
Taurochenodeoxycholate	39.8	26.5 - 53.2	18.0	15.7 - 20.2	I
Bilirubin	36.1	19.1 - 53.1	20.6	16.8 - 24.4	I

[1]Dehydroepiandrosterone sulfate

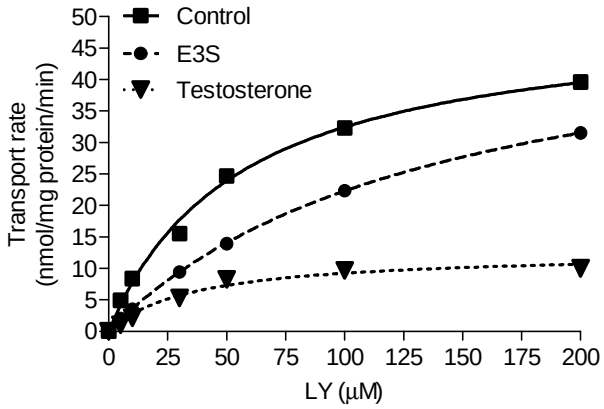

Figure 3.10. Example of dose response curves used to determine type of interaction with Oatp1d1. Kinetic analysis of LY mediated transport by HEK293/Oatp1d1 overexpressing cells in the absence of an interactor (Control) and in the presence of a competitive inhibitor (i.e. substrate) E3S at 0.8 µM concentration and in the presence of un-competitive inhibitor, testosterone at 30 µM concentration.

3.4.3. Dependence on pH gradient

Oatp1d1 mediated LY uptake is dependent on the pH gradient. The inwardly directed $[H]^+$ gradient created by lowering extracellular pH (pH_o = 5.5) caused activation of Oatp1d1 transport. This effect was apparent with both substrates; E3S uptake at pH_o 5.5 increased by 108 ± 20% and LY uptake at pH_o 5.5 increased by 158 ± 4% in comparison to pH_o 7.4 (Fig. 3.11A). To test if this effect was due to the activation of inwardly directed proton gradient, we performed the same experiment in the presence of ionophore monensin which acts as Na^+/H^+ antiporter and stops the gradient. Indeed, addition of 2 µM monensin at pH_o 5.5 resulted in the same Oatp1d1 activity as was observed at neutral extracellular pH which suggested that effect was gradient specific (Fig. 3.11A). Kinetic analysis of Oatp1d1 LY transport at pH_o 5.5 showed a significant increase in the transport rate: V_m increased from 91.2 nmol/mg protein/min (c.i. 81.4 -101) at neutral pH_o to 110 nmol/mg protein/min, c.i. 103 – 117 at pH_o 5.5 (Fig. 3.12A). On the contrary, substrate affinity remained unchanged: K_m 27.0 ± 4.4 µM (c.i. 17.5 – 36.5) at neutral pH_o and 25.8 ± 2.7 µM (c.i. 19.9 – 31.7) at pH_o 5.5 (Fig. 3.12A).

Next, we created outwardly directed proton gradient to determine its effect on Oatp1d1 activity. In order to achieve outward $[H]^+$ flux, we applied two different approaches: (i) alkalization of extracellular medium (pH_o 8), and (ii) acidification of intracellular space (pH_i). Significant reduction of Oatp1d1 activity was observed in comparison to neutral conditions in both cases: at pH_o 8 LY uptake was reduced by 58.8% in comparison to neutral pH_o, and at $pH_i < pH_o$ the uptake was decreased by 83% when compared to $pH_i \approx pH_o$ (Fig. 3.11B and 3.12A). The specificity of the gradient dependence

was further tested by monitoring the pH_i recovery to neutral pH (2 h incubation in complete growth medium at 37°C), when the protein activity was restored to the control levels (data not shown). Furthermore, we determined uptake kinetic parameters at pH_o 8 and found that transport rate and transport affinity were significantly reduced (Fig. 3.12A). K_m shifts from 27.0 ± 4.4 µM in neutral pH_o in comparison to 134 ± 13.1 µM in pH_o 8, whereas V_m is significantly reduced at pH_o 8 (83.1 nmol/mg protein/min; c.i. 76.5 – 90.0) in relation to neutral pH_o (91.2 nmol/mg protein/min; c.i. 81.4 -101) (Fig. 3.12A).

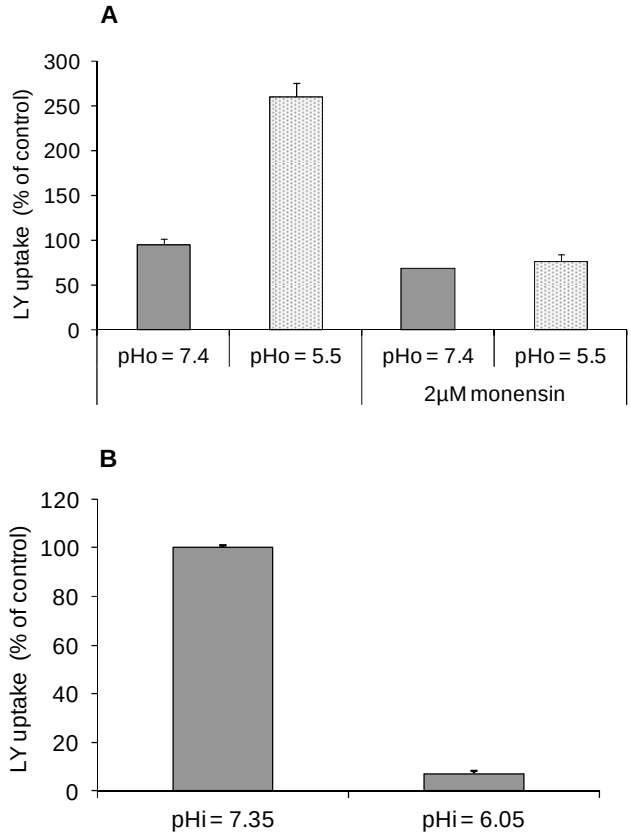

Figure 3.11. pH dependency of Oatp1d1. (**A**) extracellular acidification (pH_o) activates Oatp1d1-mediated LY uptake by 2.5-fold. When inwardly directed $[H]^+$ gradient is stopped with 2 µM monensin, LY uptake returns to control levels at neutral pH_o. (**B**) intracellular acidification after incubation in 30 mM NH_4Cl (30 minutes at 37°C), which creates outwardly directed $[H]^+$ gradient abolishes Oatp1d1 LY uptake after pH_i is reduced by 1.25 pH units (acidification from pH 7.35 to 6.05). Each data point represents the mean ± SD of three independent experiments.

The fact that Oatp1d1 transport rate is activated at acidic extracellular pH, and decreased at both, alkaline extracellular pH and acidified pH_i, indicates that Oatp1d1 transport is dependent upon proton gradient. It has been suggested that transport activation at extracellular pH is due to the

protonation of an active site, more specifically a conserved outward facing histidine residue (H) at the extracellular side of the TMD3 (Leuthold *et al*., 2009). Although protonation of the substrate binding site would cause changes in apparent K_m at pH_o < 7.4, which we did not observe, we proceeded to the site directed mutagenesis of conserved histidine (H102), to test our hypothesis that activation of Oatp1d1 transport at pH_o < 7.4 is due to the inwardly directed proton gradient and not to the H102 protonation as previously observed for certain mammalian OATP/Oatps (Leuthold *et al*., 2009). The transport rate of Oatp1d1 - H102Q mediated LY uptake increased from 119 nmol/mg protein/min (c.i. 97.7 - 134) at neutral pH_o to the 157 nmol/mg protein/min (c.i. 146 – 168) at acidic pH_o (Fig. 3.12B). Considering that Oatp1d1 - H102Q mutant showed the same increase in transport rate at pH_o 5.5 as was observed for Oatp1d1 - wt (Fig 3.12A), we conclude that the effect of pH-dependent transport activation was not due to the protonation of H102. Following similar reasoning, the observed strong reduction in Oatp1d1 transport at pH_i < 6.9 could be a consequence of outwardly directed proton flux, which affects the $[HCO_3]^-$ gradient. Alternatively, it could be a consequence of protonation of histidine residues at the intracellular side at pH < 6.9. Therefore we have searched for conserved histidines on the intracellular side of the protein, and found that H79 in the intracellular LP1 is conserved in all OATP1/Oatp1 members from fish to mammals. The constructed H79Q mutant had very low activity at neutral pH_i when LY uptake was reduced by 80% in comparison to Oatp1d1 - wt (Fig. 3.13A). The reduction of LY transport rate in the case of H79Q mutant was neither a consequence of the reduced protein expression, as seen from the western blot analysis, nor a consequence of impaired membrane localization, as shown by immunocytochemistry (Fig. 3.13A). This suggests that H79 is crucial for the Oatp1d1 transport activity. Although the importance of H79 for Oatp1d1 transport activity was an unexpected discovery, we wanted to further investigate whether protonation of inwardly facing H79 may be in part responsible for the effect of reduced transport activity at pH_i < 6.9. LY uptake in Oatp1d1 - H79Q mutant was reduced by 45% at pH_i < 6.9 in comparison to the transport activity of Oatp1d1 - H79Q at neutral pH_i. In contrast, Oatp1d1 - wt activity was more profoundly reduced at acidified pH_i in comparison to Oatp1d1 - wt at neutral pH_i (65% reduction) (Fig. 3.13B). Therefore, we conclude that protonation of H79 negatively influences Oatp1d1 transport activity and that this effect is partly responsible for the transport decrease at pH_i < 7, whereas the majority of reduction effect is due to the outwardly directed proton gradient created at pH_i < pH_o.

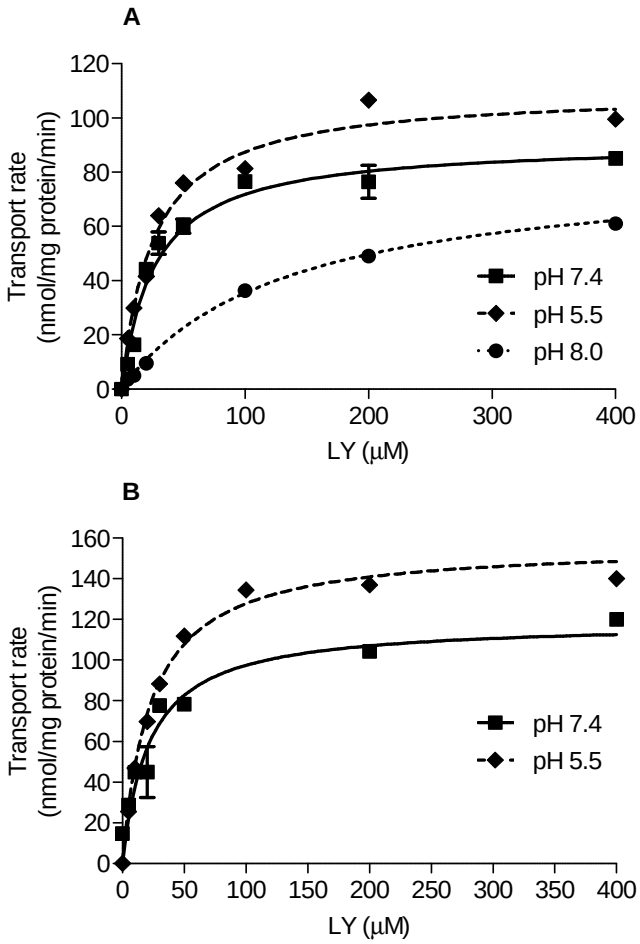

Figure 3.12. Effects of extracellular pH on Oatp1d1 - wt and Oatp1d1 - H102Q mediated LY uptake kinetics. (**A**) Oatp1d1 - wt (**B**) Oatp1d1 - H102Q.

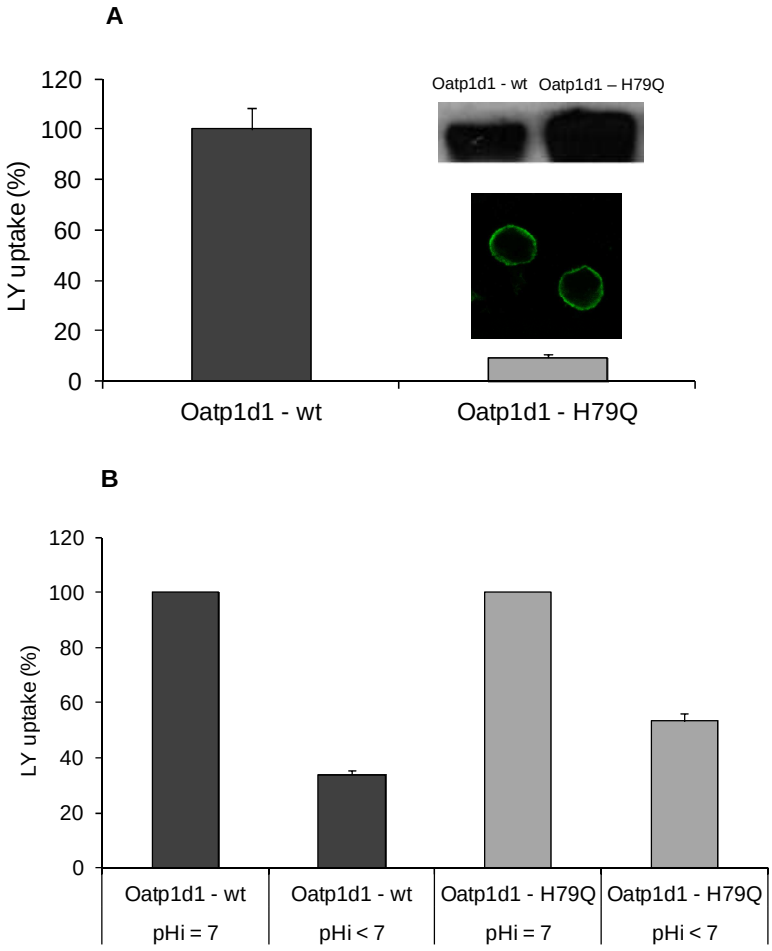

Figure 3.13. Histidine at position 79 is crucial for the Oatp1d1 transport activity and its protonation is partly responsible for the reduction of Oatp1d1 transport activity at alkaline extracellular pH. (**A**) activity of Oatp1d1 - H79Q mutant shown as a percentage of LY uptake relative to the Oatp1d1 - wt. Insets show localization of H79Q mutant in the plasma membrane and high protein levels on western blots. (**B**) change in activity of Oatp1d1 - wt and Oatp1d1 - H79Q at neutral and acidified pH_i. Results represent percentage of LY uptake relative to Oatp1d1 - wt at neutral pH_i and relative to Oatp1d1 - H79Q at neutral pH_i, respectively. Data represents mean and SDs from triplicate determinations.

3.4.4. Oligomerization of Oatp1d1

Oatp1d1 is present in three forms, as a monomeric protein of ~ 80 kDa, dimeric form of ~ 150 kDa, and as four or higher order oligomer that appears at ~ 250 kDa in western blots from the total cell lysate fraction (Fig. 3.14A). However, when the cell membrane fraction (MF) was isolated through the cell surface biotinylation, followed by binding of MF to the streptavidin magnetic beads, western blots with anti-His primary antibody showed only the oligomeric form (Fig. 3.14A).

Oligomers were not formed through disulfide bonds, since there was no breakage of the oligomeric complex in the presence of dithiothreitol (DTT) as a reducing agent (Fig. 3.14B). However, monomers appear to be linked through disulfid bonds into dimers since in the absence of reducing agent (DTT) monomers are not present, whereas after addition of DTT the monomers appear (Fig. 3.14B). The observed oligomeric state was not an experimental artifact, as it was present in all of the tested conditions, with or without thermal pretreatment (70°C) which can induce protein aggregation. To conclude, Oatp1d1 monomers are organized into dimers through disulfide bonds, whereas dimers form oligomers independently of disulfide link. Results of the rescue experiment are consistent with the dimer formation *in situ* (Fig. 3.15). When Oatp1d1 was fused to mCitrine on N terminal part of the protein, Oatp1d1/mCitrine does not localize in the membrane (Fig. 3.15A), similar to the Oatp1d1/GFP (data not shown). The fluorescent tags probably interfere with the protein folding, and thus its trafficking, which results in protein remaining in the nuclei and the cytosolic compartment (Fig. 3.15A). However, when Oatp1d1 without the mCitrine tag and Oatp1d1 with mCitrine tag are contransfected in 3:1 ratio, we detected green fluorescence in the membrane. This is confirmed by the colocalization with the red signal from the plasma membrane immunostaining, as described in the methods (Fig. 3.15A). Furthermore, protein activity in the rescue experiment was the same as in the control (Oatp1d1 - wt transfected cells), whereas Oatp1d1/mCitrine was inactive as a consequence of its inability to localize into the cell membrane (Fig. 3.15B). These findings suggest that Oatp1d1 interacts with the Oatp1d1/mCitrine. As a result, the protein complex is active and localizes to the plasma membrane, at least in the dimeric form. Whether dimers or oligomers are present remains to be further investigated.

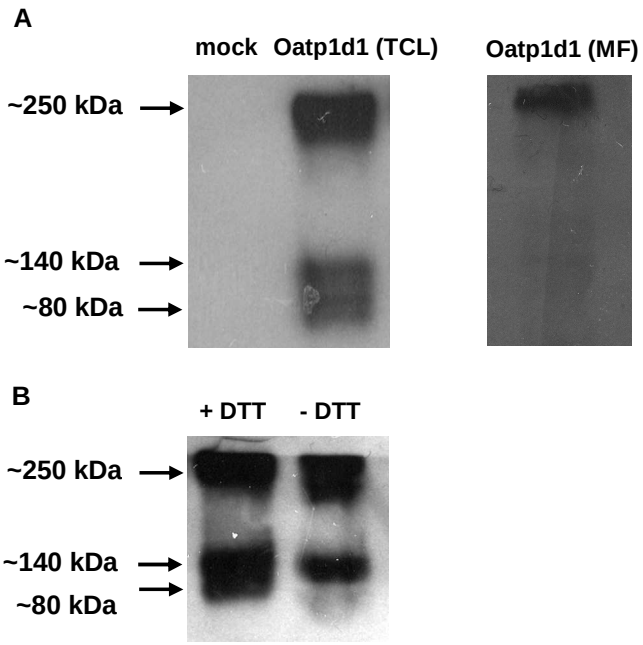

Figure 3.14. Oligomerization of Oatp1d1. (**A**) western blot analysis of total cell lysate (TCL) of HEK293/Oatp1d1 overexpressing cells shows three forms of Oatp1d1: monomeric form ~ 80 kDa, dimeric form ~ 150 kDa and oligomeric form at ~ 250 kDa. Western blot analysis of the membrane fraction (MF) of HEK293/Oatp1d1 overexpressing cells after the cell surface biotinylation with Sulfo-NHS-LC-LC-biotin and isolation of cell surface biotinylated proteins with hydrophilic streptavidin magnetic beads shows only oligomeric form. (**B**) western blot analysis of TCL with and without DTT shows that without DTT, oligomers and dimers are present, whereas after addition of DTT monomeric form appears indicating that monomers form dimers through disulfide bond.

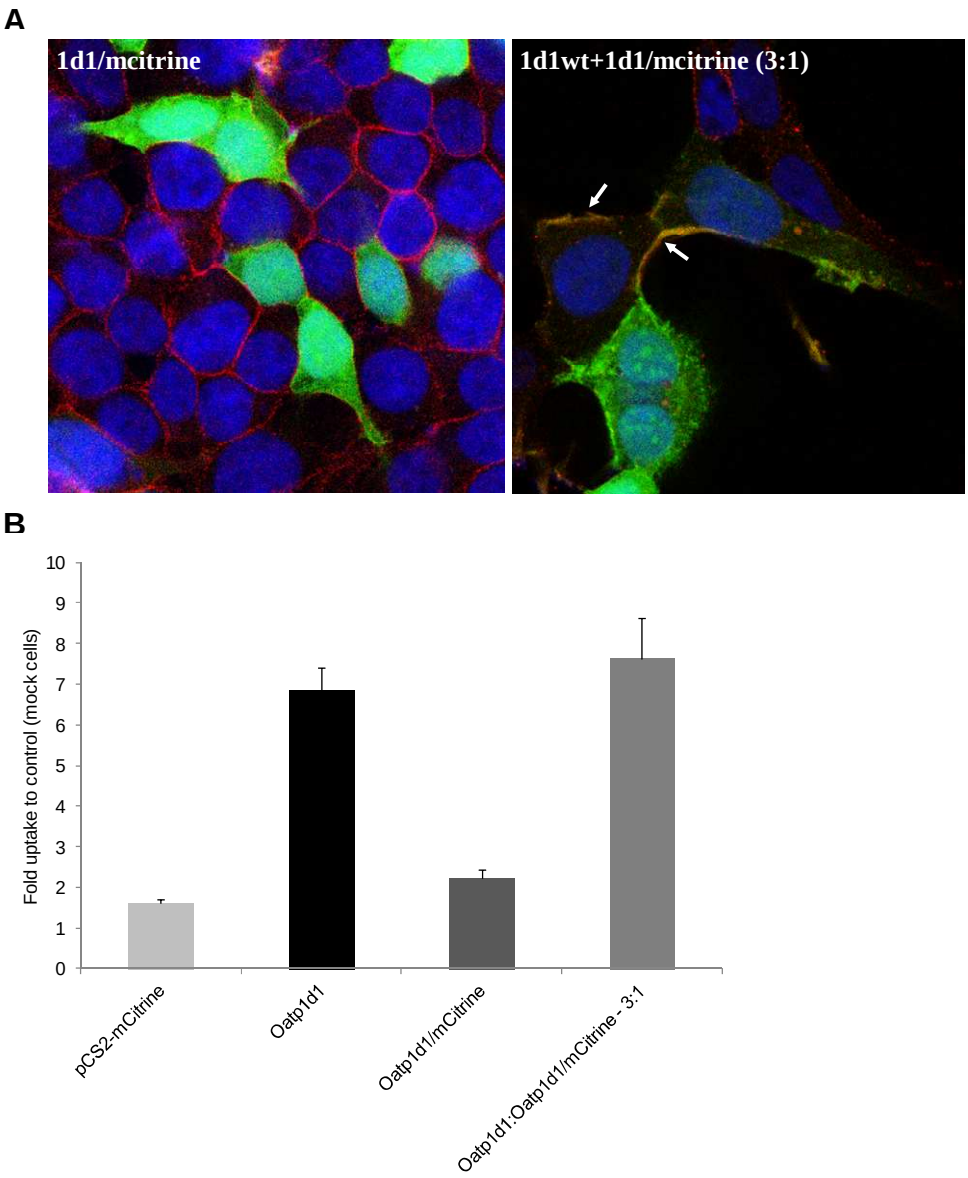

Figure 3.15. Interaction of Oatp1d1wt and Oatp1d1/mCitrine. (**A**) Cell localization of Oatp1d1 tagged on the N terminus with mCitrine (1d1/mCitrine) and cotransfection of Oatp1d1 without mCitrine and with mCitrine tag in the 3:1 ratio (1d1wt + 1d1/mCitrine). Plasma membranes are stained in red and nuclei are stained in blue. White arrows indicate cell membrane localization of Oatp1d1. If the protein is localized to the membrane, the color turns to orange because of the overlap of green signal from the mCitrine tag and red stained plasma membranes. (**B**) Uptake of LY into the Oatp1d1 - overexpressing cells in comparison to the HEK293 transiently transfected with either an empty vector pCS2-mCitrine or the Oatp1d1-mCitrine construct, and after the cotransfection of Oatp1d1 without mCitrine and with mCitrine tag in the 3:1 ratio (Oatp1d1:Oatp1d1-mCitrine = 3:1). Data are expressed as a fold of the LY uptake relative to the control (HEK293 cells transfected with pcDNA3.1 empty vector). Each value represents the mean ± SD from triplicate determinations.

The next step was to identify motifs that are responsible for the interaction among monomers. We identified three distinct Glycophorin A motifs (GXXXG): at the amino acid position 54 – 59 in the extracellular LP1, at the amino acid position 208 – 212 in the TMD5, and at the amino acid position 385 – 389 (390) in the TMD8 of Oatp1d1. Glycophorin A motif is responsible for the dimer and oligomer formation of another SLC protein, the serotonin transporter (SERT) (Horschitz *et al*., 2008). Considering high conservation of three GXXXG motifs within OATP1 subfamily in vertebrates (data not shown), site directed mutagenesis of glycine (G) to valine (V) residue was performed within the first motif, G54V (GXXXG), within the second motif, G208V and G212V (GXXXG), and within the third motif G385V, G389V and G390V (GXXXGG). We found that G208V and G212V, as well as G385V and G390V, are inactive and do not localize in the membrane (Fig. 3.16). On the contrary, G54V localizes in the membrane, but is inactive (Fig. 3.16). Western blots from total cell lysates showed that in comparison to the Oatp1d1 – wt, where monomers (~ 80 kDa), dimers (~ 140 kDa) and oligomers (> 200 kDa) are present, all GXXXG mutants (G208V, G212V, G385V, G389V and G390V) do not show > 200 kDa band, whereas G208V does not have dimeric band as well (Fig. 3.17).

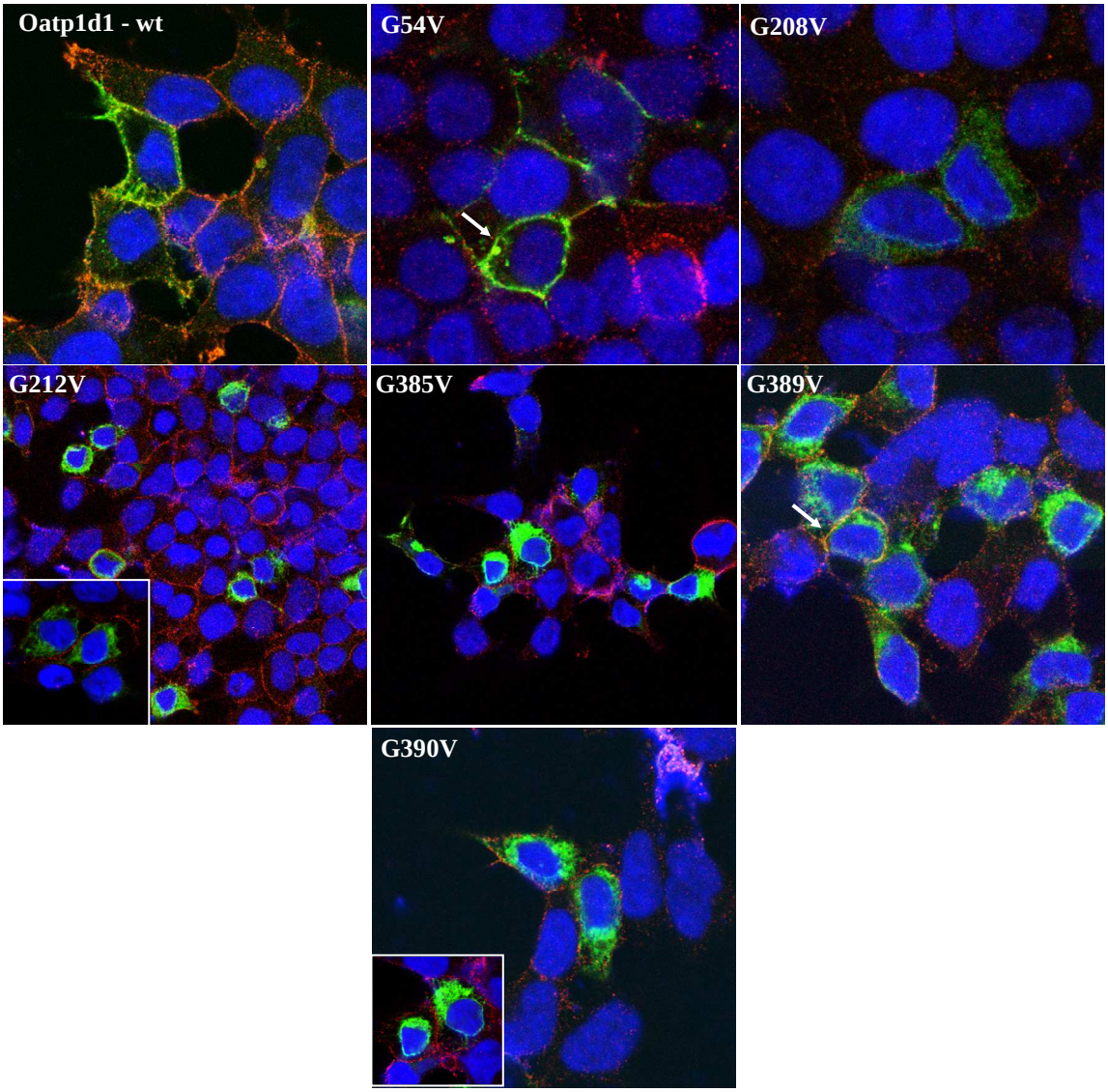

Figure 3.16. Cell localization of Oatp1d1 after mutations of conserved glycophorin motifs: G54V, G208V, G212V, G385V, G389C and G390V. Nuclei are dyed in blue with DAPI, and plasma membranes are stained in red after binding of primary antibody Na,K-ATPase and Cy3-conjugated IgG secondary antibody (all anti-mouse). White arrows indicate examples where protein is present in the cell membrane. The color turns to orange due to the overlap of green and red, or it remains light green when overexpression of protein is dominant over red stained membranes. Cytosolic forms are seen as green areas in the cytoplasm.

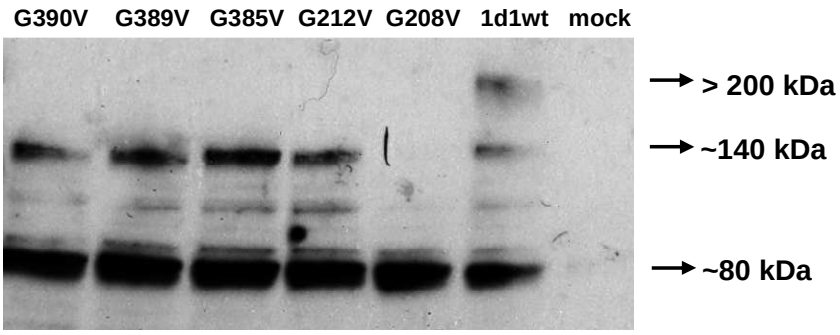

Figure 3.17. Protein expression of Oatp1d1 before and after the mutations of conserved glycophorin motifs: G208V, G212V, G385V, G389C and G390V. Western blot analysis of the total cell lysate (TCL) of HEK293/Oatp1d1 overexpressing cells shows three forms of Oatp1d1: monomeric form ~ 80 kDa, dimeric form ~ 140 kDa and oligomeric form at > 200 kDa. G208V is present as a monomer, whereas other mutants show monomeric and dimeric forms. Western blots were performed in the presence of reducing agent dithiothreitol (DTT) with anti-His antibody, and visualized with chemiluminescence.

3.4.5. N-glycosylation

In order to determine if N-glycosylation pattern is conserved within vertebrate subphylum, we treated HEK293cells overexpressing Oatp1d1 with tunicamycin and observed pronounced reduction in the protein transport activity. The uptake of both model substrates, E3S and LY, was reduced by 60% at 0.5-1 µg/ml of tunicamycin (Fig. 3.18). Furthermore, tunicamycin treatment (0.5 µg/ml, 24 h) partly impaired Oatp1d1 membrane localization which indicates the importance of N-glycosylation in membrane targeting of Oatp1d1. Subsequently, we aimed to identify the asparagine residues (N) involved in glycosylation through the analysis of conservation of asparagine residues within the OATP1 subfamily in vertebrates. We found that Oatp1d1 has five predicted N-glycosylation sites at the amino acid positions N122, N133, N499, N512 and N672. When we compared all OATP1 sequences from fish to mammals, we found that N122 is conserved in all transporters, N133, N499 and N512 are conserved in the majority of proteins, with the exception of few Oatp1c members, whereas N672 appears only sporadically throughout the OATP1 subfamily. Membrane topology prediction showed that all four conserved residues are located extracellularly, N122 and N133 in the loop 3 (LP3) (extracellular) and N499 and N512 in the LP9 (extracellular). After these four asparagines residues were changed to glutamine (Q), kinetic parameters of LY transport for each mutant were determined, as well as their cellular localizations with immunostaining. N122Q and N133Q mutants showed significantly reduced transport rates (by 2- and 1.7-fold, respectively) in comparison to the Oatp1d1 – wt, whereas their affinity remained unchanged (Table 3). Both mutants were present in the cytoplasm as well as in the plasma membrane (Fig. 3.19). N499Q showed reduced transport rate

(by 1.5-fold), whereas N512Q transport rate remained unchanged in comparison to the Oatp1d1 – wt (Table 3.5). N499Q localized mainly in the plasma membrane, whereas N512Q was found in the cytoplasm as well as in the plasma membrane (Fig. 3.19). Triple mutant (N122/133/499Q) showed reduced transport rate with unchanged affinity and was present in the cytoplasm as well as in the plasma membrane. However, when all four potential glycosylation sites were changed, membrane localization and transport activity were almost completely impaired (Fig. 3.19, Table 3.5).

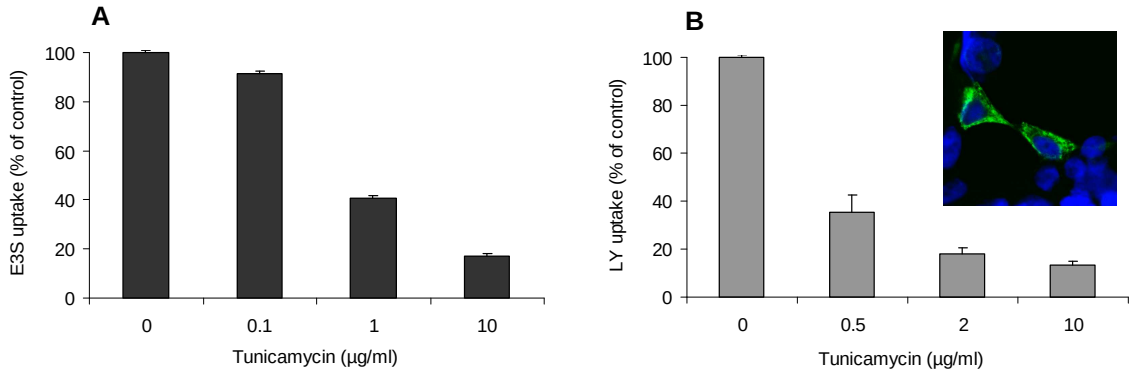

Figure 3.18. N-glycosylation is important for membrane localization of Oatp1d1. Tunicamycin, a general inhibitor of N-glycosylation, reduced (**A**) [^{3}H]E3S and (**B**) LY uptake in a dose - dependent manner and partly impaired membrane localization of Oatp1d1 (inset – nuclei are stained in blue, and protein in green). Uptake is expressed as a percentage relative to tunicamycin non-treated Oatp1d1 transiently transfected HEK293 cells. Results represent means and SE of 3 independent experiments.

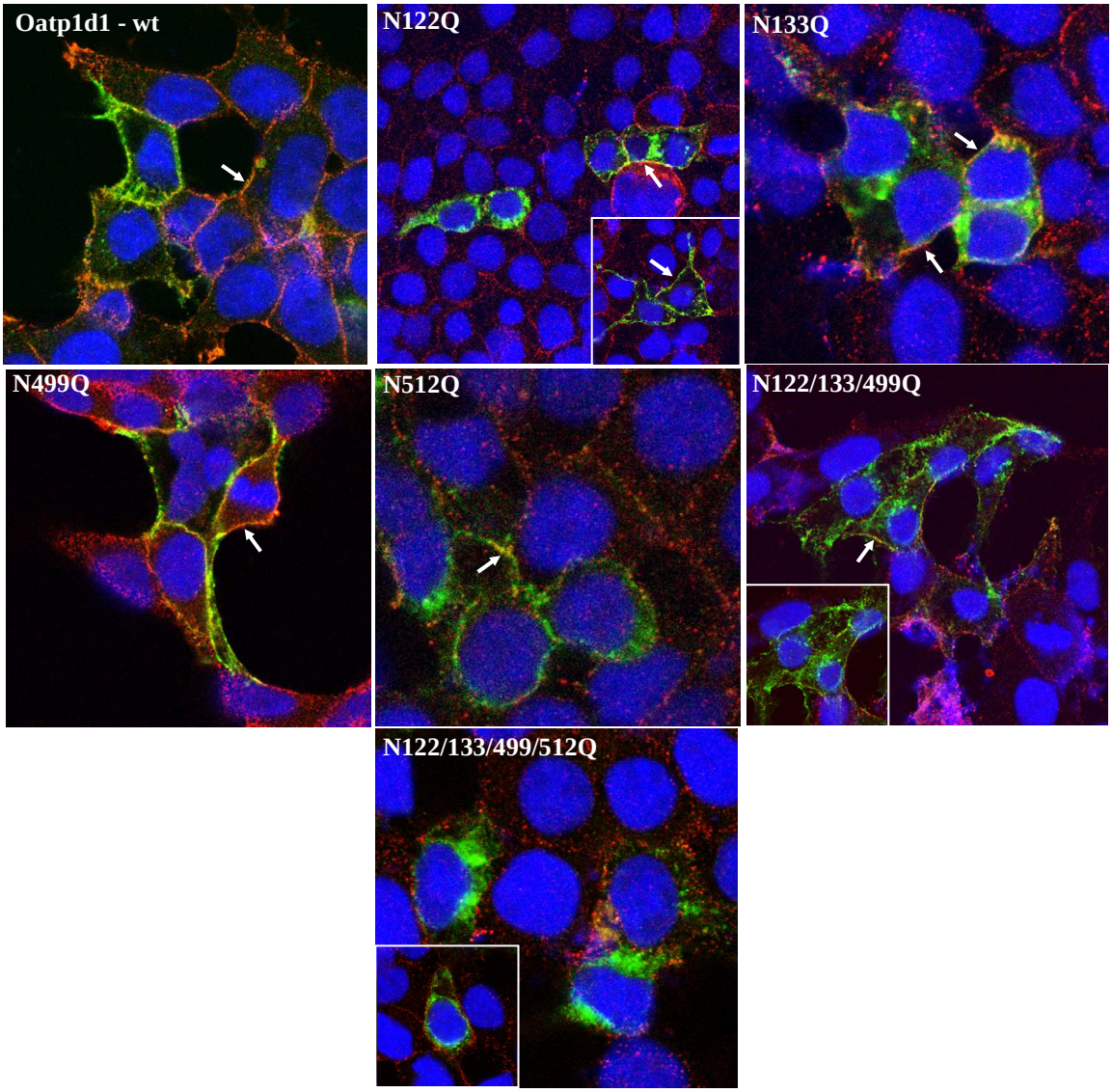

Figure 3.19. Cell localization of Oatp1d1 after mutations of conserved N-glycosylation sites. Mutagenesis of N122Q, N133Q, N499Q and N512Q, as well as simultaneous mutation of three (N122/133/499Q) and four asparagine residues (N122/133/499/512Q) was performed. Immunocytochemistry was performed with fluorescein conjugated secondary antibody (FITC) that binds to the primary Xpress antibody and stains the protein in green. Nuclei are dyed in blue with DAPI, and plasma membranes are stained in red after binding of primary antibody Na,K-ATPase and Cy3-conjugated IgG secondary antibody (all anti-mouse). White arrows indicate examples where protein is present in the cell membrane. The color turns to orange because of the overlap of green and red, or it remains light green when overexpression of protein is dominant over red stained membranes. Cytosolic forms are seen as green areas in the cytoplasm.

Table 3.5. Transport kinetics of zebrafish Oatp1d1 after disruption of four potential N-glycosylation sites (N122Q, N133Q, N499Q and N512Q) and simultaneous mutation of all four asparagine residues (N122/133/499/512).

	Km (LY)	c.i.	Vm (LY)	c.i.
Oatp1d1 - wt	28.3	23.9 - 32.6	127	119 - 135
N122Q	23.8	17.3 - 30.3	59.5	53.3 - 65.7
N133Q	24.8	19.2 - 30.4	76.9	70.1 - 83.7
N499Q	44.7	36.8 - 52.7	85.2	80.2 - 90.1
N512Q	44.7	30.7 - 58.7	111	99.2 - 122
N122/133/499Q	26.5	17.3 - 30.3	62.7	53.3 - 70.7
N122/133/499/512Q	21.3	13.9 - 28.6	18.8	16.2 - 20.7

3.4.6. Cholesterol binding domain

Considering that membrane cholesterol is important for the proper folding and function of membrane transporters (Molina *et al.*, 2008; Storch *et al*., 2007), we wanted to investigate whether Oatp1d1 contains any of the known cholesterol binding motifs and whether these motifs are conserved within the OATP1/Oatp1 subfamily. We identified the presence of the Cholesterol Recognition interaction Amino acid Consensus (CRAC) domain (L/V-$X_{(1-5)}$-Y-$X_{(1-5)}$-R/K), conserved in all OATP1/Oatp1 subfamily members from fish to mammals, with the exception of the OATP1C/Oatp1c. In Oatp1d1 this domain is positioned from the amino acid 180 to 190 and spans part of the TMD4 and IL2 according to the predicted topology. After substitution of the central tyrosine residue (Y) in the CRAC motif for alanine (Y184A), the LY transport rate was reduced by ~ 4 fold: V_{max} = 12.1 $\pm$ 1.5 nmol/mg protein/min as opposed to 43.5 $\pm$ 6.2 nmol nmol/mg protein/min in the case of Oatp1d1 - wt (Fig. 3.20A). On the contrary, the transport affinity of Oatp1d1 – Y184A (K_m = 13.0 $\pm$ 3.4 µM) increased by ~ 2 fold in comparison to Oatp1d1 - wt (K_m = 27.8 $\pm$ 8 µM) (Fig. 3.20A). Western blots of total cell lysates showed the same protein levels of Oatp1d1-Y184A as of Oatp1d1-wt. However, membrane localization revealed that part of Oatp1d1 - Y184A was localized in the cytosol, which could indicate that the decrease in transport rate was a consequence of partially impaired membrane localization (Fig. 3.20B).

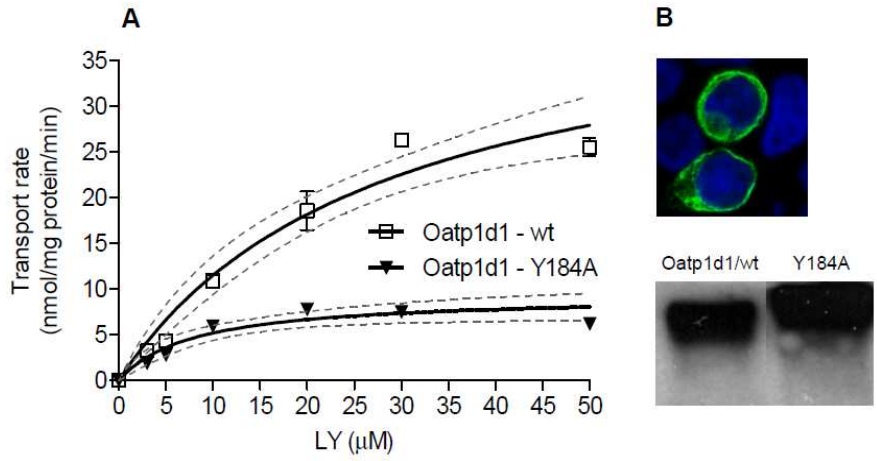

Figure 3.20. Mutation of tyrosine at the position 184 as a part of cholesterol binding motif (CRAC) impacts membrane localization and transport activity of Oatp1d1. (**A**) transport kinetics of Oatp1d1 - Y184A in comparison to Oatp1d1 - wt (**B**) Localisation of Y184A mutant obtained by immunofluorescence analysis and western blot of Oatp1d1 - wt and Oatp1d1 - Y184A proteins.

3.5. Functional characterization of zebrafish Slc22 transporters

3.5.1. DrOat3

Zebrafish Oat3 (DrOat3) is primarily expressed in kidney of females and males, where it shows very high and high expression, respectively, followed by moderate expression in testes, intestine and brain in both genders (Fig. 3.21). In gills, liver and ovaries, Oat3 is negligibly expressed. Most pronounced gender difference in Oat3 expression is found in the gonads. In ovaries, Oat3 is not expressed, as opposed to testes where it is found at the moderate expression level. In the kidney, Oat3 is 6.2 times more expressed in males (Fig. 3.21).

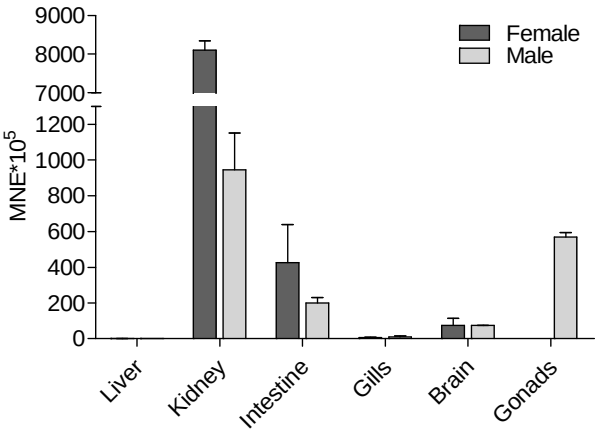

Figure 3.21. Tissue expression pattern of Oat3 in male and female zebrafish. Data represent MNE (mean normalized expression) ± SD, normalized to Ef1α.

In search for the radioactively labeled model substrates, we have performed an uptake assay on the HEK293 cells transiently expressing Oat3 using two model substrates of mammalian OAT1/Oat1 and OAT3/Oat3 transporters, [H^3]E3S and [H^3]pAH. Zebrafish Oat3 showed two-fold increase in uptake of both substrates, E3S and pAH (2.2 $\pm$ 0.1 and 1.9 $\pm$ 0.1 respectively) compared to the mock HEK293 cells. [H^3]pAH was chosen as a substrate of choice for further characterization, due to the temporary inavailability of the [H^3]E3S stock. The transport of pAH follows the classical Michaelis-Menten kinetics. Oat3 shows moderate affinity for pAH with K_m of 112 $\pm$ 16.5 µM (Fig. 3.22).

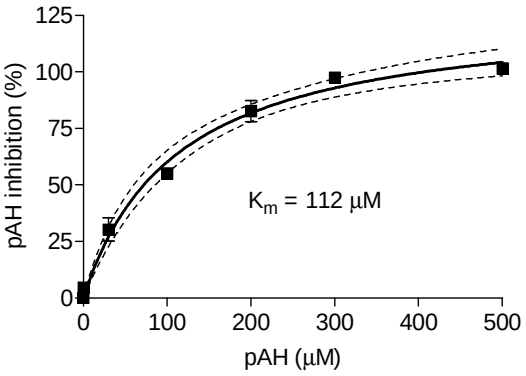

Figure 3.22. Michaelis-Menten kinetics of zebrafish Oat3 mediated uptake of p-aminohippurate (pAH). Each value represents the mean $\pm$ SD from triplicate determinations.

In order to identify interactors of DrOat3, we used radioactively labeled substrate [H^3]pAH to perform the inhibition assay as described in the Methods section. Several known substrates of mammalian OAT1/Oat1 and OAT3/Oat3 orthologs were examined including: cyclic nucleoside cGMP,

citric acid intermediates glutarate and α-ketoglutarate, monocarbxylate propionate, bile salt TCDC, and other known OAT1 and/or OAT3 substrates including urate, folate, thymidine and indoxyl-sulfate. In addition to the endogenous compounds, we analyzed several xenobiotics (mostly pharmaceuticals) that are known to interact with mammalian OATs (Fig. 3.23). Among physiological substrates, we have found that Oat3 shows strong interaction with glutarate, moderate interaction with cGMP and weak interaction with α-ketoglutarate and thymidine (Fig. 3.23). Determination of level of interaction strength (low, moderate, high, very high) is described in the Methods section.

Xenobiotic interactors of zebrafish Oat3 include strong interactors: ibuprofen, furosemide and 2,4-diphenoxyacetic acid (2,4-D), methotrexate and cimetidine as moderate interactors. Probenecid showed activation by 65% (Fig. 3.23, Table 3.6). The inhibition curves for glutarate and furosemide are shown in Figure 3.24 with the inhibition constant of 1.08 µM for glutarate and 0.353 µM for furosemide (Table 3.6).

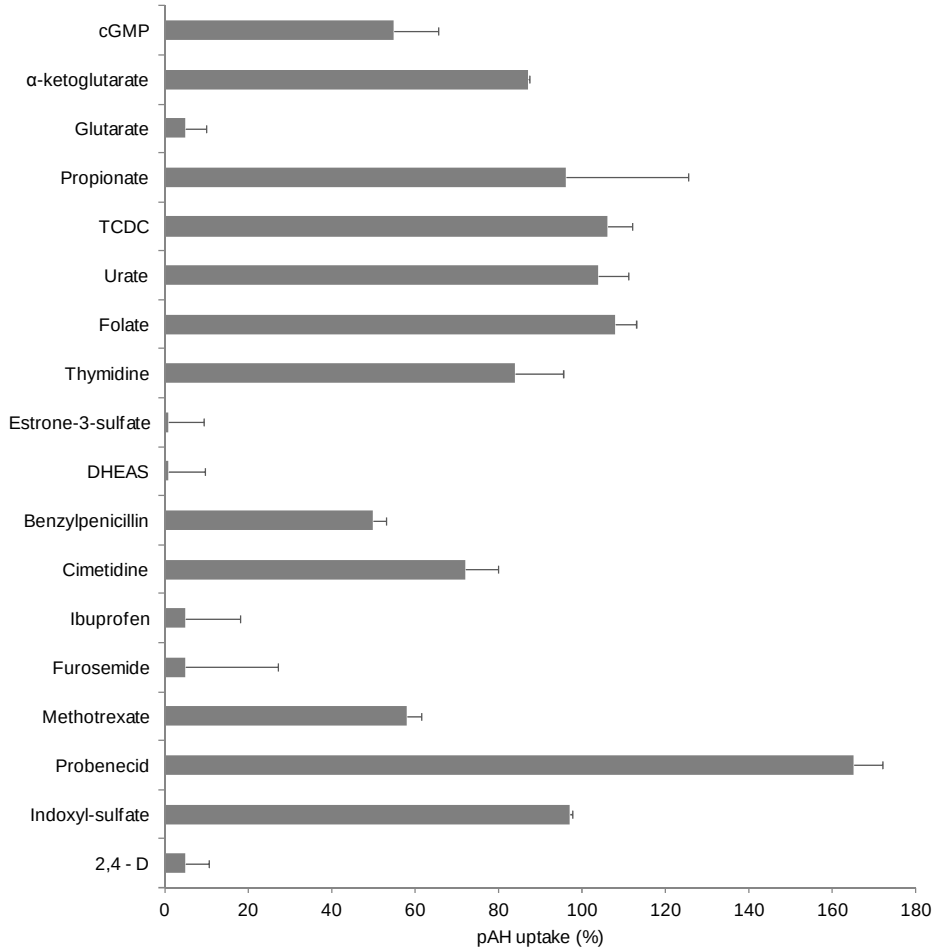

Figure 3.23. Interaction of zebrafish Oat3 with known substrates and inhibitors of mammalian OAT1/Oat1 and OAT3/Oat3. Data are expressed as percentage (%) of pAH uptake after co-incubation with each interactor (100 µM) relative to pAH uptake in the absence of an interactor which is set to 100%. Each value represents the mean ± SD from triplicate determinations.

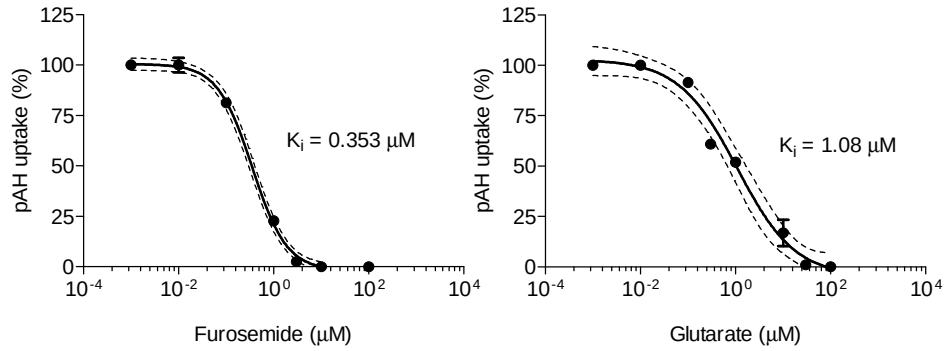

Figure 3.24. Concentration dependent inhibition of Oat3 mediated pAH uptake by glutarate and furosemide (µM). Values on X-axis were transformed to logarithmic scale (log X). Each data point represents the mean ± SD from triplicate determinations.

Table 3.6. Inhibition of Oat3 mediated pAH uptake and K_i values for a set of chosen zebrafish Oatp1d1 interactors. Physiological interactors are separated from xenobiotic interactors with the dotted line. Mean, SD and confidence intervals (c.i.) are calculated from triplicate determinations.

Compound	[H^3] pAH uptake		K_i (µM)	c.i.
	mean	SD		
Control	100	0.10	-	-
cGMP	55	10.6	-	-
α-ketoglutarate	87	0.3	-	-
Glutarate	5	5.0	1.08	0.54 - 2.16
Propionate	96	29.6	-	-
TCDC[1]	106	6.1	-	-
Urate	104	7.00	-	-
Folate	108	5.00	-	-
Thymidine	84	11.5	-	-
Estrone-3-sulfate	1	8.2	-	-
DHEAS[2]	1	8.8	-	-
Benzylpenicillin	50	3.2	-	-
Cimetidine	72	7.8	-	-
Ibuprofen	5	13.1	-	-
Furosemide	5	22.2	0.35	0.29 - 0.43
Methotrexate	58	3.4	-	-
Probenecid	165	7.00	-	-
Indoxyl-sulfate	97	0.7	-	-
2,4 - D[3]	5	5.7	-	-

[1] Taurochenodeoxycholate

[2] Dehydroepiandrosterone sulfate

[3] 2,4 - dichlorophenoxyacetic acid

3.5.2. DrOat2c

Zebrafish Oat2c (DrOat2c or Oat2c) is primarily expressed in the kidney and testes where it shows high expression (Fig. 3.25). It is found at moderate expression levels in ovaries, female brain, and male gills, whereas in other tissues, DrOat2c is expressed very low or negligibly. There are almost no differences in expression levels in kidneys of males and females. However, pronounced difference is found in the gonads, where Oat2c shows 22 times high expression in testes in comparison to ovaries. In gills, Oat2c shows 7 times higher expression in males (Fig. 3.25)

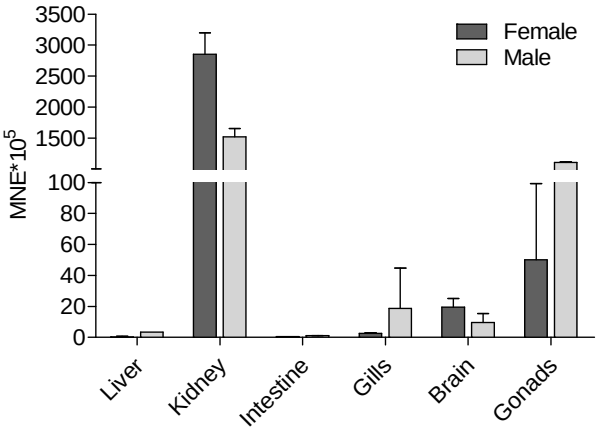

Figure 3.25. Tissue expression pattern of zebrafish Oat2c in male and female zebrafish. Data represent MNE (mean normalized expression) ± SD, normalized to Ef1α.

Similar to the Oat3, zebrafish Oat2c was examined for the transport of radioactively labeled substrates, [H^3]E3S and [H^3]pAH. The uptake of pAH was significantly stronger than the uptake of E3S with 50-fold increase in the Oat2b/HEK293 transfected cells (49.8 $\pm$ 9.71) in comparison to the mock cells. The fold increase in the transport of E3S was substantially lower (1.2 $\pm$ 0.08). We have found that Oat2c transports pAH with moderate affinity: K_m is 44.4 $\pm$ 4.7. µM (c.i. 35.2 – 55.2) (Fig. 24). The uptake follows Michaelis-Menten kinetics.

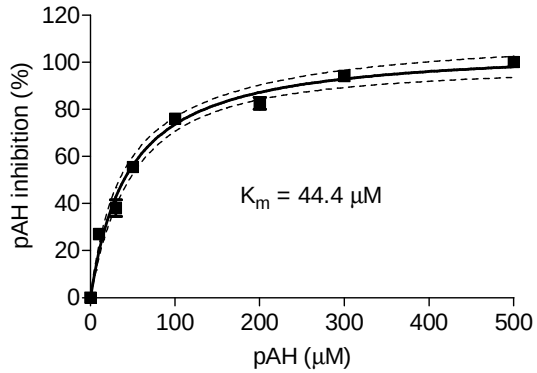

Figure 3.26. Michaelis-Menten kinetics of zebrafish Oat2c mediated uptake of pAH. Each value represents the mean ± SD from triplicate determinations.

DrOat2c mediated pAH transport enabled the use of the inhibition assay for finding physiological and xenobiotic interactors of Oat2c. The range of tested compounds included known interactors of human OAT2 which largely overlap with the interactors of human OAT1 and OAT3. Thus the set of potential interactors included: cyclic nucleoside cGMP, citric acid intermediates glutarate and α-ketoglutarate, monocarbxylate propionate, bile salts: cholate, taurocholate and TCDC, and other known OAT2 interactors including urate, folate, indoxyl-sulfate, PGE2 and bilirubin. The selected set of xenobiotic interactors (mostly pharmaceuticals) overlaps with the interactors of OAT1 and OAT3 and is the same as for zebrafish Oat3 (Table 3.6), with the addition of salicylate. We have found that Oat2c shows moderate interaction with α-ketoglutarate and indoxyl-sulfate, whereas all other physiological compounds did not inhibit pAH uptake at 100 µM concentration (Fig. 3.27, Table 3.7). Among the xenobiotic interactors, probenecid and 2,4-D strongly inhbitied pAH uptake, benzylpenicillin showed weak inhibition, and cimetidine and methotrexate had negligable interaction with Oat2c (Fig. 3.27, Table 3.7). Inhibition constants were determined for two most potent interacting compounds: probenecid and 2,4-D and inhibition curves are shown in Figure 3.28. K_i values for probenecid and 2,4-D were 5.37 µM and 24.6 µM, respectively (Table 3.7).

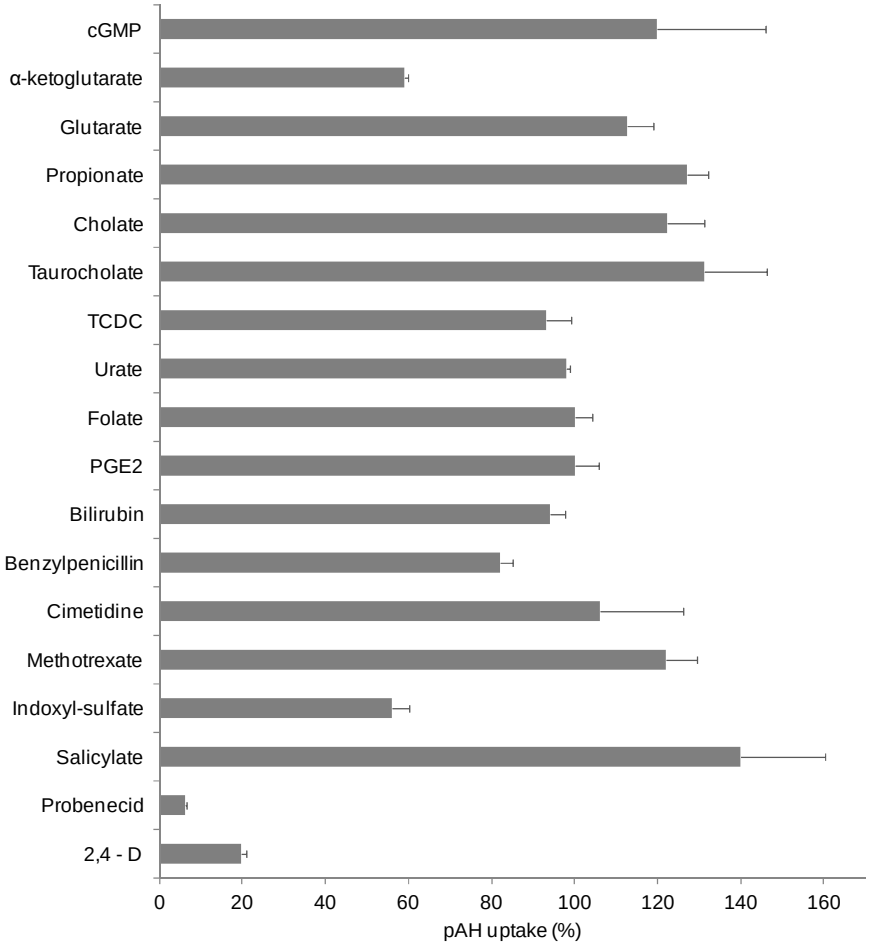

Figure 3.27. Interaction of zebrafish Oat2c with known substrates and inhibitors of mammalian OAT2/Oat2. Data are expressed as percentage (%) of pAH uptake after co-incubation with each interactor (100 µM) relative to pAH uptake in the absence of interactor which is set to 100%. Each value represents the mean ± SD from triplicate determinations.

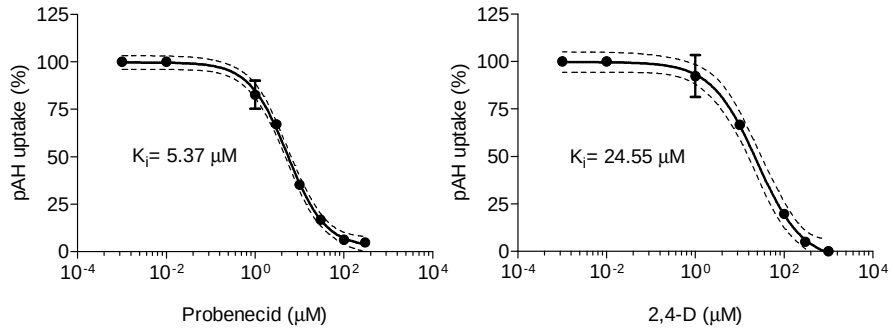

Figure 3.28. Concentration dependent inhibition of Oat2c mediated pAH uptake by probenecid and 2,4 - dichlorophenoxyacetic acid (2,4-D). Values on X-axis were transformed to logarithmic scale (log X). Each data point represents the mean ± SD from triplicate determinations.

Table 3.7. Inhibition of Oat2c mediated pAH uptake and K_i values for a set of chosen zebrafish Oatp1d1 interactors. Physiological interactors are separated from xenobiotic interactors with dotted line. Mean, SD and confidence intervals (c.i.) are calculated from triplicate determinations.

Compound	[H^3] pAH uptake		K_i (µM)	c.i.
	mean	SD		
Control	100	0.10	-	-
cGMP	120	25.8	-	-
α-ketoglutarate	59	0.9	-	-
Glutarate	113	6.5	-	-
Propionate	127	5.2	-	-
Cholate	122	9.1	-	-
Taurocholate	131	15.0	-	-
TCDC[1]	93	6.0	-	-
Urate	98	1.0	-	-
Folate	100	4.2	-	-
PGE2[2]	100	5.7	-	-
Thymidine	nd	nd	-	-
Bilirubin	94	3.6	-	-
Benzylpenicillin	82	3.2	-	-
Cimetidine	106	20.1	-	-
Methotrexate	122	7.6	-	-
Indoxyl-sulfate	56	4.3	-	-
Salicylate	140	20.5	-	-
Probenecid	6	0.0	5.37	4.33 - 6.66
2,4 - D[3]	20	1.0	24.6	14.5 - 41.5

[1] Taurochenodeoxycholate

[2] Prostaglandin E2

[3] 2,4 - dichlorophenoxyacetic acid

3.5.3. DrOat2d

DrOat2d is predominantly expressed in intestine of both genders and testes (high level of expression), followed by moderate expression in kidney of males and females and in brain and gills of males. Most pronounced gender differences are present in the gonads. Zebrafish Oat2d is not expressed in the ovaries, whereas it is highly expressed in the testes. Similar is observed in the brain, where Oat2d shows 25 times higher expression in males, and in gills where Oat2d is 6 times more expressed in males (Fig. 3.29).

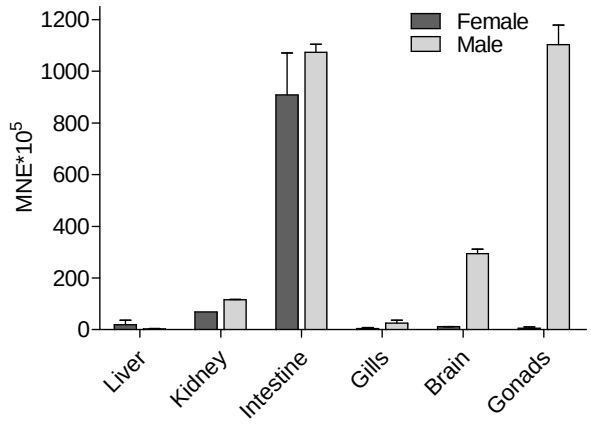

Figure 3.29. Tissue expression pattern of DrOat2d in male and female zebrafish. Data represent MNE (mean normalized expression) ± SD, normalized to Ef1α.

Oat2d was examined for the transport of radioactively labeled substrates, [H^3]E3S and [H^3]pAH. The uptake of both labeled substrates was similar, with 2-fold increase in both cases (2.0 ± 0.5 for E3S and 2.1 ± 0.3 for pAH). The kinetics of Oat2d mediated pAH transport was determined and we found that Oat2d mediated pAH uptake follows Michaelis-Menten kinetics. Oat2d shows moderate affinity towards pAH: K_m is 125 ± 34.8 μM (c.i. 48.8 - 201) (Fig. 3.30).

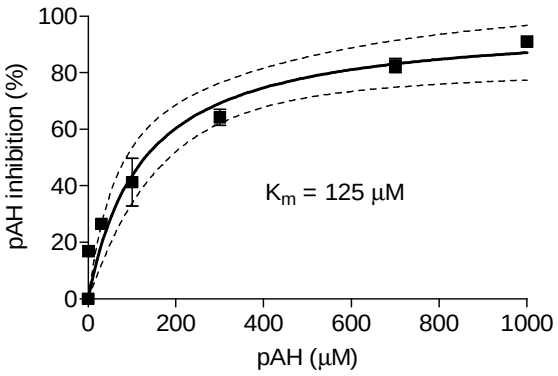

Figure 3.30. Michaelis-Menten kinetics of zebrafish Oat2d mediated uptake of pAH. Each value represents the mean ± SE from triplicate determinations.

The set of selected interactors of Oat2d was similar to the other zebrafish co-ortholog of OAT2, Oat2c, as described above (section 3.4.2.). We have found substantially more interacting compounds

for Oat2d in comparison to the Oat2c. Among physiological interactors: glutarate, α-ketoglutarate, taurocholate and folate strongly inhibited Oat2d mediated pAH uptake, followed by moderate inhibition with salicylate (Fig. 3.31, Table 3.8). On the contrary, cGMP and propionate showed weak activation of pAH uptake (by 28 ± 4.6 % and 35 ± 8.2 % respectively). Among the xenobiotic interactors: probenecid, furosemide and 2,4-D strongly inhibitied pAH uptake, whereas cimetidine, benzylpenicillin and methotrexate did not show inhibition of pAH uptake at 100 µM concentrations (Fig. 3.31, Table 3.8). Inhibition constants for most potent interactors were determined, and are shown in Figure 3.32 and Table 3.8.

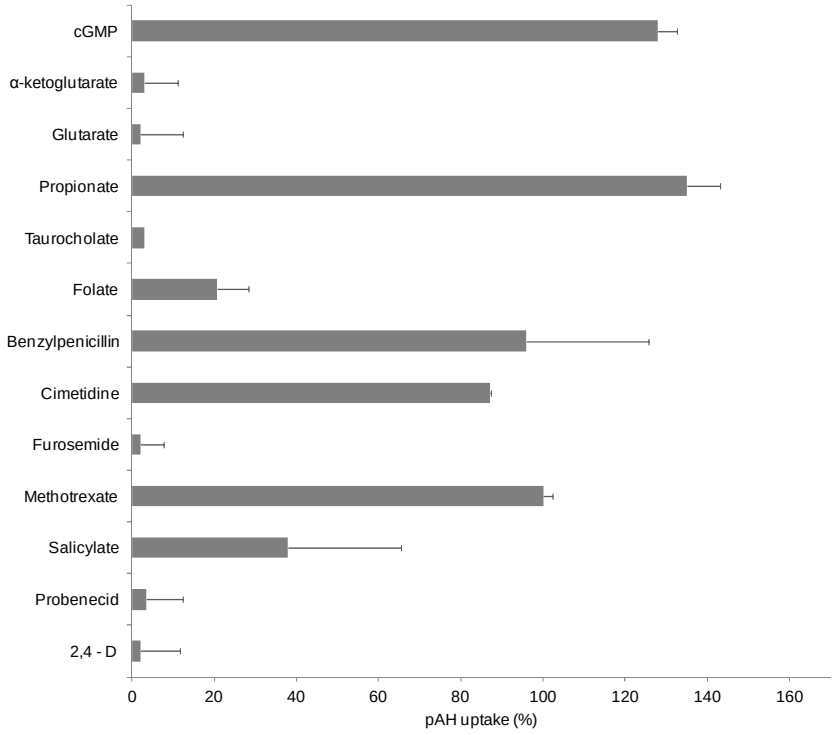

Figure 3.31. Interaction of zebrafish Oat2d with known substrates and inhibitors of mammalian OAT2/Oat2. Data are expressed as percentage (%) of pAH uptake after co-incubation with each interactor (100 µM) relative to pAH uptake in the absence of interactor which is set to 100%. Each value represents the mean ± SD from triplicate determinations.

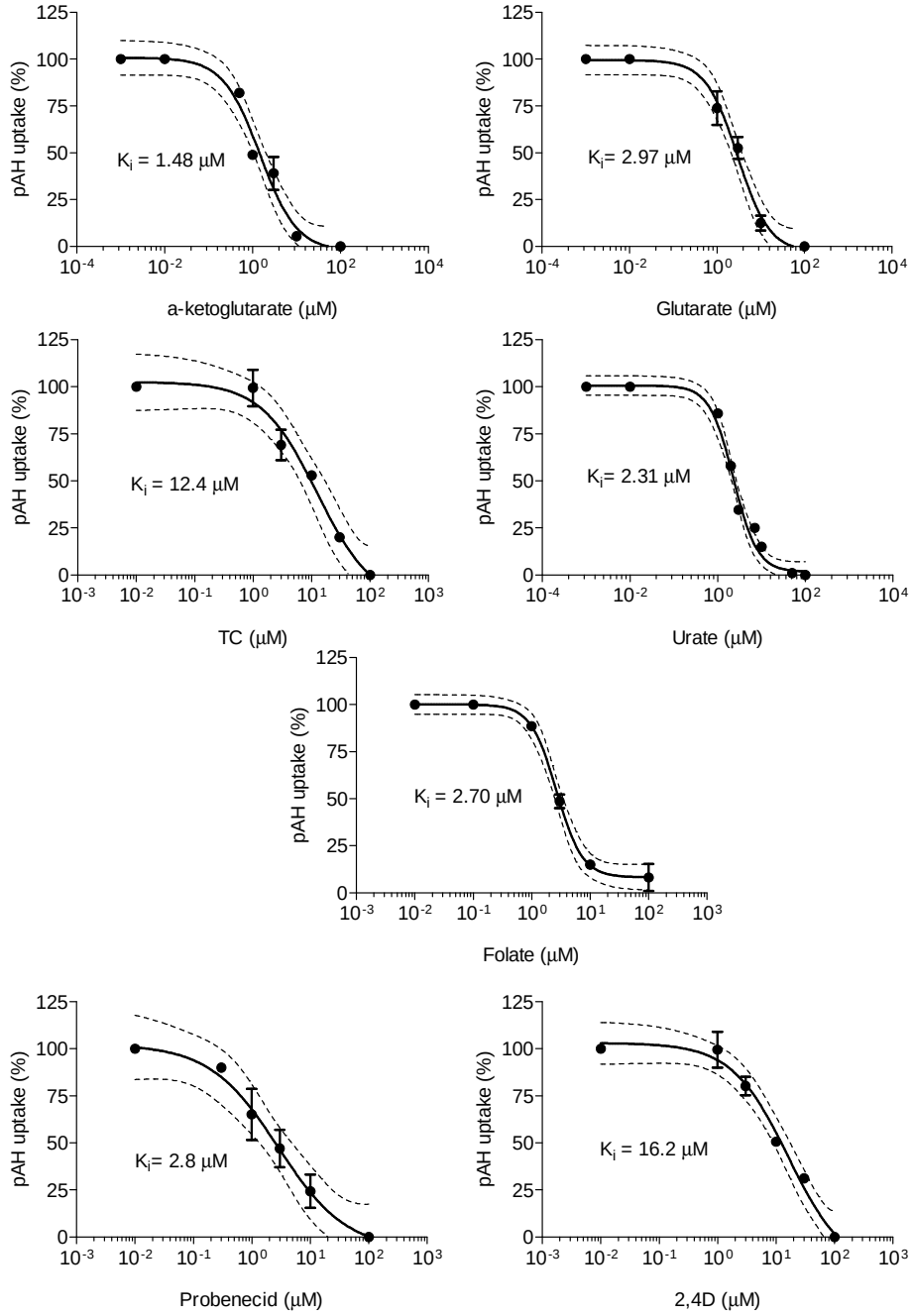

Figure 3.32. Concentration dependent inhibition of Oat2d mediated pAH uptake by most potent interacting compounds (µM) of Oat2d shown in Fig. 3.31. Values on X-axis were transformed to logarithmic scale (log X). Each data point represents the mean ± SD from triplicate determinations.

Table 3.8. Inhibition of Oat2d mediated pAH uptake and K_i values for a set of chosen zebrafish Oatp1d1 interactors. Physiological interactors are separated from xenobiotic interactors with dotted line. Mean, SD and confidence intervals (c.i.) are calculated from triplicate determinations.

Compound	[H^3] pAH uptake (%)		K_i (µM)	c.i.
	mean	SD		
Control	100	0.10	-	-
cGMP	128	4.56	-	-
α-ketoglutarate	3	8.2	1.48	0.90 - 2.44
Glutarate	2	10.4	2.97	1.97 - 4.46
Propionate	135	8.2	-	-
Taurocholate	3	0.1	12.4	3.70 - 41.6
Urate	nd	nd	2.31	1.96 - 2.71
Folate	21	7.6	2.66	2.20 - 3.21
Benzylpenicillin	96	29.6	-	-
Cimetidine	87	0.3	-	-
Furosemide	2	5.7	-	-
Methotrexate	100	2.4	-	-
Salicylate	38	27.4	-	-
Probenecid	3.5	8.8	2.80	0.90 - 8.79
2,4 - D[1]	2.1	9.6	16.2	6.01 - 43.6

[1] 2,4 - dichlorophenoxyacetic acid

3.5.4. Fluorescent substrates of zebrafish Oat3, Oat2c and Oat2d

The initial functional characterization of zebrafish Oats was possible using the radioactively labeled substrate [H^3]pAH. However, working with radioactive compounds is time and labor intensive, as well as expensive. Therefore, we have tried to identify fluorescent substrate(s) of zebrafish Oats that would enable high-throughput studies, thus making possible detailed characterization of these transporters. In that way, we could identify more interactors, and distuinguish among substrates and inhibitors of Oats, similar to the approach we applied for the characterization of Oatp1d1 (section 3.3). We have tested a range of commercially available anionic dyes from the group of fluoresceins: fluorescein, 5- and 6-carboxyfluorescein (5CF and 6CF); LY , resorufin, resazurin and EosinY for the Oat mediated transport.

DrOat3 does not transport fluorescein, resorufin and eosinY, but the uptake of 6CF was 5 times higher than in the mock transfected cells (HEK293T/pCDNA) (Fig. 3.33A). The uptake was measured after 5 minutes at room temperature at the 5 µM concentration of 6CF. Similar pattern of the fluorescent dye uptake was observed in the case of Oat2c (Fig. 3.33B), but with the 2 times lower accumulation when compared to the Oat3 mediated uptake of 6CF. Oat2d, in addition to the transport of 6CF (2.3 $\pm$ 0.2 fold), mediates uptake of 5CF. The Oat2d mediated uptake of 5CF was 2.3 ($\pm$ 0.09) times higher in comparison to the mock transfected cells. Weak uptake of EosinY was also observed (1.6 $\pm$ 0.3 fold), whereas fluorescein and resorufin were not transported by Oat2d (Fig.

3.33C). The range of different concentrations and incubation periods were tested and only selected conditions were shown in the Figure 3.33 (and described in the figure legend).

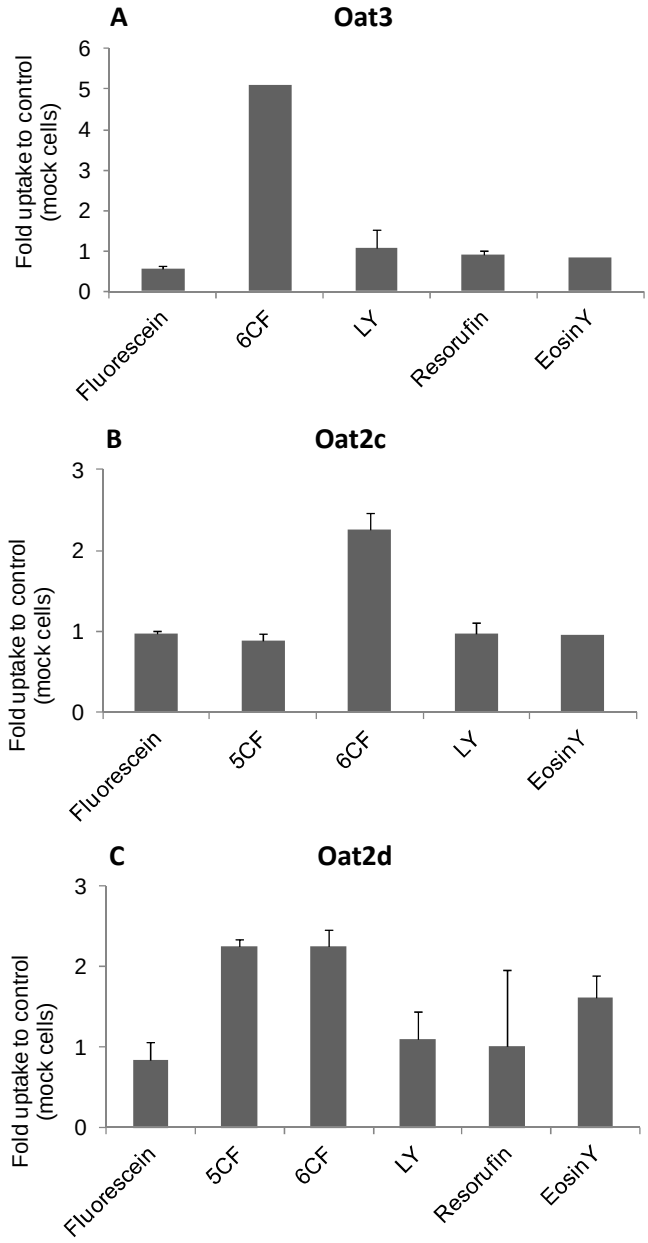

Figure 3.33. Uptake of fluorescent dyes by zebrafish Oats: (**A**) Oat3, (**B**) Oat2c, and (**C**) Oat2d. Data represent mean ± SD of triplicates from three independent experiments (note that if not visible SDs were < 5%) and are expressed as fold uptake relative to vector - transfected HEK293 cells (mock cells). Fluorescent dyes tested included fluorescein (50 µM), 5CF (5 µM), 6CF (5 µM), LY (5 µM), resorufin (20 µM) and EosinY (20 µM). Incubation time varied from 5-10 min depending on the dye.

3.6. Role of uptake transporters in the transport of environmental contaminants – case of Oatp1d1

3.6.1. Development of a novel assay for determination of Oatp1d1 interactors

Appropriate fluorescent probes for the Oatp1d1 uptake would enable a fast identification of Oatp1d1 interacting compounds, which is superior to the radioactively labeled probes that are costly and time and labor intensive. A set of 8 fluorescent compounds have been seleceted based on their anionic nature and the available knowledge from mammalian OATPs/Oatps studies (de Bruyn *et al*., 2011). We found that LY and 5CF are good substrates for Oatp1d1 (Fig. 3.34). 6CF and Eosin Y showed weak transport, whereas fluorescein (FL), dihydrofluorescein (dhFL), rhodamineB (rhB) and resazurine were not transported by Oatp1d1 (Fig. 3.34). The transport kinetics of LY and 5CF was further examined in order to determine transport affinities (K_m) and transport rates (V_m) and compare the two substrates. Oatp1d1 showed 10 times higher affinity towards LY than 5CF (Fig. 3.35B and 3.35D). Uptake of LY into vector-transfected HEK293 cells (mock cells) was absent (Fig. 3.35C), whereas 5CF showed higher passive uptake as well as increase of passive uptake within the first 5 minutes (Fig. 3.35A). This property of 5CF is unwanted, given that the concentration dependency curve is within the linear range over the first 5 minutes of uptake (Fig. 3.35B). In addition, the transport rate of 5CF could not be accurately determined due to the fact that fluorescent signal amplifies by the factor of 1000 in the cell matrix, as opposed to SDS or transport buffer alone (data not shown). Thus, LY is a superior to 5CF as a fluorescent probe for identifying compounds interacting with zebrafish Oatp1d1 due to the higher affinity and lower passive uptake in comparison to 5CF. Furthermore, considering that Oatp1d1 has one substrate binding site for LY (section 3.3), this fluorescent probe can be utilized to determine the type of interaction for the compound of interest using the shift in K_m and V_{max} values for LY Michaelis-Menten kinetics, as described in the Methods section.

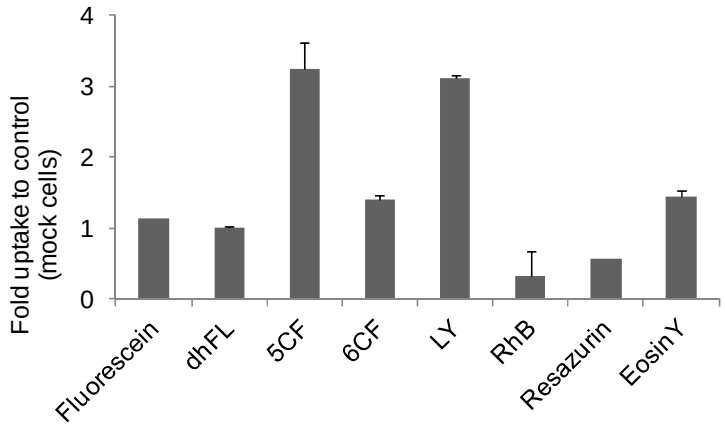

Figure 3.34. Oatp1d1 mediated uptake of fluorescent dyes into HEK293 cells transiently transfected with Oatp1d1. Data represent mean ± SD of triplicates from three independent experiments and are expressed as fold uptake relative to vector - transfected HEK293 cells (mock cells). Fluorescent dyes tested included fluorescein (10 µM), dhFL (20 µM), 5CF (5 µM), 6CF (5 µM), LY (5 µM), rhB (2 µM), resazurine (5 µM) and EosinY (50 µM). Incubation time varied from 5-10 min depending on the dye.

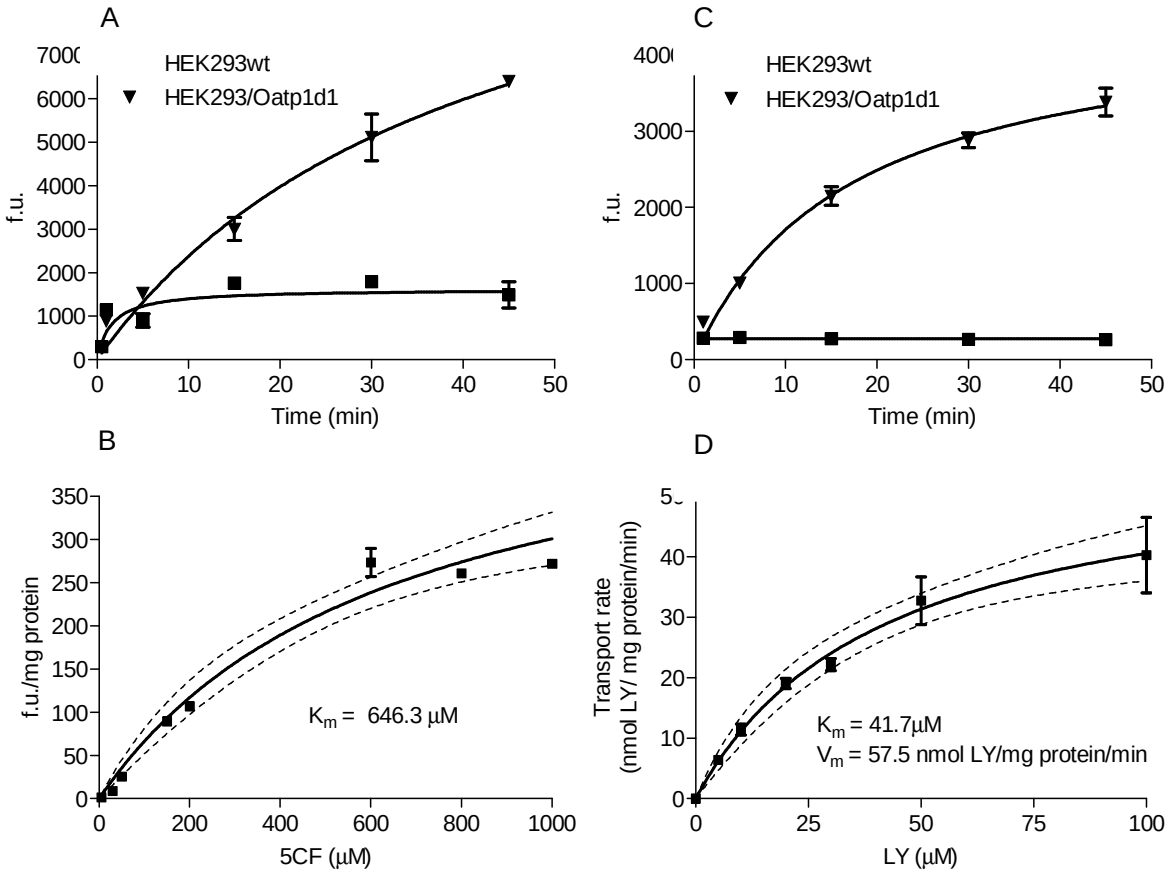

Figure 3.35. Michaelis-Menten kinetics of zebrafish Oatp1d1 mediated uptake of fluorescent dyes 5CF and LY. (**A**) Time - related response of 5CF uptake mediated by Oatp1d1. (**B**) Concentration dependence of Oatp1d1 mediated 5CF uptake expressed as increase in fluorescence normalized to mg of proteins (f.u./mg protein) over 5CF concentration (µM) after 5 min incubation at 37°C. (**C**) Time - related response of Oatp1d1 LY mediated uptake. (**D**) Concentration dependence of LY uptake expressed as transport rate (nmol/mg protein/min) over LY concentration (µM) after 15 min incubation. The uptake into vector - transfected HEK293 cells (mock cells) was subtracted to obtain transporter specific uptake. Mean, SD and confidence intervals (c.i.) were calculated from triplicate determinations in the representative experiment.

3.6.2. Interaction of environmental contaminants with Oatp1d1

Interaction of a selected set of environmental chemicals with Oatp1d1 is shown in Figure 3.36. All chemicals that inhibited Oatp1d1, resulting in 80 - 90% decrease in LY uptake compared to control, were further analyzed and their K_i values were determined (Table 3.9). All inhibition curves are given in the Supplemental Material (Figure S4), while representatives of very strong, strong and moderate interaction are shown in Figure 3.37. The type of interaction of environmental contaminants with Oatp1d1 is given in Table 3.10, and typical Michaelis-Menten curves used for determination of kinetic parameters and distinguishing among substrates and inhibitors are shown in Figure 3.38.

Oatp1d1 showed very strong and strong interaction with perfluorinated compounds, perfluorooctanoic acid (PFOA) and perfluorooctanesulfonic acid (PFOS), respectively (Fig. 3.36). PFOA is a potent un-competitive inhibitor of Oatp1d1 with K_i value of 0.39 μM. Although very similar in structure, PFOS is a high affinity Oatp1d1 substrate with K_i value of 12.9 μM (Tables 3.9 and 3.10, Fig. 3.38B). Phenols interact strongly with Oatp1d1. Nonylphenol is a high affinity substrate (K_i = 9.43 μM), whereas bisphenol A (BisA) (K_i = 105 μM) is a moderately strong inhibitor of Oatp1d1 (Tables 3.9 and 3.10, Fig. 3.38A). Most frequently occurring phthalates in surface waters, diethyl phthalate (DEP), dibutyl phthalate (DBP) and bis(2-ethylhexyl) phthalate (DEHP) showed very different interactions with Oatp1d1; DEHP showed no interaction at 100 μM concentration (Fig. 3.36), DBP acted as a weak inhibitor (K_i = 466.5 μM), whereas DEP was a moderately strong inhibitor of Oatp1d1 (K_i = 41.7 μM) (Tables 3.9 and 3.10). Butylated hydroxytoluen (BHT), a food additive, showed very weak interaction with Oatp1d1 (K_i = 1337 μM) (Fig. 3.36, Table 3.9).

Different interactions with Oatp1d1 occurred within the seven major pesticide groups. Carbamate carbaryl acted as an Oatp1d1 substrate with K_i = 67.5 μM; the herbicide metolachlor acted as a weak Oatp1d1 inhibitor (K_i = 152 μM), whereas 2,4-D showed no interaction with Oatp1d1 at 100 μM (Fig. 3.36, Tables 3.9 and 3.10). Highly persistent organochlorines including DDT, dieldrin, endosulfan and methoxychlor showed no interaction with Oatp1d1 (Fig. 3.36). In contrast, organophosphate pesticides were among the most potent Oatp1d1 interactors found in our study (Fig. 3.36). Diazinon was a moderately strong inhibitor and chlorpyrifos-methyl acted as a strong inhibitor of Oatp1d1 with K_i of 51.6 μM and 9.48 μM, respectively, whereas malathion acted as an Oatp1d1 substrate (K_i = 48.7 μM) (Tables 3.9 and 3.10). Fenvalerate and atrazine exhibited very weak interaction with Oatp1d1 (Fig. 3.36, Table 3.9). Among other widely used pesticides, isoproturon showed a weak interaction with Oatp1d1 (Fig. 3.36), whereas diuron was a moderately strong Oatp1d1 substrate with K_i of 68.7 μM (Tables 3.9 and 3.10).

We also analyzed pharmaceuticals and personal care products (PPCPs) that are present in the aquatic environment, including synthetic hormones, analgesics and anti-inflammatory drugs, lipid lowering agents, antibiotics, insect repellents and caffeine (Fent *et al*., 2006; Murray *et al*., 2010). Synthetic estrogens were among the most potent interactors of zebrafish Oatp1d1. E2 and estrone (E1) acted as strong Oatp1d1 inhibitors, whereas 17α-ethynilestradiol (EE2) was a high affinity substrate (K_i = 5.93 μM) (Tables 3.9 and 3.10). The most potent interacting compound among analgesics and non-steroidal anti-inflammatory drugs (NSAIDs) was diclofenac, which is transported by Oatp1d1 with very high affinity (K_i = 0.23 μM) (Tables 3.9 and 3.10, Fig. 3.37). In contrast, another frequently occurring NSAID, ibuprofen was transported by Oatp1d1 with lower affinity (K_i = 84.2 μM) (Tables 3.9 and 3.10). Acetaminophen, acetylsalicylic acid and carbamazepine showed weak or no interaction with Oatp1d1 (Fig. 3.36). The lipid lowering drugs gemfibrozil, clofibric acid, and

fenofibric acid exhibited different interactions with Oatp1d1; Gfb acted as a high affinity Oatp1d1 substrate (K_i = 7.44 µM), whereas fenofibrate and clofibrate acted as inhibitors of different potencies: fenofibrate was a moderately strong inhibitor (K_i = 54.4 µM) and clofibrate was a weak inhibitor (K_i = 345 µM) of Oatp1d1 (Tables 3.9 and 3.10). Erythromycin and triclosan showed weak interactions (Fig. 3.36), whereas polycyclic musk fragrance 7-acetyl -1,1,3,4,4,6-hexamethyl-1,2,3,4 tetrahydronapthalene (AHTN) acted as a weak un-competitive inhibitor (Tables 3.9 and 3.10). Two other frequently occurring compounds were tested, caffeine and insect repellent, N,N-diethyl meta-toluamide (DEET). Caffeine was found to be a moderate affinity substrate of Oatp1d1 (K_i = 31.3 µM) (Table 3.10), and DEET showed a very weak interaction (Fig. 3.36).

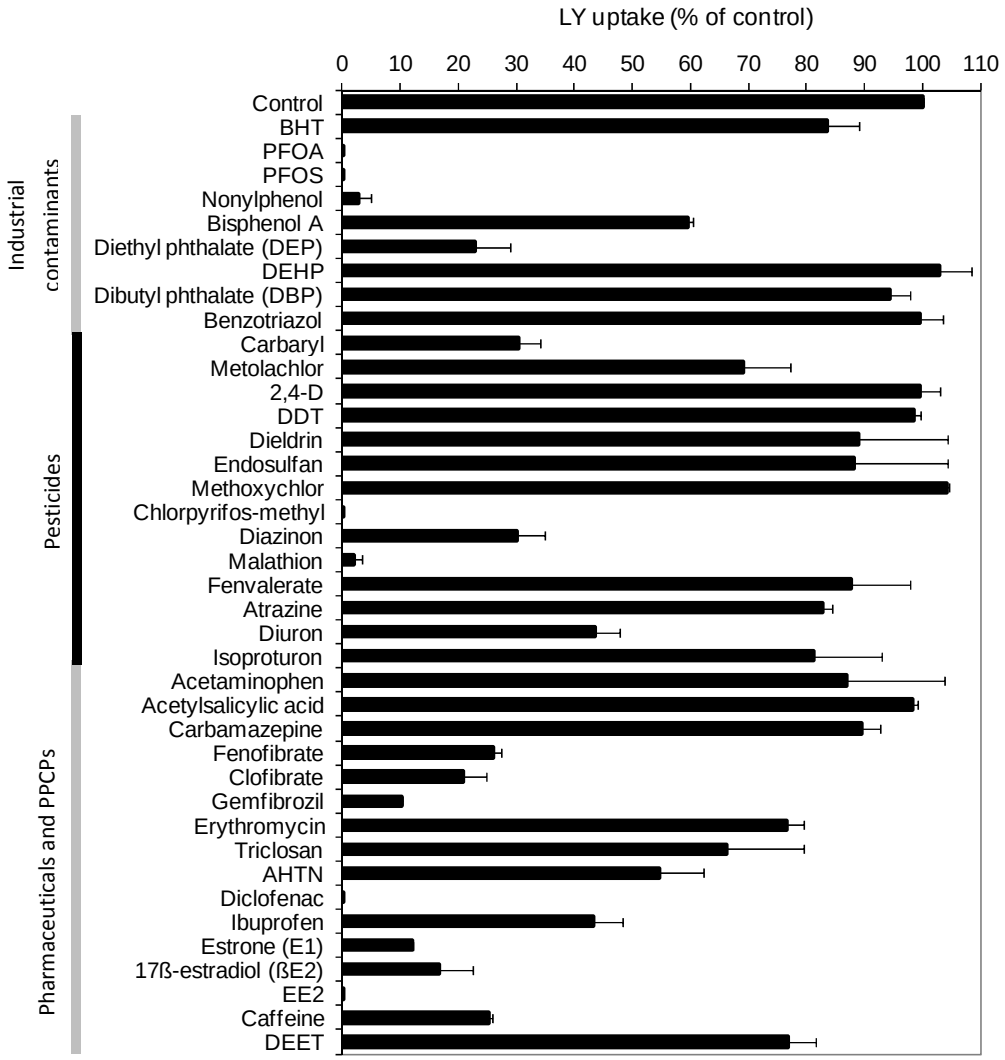

Figure 3.36. Interaction of zebrafish Oatp1d1 with environmental contaminants. Data are expressed as percentage (%) of the LY uptake after co-incubation with each tested substance (100 µM) relative to LY uptake in the absence of the substance, which is set to 100%. Xenobiotic interactors are divided into three groups: industrial contaminants, pesticides and pharmaceuticals and personal care products (PPCPs). Data represent mean ± SD of triplicates from three independent experiments (note that SD was < 5% when not visible on the chart). Abbreviations used are listed in Chapter 9.

Table 3.9. Inhibition constants (K_i) of xenobiotic compounds that showed interaction with Oatp1d1.

Compound	K_i (µM)	95 % c.i.
BHT[1]	1337	1006 - 1777
PFOA[2]	0.39	0.23 - 0.67
PFOS[3]	12.9	2.76 - 60.0
Nonylphenol	9.43	4.56 - 19.5
Bisphenol A	105	90.9 - 121
Diethyl phthalate (DEP)	41.7	35.2 - 49.6
Dibutyl phthalate (DBP)	467	285 - 764
Carbaryl	67.5	48.0 - 94.9
Metolachlor	152	97.5 - 238
Chlorpyrifos methyl	9.48	7.55 - 11.9
Diazinon	51.6	25.9 - 102
Malathion	48.7	29.8 - 79.4
Fenvalerate	862	465 - 1595
Atrazine	722	570 - 914
Diuron	68.7	32.1 - 148
Fenofibrate	54.4	37.8 - 78.3
Clofibrate	345	252 - 470
Gemfibrozil	7.44	4.37 - 12.7
Erythromycin	882	639 - 1216
AHTN[4]	120	57.7 - 250
Diclofenac	0.23	0.18 - 0.29
Ibuprofen	84.2	64.0 - 111
17ß-estradiol (E2)	2.83	2.27 - 3.52
EE2[5]	5.93	4.41 - 7.97
Estrone (E1)	1.04	0.68 - 1.58
Caffeine	31.3	23.6 - 41.5

[1]Butylated hydroxytoluen

[2]Perfluorooctanoic acid

[3]Perfluorooctanesulfonic acid

[4]Acetyl-hexamethyltetrahydro-naphthalene

[5]17a-ethynilestradiol

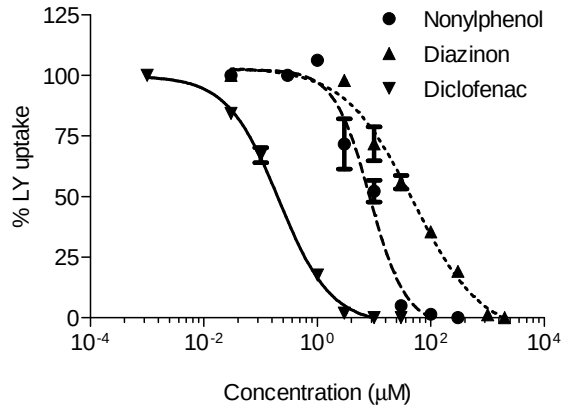

Figure 3.37. Concentration dependent inhibition of Oatp1d - mediated LY uptake by exemplary modulators of a high (diclofenac), moderate (nonylphenol) and low potency (diazinon). The specific uptake of LY is expressed as percentage relative to the LY uptake in the absence of an interactor (set to 100%). Values on X-axis were transformed to logarithmic scale (log X).

Table 3.10. Distinguishing among substrates and inhibitors of Oatp1d1 using LY uptake kinetics. Kinetic parameters of LY uptake are given as apparent Km (Km app) (µM), apparent Vm (Vm app) (nmol LY/mg protein/min), and 95% confidence intervals (c.i.) for each. The mark "I" denotes inhibitors and the "S" denotes Oatp1d1 substrates.

Interactor	Km_{app} (LY)	c.i.	Vm_{app} (LY)	c.i.	Interaction type
Control	30.3	24.6 - 35.9	197	184 - 209	
PFOA[1]	27.5	16.9 - 38.1	126	106 - 145	I
PFOS[2]	158	63.4 - 253	147	96.7 - 197	S
Nonylphenol	57.1	33.5 - 80.7	180	142 - 219	S
Bisphenol A	31.1	17.3 - 44.8	112	94.5 - 129	I
Diethyl phthalate	32.7	20.0 - 45.4	159	132 - 185	I
Carbaryl	148	109 - 186	271	242 - 300	S
Metolachlor	80.2	44.7 - 116	219	163 - 275	S
Chlorpyrifos-methyl	30.4	22.7 - 38.2	101	91.2 - 111	I
Diazinon	57.7	43.8 - 71.7	232	203 - 260	S
Malathion	219	81.0 - 356	188	126 - 250	S
Diuron	54.3	42.6 - 66.1	313	289 - 337	S
Clofibrate	14.1	4.87 - 23.4	41	32.5 - 49.5	I
Gemfibrozil	160	95.7 - 224	294	227 - 362	S
AHTN[3]	5.56	0.66 - 10.5	11.5	9.12 - 13.9	I
Diclofenac	59.7	34.7 - 84.7	202	166 - 238	S
Ibuprofen	188	91.3 - 284	220	168 - 271	S
EE2[4]	62.1	30.3 - 93.9	194	147 - 241	S
17ß-estradiol (E2)	29.3	21.5 - 34.7	118	99.3 - 134	I
Estrone	30.8	15.7 - 45.9	25	21.8 - 29.0	I
Caffeine	132	90.8 - 173	246	204 - 287	S

[1]Perfluorooctanoic acid
[2]Perfluorooctanesulfonic acid
[3]Acetyl-hexamethyltetrahydro-naphthalene
[4]17a-ethynilestradiol

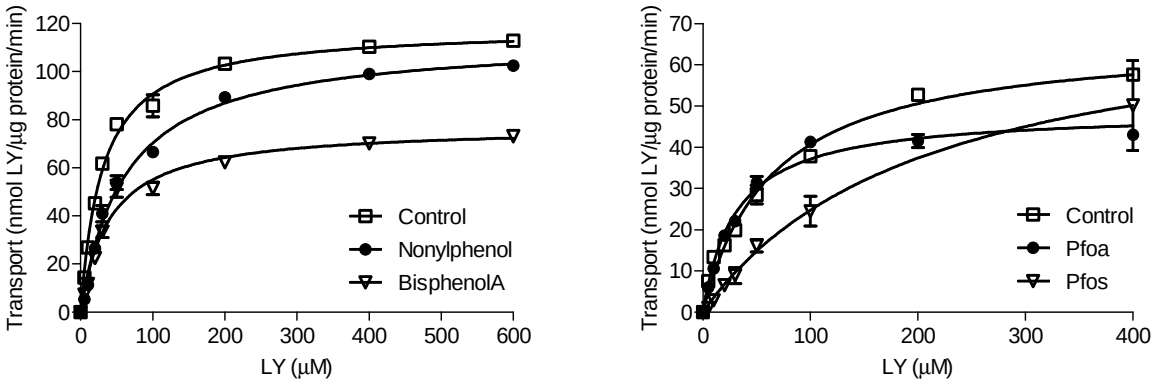

Figure 3.38. Example of dose-response curves used to determine type of interaction with Oatp1d1. Kinetic analysis of LY transport by HEK293/Oatp1d1 overexpressing cells in the absence of an interactor (Control), and in the presence (**A**) competitive inhibitor (i.e. substrate) nonylphenol (at the concentration of 9.4 µM) and an un-competitive inhibitor BisA (110 µM). (**B**) competitive inhibitor (i.e. substrate) PFOS (12.9 µM) and an un-competitive inhibitor, PFOA (0.39 µM).

In summary, our data show that numerous environmental contaminants present in the aquatic environment interact with zebrafish Oatp1d1. Oatp1d1 mediates uptake of diclofenac with very high affinity, followed by high affinity towards PFOS, nonylphenol, Gfb and EE2; moderate affinity towards DEP, carbaryl, diazinon and caffeine; and low affinity towards metolachlor (Tables 3.9 and 3.10). Importantly, many environmental contaminants clearly act as potent inhibitors of Oatp1d1. A strong inhibition of Oatp1d1 transport activity was found by PFOA, chlorpyrifos-methyl, E1 and E2, followed by moderate to low inhibition by DEP, BisA, AHTN and clofibrate (Tables 3.9 and 3.10).

4. Discussion

4.1. OATP family

Our results represent the first comprehensive analysis of the OATP/Oatp family in zebrafish. In addition to previously annotated Oatp1c1, 2a1, 3a1 and 4a1 (Meier-Abt et al., 2005), we have identified and classified 10 new zebrafish Oatps: Oatp1d1, Oatp1d2, Oatp1f1-4, Oatp2b1, Oatp3a2 and Oatp5a1-2 (Fig. 3.1, Table 3.1, Table S1).

Membrane topology analysis revealed that zebrafish Oatps most probably have 12 TMDs. Similar structure has already been predicted for mammalian Oatps (Hagenbuch and Meier, 2004) and for the Oatp1d1 in little skate (Cai *et al*., 2002). Furthermore, topology prediction showed that organization of TMDs and LPs is highly conserved throughout the whole vertebrate lineage, which was previously observed only for mammals (reviewed in Hagenbuch and Gui, 2008). However, further studies and experimental evidence are necessary to confirm the predicted topology of zebrafish Oatps. As expected, conserved motifs specific for Oatp family were identified in zebrafish Oatps as well. These include the family signature, a large extracellular LP9 with 10 conserved cysteines, and the Kazal SLC21 domain. Function of family signature sequence and Kazal21 domain is unknown (Kawaji *et al*. 2002; Hagenbuch and Gui, 2008), while cysteine residues are important for protein trafficking and function (Hanggi *et al*., 2006). Our data showed that all mentioned motifs are conserved not just within mammals, but within the entire vertebrate subphylum.

The schematic representation of the OATP1/Oatp1 subfamily evolution (Fig. 4.1) derived from phylogenetic analysis (Fig. 3.1 and Fig. S1) shows the emergence of Oatp1 groups from tunicates to mammals. We suggest that diversification of the OATP1/Oatp1 subfamily occurred after the emergence of jawed fish which followed the second round of the whole genome duplication (WGD) event after the split of jawless and jawed fish, but before the split of cartilaginous and bony fish (Froschauer *et al*., 2006). OATP1A/Oatp1a and OATP1B/Oatp1b groups that emerged at the root of tetrapods (OATP1A/Oatp1a is found in primitive tetrapod *Latimeria chalumnae*) long after two rounds of WGD events in vertebrate evolution, probably arose independently by chromosomal duplications. OATP1C/Oatp1c, as the only group found in all vertebrate representatives from cartilaginous fish (little skate) to humans, might represent a genes most similar to the common ancestor of the OATP1/Oatp1 subfamily, as was previously suggested by Pizzagalli, 2002. In fish, three Oatp1 groups are present: Oatp1c, Oatp1d and Oatp1f (Table 4.1). Oatp1d1 orthologs are strongly conserved in fish and Oatp1d1 is ubiquitously expressed in zebrafish tissues of both genders, with dominant expression in liver, brain and testes. In human, OATP1A proteins are expressed in various tissues and transport a wide range of substrates, including numerous physiological substrates (e.g., bile salts, thyroxine, E3S) and xenobiotics (e.g., methotrexate, fexofenadine, microcystin) (Hagenbuch and Gui, 2008). Unlike OATP1A/Oatp1a, OATP1B/1b members (mouse Oatp1b2 and

human OATP1B1, 1B3) are expressed specifically in liver, where they are involved in elimination of toxic compounds from the blood (Hagenbuch and Meier, 2003). Zebrafish Oatp1d1 expression pattern is most similar to the mouse Oatp1a4, and partly to human OATP1A2 (Cheng et al., 2005, Nishimura and Naito, 2005). Apart from similarity in expression with OATP1A2, Oatp1d1 is the only member of Oatp1 subfamily expressed in zebrafish liver and is thus similar to the OATP1B/1b as well. Considering that in mammalian liver, OATP1B/1b members (mouse Oatp1b2 and human 1B1, 1B3) are predominantly expressed, and their primary role is the transport of xenobiotics, we suggest that zebrafish Oatp1d1 could play similar role in zebrafish liver and that overall it would resemble both groups, OATP1A/1a and OATP1B/1b. Unfortunately, syntenic relationship to mammalian OATP1/Oatp1 members cannot be determined, because zebrafish Oatps are not yet mapped within the chromosomes.

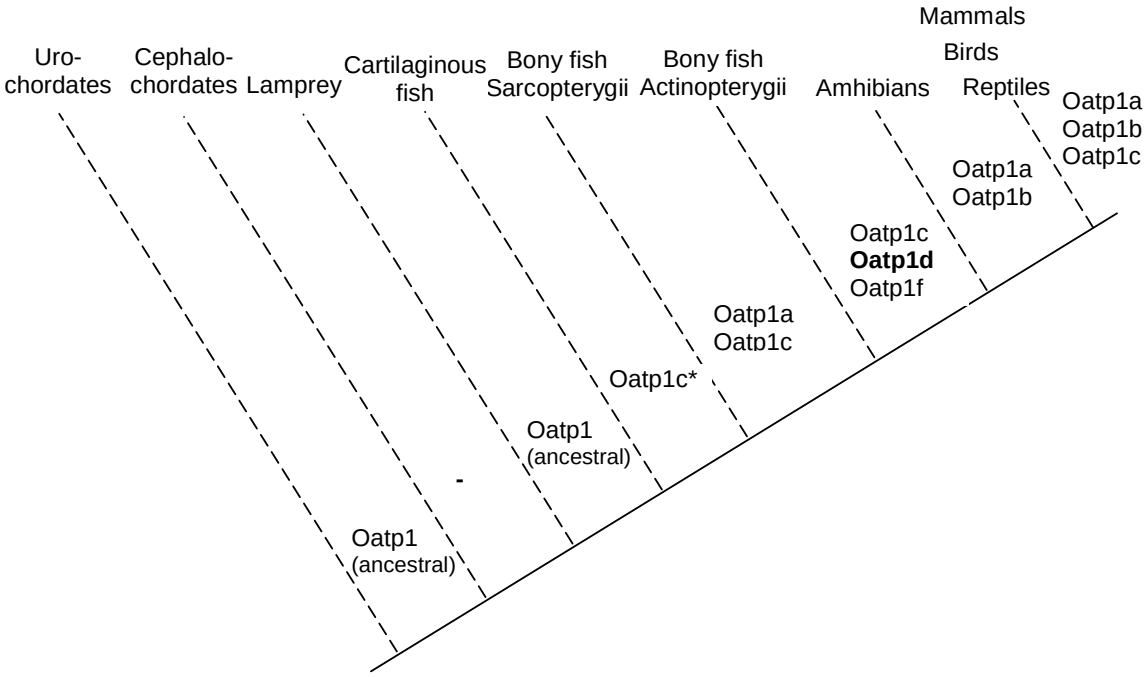

Figure 4.1. Schematic presentation of OATP1/Oatp1 subfamily evolution in chordates. Mammals include human, mouse and rat; birds include chicken (*Gallus gallus*) and zebra finch (*Taeniopygia guttata)*. Reptiles are represented with anole lizard (*Anolis carolinensis*) and amphibians with frog *Xenopus tropicalis*. Teleosts included in the analysis are acanthopterygians: zebrafish (*Danio rerio*), pufferfishes (*Tetraodon nigroviridis* and *Takifugu rubripes*), stickleback (*Gastrosteus aculeatus*), medaka (*Oryzias latipes*), Atlantic cod (*Gadus morhua*) and a sarcopterygian *Latimeria chalumnae*. Cartilaginous fish include little skate (*Raja erinacea*), while representatives of primitive chordates are cephalochordate lancelet (*Branchiostoma floridae*) and tunicate sea squirt (*Ciona intestinalis*).

Apart from Oatp1d1, the second newly identified member of Oatp1d group, Oatp1d2, exhibits comparatively lower expression in all analyzed tissues. Notable expression is detected only in brain.

In the mammalian brain, OATP1C1, OATP1A2 and OATP3A1 are major Oatps that are involved in the transport of thyroid hormones (Cheng *et al*., 2005; Nishimura and Naito, 2005). In zebrafish brain, Oatp1c1 expression was not detected, while Oatp3a1 (a co-ortholog of human OATP3A1) is more than an order of magnitude higher expressed than Oatp1d2. Consequently, our results indicate that beside Oatp1d1, Oatp3a1 may be a major thyroid hormone transporter in zebrafish brain, while Oatp1d2 is probably of lesser physiological importance.

Oatp1f group is specific for zebrafish. Whether Oatp1f is specific only for Cyprinidae family remains to be determined after more Cyprinids genomes become available. Considering very high expression of Oatp1f2 in kidney, this gene probably has important physiological function in the transport of organic anions in the zebrafish kidney. However, considering that tissue distribution pattern of Oatp1f2 does not resemble any of the mammalian OATPs/Oatps (Cheng *et al*., 2005; Nishimura and Naito, 2005), without functional characterization it is hard to speculate about the role of Oatp1f group and its specific presence in zebrafish (or potentially entire Cyprinidae family).

OATP2A group is conserved in vertebrates: all vertebrate species analyzed have a single ortholog, OATP2A1/Oatp2a1. This is in line with the important physiological function of OATP2A1 as a transporter of prostaglandins in various tissues including brain, colon, heart, kidney, liver, lung, ovary, pancreas, placenta, prostate, skeletal muscle, spleen and small intestine (Kanai *et al*., 1995; Schuster, 2002; Nomura *et al*., 2004, 2005). Proposed physiological role of OATP1A2 could be in terminating prostaglandin signaling by transporting prostaglandins into the cells as hypothesized by Nomura *et al*. (2004, 2005). Zebrafish Oatp2a1 appears to be a direct ortholog of the human and mouse OATP2A1/Oatp2a1 with ubiquitous tissue expression similar to human OATP2A1 and mouse Oatp2a1. Its relative tissue distribution pattern is in line with the mammalian OATP2A1/Oatp2a1, with the exception of comparatively higher expression of Oatp1a2 in the mouse brain (Cheng *et al*., 2005; Nishimura and Naito, 2005). Considering mentioned similarities, we suggest that zebrafish Oatp2a1 is a functional ortholog of the prostaglandin transporter OATP2A1. This hypothesis remains to be proven after the functional characterization of DrOat2a1.

Another OATP2 subfamily member, zebrafish Oatp2b1, shows ubiquitously high expression similar to human OATP2B1 and mouse Oatp2b1 (Tamai *et al*., 2000; Kullak-Ublick *et al*., 2001; Cheng *et al*., 2005) with dominant expression in liver at the basolateral membrane of hepatocytes. Given the fact that OATP2B1/Oatp2b1 cluster shows clear one-to-one orthology relationships, and that DrOatp2b1 shares similar expression profile to mammalian OATP2B1/Oatp2b1 transporters, we suggest that zebrafish Oatp2b1 is a functional ortholog of OATP2B1. Thus, the function of DrOatp2b1 would include absorption and disposition of numerous endo- and xenobiotics within the body with the principal role in the first step of xenobiotic elimination through the liver (Roth *et al*., 2012), along with Oatp1d1. In addition to the important function in mammalian liver, OATP2B1/Oatp2b1 is an

essential transporter at the apical membrane of enterocytes (Kobayashi *et al*., 2003), as well as at the luminal membrane of the endothelial cells of the blood – brain barrier (Bronger *et al*., 2005). Considering clear orthology relationship of DrOatp2b1, and its expression in intestine and brain, we hypothesize that zebrafish Oatp2b1 would fulfill the same role as does human OATP2B1 in these tissues.

We showed that OATP3/Oatp3 subfamily is most highly conserved within the vertebrate OATP/Oatp family and not only in mammals as previously noted (Maier-Abt *et al*., 2005) which would suggest an important physiological role within the vertebrate subphylum. Two co-orthologs of human OATP3A1 transporter are found within the zebrafish genome. Zebrafish Oatp3a1 showed high sequence identity and similar tissue distribution pattern as human and mouse OATP3A1/Oatp3a1 (Cheng *et al*., 2005; Nishimura and Naito, 2005) with the highest expression in the brain. OATP3A1 is ubiquitously expressed in mammals including testes, brain and heart, followed by lung, spleen, peripheral blood leukocytes and thyroid gland (Adachi *et al*., 2003; Huber *et al*., 2007). Considering all mentioned, it is possible that DrOatp3a1 is a functional ortholog of OATP3A1 which is suggested to be involved in the transport of thyroid hormones and/or neuron-active peptides (Hagenbuch and Gui, 2008; Huber *et al*., 2007) across the BBB. The other co-ortholog of OATP3A1, zebrafish Oatp3a2, shows quite different tissue distribution pattern from human OATP3A1, mouse Oatp3a1 and zebrafish Oatp3a1. Considering its low expression in all tissues except brain, it could possibly have similar function to its co-ortholog DrOatp3a1, but the function in the thyroid hormone transport would be limited to the brain.

After 4 primer pairs were tried out, we conclude that DrOatp4a1 (and DrOatp1c1 and DrOatp5a2) transcripts were not expressed in the analyzed tissues. The other OATP/Oatp4 subfamily member, OATP4c/Oatp4c appeared in the ancestor of tetrapods (it is present in the ancient tetrapod representative *L. chalumnae*) and is not found in fish (Fig 1., Fig. S1). It is not clear why there was a need for another anion transporter at the basolateral membrane of renal cells in tetrapods, but what we can derive from our results is that there is a higher number of organic anion transporters from OATP/Oatp family and OAT/Oat subfamily present in fish kidney. Some of those transporters might have similar substrate specificity to Oatp4c1 (Table 1.1), possibly Oatp1d1, Oatp2a1 and 2b1, Oatp3a1 and 5a1 which are all found at the moderate to high expression levels in zebrafish kidney (Fig 3.3B).

Zebrafish Oatp5a1 and Oatp5a2 are probable co-orthologs of OATP5A1. Unfortunately, tissue distribution patterns of human and rodent OATP5A1/Oatp5a1 are still unknown and our study represent the first insight into the tissue expression profile of OAT5/Oatp5 subfamily members in general. We found that Oatp5a1 is weakly to moderately expressed across all zebrafish tissues. Given the fact that Oatp5 subfamily is most highly conserved within vertebrate lineage (along with Oatp3

subfamily), with high amino acid sequence identity among the members of different species (section 3.1.1), and the fact that zebrafish Oatp5a1 transcript is ubiquitously expressed, DrOatp5a1 probably has an important physiological function that remains to be determined in future studies. The expression of Oatp5a2 should be considered in future research, as well as DrOatp4a1, which could not be quantified within this study.

OATP6 subfamily is specific to mammals. Considering predominant expression in testes where Oatp6 co-orthologs in rodents are involved in the uptake of DHEA and DHEAS (Lee *et al*., 2004; Suzuki *et al*., 2003), this subfamily seems to be developed to accommodate this specific function. In zebrafish, any of the OATPs or OATs expressed in testes could fulfill this role. For example, Oatp1d1 which we showed to transport DHEAS could compensate for the function of OATP6/Oatp6 in zebrafish testes.

In summary, our up to date phylogenetic analysis of OATP/Oatp family in vertebrates has in part resolved phylogenetic relationships among the OATPs/Oatps in vertebrates, and resulted in the annotations of 14 zebrafish Oatps, whereas tissue expression analysis revealed the highest gene expression in toxicologically important tissues, primarily liver, kidney, intestine and gills. Drawing together from the phylogenetic similarity to mammalian OATPs/Oatps with known function, and from the tissue expression pattern, we suggest that most likely candidates for further (eco)toxicological research on Oatp-mediated xenobiotic uptake in fish are Oatp1d1 and Oatp2b1. Oatp1f would be included as well, but considering that it is found only in zebrafish it is probably not relevant for the entire teleost group. Its functional analysis would nonetheless be important for the characterization of zebrafish as a model species. Overall, following the results form phylogenetic and expression analysis, our first focus was the detailed molecular characterization of Oatp1d1.

4.2. Oatp1d1

Based on the kinetic analysis we propose that Oatp1d1 probably has one and the same substrate binding site for E3S and LY. In that sense it is similar to OATP1A2, whereas OATP1B1 and probably OATP1B3 have two binding sites for E3S (Hirano *et al*., 2006; Noe *et al*., 2007; Tamai *et al*., 2000; Roth *et al*., 2011). Biphasic transport kinetics was also suggested for the OATP1C1 mediated transport of estradiol-17β-glucuronide and T4 (Kindla *et al*., 2011). Affinity of Oatp1d1 for E3S is more similar to OATP1A2 (K_m = 6 - 35 µM) than to the skate Oatp1 member (K_m = 61 ± 11 µM) and is several times higher than the affinities of OATP1B3 and OATP1C1 for E3S (Cai *et al*., 2002; Pizzagalli *et al*., 2002; Lee *et al*., 2003, 2005; Hirano *et al*., 2006).

We showed that zebrafish Oatp1d1 is a high affinity transporter of conjugated steroid hormones: E3S, estradiol-17β-glucuronide and DHEAS, whereas non-conjugated steroids: estradiol,

progesterone, androstenedione, dihydrotestosterone and testosterone are potent inhibitors of Oatp1d1 (Table 3.4). Considering high expression of Oatp1d1 in liver, we propose that Oatp1d1 is crucial for the uptake and subsequent elimination of excess steroid hormone metabolites through bile, similar to the role of OATP1A2, OATP1B1 and OATP1B3 (Hagenbuch and Gui, 2008). Furthermore, its high expression in testes implies possible involvement in the uptake of DHEAS as a precursor for androgen synthesis in gonads, a role that OATP6/Oatp6 subfamily has in mammalian testes (Suzuki *et al*., 2003; Klaasen and Lu, 2008). Additionally, uptake of DHEAS by Oatp1d1 may be of critical importance in the brain, considering its action as a neurosteroid and high expression of Oatp1d1 in the brain (similar to OATP1A2). Inhibition of Oatp1d1 by non-conjugated steroids could reduce the uptake of conjugated steroid hormones in target tissues, depending on the fine hormonal balance in the plasma. In that sense, transporters, and more specifically Oatp1d1, would be involved in the negative feedback loop regulation of steroid hormone synthesis (James, 2011). Corticosteroid metabolism is also in part regulated by transporters. Oatp1d1, similarly to OATP1A2, transports cortisol, a crucial hormone in fish that acts as both glucocorticoid and mineralocorticoid given that fish do not possess corticosterone and aldosterone (James, 2011; Pippal *et al*., 2011). In summary, our data strongly suggest that the role of OATP/Oatp transporters in steroid catabolism is conserved from fish to mammals and that Oatp1d1 fulfills that role in zebrafish.

The most pronounced difference between mammalian OATP1/Oatp1 members and zebrafish Oatp1d1 is the fact that Oatp1d1 does not transport thyroid hormones, thyroxine (T4) and triiodothyronine (T3) (Fig. 3.3, Fig. 3.8). In mammals, thyroid hormones are primarily transported by OATP1C1 and OATP1A2 in the brain, whereas OATP1B1 is crucial for their elimination through liver (Deure *et al*., 2010; Fujiwara *et al*., 2001). Considering that Oatp1d1 is inhibited by T3 and no allosteric interaction for Oatp1d1 was found for the wide range of interactors, T3 possibly enters the substrate binding pocket without actually being transported. The substrate binding site of OATP1A2 in mammals possibly evolved in order to transport thyroid hormones. In fish however, this role might be fulfilled by Oatp3a1 and Oatp3a2 which are highly expressed in zebrafish brain, especially considering that the OATP3/Oatp3 subfamily is involved in thyroid uptake in mammalian brain (Huber *et al*., 2007).

Another major group of OATP1/Oatp1 substrates includes bile salts. Bile acids metabolism is conserved within the vertebrate lineage, with certain variations in bile content. Bile acid uptake from blood into liver is largely mediated by Na-taurocholate cotransporting polypeptide (MTCP) that accounts for 70% of the bile acid uptake in humans. The rest is mediated by OATPs, namely OATP1A2, OATP1B1 and OATP1B3. The dominant forms of bile acids in teleosts and mammals are cholic and deoxycholic acid and their glyco- and tauroconjugates. However, in cyprinid fishes, unlike

in other teleost species, the dominant bile alcohol is 5α-cyprinol, a C_{27} bile alcohol (Hagey *et al*., 2010). We have shown that in zebrafish, cholate, deoxycholate and their taurine conjugates are inhibitors of Oatp1d1 (Table 3.4). Considering significant structural differences between these bile salts and 5α-cyprinol, we propose that Oatp1d1 might transport cyprinol. Unfortunately, this hypothesis could not be tested in this study due to commercial unavailability of 5α-cyprinol. In favor of the hypothesis that Oatp1d1 is important for cyprinol excretion into bile is the fact that Oatp1d1 is the only Oatp1 present in zebrafish liver and OATP1/Oatp1 subfamily is crucial for bile acid homeostasis in mammals.

Comparison of substrate and inhibitor preferences of Oatp1d1 with mammalian OATP1/Oatp1 transporters clearly indicates that zebrafish Oatp1d1 is more similar to OATP1A2, OATP1B1 and OATP1B3 than to OATP1C1. Nevertheless, notable differences are present in terms of its substrate selectivity and affinity in comparison to OATP1A2, OATP1B1 and OATP1B3. Firstly, Oatp1d1 does not transport bilirubin, T3, T4, bile salts and ouabain which are transported by OATP1A2, 1B1 and 1B3. Secondly, differences are present in the substrate affinity: Oatp1d1 shows higher affinity for DHEAS in comparison to mammalian OATP1/Oatp1 members and finally, inhibition potency of model compounds warfarin, Gfb and fenofibrate is higher for Oatp1d1 than for OATP1A2, 1B1 and 1B3. Since the skate Oatp1 member, which we annotated as Oatp1c1, was not characterized in detail (Cai *et al*., 2002; Maier-Abt *et al*., 2007), it can be compared only in terms of E3S, BSP and ouabain transport, which generally showed similarities between skate Oatp1c1 and zebrafish Oatp1d1. In summary, Oatp1d1 appears to be crucial for the balance of steroid hormones in zebrafish, and might be responsible for uptake of bile alcohol cyprinol and conjugated bilirubin in zebrafish liver.

The transport mechanism of OATPs/Oatps has not been elucidated conclusively, although the anion antiport has been suggested as a presumable driving force. The majority of OATPs/Oatps, including OATP1A2, OATP1B1 and OATP1B3, function as [HCO_3^-] antiporters (Satlin *et al*, 1997; Kobayashi *et al*. 2003; Martinez-Becerra *et al*., 2011; Yao *et al*., 2012). However, some rat transporters, namely Oatp1a1 and Oatp1a4 use glutathione for the antiport (Li *et al*., 1998; Li *et al*., 2000). Therefore we wanted to address the transport mechanism of Oatp1d1 and gain insight into the evolutionary conservation of OATP1/Oatp1 transport in vertebrates. Oatp1d1 activity was affected by extracellular pH (pH_o) and intracellular pH (pH_i) changes which in turn induced changes in proton fluxes across the plasma membrane (Figs. 3.11A, 3.11B and 3.12A). These proton fluxes are linked to [HCO_3^-] concentrations. When extracellular [H^+] concentration is increased (pH_o 5.5), [HCO_3^-] with excess [H^+] forms H_2O and CO_2 which in turn stimulates the outwardly directed [HCO_3^-] gradient. The opposite effect is achieved when $pH_i < pH_o$ after intracellular acidification or extracellular alkalinization (pH_o 8.0). In our experiments, acidification of extracellular space (pH_o 5.5) significantly

increased Oatp1d1 transport rate, while at the same time apparent K_m was not significantly changed (Fig. 3.12A). This suggests that the inwardly directed proton gradient enhances protein activity, either through [H^+] cotransport (uptake) or through [HCO_3^-] or [OH^-] antiport. Since [H^+] cotransport or [OH^-] antiport as driving forces for OATP/Oatp transport have not been reported for any of the OATPs/Oatps studied, we regard it as less probable than [HCO_3^-] antiport, which was previously proven for several mammalian OATPs/Oatps (Leuthold *et al*., 2009; Martinez-Becerra *et al*., 2011). In contrast, when [H^+] gradient was reversed ($pH_i < pH_o$) through intracellular acidification or extracellular alkalization, we observed significant reduction in Oatp1d1 transport activity (Fig. 3.11B). To summarize, when proton gradient is inwardly directed, [HCO_3^-] is outwardly directed and Oatp1d1 activity is stimulated. The opposite effect was observed when proton gradient is outwardly directed and Oatp1d1 activity is significantly reduced. Altogether, our results suggest that Oatp1d1 is pH gradient dependant which is an indication of the bicarbonate antiport as a driving force for the substrate uptake, similar to the mammalian OATP/Oatps.

Since the pH dependence of protein activity could be a consequence of the protonation of histidine residues, we analyzed the conservation of relevant His residues within the OATP1/Oatp1 subfamily. Through mutagenesis studies we showed that H102 is not involved in the pH sensitivity of the transport (Fig. 3.12B), unlike in mammalian transporters (Leuthold *et al*., 2009). However, we showed that protonation of H79 in the intracellular LP1 is crucial for Oatp1d1 activity (Fig. 3.13A) and is in part responsible for the reduction of transport activity at acidified intracellular pH (Fig. 3.13B). Considering that H79 is highly conserved within vertebrate OATP1/Oatp1 subfamily, this new finding suggests that H79 may be important for the transport activity of mammalian OATPs/Oatps as well.

N-glycosylation is known to be involved in posttranslational processing of mammalian OATPs/Oatps (Wang *et al*., 2008). Considering that each individual mutation of four highly conserved potential glycosylation sites in Oatp1d1 only partly impaired membrane localization and protein activity, whereas only quadruple mutant was completely inactive and remained in the cytosol (Table 3.5 and Fig. 3.19), we propose that N122, N133, N499 and N512 are responsible for protein glycosylation which in turn influences membrane targeting and thus protein activity. Interestingly, when only N512 was modified, protein transport rate remained unchanged. However, the triple mutant that excluded N512 (N122/133/499) was active (with 50% reduced transport rate), and it partly localized in the membrane. When N512 was also changed (in the quadruple mutant), protein was inactive and remained in the cytosol which indicates that N512 is also involved in the N-glycosylation, but in the N512Q mutant, the other three residues compensate for the inability of glycan binding to N512. Similar pattern was observed for rat Oatp1a1 where residues N124, N135 and N492 that correspond to the residues N122, N133 and N499 in Oatp1d1, are responsible for

protein glycosylation (Lee *et al*., 2003; Wang *et al*., 2008), whereas N133 was identified as crucial for the glycosylation of human OATP1A2. Importance of glycosylation for protein folding and membrane targeting was also observed for human OATP2B1 (Tschantz *et al*., 2008). Based on the high degree of conservation of residues N122, N133, N499 and N512 within the OATP1 subfamily of vertebrates, we propose that N-glycosylation is an important factor for membrane localization of OATP1/Oatp1 subfamily and that these four conserved rasidues in extracellular LPs 2 and 5 are being glycosilated.Dependence of OATP/Oatps on membrane cholesterol has not been investigated so far. Cholesterol reckognition motif, CRAC motif is conserved in all OATP1/Oatp1 subfamily members from fish to mammals, with the exception of OATP1C/Oatp1c group. Furthermore, this motif is known to be present in many proteins that interact with cholesterol (Jafurulla *et al*., 2011). Since our data show that mutation in CRAC motif (Y184A) significantly impairs zebrafish Oatp1d1 membrane targeting (Fig. 3.20B), we propose that this motif is important for the localization of Oatp1d1 in the plasma membrane, possibly through the interaction with membrane cholesterol. Considering that the CRAC motif is well conserved within OATP1/Oatp1 subfamily, we suggest its importance for the membrane localization of mammalian OATPs, possibly through the interaction with membrane cholesterol, a topic that remains to be addressed in further studies.

Oatp1d1 is present in the plasma membrane as a dimer and potentially as a higher order oligomer. Monomers are linked into dimers through disulfide bonds and dimers organize into oligomers independent of disulfide bonds (Figs. 3.14A and B). Dimerization through disulfide bonds has been shown for OATP2B1 (Hanggi *et al*., 2006). Considering that cotransfection of Oatp1d1 - wt and Oatp1d1/mCitrine showed plasma membrane localization (Fig. 3.15A), Oatp1d1 - wt is present in the membrane at least in the dimeric form. Although the surface biotinylation experiment is an indication of the presence of only oligomeric form in the plasma membrane (Fig. 3.14A), due to the possibility of the chemical crosslinking it is not conclusive. However, we have a strong indication that highly conserved glycophorin A motifs (GXXXG) within the TMD5 (208-212) and TMD8 (385-390) are involved in the oligomer formation, considering that change in these motifs impairs protein activity due to the inability to localize to the plasma membrane, and considering the absence of oligomeric form in total cell lysates after their mutation (Fig. 3.16 and Fig. 3.17). This motif has been found to be responsible for the dimer and oligomer formation of another SLC transporter, serotonin transporter (SERT) (Horschitz *et al*., 2008). Overall, although more than 35% of all cellular proteins act as oligomers, investigation of oligomeric forms of membrane proteins has been scarce (Goodsell and Olson, 2000; Ali and Imperiali, 2005), probably due to the fact that oligomers are “lost” on western blots due to the often harsh experimental conditions. However, oligomeric state is preferable over monomers or dimers, due to the allosteric regulation between monomers (Hanggi *et al*., 2006). In addition, members of the SLC22, a closely related transporter family, human OAT1 and rat Oat1, Oct1

and Oct2 form homo-oligomers (Hong *et al*., 2005; Keller *et al*., 2011). In the case of rat Oct1 and Oct2 monomeric units are linked through disulfide bond (Keller *et al*., 2011), whereas OAT1 oligomers are formed independently of disulfide link (Hong *et al*., 2005), similar to zebrafish Oatp1d1.

In summary, we have characterized a novel Oatp in zebrafish, Oatp1d1. This is the first characterization of a *Slc21* transporter in zebrafish which provides important insights into the functional evolution of OATP1/Oatp1 subfamily. Diversification of the OATP1/Oatp1 subfamily occurred after the emergence of jawed fish; the Oatp1d group emerged in teleosts and is absent in tetrapods, whereas OATP1A/Oatp1a and OATP1B/Oatp1b emerged at the root of tetrapods. Substrate specificity analysis and tissue expression analysis revealed similarities with mammalian OATP1A/Oatp1a and OATP1B/Oatp1b transporters and differences from mammalian OATP1C/Oatp1c proteins. We suggest an important role of Oatp1d1 in hormonal balance in fish, as well as its involvement in elimination of steroid hormones metabolites and foreign compounds through bile. Based on the results on extracellular and intracellular pH manipulations, we propose that Oatp1d1 activity is pH gradient dependant. Analysis of evolutionary conservation and importance of structural properties revealed that: (i) H79 located in the intracellular LP3 is conserved within the OATP1/Oatp1 subfamily and is crucial for transport activity; (ii) N-glycosylation pattern is conserved within OATP1/Oatp1 subfamily and is important for membrane localization with the four N-linked glycosylation sites involved (N122, N133, N499, N512); (iii) evolutionary conserved CRAC motif is important for the membrane localization of Oatp1d1; and finally (iv), our results show that Oatp1d1 is present in the plasma membrane as a dimer and possibly as a higher order oligomer, with highly conserved glycophorin motifs in TMD5 and TMD8 involved in the oligomer formation. Our results contribute to the better understanding of the OATP/Oatp evolution in vertebrates and offer the first insight into the function and structural properties of a novel zebrafish Oatp1 ortholog.

4.3. Slc22 family

Our results represent the first insight into the Slc22 transporter family in zebrafish. As it was expected, zebrafish Slc22 transporters share structural similarity with mammalian SLC22 in respect to 12 α-helical TMDs, large extracellular LP1 and intracellular LP6, and intracellular orientation of C and N termini (Burckhardt and Wolff, 2000; Koepsell *et al*., 2011), indicating high degree of conservation of secondary structure in the vertebrates. Two motifs, so far found in mammalian SLC22/Slc22 transporters (Wright and Dantzler 2004), are present in zebrafish Slc22 proteins as well. Presence of the major facilitator superfamily motif was expected, but nonetheless, our results confirm high degree of conservation of MSF motifs within the SLC22/Slc22 family in vertebrates. What is more

interesting is a very high degree of conservation of the second motif, ASF domain, in all three subgroups: OATs, OCTs and OCTNs (Fig 3.4). This motif was previously identified by Schomig *et al.* (1998) as OCT specific motif localized before the TMD2 in mammalian OCT/Octs. Our results show that ASF motif is conserved within the whole SLC22/Slc22 family from fish to mammals (and not just within OCTs), whereas its function remains to be determined.

OAT1/Oat1 and OAT3/Oat3 cluster shows one-to-one orthology relationship in each vertebrate species (Fig. 3.2, Table 3.2) which indicates high degree of conservation of OAT1 and OAT3 function in the physiology of vertebrates. This is not surprising, considering crucial physiological role of these transporters in the uptake of endogenous compounds including medium chain fatty acids cAMP and cGMP, prostaglandins, urate and neurotransmitter metabolites (Rizwan and Burckhardt, 2007; Cropp *et al*., 2008; Nakakariya *et al*., 2009). Fish Oat1 and Oat3 proteins form a cluster separated from the tetrapod OAT1/3 cluster, thus it is not possible to decipher clear orthologs of mammalian OAT1/Oat1 and OAT3/Oat3 in fish based solely on the phylogentic analysis. However, considering that zebrafish Oat3 is expressed predominantly in kidney, it seems that this protein would resemble both, human OAT1 and OAT3 which are dominant in mammalian kidney (Motohashi *et al*., 2002). Moderate expression in brain and intestine also fits well with the expressions of human OAT1 (brain) and OAT3 (intestine and brain) (Motohashi *et al*., 2002), thus indicating possible involvement of zebrafish Oat3 in the renal elimination of drugs similar to the function of mammalian OAT1 and 3 (Koepsell, 2013). The distinct difference in transcript expression is present in testes where DrOat3 is highly expressed, followed by moderate expression of DrOat1, whereas human OAT1 and 3 have been so far detected in testes (Koepsel *et al*., 2013). We suggest that possible role of DrOat3 in testes would be uptake of DHEAS (a testosterone precursor) from the circulation, given that our functional studie showed strong interaction of DrOat3 with DHEAS (Table 3.6).

OAT2/Oat2 transporters have greatly diversified in teleosts, a typical pattern observed in many genes when comparing teleost fish with other vertebrates which is probably a consequence of the fish specific WGD (Stegeman *et al*., 2010). However, in the case of OAT2, we would expect 2 orthologs in fish, as opposed to five observed in zebrafish, and 2-4 in other teleost fish (Table 3.2). Considering that all 5 zebrafish Oat2 co-orthologs are expressed at the mRNA level across zebrafish tissues that these proteins are functional *in vitro* (Figs 3.26, 3.30 and data not shown), we conclude that these are not pseudogenes.and that they are probably functional *in vivo*. We propose that diverse number of OAT2/Oat2 co-orthologs across the teleost species is a consequence of differential gene silencing after the WGD (Froschauer *et al*., 2006). While only one ortholog in all other tetrapods indicate that probably diversification of OAT2 proteins in teleosts happened after the emergence of jawed fish which followed the second round of the WGD (Froschauer *et al*., 2006). When we compare tissue expression pattern of 5 zebrafish OAT2 co-orthologs with human OAT2 that is highly

expressed in liver, moderately in kidney and low in testes, intestine and uterus (Simonson *et al*., 1994), none of the zebrafish Oat2 genes follows this pattern, and surprisingly none is expressed notably in liver (Fig. 3.5A). In kidney, Oat2c and Oat2e are found at moderate expression levels which resemble the pattern of human OAT2 and rat Oat2 (Simonson *et al*., 1994; Rizwan and Burckhardt, 2007). Apart for liver, a notable difference is the expression of DrOat2 members brain where Oat2b, 2d and 2e are moderately expressed as opposed to the lack of expression of OAT2/Oat2 in the mammalian brain (Rizwan and Burckhardt, 2007). Therefore, we suggest that Oat2 proteins in zebrafish have distinct function from mammalian OAT2/Oat2 transporters, with the only overlap in respect to the renal expression of Oat2c and Oat2e. It would be interesting to decipher substrate specificity of zebrafish OAT2 co-orthologs which could provide a window into the evolution of OAT2/Oat2 proteins in vertebrates.

A distinct OAT/Oat cluster that is specific to mammals and/or humans includes OAT4-7 and URAT1 (Fig 3.1). OAT4 is localized to the apical membranes of renal tubule cells, where it is responsible for the reabsorption of urate, prostaglandins and xenobiotics (Koepsell, 2013). In other vertebrates, this role is obviously fulfilled by another OAT. In fish, including zebrafish, considering wide diversification of OAT2 cluster, it is possible that Oat2c or/and Oat2e fulfil the function of OAT4. This could be determined only after the production of zebrafish specific antibodies in order to explore protein localization in the kidney and determination of substrate specificity for Oat2c and Oat2e. OAT5 function is currently unknown (Koepsell, 2013), whereas rat Oat6 has a very specific role in the olfactory sensing (Kaller *et al*., 2006). Since olfactory sensing is a trait very different in each vertebrate group, it is not surprising that in mammals a specific transporter emerged for the transport of negatively charged odor type molecules (Kaller *et al*., 2006). OAT7 is a liver specific transporter, localized to the basolateral membrane of hepatocytes and is specific for mammals (Fig 3.2). Considering the substrate overlap between OAT7 and OATP/Oatp transporters in terms of transport of steroid hormones conjugates (Table 1.1 and 1.2), and more particularly the overlap with the substrate specificity of Oatp1d1 (Table 3.4) and possibly Oatp2b1 which are both highly expressed in liver, we suggest that these transporters might compensate for the function of OAT7 in zebrafish and other teleosts. URAT1 is a kidney specific transporter localized to the apical membranes of renal proximal tubule cells with the function in urate reabsorption. Like OAT7, we have found that it is specific for mammals (Fig. 3.2). Given the fact that birds and reptiles do not excrete uric acid through the kidney, but rather through the intestine, we suggest that there is no need for the Urat1 transporter in their kidney. In fish, end product of purine metabolism is not uric acid, but ammonia, thus also making urate specific transporter unnecessary.

Within the ORCTL/Ocrtl3/4 cluster, one-to-one orthology relationships are present in all vertebrate groups (Table 3.2) indicating high degree of conservation and important physiological role of these transporters. ORCTL4 transporter is not yet characterized, and has so far been identified only on the genome level (Koepsell, 2013). ORCTL3 (novel annotation OAT10) (Koespell, 2013) was recently characterized and its main physiological role is proposed to be the uptake of vitamine nicotinate in the intestine and the uptake of urate in the kidney (Bahn *et al*., 2008). However, considering that we identified very clear one-to-one orthologies of ORCTL3/Orctl3 within the vertebrate subphylum, our results would suggest more conserved physiological role. In vertebrate groups, apart from mammals, there is no need for the urate reapsorption in kidneys, given the differences in the purine metabolism, whereas uptake of vitamin appears too specific. Our results regarding the tissue distribution of zebrafish Ortcl3 correspond to the human ORCTL3 expression (high expression in kidneys, moderate in intestine) (Fig. 3.5), which would suggest similar physiological role of ORCTL3/Ortcl3 from zebrafish to mammals.

OCT1/Oct1 and OCT2/Oct2 form a distinct cluster separate from the OCT3/Oct3 cluster. Within the OCT1/2 cluster, it is not possible to identify direct orthologs of human OCT1 and OCT2 genes in fish and other vertebrates (Fig. 3.2), but it is clear that all vertebrate species have 2 co-orthologs of mammalian OCT1/Oct1 and OCT2/Oct2. Our results indicate that zebrafish Oct1 resembles mammalian OCT1/Oct1, considering high expression of DrOct1 in zebrafish liver, while high expression in kidney goes in line with the high renal expression of rat and mouse Oct1 (but not human OCT1). Moderate expression of Oct1 in zebrafish brain resembles both, OCT1/Oct1 and OCT2/Oct2 in human and rodents (Koepsell *et al*, 2007, 2013; Nies *et al*., 2009). The only difference to the mammalian expression of OCT1/Oct1 genes is moderate expression in zebrafish testes, which was not observed in mammals. Zebrafish Oct2 on the other hand, differs in terms of tissue expression pattern from both mammalian co-orthologs, OCT1/Oct1 and OCT2/Oct2: it is highly expressed in testes, followed by moderate expression in the kidney and intestine. On the contrary, human OCT2 is primarily expressed in kidney, followed by brain, intestine, placenta and lungs (Koepsell *et al*., 2003; Ciarimboli *et al*., 2010). Similarity is present in respect that all three transporters, DrOct2, OCT1 and OCT2 are expressed in kidney and intestine (Table 1.2). Given that primary physiological role of OCT1 is elimination of compounds through the liver, while primary role of OCT2 is the elimination of compounds through kidney (Koepsell *et al*., 2013), and based on the comparions of their expression patterns, we suggest that zebrafish Oct1 might have a role similar to both, human OCT1 and OCT2, whereas zebrafish Oct2 could, given its moderate renal expression, be involved in the elimination of endogenus cations and drugs through the kidneys. In addition, considering moderate expression of zebrafish Oct1 in the brain, DrOct1 might be important in the transport of neurotransmitters and regulation of brain function, the role that both, OCT1 and OCT2,

fulfill in the mammalian brain (Koepsell *et al*., 2013). OCT3/Oct3 transporters emerged in higher tetrapods: they are found in the genomes of anole lizard, chicken and mammals, and are not present in amphibian *X. laevis* and fish (Fig. 3.2, Table 3.2). It is possible that due to the extensive substrate overlap among mammalian OCT1, 2 and 3 (Koepsell *et al*. 2003, 2007; Nies *et al*., 2010), Oct1 and 2 in zebrafish (and other fish) compensate for the function of Oct3.

OCTN group is highly conserved in vertebrates considering that two members are present in the majority of analyzed species (Fig 3.2, Table 3.2) and considering the presence of Octn transporters in a primitive chordate, *Ciona intestinalis* (Fig 3.2). High degree of evolutionary conservation would suggest crucial physiological role of these proteins, which is in line with the fact that their main physiological substrate is L-carnitine (Tamai *et al*., 1997), indispensible for the transport of long chain fatty acids into mitochondria, thus enabling their oxidation. The expression pattern of zebrafish Octn1 largely differs from its human counterpart: DrOctn1 is overall weakly expressed in all analyzed tissues, whereas human OCTN1 is ubiquitously expressed including kidney, intestine, brain, testes, lung and heart(Meier *et al*., 2007; Markova *et al*., 2009; Gilchrist and Alcorn, 2010; Lamhonwah *et al*., 2011). Considering that the main physiological role of OCTN1 is transport of ergothioneine, a naturally occurring amino acid, histidine derivative of unknown function (Nakamura *et al*., 2007), it seems possible that the transport of a given compound is not of importance in the analyzed zebrafish tissues and possibly DrOctn1 is expressed elsewhere. On the contrary, zebrafish Octn2 (DrOctn2) is highly expressed in kidney and testes and moderately expressed in intestine, which partly corresponds to the expression of human and rodent OCTN2/Octn2: OCTN2/Octn2 is expressed in the kidney and intestine, but not in the testes of mammals (Meier *et al*., 2007; Koepsell *et al*., 2013). Mammalian OCTN2/Octn2 plays a role in the absorption of L-carnitine in the small intestine, and its reapsorption in the renal proximal tubule. We propose the same role for zebrafish Octn2, considering similar expression levels in intestine and kidney. Additionally, zebrafish Octn2, given its high renal expression, might be responsible for the secretion and reapsorption of organic cations in the renal proximal tubule, similar to its mammalian counterpart OCTN2 which is localized to the apical side of renal cells (Tamai *et al*., 2001).

OCT6/Oct6 is the most conserved transporter of the SLC22/Slc22 family, with single ortholog found in all vertebrate species from fish to mammals (Fig. 3.1, Table 3.1). Apart from OCTN/Octn group, OCT6/Oct6 cluster is the only one that includes co-orthologs in tunicate *Ciona intestinalis*. This wouldsuggest an important physiological role in the cation transport which is in line with the fact that OCT6 is a high affinity L-carnitine transporter, similar to the OCTN2 (Enomoto *et al*., 2002). However, tissue expression pattern of OCT6/Oct6 partly differs in zebrafish when compared to mammals. In zebrafish, Oct6 is moderately expressed in kidney, followed by testes and intestine (Fig. 3.5), whereas in mammals, OCT6 is primarily expressed in testes where it regulates the

concentrations of L-carnitine and spermidine in spermatozoa (Koepsell *et al*., 2013). However, OCT6/Oct6 in mammals is also expressed in kidney, liver, brain, heart and other organs, although its physiological role in those tissues is not known (Enomoto *et al*., 2002; Eraly and Nigam, 2002; Kwok *et al*., 2006; Sato *et al*., 2007). In summary, zebrafish Oct6 most probably transports L-carnitine, given high degree of conservation of OCT6 orthologs and importance of L-carnitine transport, and it is possibly involved in the spermidine transport in testes. The role of DrOct6 in the kidney and intestine remains to be resolved after the functional characterization of DrOct6.

In summary, based on the phylogenetic analysis, tissue distribution patterns and comparison to mammalian SLC22/Slc22 transporters, we propose that zebrafish Slc22 transporters of potential ecotoxicological relevance and candidates for functional characterization are Oat3, Oat2c and Oat2e in the kidney, Oct2 in liver, and Oat2d in intestine.

4.4. Zebrafish Oat3, Oat2c and Oat2d

Function of mammalian OAT1/Oat1 and OAT3/Oat3 transporters is similar in the respect that they are both dominant in the kidney where they uptake compounds from the circulation into the renal tissue, and that they both play important role in the anion transport across the blood-brain barrier (BBB) (Rizwan and Bueckhardt, 2007). Zebrafish Oat3 resembles the expression pattern of mammalian OAT1/Oat1 and OAT3/Oat3 (Fig. 3.21), as opposed to the DrOat1 which is primarily expressed in the testes and moderately expressed in the brain. Considering that DrOat3 is the only OAT1/3 co-ortholog in zebrafish kidney, we propose that it plays a role in the elimination of endogenous anions and xenobiotcs in zebrafish kidney, similar to the mammalian co-orthologs OAT1/Oat1 and OAT3/Oat3. When we compare substrate affinities for two model substrates of OATs (pAH and E3S) between zebrafish Oat3 and mammalian OAT1/Oat1 and OAT3/Oat3 (human, mouse and rat), we have found that: (1) Oat3 transports E3S which is similar to OAT3, but not to OAT1 (E3S transport by rat and mouse Oat1 is inconclusive) (Rizwan and Burckhardt, 2007); and (2) affinity of DrOat3 towards model anion pAH is 112 µM, which resembles OAT1/Oat1 orthologs in human and mouse (OAT1, K_m = 3.1 - 133 µM depending on the expression system; rat Oat1, K_m = 42 µM; mouse Oat1, K_m = 37 - 162 µM depending on the expression system), as well as human OAT3 (K_m = 20 - 87 µM) (Burckhardt, 2012).

Comparison of interactors and their interaction strengths between zebrafish Oat3 and mammalian OAT1/Oat1 and OAT3/Oat3 are summarized in Table 4.1. Among the physiological interactors, DrOat3 shows strong to moderate interaction with glutarate, DHEAS and cGMP. Given that these three physiologically important compounds are substrate of mammalian OAT1/Oat1

and/or OAT3 transporters, we suggest that these are in fact substrates of DrOat3,. Importantly, although substrate overlap of OAT1 and OAT3 is substantial (Ahn and Nigam, 2009), one of the differences among these transporters is the transport of DHEAS by OAT3, important steroid hormone precursor which is not transported by human and rat OAT1/Oat1. Our results would therefore suggest that DrOat3 is more similar to OAT3 than to OAT1. Considering that DrOat3 transports E3S and probably DHEAS, we suggest that DrOat3 is important for the uptake of sulfated steroid hormones from the circulation into the kidney, brain and testes. Zebrafish Oat3 does not show interaction with propionate at 100 μM concentration. Considering that propionate is a typical substrate of OATs (Burckhardt, 2012), there is a possibility that Oat3 transports the compound with smaller affinities (K_m > 300 μM). Lack of urate transport by DrOat3 (Table 4.1) was partly expected considering that fish mainly excrete nitrogen waste metabolites as ammonia through the gills (Forster and Goldstein, 1969). Considering studies on the mouse knock out (KO) models which showed that thymidine transport is one of the important roles of OAT3/Oat3 *in vivo* (Ahn and Nigam, 2009), it seems that this particular function of Oat3 is not conserved in zebrafish. Therefore, another anion transporter may be responsible for the thymidine elimination through zebrafish kidney, possibly Oat2d or Oat2e which are strongly expressed there.

Typical pharmaceuticals transported by OAT1 and OAT3 and eliminated through the kidney include benzylpenicillin, H2 receptor agonist cimetidine, NSAID ibuprofen, diuretic furosemide and methotrexate, whereas typical inhibitor drug is probenecid. Strong interaction of DrOat3 with ibuprofen and furosemide resembles mammalian transporters (Table 4.1), as well as moderate interaction with benzylpenicillin and cimetidine. Pronounced difference is present in the interaction with probenecid, a strong inhibitor of OAT1/Oat1 and OAT3 (Table 4.1) which does not inhibit DrOat3 at 100 μM concentration. On the contrary, we have observed activation of DrOat3 mediated pAH transport by probenecid which could indicate allosteric activation as well as possible difference between inhibitor binding site/s of mammalian and zebrafish OAT1/Oat1 and OAT3/Oat3 co-orthologs.

Table 4.1. Comparison of interaction profiles of zebrafish Oat3 with human OAT1 and OAT3 and rat and mouse Oat1 (rOat1 and mOat1) for a set of selected interactors. Physiological interactors are separated from xenobiotic interactors with dotted line (S, substrate; I, inhibitor; na, not available).

	DrOat3	**OAT1**	**OAT3**	**rOat1**	**mOat1**
E3S[H^3]	S	no transport	Km = 3.1uM	inconclusive	inconclusive
pAH [H^3]	K_m = 112 µM	K_m = 3 - 113 µM	K_m = 20 - 187 µM	K_m = 42 µM	K_m = 37 - 162 µM
cGMP	moderate interaction	S	na	na	na
α-ketoglutarate	weak interaction	S	S	na	na
Glutarate	K_i = 2.2 µM	S	K_m = 5 - 38 µM	I	K_i = 6.7 µM (S)
Propionate	no interaction	S	S	na	na
TCDC[1]	no interaction	no interaction	na	no interaction	na
Urate	no interaction	K_m = 200 - 943 µM	S	na	na
DHEAS[2]	strong interaction	no transport	S	no transport	na
Folate	no interaction	na	na	na	na
Thymidine	weak interaction	na	na	na	na
Indoxyl-sulfate	no interaction	na	na	na	na
Benzylpenicillin	moderate interaction	I	na	K_m = 2007 µM	na
Cimetidine	moderate interaction	K_i = 492 µM (S)	I	inconclusive	K_i = 1038 µM
Ibuprofen	strong interaction	K_i = 1.4 - 8 µM (S)	na	K_i = 4 µM	K_i = 4.7 µM
Furosemide	K_i = 0.35 µM	K_i = 14 - 20 µM (S)	na	K_i=9.5 (S)	K_i = 8.1 µM
Methotrexate	moderate interaction	K_m = 724 µM	na	K_m = 0.9 - 15 µM	K_i = 901 µM (S)
Probenecid	activation	K_i = 4 - 13 µM (S)	I	K_i = 1.4 - 31 µM	K_i = 6.4 µM

[1] Taurochenodeoxycholate

[2] Dehydroepiandrosterone sulfate

The comparison of interacting compounds of zebrafish Oat3 and flounder Oat1 (fOat1) is unfortunately not possible, because in the study by Ashlamkan *et al*. (2006) only three compounds were examined for their interaction with fOat1: E3S, antiviral drug adefovir and herbicide 2,4-D. The similarity is present inrespect to E3S and 2,4-D, which showed strong interaction with both transporters, but the dataset is too small for the strong conclusions about the similarity of these two fish transporters.

In summary, zebrafish Oat3 is involved in the transport of pAH, cGMP, glutarate and conjugated steroid hormones, E3S and DHEAS, similar to the human OAT3 and partly to the human and rodent OAT1/Oat1, whereas interaction of DrOat3 with a range of xenobiotics indicates its function in the elimination of xenobiotics through the kidney, similar to the role of its human counterparts, OAT1 and OAT3 (Sekine *et al*., 1997; Kobayashi *et al*., 2005a). Given that the other Oat1/3 co-ortholog, zebrafish Oat1, is primarily expressed in testes and to a lesser extent in the brain, this transporter is probably not crucial for the elimination of xenobiotics in zebrafish.

Human OAT2 transports pAH and E3S, but kinetic parameters were not determined for neither of them (Kobayahi *et al*., 2005). It was observed that pAH uptake mediated by OAT2 was much lower than for OAT1 and 3 (Rizwan and Burckhardt, 2007). Both zebrafish OAT2 co-orthologs differ from

their mammalian counterparts in these aspects: E3S uptake by zebrafish Oat2c and 2d is comparable to the E3S uptake of DrOat3 (Table 4.1 and 4.2), whereas Oat2c affinity towards pAH is 2 times higher than the one for DrOat3 (Table 4.1 and 4.2). DrOat2d affinity towards pAH is similar to the DrOat3 (Table 4.1 and 4.2). Both zebrafish Oat2 transporters substantially differ from mammalian co-orthologs, human and rat OAT2/Oat2, if comparison of interactors is taken into account (Table 4.2). Most pronounced difference is the lack of interaction of zebrafish Oat2c and 2d with cGMP, a second messenger that is one of the principal substrates of OAT2 (Cropp *et al*., 2008).

Physiological substrates of Oat2c include only E3S, pAH, and possibly α-ketoglutarate, which differentiates this transporter from human OAT2 and rat Oat2 that transport a wide range of physiological substrates including prostaglandins, cGMP, glutarate and α-ketoglutarate (Table 4.2). Similarly, comparison of xenobiotic interactors of DrOat2c differs from the human and rat OAT2/Oat2, with only resemblance in the interaction with ibuprofen and probenecid. However, while ibuprofen is in the same range of moderate interaction strength among these transporters, probenecid is considerably stronger inhibitor of DrOat2c than of OAT2 (Table 4.2). Tissue distribution of Oat2c differs significantly from mammalian co-orthologs which are found in liver and kidney, followed by intestine, brain, lung and heart (Cropp *et al*., 2008), whereas Oat2c is expressed predominantly in the kidney and testis. In human kidney, OAT2 is located at the basolateral membrane of renal cells where it transports urate, organic anions and drugs into the kidney, thus playing important role in the renal elimination of metabolites and drugs. It is possible that Oat2c, which shows high expression in kidneys, fulfills this role. However, two facts go against this hypothesis: (1) Oat2c did not interact with any of the tested drugs apart from ibuprofen, probenecid and herbicide 2,4D (Fig. 3.27), and (2) the localization of Oat2c in kidneys remains unknown. Contrary to the majority of OATP and OAT transporters, where tissue localization is conserved among the species (Burckhardt, 2012; Hagenbuch and Stieger, 2013), OAT2 localization differs among human and rodents. In humans, OAT2 is found on the basolateral side of renal proximal tubule cells, whereas in rats and mouse, Oat2 is localized on the apical side of renal cells (Enomoto *et al*., 2002; Ljubojevic *et al*., 2007). Thus, the function of the transporters differ as well: human OAT2 primarily mediates uptake of compounds from the circulation into the liver and kidney, whereas rodent Oat2 at the brush-border of renal tubular cells mediates reapsorption of urate and other organic anions from renal lumen (Rizwan and Burckhardt, 2007). It is important to mention that OAT2 is capable of bidirectional transport, thus transporting compounds back to the circulation at the basolateral side of renal cells in humans, as well as transporting them to the renal lumen at the apical membrane (Cropp *et al*., 2008). Considering the complexity and differences in OAT2/Oat2 mediated transport in mammals, without the specific antibody to determine localization of zebrafish Oat2c it is difficult to infer its possible function based solely on the knowledge about mammalian co-orthologs.

Table 4.2. Comparison of interaction profiles of zebrafish Oat2c and Oat2d with human OAT2 (OAT1) and rat Oat2 (rOat2) for a set of chosen interactors. Physiological interactors are separated from xenobiotic interactors with dotted line (S, substrate; I, inhibitor; na, not available).

	DrOat2c	**DrOat2d**	**OAT2**	**rOat2**
E3S[H^3]	1.4 fold	2.2 fold	S (weak)	not transported
pAH [H^3]	K_m = 44.4 µM	K_m = 125 µM	S	S
cGMP	120	128	K_m = 88 µM	na
α-ketoglutarate	moderate interaction	K_i = 1.2 µM	inconclusive	inconclusive
Glutarate	no interaction	K_i = 3.0 µM	S	na
Propionate	127	135	na	na
Cholate	122	na	no interaction	no interaction
Taurocholate	131	K_i = 13 µM	no interaction	I
PGE2[1]	no interaction	-	K_m = 0.7 µM	K_m = 39 µM
Urate	no interaction	K_i = 2.2 µM	na	na
Folate	no interaction	K_i = 2.8 µM	na	na
Salicylate	140	38	no interaction	S
Benzylpenicillin	weak interaction	96	na	inhibitor
Cimetidine	no interaction	38	S	weak interaction
Ibuprofen	moderate interaction	na	K_i = 692 µM	K_i = 155 µM
Furosemide	-	42	K_i = 603 µM	-
Methotrexate	no interaction	78	K_i = 8.9 µM (S)	inconclusive
Probenecid	K_i = 5.4 µM	K_i = 3.0 µM	K_i = 766 µM	na
2,4D[2]	K_i = 25.1 µM	K_i = 16.2 µM	na	na

[1] Prostaglandin E2

[2] 2,4 - dichlorophenoxyacetic acid

Contrary to the zebrafish Oat2c, Oat2d shows some similarity with human OAT2 and rat Oat2 in respect to interactions with endogenous and xenobiotic substrates of human and rat OAT2/Oat2 (Table 4.2). However, tissue distribution profiles differ significantly: Oat2d is primarily expressed in intestine, testes and brain, as opposed to primary expression of human and rodent OAT2/Oat2 in the liver and kidney (Burckhardt, 2012). Similar to the mammalian co-orthologs, Oat2d strongly interacts with glutarate and α-ketoglutarate, as well as with a wide range of pharmaceuticals, including salicylate, cimetidine, furosemide, methotrexate and probenecid (Table 4.2). Difference is present in respect to cGMP transport, as mentioned above, as well as to taurocholate transport (Table 4.2). Overall, our data show that Oat2c and Oat2d do not resemble their mammalian co-orthologs, human and rodent OAT2/Oat2 in respect to tissue distribution and interaction with endogenous and xenobiotic compounds. Considering that none of the zebrafish co-orthologs is expressed in liver (Fig. 3.5A), while OAT2 in humans have indispensable role at the basolateral membrane of hepatocytes in the uptake of glutamate and various drugs and toxins, thus enabling their elimination (Burckhardt, 2012), we suggest that other organic anion transporters, probably from the OATP family, compensate for this role in zebrafish liver (Fig. 3.5A).

In summary, we have performed initial characterization of the three zebrafish OATs of potential toxicological relevance. We suggest that Oat3 is important for the elimination of foreign compounds through the kidney. Oat2c might also be of considerable importance for renal elimination of xenobiotics, which remains to be confirmed after localization of Oat2c is determined and more xenobiotic interactors are tested. Similar to Oat2c, after determining the localization of Oat2d its importance in the elimination of endogenous and xenobiotic compounds through intestine could be determined. The next research steps for all three zebrafish Oats should include optimization of the uptake assay with the fluorescently labeled model substrates which would enable distinguishing substrates from inhibitors of zebrafish Oats through the Michaelis-Menten analysis similar to the approach applied for the detailed characterization of Oatp1d1. So far, we have identified 6CF as a substrate of DrOat3 and Oat2c, and 5CF and 6CF as substrates of DrOat2d.

4.5. Interaction of environmental contaminants with the uptake transporter, Oatp1d1

Liver is the principal organ of xenobiotic metabolism and their subsequent elimination through bile (and later on feces). Physiological metabolites, including steroid hormones and their conjugates, as well as many xenobiotics and their metabolites are eliminated through this pathway. Given that functional orthologs of Oatp1d1 – human OATP1B1 and OATP1B3 – are expressed on the basolateral membrane of hepatocytes, we presumed the same for zebrafish Oatp1d1. In that case, Oatp1d1 would mediate the uptake of compounds from the circulation into hepatocytes, thus enabling their metabolism and subsequent elimination. We have shown that zebrafish Oatp1d1 transports conjugated steroid hormones E3S, estradiol-17β-glucuronide and DHEAS with high affinity (Table 3.4). Therefore, potent modulators of Oatp1d1 activity present in the aquatic environment could disrupt the uptake of excess steroid hormone conjugates from the circulation, ultimately resulting in hormonal disbalance and changes in the reproduction behavior (James, 2011). Very potent inhibitors of Oatp1d1, like PFOA, E1 and E2 (Tables 3.9 and 3.10) may block the Oatp1d1 mediated entry of conjugated steroids into hepatocytes, resulting in the alteration of plasma levels of steroid hormones and subsequent endocrine disruption. On the other hand, substrates of Oatp1d1, including PFOS, nonylphenol, EE2, Gfb and diclofenac, would enter hepatocytes through Oatp1d1 mediated uptake, which would enable their metabolization in fish liver, and in some cases elimination through bile.

Considering high expression of Oatp1d1 in testes (Fig 3.6), disruption of Oatp1d1 transport activity by environmental chemicals would prevent the uptake of the Oatp1d1 high affinity substrate DHEAS, a testosterone precursor, into testes. Alteration of DHEAS concentration in testes, caused by

the impaired transport activity of Oatp1d1, could in turn lead to the alteration of testosterone levels, and potentially to endocrine disruption effects. Therefore, we hypothesize that very potent Oatp1d1 inhibitors including PFOA, estrone and E2 could interfere with testosterone synthesis in the testes through the inhibition of Oatp1d1 mediated DHEAS transport. In contrast, Oatp1d1 mediated uptake of high affinity xenobiotic substrates, including PFOS, nonylphenol, EE2, diclofenac and Gfb, may lead to the entry of these compounds from the circulation into the testicular tissue where they can exert their effects.

Endocrine disruption effects of PFOA, PFOS, nonylphenol and EE2 have been well documented in fish (Kudo *et al*., 2002; Sumpter, 2002; Du *et al*., 2009; White *et al*., 2011). PFOA and PFOS may occur in high concentrations in the liver, plasma and kidneys of fish, with maximum levels reaching 2 mg/kg wet mass (Du *et al*., 2009). These concentrations are in the range of the effective values for Oatp1d1 modulation determined in this study, with K_i of 0.4 and 9 µM for PFOA and PFOS, respectively (Table 3.9). Consequently, environmentally relevant concentrations of PFOA and PFOS could interfere with the Oatp1d1 mediated uptake of excess steroid hormone conjugates into hepatocytes. That inhibition could in turn result in the alteration of the steroid hormone plasma levels, as was observed in fish after exposure to PFOS and/or PFOA (Kudo *et al.,* 2002; Hagenaars *et al*., 2008; Du *et al.*, 2009). In testes, considering very high affinity of Oatp1d1 for DHEAS uptake, presumably from the circulation (K_i = 0.68 µM) (Tables 3.3 and 3.4), PFOS would not interfere with the DHEAS transport, given its 20-times lower affinity in comparison to DHEAS (Tables 3.3 and 3.9). On the contrary, very strong inhibition of Oatp1d1 activity by PFOA (K_i = 0.39 µM) could be significant. Therefore, our data indicate that modulation of Oatp1d1 uptake activity may be considered as a novel factor explaining adverse effects of PFOA and PFOS.

Nonylphenol bioaccumulates in fish up to 1.59 mg/kg (Snyder *et al*., 2001), which is in the range of concentrations required to modulate Oatp1d1 activity (K_i = 9.4 µM) (Table 3.9, Fig. 3.37). Metabolism of nonylphenol results in formation of the glucuronide conjugate, which is excreted through bile (Vazquez-Duhalt *et al*., 2005). Based on our analysis we suggest that Oatp1d1 is the principal transporter for the uptake of nonylphenol into hepatocytes, thus enabling its glucuronidation. We also propose that Oatp1d1 may be the major transporter implicated in the uptake of nonylphenol in testes, enabling nonylphenol mediated alteration of gene expression through the interaction with androgen (AR) and estrogen receptors (ER) (Vazquez-Duhalt *et al*., 2005).

Most abundant synthetic estrogens found in surface waters include E2, EE2 and E1 (Murray *et al*., 2010; Sumpter and Jobling, 2013). Given that EE2 is a high affinity substrate of Oatp1d1 (K_i = 5.93 µM), and E1 and E2 are potent Oatp1d1 inhibitors (K_i = 1.04 µM and 2.83 µM), these compounds

could modulate Oatp1d1 transport activity in liver, testes and brain at the environmentally relevant concentrations (Murray *et al*., 2010). In addition, since EE2 acts as an Oatp1d1 substrate, it probably enters these target tissues through the Oatp1d1 mediated uptake from the circulation. Consequently, based on our data we propose that modulation of Oatp1d1 uptake activity may be considered as a novel factor that contributes to the endocrine disruption effects of synthetic estrogens.

In addition to perfluorinated compunds (PFCs) and synthetic estrogens, it has been observed in recent studies that Gfb, a lipid lowering drug, may be implicated in the endocrine disruption effects in fish (Mimeault *et al*., 2005; Fent *et al*., 2006). Fibrates are one of the most abundant pharmaceuticals occurring in surface waters where Gfb is found at 0.048 - 0.052 µg/L (Corcoran *et al*., 2010). Despite low water concentration, Gfb has a high bioaccumulation factor and therefore higher concentrations might actually be present in the organism (Mimeault *et al*., 2005). Considering that Gfb is a potent modulator of Oatp1d1 (K_i = 7.45 µM), and given its high bioaccumulation factor, our data indicate that Gfb could interfere with the steroid hormone transport mediated by Oatp1d1 in liver and testes. This may partly explain the reduced plasma concentrations of androgen and testosterone observed in testes of goldfish after Gfb exposure (Mimeault *et al*., 2005).

Overall, considering that zebrafish is recognized as an excellent model to study endocrine disruption (Segner, 2009), characterization of the uptake processes of endocrine disrupting chemicals is a necessary prerequisite for the reliable utilization of this valuable model.

The most potent Oatp1d1 interactor found in our study is diclofenac, a high affinity substrate of Oatp1d1 (K_i = 0.23 µM) (Table 3.10). Diclofenac occurs in surface waters at concentrations up to 1.8 µg/L (Murray *et al*., 2010). Considering that the affinity of Oatp1d1 towards diclofenac was 5-fold, 10-fold and 60-fold higher than towards the physiological substrates of Oatp1d1: estrone 3-sulfate, estradiol-17β-glucuronide and cortisol, respectively, we hypothesize that environmentally relevant concentrations of diclofenac may significantly interfere with the Oatp1d1-mediated transport of these hormones.

The blood brain barrier (BBB) prevents the uptake of xenobiotics into brain and delivers essential nutrients and hormones to the brain through the action of membrane transporters belonging to the ABC superfamily (ATP Binding Cassette), and OATP/Oatp and SLC22/Slc22 families (Gao *et al.*, 2000; Pizagalli, 2002; Uchida *et al.*, 2011). High expression of Oatp1d1 in the zebrafish brain and its similarity in substrate specificities to the OATP1A/Oatp1a group suggests that Oatp1d1 may have a potentially important role at the BBB, similar to the OATP1A/Oatp1a transporters in mammals (Badagnani *et al*., 2006). Furthermore, high expression of Oatp1d1 in the zebrafish brain, the high affinity towards DHEAS, and the high inhibition potencies of PFOA, E2 and E1 at environmental

relevant concentrations, implies that these compounds may reduce the transport of DHEAS across the BBB, thus interfering with the balance of this essential neurosteroid. On the other hand, environmental contaminants that act as high affinity substrates of Oatp1d1, including diclofenac, Gfb, nonylphenol and PFOS, would be transported by Oatp1d1 across the BBB.

Another frequently occurring environmental chemical, caffeine, primarily acts through the interaction with adenosine receptors in the brain, which leads to the increase in the level of neurotransmitters. So far it was not known how caffeine enters the brain. Here we showed that Oatp1d1 transports caffeine with moderate affinity (Tables 3.9 and 3.10), in the range of environmentally relevant concentrations (Murray *et al*., 2010), as well as within the range (mg/L) of reported plasma levels of caffeine in fish (Gomez-Martinez, 2011). To our knowledge, this is the first report about the interaction of caffeine with OATPs/Oatps, a finding that could be relevant for the evaluation of adverse drug interactions in medical studies, especially considering high plasma concentrations of caffeine in humans (Fisone *et al*., 2004).

Organophosphate pesticides, diethyl phthalate (DEP) and ibuprofen showed strong to moderate interaction with Oatp1d1. However, their environmental loads (Murray *et al*., 2010) are not sufficient to reach effective concentrations required to modulate Oatp1d1 activity (Table 3.9). The same is true for the low affinity Oatp1d1 substrates: BisA, clofibrate and AHTN (Murray *et al*., 2010).

In summary, this is the first study that addressed the uptake phase in the disposition of contaminants in any aquatic organism, and Oatp1d1 is the first xenobiotic uptake transporter characterized in fish. Our data clearly indicated the involvement of zebrafish Oatp1d1 in the transport of a considerable diversity of environmentally relevant compounds. We determined that PFOS, nonylphenol, Gfb, diclofenac, EE2 and caffeine are high affinity substrates of zebrafish Oatp1d1, while PFOA and synthetic estrogens, E2 and E1 are potent Oatp1d1 inhibitors at the environmentally relevant concentrations. Although acting differently, both groups of compounds could potentially disrupt normal Oatp1d1 transport function in fish.

Most importantly, considering the tissue localization of Oatp1d1 and data on its detailed functional characterization obtained in this study, we can reliably hypothesize that its inhibition could be implicated in:

(1) the inhibition of Oatp1d1-mediated uptake of excess steroid hormone conjugates into hepatocytes, and

(2) the inhibition of Oatp1d1-mediated DHEAS uptake in the brain and testes, which could in turn potentially cause physiological effects in fish.

Likewise, the inhibition of Oatp1d1 by many environmental contaminants further emphasizes their potential effects in modulating uptake processes. We believe the presented characterization of

Oatp1d1 in relation to its interaction with environmentally relevant contaminants will foster better understanding of the mode(s) of action of tested compounds, and enable more accurate predictions of their disposition and possible harmful effects in fish.

Finally, considering that zebrafish is recognized as an excellent model in (eco)toxicological research and a detailed characterization of the uptake processes is a necessary prerequisite for its reliable use, we believe data from this work will significantly contribute to this overall goal.

5. Conclusions

1. Polyspecific uptake transporters in zebrafish are encoded with 14 *Slc21* genes and 14 *Slc22* genes. Organic anion transporting polypeptides (Oatps; gene name *Slc21/Sl*) encompass 5 subfamilies: (1) Oatp1 with 7 genes: Oatp1c1, 1d1, 1d2, and 1f1-1f4; (2) Oatp2 that includes Oatp2a1 and 2b1; (3) Oatp3 with Oatp3a1 and 3a2; (4) Oatp4 with a single member, Oatp4a1; and (5) Oatp5 subfamily with Oatp5a1 and 5a2. *Slc22* genes in zebrafish encode: (1) seven Organic anion transporters (Oats): Oat1, Oat2a-e and Oat3, (2) five organic cation and carnitine transporters (Octs and Octns): Oct1, Oct2, Oct6, Octn1 and Octn2, and (3) two organic anion transporter-like genes: Ocrtl3 (syn. Oat10) and Orctl4.

2. Tissue expression analysis and phylogenetic relationships with mammalian co-orthologs suggest that following transporters could be crucial for cellular ADME (Apsorption, Distribution, Elimination and Excretion) processes in fish: Oatp1d1 in liver; Oatp2b1 in liver, kidney and gills; Oat3 Oat2c and 2e in kidney; Oat2d in intestine; and Oct1 in liver.

3. Molecular characterization of Oatp1d1, a novel zebrafish transporter, offered important insights into the functional evolution of OATP1/Oatp1 subfamily and the physiological role of Oatp1d1:

a) diversification of the OATP1/Oatp1 subfamily occurred after the emergence of jawed fish, OATP1A/Oatp1a and OATP1B/Oatp1b groups appeared at the root of tetrapods and Oatp1d group emerged in teleosts and is absent in tetrapods;
b) zebrafish Oatp1d1 is functional ortholog of mammalian OATP1A/Oatp1a and OATP1B/Oatp1b members, with the main physiological role in transport and balance of steroid hormones, and
c) Oatp1d1 activity is dependent upon pH gradient which could indicate bicarbonate exchange as a mode of transport.

4. Our analysis of evolutionary conservation and structural properties of Oatp1d1 revealed that:
a) H79 in the intracellular LP3 is conserved within OATP1/Oatp1 subfamily and is crucial for the transport activity;
b) N-glycosylation impacts membrane targeting and is conserved within the OATP1/Oatp1 subfamily with N122, N133, N499 and N512 residues involved;
c) Evolutionary conserved CRAC motif is important for membrane localization;
d) Oatp1d1 is present in dimeric and probably oligomeric form in the cell membrane with highly conserved glycophorin motifs in TMD5 and TMD8 involved in the oligomer formation.

5. Initial characterization of the three zebrafish Oats of potential toxicological relevance revealed that:

a) Oat3 transports physiologically important compounds including pAH, cGMP, glutarate and conjugated steroid hormones (E3S and DHEAS), similar to the human and rodent OAT3/Oat3 and it is probably important for the elimination of foreign compounds through the kidney;

b) Mammalian OAT2/Oat2 co-ortholog in zebrafish, Oat2c, might be of considerable importance for renal elimination of xenobiotics, whereas Oat2d probably has a role in the xenobiotic transport in intestine.

6. Oatp1d1 is the first characterized *Slc* (*Solute carrier*) transporter in aquatic organisms in the context of interaction with environmental contaminants. It transports wide range of environmental contaminants at the environmentally relevant concentrations, including diclofenac, PFOS, nonylphenol, Gfb, EE2 and caffeine. Furthermore, its transport activity can be inhibited by PFOA and estrone, at the concentrations found in the aquatic environment.

7. Considering tissue localization of Oatp1d1 and data on its substrate specificity, we can hypothesize that its inhibition by environmental contaminants could be implicated in:

a) the inhibition of Oatp1d1-mediated uptake of excess steroid hormone conjugates into hepatocytes, and

b) the inhibition of DHEAS uptake in the brain and testes, which could in turn cause physiological effects in fish.

In summary, this PhD thesis represents the first comprehensive characterization of membrane proteins from OATP/Oatp and SLC22/Slc22 families in fish and provides important insights into the function of these important cellular determinants of toxicological response.

6. References

Abrahamson, A., Andersson, C., Jönsson, M.E., Fogelberg, O., Orberg, J., Brunström, B., Brandt, I., 2007. Gill EROD in monitoring of CYP1A inducers in fish: a study in rainbow trout (Oncorhynchus mykiss) caged in Stockholm and Uppsala waters. Aquat. Toxicol. 85, 1–8.

Adachi,H., Suzuki, T., Abe, M., Asano, N., Mizutamari, H., Tanemoto, M., Nishio, T., Onogawa, T., Toyohara, T., Kasai, S., Satoh, F., Suzuki, M., Tokui, T., Unno, M., Shimosegawa, T., ..., Abe, T., 2003. Molecular characterization of human and rat organic anion transporter OATP-D. Am. J. Physiol. Renal Physiol. 285, 1188–97.

Ahn, S-Y. and Nigam, S.K., 2009. Toward a systems level understanding of organic anion and other multispecific drug transporters: A remote sensing and signaling hypothesis. Mol. Pharmacol. 76, 481–490.

Ahn, S-Y. and Bhatnagar, V., 2008. Update on the molecular physiology of organic anion transporters. Curr. Opin. Nephrol. Hypertens. 17, 499–505.

Alebouyeh, M., Takeda, M., Onozato, M.L., Tojo, A., Noshiro, R., 2003. Expression of human organic anion transporters in the choroid plexus and their interactions with neurotransmitter metabolites. J. Pharmacol. Sci. 436, 430–436.

Ali, M.H. and Imperiali, B., 2005. Protein oligomerization: how and why. Bioorg. Med. Chem. 13, 5013–20.

Amores, A., Force, A., Yan, Y.-L., Joly, L., Amemiya, C., Fritz, A., Ho, R.K., Langeland, J., Prince, V., Wang, Y.-L., Westerfield, M., Ekker, M., Postlethwait, J.H.1998. Zebrafish hox Clusters and Vertebrate Genome Evolution. Science. 282, 1711–14.

Aouida, M., Poulin, R., Ramotar, D., 2010. The human carnitine transporter SLC22A16 mediates high affinity uptake of the anticancer polyamine analogue bleomycin-A5. J. Biol. Chem. 285, 6275–84.

Aslamkhan, A.G., Thompson, D.M., Perry, J.L., Bleasby, K., Wolff, N. A, Barros, S., Miller, D.S., Pritchard, J.B., 2006. The flounder organic anion transporter fOat has sequence, function, and substrate specificity similarity to both mammalian Oat1 and Oat3. Am. J. Physiol. Regul. Integr. Comp. Physiol. 291, R1773–80.

Badagnani, I., Castro, R.A., Taylor, T.R., Brett, C.M., Huang, C.C., Stryke, D., Kawamoto, M., Johns, S.J., Ferrin, T.E., Carlson, E.J., Burchard, E.G., Giacomini, K.M., 2006. Interaction of methotrexate with Organic-Anion Transporting Polypeptide 1A2 and its genetic variants. J. Pharmacol. Exp. Ther. 318, 521–529.

Bahn, A., Hagos, Y., Reuter, S., Balen, D., Brzica, H., Krick, W., Burckhardt, B.C., Sabolic, I., Burckhardt, G., 2008. Identification of a new urate and high affinity nicotinate transporter, hOAT10 (SLC22A13). J. Biol. Chem. 283, 16332–41.

Bendayan, R., Silverman, M., Cells, L., Bendayan, P., 1994. Characterization of cimetidine transport in LLCPKI cells. J. Am. Soc. Nephrol. 5, 75-84.

Biran, J., Ben-Dor, S., Levavi-Sivan, B., 2008. Molecular identification and functional characterization of the kisspeptin/kisspeptin receptor system in lower vertebrates. Biol. Reprod. 79, 776–86.

Bleasby, K., Castle, J.C., Roberts, C.J., Cheng, C., Bailey, W.J., Sina, J.F., Kulkarni, A.V., Hafey, M.J., Evers, R., Johnson, J.M., Ulrich, R.G., Slatter, J.G., 2006. Expression profiles of 50 xenobiotic transporter genes in humans and pre-clinical species: a resource for investigations into drug disposition. Xenobiotica 36, 963–88.

Boaru, D.A., Dragoş, N., Schirmer, K., 2006. Microcystin-LR induced cellular effects in mammalian and fish primary hepatocyte cultures and cell lines: a comparative study. Toxicology 218, 134–48.

Boussif, O., Lezoualc'h, F., Zanta, M.A., Mergny, M.D., Scherman, D., Demeneix, B., Behr, J.P., 1995. A versatile vector for gene and oligonucleotide transfer into cells in culture and in vivo: Polyethylenimine. Proc. Natl. Acad. Sci., 92, 7297-301.

Boron, W. F. and Weer, de P., 1976. Intracellular pH transients in squid giant axons caused by C02, NH3 and metabolic inhibitors. J.Gen. Physiol. 67, 91-112.

Boyarsky, G., Hanssen, C., Clyne, L.A., 1996. Superiority of in vitro over in vivo calibrations of BCECF in vascular smooth muscle cells. FASEB J. 10, 1205-12

Boyer, J.L., Schwarz, J. , Smith, N., 1976. Biliary secretion in elasmobranchs. II. Hepatic uptake and biliary excretion of organic anions. Am. J. Physiol. 230, 974-81.

Boyer, J.L., Hagenbuch, B., Ananthanarayanan, M., Suchy, F., Stieger, B., Meier, P.J., 1993. Phylogenic and ontogenic expression of hepatocellular bile acid transport. Proc. Natl. Acad. Sci. 90, 435-38.

Brast, S., Grabner, A., Sucic, S., Sitte, H.H., Hermann, E., Pavenstädt, H., Schlatter, E., Ciarimboli, G., 2012. The cysteines of the extracellular loop are crucial for trafficking of human organic cation transporter 2 to the plasma membrane and are involved in oligomerization. FASEB J. 26, 976–86.

Bronger, H., König, J., Kopplow, K., Steiner, H.-H., Ahmadi, R., Herold-Mende, C., Keppler, D., Nies, A.T., 2005. ABCC drug efflux pumps and organic anion uptake transporters in human gliomas and the blood-tumor barrier. Cancer Res. 65, 11419–28.

Budiman, T., Bamberg, E., Koepsell, H., Nagel, G., 2000. Mechanism of electrogenic cation transport by the cloned organic cation transporter 2 from rat. J. Biol. Chem. 275, 29413–20.

Burckhardt, G., 2012. Drug transport by Organic Anion Transporters (OATs). Pharmacol. Ther. 136, 106–30.

Burckhardt, G. and Wolff, N. A, 2000. Structure of renal organic anion and cation transporters. Am. J. Physiol. Renal Physiol. 278, F853–66.

Busby, E., Roch, G.J., Sherwood, N.M., 2010. Endocrinology of zebrafish; a small fish with a large gene pool. In Perry, S.F., Ekker, M., Farrell, A.P., Brauner, C.J. (Eds.), Zebrafish Elsevier, MA ,US , pp. 173-247.

Busch, A. E., Quester, S., Ulzheimer, J.C., Waldegger, S., Gorboulev, V., Arndt, P., Lang, F., Koepsell, H., 1996. Electrogenic properties and substrate specificity of the polyspecific rat cation transporter rOCT1. J. Biol. Chem. 271, 32599–604.

Cai, S.-Y., Wang, W., Soroka, C.J., Ballatori, N., Boyer, J.L., 2002. An evolutionarily ancient Oatp: insights into conserved functional domains of these proteins. Am. J. Physiol. Gastrointest. Liver Physiol. 282, G702–10.

Carvan, M. J., Gallagher, E. P., Goksoyr, A., Hahn, M. E., and Larsson, D. G., 2007. Fish models in toxicology. Zebrafish 4, 9-20.

Cheng, X., Maher, J., Chen, C., Klaassen, C.D., 2005. Tissue distribution and ontogeny of mouse organic anion transporting polypeptides (Oatps). Drug. Metab. Dispos. 33, 1062-73.

Ciarimboli, G., Deuster, D., Knief, A., Sperling, M., Holtkamp, M., Edemir, B., Pavenstädt, H., Lanvers-Kaminsky, C., am Zehnhoff-Dinnesen, A., Schinkel, A.H., 2010. Organic cation transporter 2 mediates cisplatin-induced oto- and nephrotoxicity and is a target for protective interventions. Am. J. Pathol. 176, 1169–80.

Clelland, E. and Peng, C., 2009. Endocrine/paracrine control of zebrafish ovarian development. Mol. Cell. Endocrinol. 312, 42–52.

Corcoran, J., Winter, M.J., Tyler, C.R., 2010. Pharmaceuticals in the aquatic environment: a critical review of the evidence for health effects in fish. Crit. Rev. Toxicol. 40, 287–304.

Cropp, C.D., Komori, T., Shima, J.E., Urban, T.J., Yee, S.W., More, S.S., Giacomini, K.M., 2008. Organic Anion Transporter 2 (SLC22A7) is a facilitative transporter of cGMP. Mol. Pharmacol. 73, 1151–58.

Csanaky, I.L., Lu, H., Zhang, Y., Ogura, K., Choudhuri, S., Klaassen, C.D., 2011. Organic anion-transporting polypeptide 1b2 (Oatp1b2) is important for the hepatic uptake of unconjugated bile acids: Studies in Oatp1b2-null mice. Hepatology 53, 272–81.

De Bruyn, T., Fattah, S., Stieger, B., Augustijns, P., Annaert, P. J., 2011. Sodium fluorescein is a probe substrate for hepatic drug transport mediated by OATP1B1 and OATP1B3. J. Pharm. Sci. 100, 5018-30.

Du, Y., Shi, X., Liu, C., Yu, K., Zhou, B., 2009. Chronic effects of water-borne PFOS exposure on growth, survival and hepatotoxicity in zebrafish: A partial life-cycle test. Chemosphere 74, 723–729.

Enomoto, A., Wempe, M.F., Tsuchida, H., Shin, H.J., Cha, S.H., Anzai, N., Goto, A., Sakamoto, A., Niwa, T., Kanai, Y., Anders, M.W., Endou, H., 2002. Molecular identification of a novel carnitine transporter

specific to human testis. Insights into the mechanism of carnitine recognition. J. Biol. Chem. 277, 36262–71.

Eraly, S. A., 2008. Implications of the alternating access model for organic anion transporter kinetics. J. Membr. Biol. 226, 35–42.

Eraly, S. A, Monte, J.C., Nigam, S.K., 2004. Novel slc22 transporter homologs in fly, worm, and human clarify the phylogeny of organic anion and cation transporters. Physiol. Genomics 18, 12–24.

Eraly, S. A and Nigam, S.K., 2002. Novel human cDNAs homologous to Drosophila Orct and mammalian carnitine transporters. Biochem. Biophys. Res. Commun. 297, 1159–66.

Eraly, S. A, Vallon, V., Vaughn, D. A, Gangoiti, J. A, Richter, K., Nagle, M., Monte, J.C., Rieg, T., Truong, D.M., Long, J.M., Barshop, B. A, Kaler, G., Nigam, S.K., 2006. Decreased renal organic anion secretion and plasma accumulation of endogenous organic anions in OAT1 knock-out mice. J. Biol. Chem. 281, 5072–83.

Evers, R. and Chu, X., 2008. Role of the murine Organic anion-transporting polypeptide 1b2 (Oatp1b2) in drug disposition and hepatotoxicity. Mol. Pharmacol. 74, 309–311.

Felsenstein, J., 1985. Confidence-limits on phylogenies - an approach using the bootstrap. Evolution 39, 783-791.

Feng, B., Dresser, M.J., Shu, Y., Johns, S.J., Giacomini, K.M., 2001. Arginine 454 and Lysine 370 are essential for the anion specificity of the Organic anion transporter, rOat3. Biochemistry 40, 5511–20.

Fent, K., Weston, A., Caminada, D., 2006. Ecotoxicology of human pharmaceuticals. Aquat. Toxicol. 76, 122–59.

Fischer, S., Klüver, N., Burkhardt-Medicke, K., Pietsch, M., Schmidt, A.-M., Wellner, P., Schirmer, K., Luckenbach, T., 2013. Abcb4 acts as multixenobiotic transporter and active barrier against chemical uptake in zebrafish (Danio rerio) embryos. BMC Biol. 11, 69.

Fisone, G., Borgkvist, A., Usiello, A., 2004. Caffeine as a psychomotor stimulant: Mechanism of action. Cell. Mol. Life Sci. 61, 857-72.

Forster, R.P., Goldstein, L., 1969. Formation of excretory products. In Hoar, W.S., Randall, D.J. (Eds), Fish physiology, Academic Press, NY, USA, pp. 56-90.

Fricker, G., Hugentobler, G., Meier, P.J., Kurz, G., Boyer, J.L., 1987. Identification of a single sinusoidal bile salt uptake system in skate liver. Am. J. Physiol. 253, G816-822.

Fricker, G., Dubost, V., Finsterwald, K., Boyer, J.L., 1994. Characteristics of bile salt uptake into skate hepatocytes. Biochemical J. 299, 665-670.

Froschauer, A., Braasch, I., Volff, J., 2006. Fish Genomes, Comparative Genomics and Vertebrate Evolution. Curr. Genomics 7, 43–57.

Fujiya, M., Musch, M.W., Nakagawa, Y., Hu, S., Alverdy, J., Kohgo, Y., Schneewind, O., Jabri, B., Chang, E.B., 2007. The Bacillus subtilis quorum-sensing molecule CSF contributes to intestinal homeostasis via OCTN2, a host cell membrane transporter. Cell Host Microbe 1, 299–308.

Furuichi, Y., Sugiura, T., Kato, Y., Shimada, Y., Masuda, K., 2010. OCTN2 is associated with carnitine transport capacity of rat skeletal muscles. Acta Physiol. 200, 57–64.

Gao, B., Hagenbuch, B., Kullak-Ublick, G. a, Benke, D., Aguzzi, A., Meier, P.J., 2000. Organic anion-transporting polypeptides mediate transport of opioid peptides across blood-brain barrier. J. Pharmacol. Exp. Ther. 294, 73–9.

George, R.L., Wu, X., Huang, W., Fei, Y.J., Leibach, F.H., Ganapathy, V., 1999. Molecular cloning and functional characterization of a polyspecific organic anion transporter from Caenorhabditis elegans. J. Pharmacol. Exp. Ther. 291, 596–603.

Gilchrist, S.E., Alcorn, J., 2010. Lactation stage-dependent expression of transporters in rat whole mammary gland and primary mammary epithelial organoids. Fundam. Clin. Pharmacol. 24, 205–14.

Goldstone, J. V., Hamdoun, A., Cole, B. J., Howard-Ashby, M., Nebert, D. W., Scally, M., Dean, M., Epel, D., Hahn, M. E., and Stegeman, J. J., 2006. The chemical defensome: Environmental sensing and response genes in the Strongylocentrotus purpuratus genome. Dev. Biol. 300, 366-84.

Gomez-Martinez, L.E., 2011. Disposition kinetics of caffeine and paraxanthine in Nile tilapia (Oreochromis niloticus): Characterization of the main metabolites. Arch. Environ. Con. Tox. 64, 654-64.

Goodsell, D.S., Olson, A.J., 2000. Structural symmetry and protein function. Annu. Rev. Biophys. 29, 105-153.

Gui, C., Wahlgren, B., Lushington, G. H., Hagenbuch, B., 2009. Identification, Ki determination and CoMFA analysis of nuclear receptor ligands as competitive inhibitors of OATP1B1-mediated estradiol-17beta-glucuronide transport. Pharmacol. Res. 60, 50-56.

Hagenaars, A., Knapen, D., Meyer, I.J., Ven, van der K., Hoff, P., Coen, de W., 2008. Toxicity evaluation of perfluorooctane sulfonate (PFOS) in the liver of common carp (Cyprinus carpio). Aquat. Toxicol. 88, 155–63.

Hagenbuch, B., Gui, C., 2008. Xenobiotic transporters of the human organic anion transporting polypeptides (OATP) family. Xenobiotica. 38, 778–801.

Hagenbuch, B., Meier, P.J., 2004. Organic anion transporting polypeptides of the OATP/ SLC21 family: phylogenetic classification as OATP/ SLCO superfamily, new nomenclature and molecular/functional properties. Pflugers Arch. 447, 653–65.

Hagenbuch, B., Stieger, B., 2013. Molecular Aspects of Medicine The SLCO (former SLC21) superfamily of transporters. Mol. Aspects Med. 34, 396–412.

Hagey, L.R., Iida, T., Tamegai, H., Ogawa, S., Une, M., Mushiake, K., Goto, T., Mano, N., Goto, J., Matthew, D., Hofmann, A.F., 2010. Major biliary bile acids of the Medaka (Oryzias latipes): 25R- and 25S-epimers of 3α,7α,12α-trihydroxy-5β-cholestanoic. Zool. Sci. 27, 565–573

Hänggi, E., Grundschober, A.F., Leuthold, S., Meier, P.J., St-Pierre, M. V, 2006. Functional analysis of the extracellular cysteine residues in the human Organic Anion Transporting Polypeptide, OATP2B1. Mol. Pharmacol. 70, 806–817.

Hilgendorf, C., Ahlin, G., Seithel, A., Artursson, P., Ungell, A., Karlsson, J., 2007. Expression of thirty-six drug transporter genes in human intestine, liver, kidney, and organotypic cell lines. Drug Metab. Dispos. 35, 1333–1340.

Hirano, M., Maeda, K., Shitara, Y., Sugiyama, Y., 2006. Drug-drug interaction between pitavastatin and various drugs via OATP1B1. Drug Metab. Dispos. 34, 1229–36.

Höglund, P.J., Nordström, K.J.V., Schiöth, H.B., Fredriksson, R., 2011. The solute carrier families have a remarkably long evolutionary history with the majority of the human families present before divergence of Bilaterian species. Mol. Biol. Evol. 28, 1531-41.

Holmberg, A., Blomstergren, A., Nord, O., Lukacs, M., Lundeberg, J., Uhlén, M., 2005. The biotin-streptavidin interaction can be reversibly broken using water at elevated temperatures. Electrophoresis. 26, 501-10.

Hong, M., Schlichter, L., Bendayan, R., 2001. A novel zidovudine uptake system in microglia. Pharmacol. Exp. Ther. 296, 141–9.

Hong, M., Xu, W., Yoshida, T., Tanaka, K., Wolff, D.J., Zhou, F., Inouye, M., You, G., 2005. Human organic anion transporter hOAT1 forms homooligomers. J. Biol. Chem. 280, 32285–90.

Horschitz, S., Lau, T., Schloss, P., 2008. Glycine residues G338 and G342 are important determinants for serotonin transporter dimerisation and cell surface expression. Neurochem. Int. 52, 770–5.

Horvath, G., Schmid, N., Fragoso, M.A., Schmid, A., Conner, G.E., Salathe, M., Wanner, A., 2007. Epithelial organic cation transporters ensure pH-dependent drug absorption in the airway. Am. J. Respir. Cell Mol. Biol. 36, 53–60.

Huang, H. and Wu, Q., 2010. Cloning and comparative analyses of the zebrafish Ugt repertoire reveal its evolutionary diversity. PLoS ONE 5, e9144.

Huber, R.D., Gao, B., Sidler Pfändler, M.-A., Zhang-Fu, W., Leuthold, S., Hagenbuch, B., Folkers, G., Meier, P.J., Stieger, B., 2007. Characterization of two splice variants of human organic anion transporting polypeptide 3A1 isolated from human brain. Am. J. Physiol. Cell Physiol. 292, C795–806.

Hugentobler, G., Fricker, G., Boyer, J.L., Meier, P.J., 1987. Anion transport in basolateral (sinusoidal) liver plasma-membrane vesicles of the little skate (Raja erinacea). Biochemical J. 247, 589-595.

Jafurulla, M., Tiwari, S., Chattopadhyay, A., 2011. Identification of cholesterol recognition amino acid consensus (CRAC) motif in G-protein coupled receptors. Biochem. Biophys. Res. Commun. 404, 569–73.

James, M.O., 2011. Steroid catabolism in marine and freshwater fish. J. Steroid Biochem. Mol. Biol. 127, 167–75.

Januszewicz, E., Bekisz, M., Mozrzymas, J.W., Nałecz, K. A., 2010. High affinity carnitine transporters from OCTN family in neural cells. Neurochem. Res. 35, 743–8.

Kawaji, H., Schönbach, C., Matsuo, Y., Kawai, J., Hayashizaki, Y., Matsuda, H., 2002. Exploration of Novel Motifs Derived from Mouse cDNA Sequences. Genome Res. 12, 367–378.

Keller, T., Egenberger, B., Gorboulev, V., Bernhard, F., Uzelac, Z., Gorbunov, D., Wirth, C., Koppatz, S., Dötsch, V., Hunte, C., Sitte, H.H., Koepsell, H., 2011. The large extracellular loop of organic cation transporter 1 influences substrate affinity and is pivotal for oligomerization. J. Biol. Chem. 286, 37874–86.

Kindla, J., Mu, F., Mieth, M., Fromm, M.F., 2011. Influence of Non-Steroidal Anti-Inflammatory Drugs on Organic Anion Transporting Polypeptide (OATP) 1B1- and OATP1B3- Mediated Drug Transport. Drug Metab. Dispos. 39, 1047–1053.

Klaassen, C.D. and Lu, H., 2008. Xenobiotic transporters: ascribing function from gene knockout and mutation studies. Toxicol. Sci. 101, 186–96.

Kobayashi, D., Nozawa, T., Imai, K., Nezu, J., Tsuji, A., Tamai, I., 2003. Involvement of human Organic Anion Transporting Polypeptide OATP-B (SLC21A9) in pH-dependent transport across intestinal apical membrane. J. Pharmacol. Exp. Ther. 306, 703–708.

Kobayashi, Y., Ohbayashi, M., Kohyama, N., Yamamoto.,T. 2005a. Mouse organic anion transporter 2 and 3 (mOAT2/3[Slc22a7/ 8]) mediated the renal transport of bumetanide. Eur. J. Pharmacol. 524, 44-8.

Kobayashi, Y., Ohshiro, N., Sakai, R., Ohbayashi, M., Kohyama, N., Yamamoto, T., 2005b. Transport mechanism and substrate specificity of human organic anion transporter 2 (hOat2 [SLC22A7]). J. Pharm. Pharmacol. 57, 573–8.

Kanai, N., Lu, R., Satriano, J.A., Bao, Y., Wolkoff, A.W., Schuster, V.L., 1995. Identification and characterization of a prostaglandin transporter. Science 268, 866–69.

Koepsell, H. and Endou, H., 2004. The SLC22 drug transporter family. Pflugers Arch. 447, 666–76.

Koepsell, H., Lips, K., Volk, C., 2007. Polyspecific organic cation transporters: structure, function, physiological roles, and biopharmaceutical implications. Pharm. Res. 24, 1227–51.

Koepsell, H., Jürgens, H., Schlatter, E., 2010. Organic cation transporter 2 mediates cisplatin-induced oto- and nephrotoxicity and is a target for protective interventions. Am. J. Pathol. 176, 1169–80.

Koepsell, H., 2011. Substrate recognition and translocation by polyspecific organic cation transporters. Biol. Chem. 392, 95–101.

Koepsell, H., 2013. The SLC22 family with transporters of organic cations, anions and zwitterions. Mol. Aspects Med. 34, 413–35.

Kudo, N., Katakura, M., Sato, Y., Kawashima, Y., 2002. Sex hormone-regulated renal transport of perfluorooctanoic acid. Chem. Biol. Interact. 139, 301–16.

Küfner, I. and Koch, W., 2008. Stress regulated members of the plant organic cation transporter family are localized to the vacuolar membrane. BMC Res. Notes 1, 43.

Kullak-Ublick, G.A., Ismair, M.G., Stieger, B., Landmann, L., Huber, R., Pizzagalli, F., Fattinger, K., Meier, P.J., Hagenbuch, B., 2001. Organic anion-transporting polypeptide B (OATP-B) and its functional comparison with three other OATPs of human liver. Gastroenterology 120, 525–33.

Kwok, B., Yamauchi, A., Rajesan, R., Chan, L., Dhillon, U., Gao, W., Xu, H., Wang, B., Takahashi, S., Semple, J., Tamai, I., Nezu, J., Tsuji, A., Harper, P., Ito, S., 2006. Carnitine/xenobiotics transporters in the human mammary gland epithelia, MCF12A. Am. J. Physiol. Regul. Integr. Comp. Physiol. 290, R793–R802.

Lamhonwah, A.-M., Mai, L., Chung, C., Lamhonwah, D., Ackerley, C., Tein, I., 2011. Upregulation of mammary gland OCTNs maintains carnitine homeostasis in suckling infants. Biochem. Biophys. Res. Commun. 404, 1010–15.

Lee, T.K., Koh, A.S., Cui, Z., Pierce, R.H., Ballatori, N., 2003. N-glycosylation controls functional activity of Oatp1, an organic anion transporter. Am. J. Physiol. Gastrointest. Liver Physiol. 285, G371–81.

Lee, S.Y., Williamson, B., Caballero, O.L., Chen, Y.T., Scanlan, M.J., Ritter, G., Jongeneel, C.V., Simpson, A.J., Old, L.J., 2004. Identification of the gonad-specific anion transporter SLCO6A1 as a cancer/testis (CT) antigen expressed in human lung cancer. Cancer Immun. 4, 13.

Lee, W., Glaeser, H., Smith, L.H., Roberts, R.L., Moeckel, G.W., Gervasini, G., Leake, B.F., Kim, R.B., 2005. Polymorphisms in human organic anion-transporting polypeptide 1A2 (OATP1A2): implications for altered drug disposition and central nervous system drug entry. J. Biol. Chem. 280, 9610–7.

Lelandais-Brière, C., Jovanovic, M., Torres, G. A. M., Perrin, Y., Lemoine, R., Corre-Menguy, F., Hartmann, C., 2007. Disruption of AtOCT1, an organic cation transporter gene, affects root development and carnitine-related responses in Arabidopsis. Plant J. 51, 154–64.

Lennard, M.L., Wilson, M.R., Miller, N.W., Clem, L.W., Warr, G.W., Hikima, J., 2006. Oct2 transcription factors in fish-a comparative genomic analysis. Fish Shellfish Immunol. 20, 227–38.

Leuthold, S., Hagenbuch, B., Mohebbi, N., Wagner, C. A., Meier, P.J., Stieger, B., 2009. Mechanisms of pH-gradient driven transport mediated by organic anion polypeptide transporters. Am. J. Physiol. Cell Physiol. 296, C570–82.

Levavasseur, F., Mandemakers, W., Visser, P., Broos, L., Grosveld, F., Zivkovic, D., Meijer, D., 1998. Comparison of sequence and function of the Oct-6 genes in zebrafish, chicken and mouse. Mech. Dev. 74, 89–98.

Li, L., Lee, T.K., Meier, P.J., Ballatori, N., 1998. Identification of glutathione as a driving force and leukotriene C4 as a substrate for oatp1, the hepatic sinusoidal organic solute transporter. J. Biol. Chem. 273, 16184–91.

Li, L., Meier, P.J., Ballatori, N., 2000. Oatp2 mediates bidirectional organic solute transport: a role for intracellular glutathione. Mol. Pharmacol. 58, 335–40.

Lovejoy, K.S., Todd, R.C., Zhang, S., McCormick, M.S., D'Aquino, J.A., Reardon, J.T., Sancar, A., Giacomini, K.M., Lippard, S.J., 2008. Cis-Diammine(pyridine)chloroplatinum(II), a monofunctional platinum(II) antitumor agent: Uptake, structure, function, and prospects. Proc. Natl. Acad. Sci. U.S.A. 105, 8902–07.

Lu, R., Kanai, N., Bao, Y., Schuster, V.L., 1996. Cloning, in vitro expression, and tissue distribution of a human prostaglandin transporter cDNA (hPGT). J. Clin. Invest. 98, 1142-1149.

Lu, H., Choudhuri, S., Ogura, K., Csanaky, I.L., Lei, X., Cheng, X., Song, P., Klaassen, C.D., 2008. Characterization of organic anion transporting polypeptide 1b2-null mice: essential role in hepatic uptake/toxicity of phalloidin and microcystin-LR. Toxicol. Sci. 103, 35–45.

Ljubojević, M., Balen, D., Breljak, D., Kusan, M., Anzai, N., Bahn, A., Burckhardt, G., Sabolić, I., 2007. Renal expression of organic anion transporter OAT2 in rats and mice is regulated by sex hormones. Am. J. Physiol. Renal Physiol. 292, F361–72.

Fujiwara, K., Adachi, H., Nishio, T., Unno, M., Tokui, T., Okabe, M., Onogawa, T., Suzuki, T., Asano, N., Tanemoto, M., Seki, M., Shiiba, K., Suzuki, M., Kondo, Y., ... , Abe T., 2005. Identification of thyroid hormone transporters in humans: different molecules are involved in a tissue-specific manner. Endocrinology. 142, 2005–2012.

Marchler-Bauer, A., Anderson, J. B., Cherukuri, P. F., DeWeese-Scott, C., Geer, L. Y., Gwadz, M., He, S., Hurwitz, D. I., Jackson, J. D., Ke, Z., Lanczycki, C. J., Liebert, C. a, Liu, C., Lu, F., Marchler, G. H., ..., Bryant, S. H., 2005. CDD: a Conserved Domain Database for protein classification. Nucleic Acids Res. 33, D192–6.

Markova, N.G., Karaman-Jurukovska, N., Dong, K.K., Damaghi, N., Smiles, K.A., Yarosh, D.B., 2009. Skin cells and tissue are capable of using L-ergothioneine as an integral component of their antioxidant defense system. Free Radical Biol. Med. 46, 1168–76.

Martinez-Becerra, P., Briz, O., Romero, M.R., Macias, R.I.R., Perez, M.J., Sancho-Mateo, C., Lostao, M.P., Fernandez-Abalos, J.M., Marin, J.J.G., 2011. Further characterization of the electrogenicity and pH sensitivity of the human Organic Anion-Transporting polypeptides OATP1B1 and OATP1B3. J. Pharmacol. Exp. Ther. 79, 596–607.

Mayerl, S., Visser, T.J., Darras, V.M., Horn, S., Heuer, H., 2012. Impact of Oatp1c1 deficiency on thyroid hormone metabolism and action in the mouse brain. Endocrinology 153, 1528–37.

Meier, Y., Eloranta, J.J., Darimont, J., Ismair, M.G., Hiller, C., Fried, M., Kullak-Ublick, G.A., Vavricka, S.R., 2007. Regional distribution of Solute Carrier mRNA expression along the human intestinal tract. Drug. Metab. Dispos. 35, 590–594.

Meier-Abt, F., Hammann-Hänni, A., Stieger, B., Ballatori, N., Boyer, J.L., 2007. The organic anion transport polypeptide 1d1 (Oatp1d1) mediates hepatocellular uptake of phalloidin and microcystin into skate liver. Toxicol. Appl. Pharmacol. 218, 274–9.

Meier-Abt, F., Mokrab, Y., Mizuguchi, K., 2005. Organic anion transporting polypeptides of the OATP/SLCO superfamily: identification of new members in nonmammalian species, comparative modeling and a potential transport mode. J. Membr. Biol. 208, 213–27.

Mikkaichi, T., Suzuki, T., Onogawa, T., Tanemoto, M., Mizutamari, H., Okada, M., Chaki, T., Masuda, S., Tokui, T., Eto, N., Abe, M., Satoh, F., Unno, M., Hishinuma, T., Inui, K.-I., Ito, S., Goto, J., Abe, T., 2004. Isolation and characterization of a digoxin transporter and its rat homologue expressed in the kidney. Proc. Natl. Acad. Sci. 101, 3569–74.

Mimeault, C., Woodhouse, A. J., Miao, X.-S., Metcalfe, C.D., Moon, T.W., Trudeau, V.L., 2005. The human lipid regulator, gemfibrozil bioconcentrates and reduces testosterone in the goldfish, Carassius auratus. Aquat. Toxicol. 73, 44–54.

Molina, H., Azocar, L., Ananthanarayanan, M., Arrese, M., Miquel, J. F., 2008. Localization of the Sodium-Taurocholate cotransporting polypeptide in membrane rafts and modulation of its activity by cholesterol in vitro. BBA - Biomembranes. 1778, 1283–91.

More, S.S., Li, S., Yee, S.W., Chen, L., Xu, Z., Jablons, D.M., Giacomini, K.M., 2010. Organic cation transporters modulate the uptake and cytotoxicity of picoplatin, a third-generation platinum analogue. Mol. Cancer Ther. 9, 1058–69.

Motohashi, H., Sakurai, Y., Saito, H., Masuda, S., Urakami, Y., Goto, M., Fukatsu, A., Ogawa, O., Inui, K.I., 2002. Gene expression levels and immunolocalization of organic ion transporters in the human kidney. J. Am. Soc. Nephrol. 13, 866–74.

Mulenga, A., Khumthong, R., Chalaire, K.C., Strey, O., Teel, P., 2008. Molecular and biological characterization of the Amblyomma americanum organic anion transporter polypeptide. J. Exp. Biol. 211, 3401–8.

Muller, P.Y., Janovjak, H., Miserez, A.R., Dobbie, Z., 2002. Processing of gene expression data generated by quantitative real-time RT-PCR. BioTechniques 32, 1372-79.

Murray, K.E., Thomas, S.M., Bodour, A.A., 2010. Prioritizing research for trace pollutants and emerging contaminants in the freshwater environment. Environ. Pollut. 158, 3462–71.

Nakakariya, M., Shima, Y., Shirasaka, Y., Mitsuoka, K., Nakanishi, T., Tamai, I., 2009. Organic anion transporter OAT1 is involved in renal handling of citrulline. Am. J. Physiol. Renal Physiol. 297, F71–9.

Nakamura, T., Sugiura, S., Kobayashi, D., Yoshida, K., Yabuuchi, H., Aizawa, S., Maeda, T., Tamai, I., 2007. Decreased proliferation and erythroid differentiation of K562 cells by siRNA-induced depression of OCTN1 (SLC22A4) transporter gene. Pharm. Res. 24, 1628–35.

Nakao, N., Takagi, T., Iigo, M., Tsukamoto, T., Yasuo, S., Masuda, T., Yanagisawa, T., Ebihara, S., Yoshimura, T., 2006. Possible involvement of organic anion transporting polypeptide 1c1 in the photoperiodic response of gonads in birds. Endocrinology 147, 1067–73.

Nies, A.T., Koepsell, H., Winter, S., Burk, O., Klein, K., Kerb, R., Zanger, U.M., Keppler, D., Schwab, M., Schaeffeler, E., 2009. Expression of organic cation transporters OCT1 (SLC22A1) and OCT3 (SLC22A3) is affected by genetic factors and cholestasis in human liver. Hepatology 50, 1227–40.

Nies, A.T., Koepsell, H., Damme, K., Schwab, M., 2010. Organic cation transporters (OCTs, MATEs), in vitro and in vivo evidence for the importance in drug therapy. Handb. Exp. Pharmacol. 201, 105–67.

Nishimura, M.N. and Naito, S.N., 2005. Tissue-specific mRNA expression profiles of human ATP-binding cassette and Solute Carrier transporter superfamilies. Drug Metab. Pharmacokinetics 20, 452–477.

Noe, J., Portmann, R., Brun, M.E. and Funk, C., 2007. Substrate-dependent drug-drug interactions between gemfibrozil, fluvastatin and other Organic Anion-Transporting Peptide (OATP) substrates on OATP1B1, OATP2B1, and OATP1B3. Drug Metab. Dispos. 35, 1308–14.

Nomura, T., Lu, R., Pucci, M.L., Schuster, V.L., 2004. The two-step model of prostaglandin signal termination: in vitro reconstitution with the prostaglandin transporter and prostaglandin 15 dehydrogenase. Mol. Pharmacol. 65, 973–8.

Ose, A., Kusuhara, H., Endo, C., Tohyama, K., Miyajima, M., Kitamura, S., Sugiyama, Y., 2010. Functional characterization of mouse Organic anion transporting peptide 1a4 in the uptake and efflux of drugs across the blood-brain barrier. Drug. Metab. Dispos. 38, 168–176.

Ozkan, P. and Mutharasan, R., 2002. A rapid method for measuring intracellular pH using BCECF-AM. BBA-Gen. 1572, 143-148.

Pelis, R.M., Zhang, X., Dangprapai, Y., Wright, S.H., 2006. Cysteine accessibility in the hydrophilic cleft of human organic cation transporter 2. J. Biol. Chem. 281, 35272–80.

Perry, J.L., Dembla-Rajpal, N., Hall, L. a, Pritchard, J.B., 2006. A three-dimensional model of human organic anion transporter 1: aromatic amino acids required for substrate transport. J. Biol. Chem. 281, 38071–9.

Pippal, J.B., Cheung, C.M.I., Yao, Y.-Z., Brennan, F.E., Fuller, P.J., 2011. Characterization of the zebrafish (Danio rerio) mineralocorticoid receptor. Mol. Cell. Endocrinol. 332, 58–66.

Pizzagalli, F., 2002. Identification of a novel human Organic Anion Transporting Polypeptide as a high affinity thyroxine transporter. Mol. Endocrinol. 16, 2283–2296.

Popp, C., Gorboulev, V., Mu, T.D., Gorbunov, D., Shatskaya, N., Koepsell, H., 2005. Amino acids critical for substrate affinity of rat Organic cation transporter 1 line the substrate binding region in a model derived from the tertiary structure of lactose permease. Mol. Pharmacol. 67, 1600–1611.

Rabergh, C.M., Ziegler, K., Isomaa, B., Lipsky, M.M., Eriksson, J.E., 1994. Uptake of taurocholic acid and cholic acid in isolated hepatocytes from rainbow trout. Am. J. Physiol. 267, G380-86.

Ravi, V. and Venkatesh, B., 2008. Rapidly evolving fish genomes and teleost diversity. Curr. Opin. Genet. Dev. 18, 544–50.

Reed, J.S., Smith, N.D., Boyer, J.L., 1982. Hemodynamic effects on oxygen consumption and bile flow in isolated skate liver. Am. J. Physiol. 242, G313-18.

Rizwan, A.N., Burckhardt, G., 2007. Organic anion transporters of the SLC22 family: biopharmaceutical, physiological, and pathological roles. Pharm. Res. 24, 450–70.

Roth, M., Araya, J.J., Timmermann, B.N., Hagenbuch, B., 2011. Isolation of modulators of the liver-specific Organic Anion-Transporting Polypeptides (OATPs) 1B1 and 1B3 from Rollinia emarginata Schlecht (Annonaceae). J Pharmacol Exp Ther. 339, 624–32.

Roth, M., Obaidat, A., Hagenbuch, B., 2012. OATPs, OATs and OCTs: the organic anion and cation transporters of the SLCO and SLC22A gene superfamilies. Br. J. Pharmacol. 165, 1260–87.

Sambrook, J. F., Fritsch, E.F., Maniatis, T. 1989. Molecular Cloning - A Laboratory Manual. Cold Spring Harbor Laboratory Press. Cold Spring Harbor, NY, USA.

Satlin, L.M., Amin, V., Wolkoff, A. W., 1997. Organic anion transporting polypeptide mediates organic anion/HCO3- exchange. J. Biol. Chem. 272, 26340–5.

Sato, N., Ito, K., Onogawa, T., Akahira, J., Unno, M., Abe, T., Niikura, H., Yaegashi, N., 2007. Expression of organic cation transporter SLC22A16 in human endometria. Int. J. Gynecol. Pathol. 26, 53–60.

Sato, M., Mamada, H., Anzai, N., Shirasaka, Y., Nakanishi, T., Tamai, I., 2010. Renal secretion of uric acid by organic anion transporter 2 (OAT2/SLC22A7) in human. Biol. Pharm. Bull. 33, 498–503.

Schlessinger, A., Yee, S.W., Sali, A., Giacomini, K.M., 2013. SLC Classification: An Update. Clin. Pharmacol. Ther. 94, 19-23.

Schmidt, U.G., Endler, A., Schelbert, S., Brunner, A., Schnell, M., Neuhaus, H.E., Marty-Mazars, D., Marty, F., Baginsky, S, Martinoia, E., 2007. Novel tonoplast transporters identified using a proteomic approach with vacuoles isolated from cauliflower buds. Plant. Physiol. 145, 216-29.

Schomig, E., Spitzenberger, F., Engelhardt, M., Martel, F., Ording, N., Gründemann, D., 1998. Molecular cloning and characterization of two novel transport proteins from rat kidney. FEBS Lett. 425, 79–86.

Sekine, T., Watanabe, N., Hosoyamada, M., Kanai, Y., Endou, H., 1997. Expression cloning and characterization of a novel multispecific organic anion transporter. J. Biol. Chem. 272, 18526-29.

Segner, H., 2009. Zebrafish (Danio rerio) as a model organism for investigating endocrine disruption. Comp. Biochem. Physiol. C. Toxicol. Pharmacol. 149, 187–95.

Shekhawat, P.S., Srinivas, S.R., Matern, D., Bennett, M.J., Boriack, R., George, V., Xu, H., Prasad, P.D., Roon, P., Ganapathy, V., 2007. Spontaneous development of intestinal and colonic atrophy and inflammation in the carnitine-deficient jvs (OCTN2-/-) mice. Mol. Genet. Metab. 92, 315–24.

Simonson, G.D., Vincent, A.C., Roberg, K.J., Huang, Y., Iwanij, V., 1994. Molecular cloning and characterization of a novel liver-specific transport protein. J. Cell Sci. 107, 1065–72.

Smith, N.F., Figg, W.D., Sparreboom, A., 2005. Role of the liver-specific transporters OATP1B1 and OATP1B3 in governing drug elimination. Expert Opin. Drug. Metab. Toxicol. 1, 429-45.

Snyder, S. A., Keith, T.L., Pierens, S.L., Snyder, E.M., Giesy, J.P., 2001. Bioconcentration of nonylphenol in fathead minnows (Pimephales promelas). Chemosphere 44, 1697–702.

Srimaroeng, C., Perry, J.L., Pritchard, J.B., 2008. Physiology, structure, and regulation of the cloned organic anion transporters. Xenobiotica. 38, 889–935.

Steeg, E. Van De, Wagenaar, E., Kruijssen, C.M.M. Van Der, Burggraaff, J.E.C., Waart, D.R. De, Elferink, R.P.J.O., Kenworthy, K.E., Schinkel, A.H., 2010. Organic anion transporting polypeptide 1a / 1b – knockout mice provide insights into hepatic handling of bilirubin, bile acids, and drugs. J. Clin. Invest. 120, 2942–52.

Stegeman, J., Goldstone, J., Hahn, M., 2010. Perspectives on zebrafish as a model in environmental toxicology. In Perry, S.F., Ekker, M., Farrell, A.P., Brauner, C.J. (Eds.), Zebrafish Elsevier, MA ,US , pp. 367-439.

Sugiyama, D., Kusuhara, H., Taniguchi, H., Ishikawa, S., Nozaki, Y., Aburatani, H., Sugiyama, Y., 2003. Functional characterization of rat brain-specific Organic anion transporter (Oatp14) at the blood-brain barrier: high affinity transporter for thyroxine. J. Biol. Chem. 278, 43489-95.

Sukardi, H., Chng, H.T., Chan, E.C.Y., Gong, Z., Lam, S.H., 2011. Zebrafish for drug toxicity screening: bridging the in vitro cell-based models and in vivo mammalian models. Expert Opin. Drug Metab. Toxicol. 7, 579–89.

Sumpter, J.P. and Jobling, S., 2013. The occurrence, causes, and consequences of estrogens in the aquatic environment. Environ. Toxicol. Chem. 32, 249-51.

Suzuki, T., Onogawa, T., Asano, N., Mizutamari, H., Mikkaichi, T., Tanemoto, M., Abe, M., Satoh, F., Unno, M., Nunoki, K., Suzuki, M., Hishinuma, T., Goto, J., Shimosegawa, T., Matsuno, S., Ito, S., Abe,T., 2003. Identification and characterization of novel rat and human gonad-specific organic anion transporters. Mol. Endocrinol. 17, 1203–15.

Schuster, V., L., 2002. Prostaglandin transport. Prostaglandins Other Lipid Mediat 68–69, 633–647.

Simon, P., 2003. Q-Gene: processing quantitative real-time RT–PCR data. Bioinformatics 19, 1439–40.

Simonson, G. D., Vincent, A. C., Roberg, K. J., Huang, Y. , Iwanij, V., 1994. Molecular cloning and characterization of a novel liverspecific transport protein. J. Cell Sci. 107, 1065-72.

Storch, C. H., Ehehalt, R., Haefeli, W. E., Weiss, J., 2007. Localization of the human Breast Cancer Resistance Protein (BCRP/ABCG2) in lipid rafts/caveolae and modulation of its activity by chlesterol in vitro. J. Pharmacol. Exp. Ther. 323, 257-64.

Tachampa, K., Takeda, M., Khamdang, S., Noshiro-Kofuji, R., Tsuda, M., Jariyawat, S., Fukutomi, T., Sophasan, S., Anzai, N., Endou, H., 2008. Interactions of organic anion transporters and organic cation transporters with mycotoxins. J. Pharmacol. Sci. 106, 435–43.

Tachikawa, M., Takeda, Y., Tomi, M., Hosoya, K., 2010. Involvement of OCTN2 in the transport of acetyl-L-carnitine across the inner blood-retinal barrier. Invest. Ophthalmol. Vis. Sci. 51, 430–36.

Tamai, I., Yabuuchi, H., Nezu, J., Sai, Y., Oku, A., Shimane, M., Tsuji, A., 1997. Cloning and characterization of a novel human pH-dependent organic cation transporter, OCTN1. FEBS Lett. 419, 107–11.

Taylor, J. S., Peer, van der Y., Braasch, I., Meyer, A., 2001. Comparative genomics provides evidence for an ancient genome duplication event in fish. Philos. Trans. R. Soc. Lond. B Biol. Sci. 356, 1661–79.

Tom, R., Bisson, L., Durocher, Y., 2008. Transfection of adherent HEK293-EBNA1 cells in a six-well plate with branched PEI for production of recombinant proteins. Cold Spring Harb Protoc. 3.

Torres, G.A., Lelandais-Briere, C., Besin, E., Jubier, M.F., Roche, O., Mazubert, C., Corre-Menguy, F., Hartmann, C., 2003. Characterization of the expression of Phaseolus vulgaris OCT1, a dehydration-regulated gene that encodes a new type of phloem transporter. Plant. Mol. Biol. 51, 341-349.

Tusnady, G.E. and Simon, I., 2001. The HMMTOP transmembrane topology prediction server. Bioinformatics 17, 849-850.

Tamai, I., Nezu, J., Uchino, H., Sai, Y., Oku, A., Shimane, M., Tsuji, A., 2000. Molecular identification and characterization of novel members of the human organic anion transporter (OATP) family. Biochem. Biophys. Res. Commun. 273, 251–60.

Tschantz, W.R., Pfeifer, N.D., Meade, C.L., Wang, L., Lanzetti, A., Kamath, A. V, Berlioz-Seux, F., Hashim, M.F., 2008. Expression, purification and characterization of the human membrane transporter protein OATP2B1 from Sf9 insect cells. Protein Expr. Purif. 57, 163–71.

Uchida, Y., Ohtsuki, S., Katsukura, Y., Ikeda, C., Suzuki, T., Kamiie, J., Terasaki, T., 2011. Quantitative targeted absolute proteomics of human blood-brain barrier transporters and receptors. J. Neurochem. 117, 333–45.

Ugele, B., St-Pierre, M.V., Pihusch, M., Bahn, A., Hantschmann, P., 2003. Characterization and identification of steroid sulfate transporters of human placenta. Am. J. Physiol. Endocrinol. Metab. 284, E390–E98.

Urban, T.J., Yang, C., Lagpacan, L.L., Brown, C., Castro, R.A., Taylor, T.R., Huang, C.C., Stryke, D., Johns, S.J., Kawamoto, M., Carlson, E.J., Ferrin, T.E., Burchard, E.G., Giacomini, K.M., 2007. Functional effects of protein sequence polymorphisms in the organic cation/ergothioneine transporter OCTN1 (SLC22A4). Pharmacogenet. Genomics 17, 773–82.

Vallon, V., Rieg, T., Ahn, S.Y., Wu, W., Eraly, S. A., Nigam, S.K., 2008. Overlapping in vitro and in vivo specificities of the organic anion transporters OAT1 and OAT3 for loop and thiazide diuretics. Am. J. Physiol. Renal Physiol. 294, F867–73.

Deure, van der W.M., Peeters, R.P., Visser, T.J., 2010. Molecular aspects of thyroid hormone transporters, including MCT8, MCT10, and OATPs, and the effects of genetic variation in these transporters. J. Mol. Endocrinol. 44, 1–11.

Vanwert, A.L., Gionfriddo, M.R., Sweet, D.H., 2010. Organic anion transporters: discovery, pharmacology, regulation and roles in pathophysiology. Biopharm. Drug Dispos. 31, 1–71.

Vazquez-Duhalt, R., Marquez-Rocha, F., Ponce, E., Licea, A.F., Viana, M.T., 2005. Nonylphenol, an integrated vision of a pollutant. AEER 4, 1-25.

Wang, P., Hata, S., Xiao, Y., Murray, J.W., Wolkoff, A.W., 2008. Topological assessment of oatp1a1: a 12-transmembrane domain integral membrane protein with three N-linked carbohydrate chains. Am. J. Physiol. Gastrointest. Liver Physiol. 294, G1052–9.

Westholm, D.E., Salo, D.R., Viken, K.J., Rumbley, J.N., Anderson, G.W. 2009. The blood-brain barrier thyroxine transporter organic anion-transporting polypeptide 1c1 displays atypical transport kinetics. Endocrinology 150, 5153-62.

Winter, T.N., Elmquist, W.F., Fairbanks, C.A., 2011. OCT2 and MATE1 provide bidirectional agmatine transport. Mol. Pharm. 8, 133–42.

Wolff, N. A., Grünwald, B., Friedrich, B., Lang, F., Godehardt, S., Burckhardt, G., 2001. Cationic amino acids involved in dicarboxylate binding of the flounder renal organic anion transporter. J. Am. Soc. Nephrol. 12, 2012–8.

Wong, C.C., Botting, N.P., Orfila, C., Al-Maharik, N., Williamson, G., 2011. Flavonoid conjugates interact with organic anion transporters (OATs) and attenuate cytotoxicity of adefovir mediated by organic anion transporter 1 (OAT1/SLC22A6). Biochem. Pharmacol. 81, 942–9.

Wright, S.H. and Dantzler, W.H., 2004. Molecular and cellular physiology of renal organic cation and anion transport. Physiol. Rev. 84, 987–1049.

Wu, X., Fei, Y.J., Huang, W., Chancy, C., Leibach, F.H., Ganapathy, V., 1999. Identity of the F52F12.1 gene product in Caenorhabditis elegans as an organic cation transporter. Biochim. Biophys. Acta. 1418, 239-44.

Xiao, Y.H., Yin, M.H., Hou, L., Luo, M., Pei, Y., 2007. Asymmetric overlap extension PCR method bypassing intermediate purification and the amplification of wild-type template in site-directed mutagenesis. Biotechnol. Lett. 29, 925-30.

Xu, C., Yong-Tao, L., Kong, T., 2005. Induction of Phase I, II and III drug metabolism/transport by xenobiotics. Arch. Pharm. Res. 28, 249-268.

Xu, C. and Zon, L.I. 2010. The zebrafish as a model for human disease. In Perry, S.F., Ekker, M., Farrell, A.P., Brauner, C.J. (Eds.), Zebrafish Elsevier, MA ,US , pp. 345-365.

Yamazaki, M., Li, B., Louie, S.W., Pudvah, N.T., Stocco, R., Wong, W., Abramovitz, M., Demartis, a, Laufer, R., Hochman, J. H., Prueksaritanont, T., Lin, J. H., 2005. Effects of fibrates on human organic anion-transporting polypeptide 1B1-, multidrug resistance protein 2- and P-glycoprotein-mediated transport. Xenobiotica 35, 737–53.

Yao, J., Hong, W., Huang, J., Zhan, K., Huang, H., Hong, M., 2012. N-Glycosylation dictates proper processing of organic anion transporting polypeptide 1B1. PLoS One 7, e52563.

Zaher, H., Meyer, H.E., Tirona, R.G., Cox, M.L., Obert, L.A., Agrawal, N., Palandra, J., Stock, J.L., Kim, R.B., Ware, J.A., 2008. Targeted Disruption of Murine Organic Anion-Transporting Polypeptide 1b2 (oatp1b2/Slco1b2) Significantly Alters Disposition of Prototypical Drug Substrates Pravastatin and Rifampin. Mol. Pharmacol, 74, 320-29.

Zair, Z.M., Eloranta, J.J., Stieger, B., Kullak-Ublick, G.A., 2008. Pharmacogenetics of OATP (SLC21/SLCO), OAT and OCT (SLC22) and PEPT (SLC15) transporters in the intestine, liver and kidney. Pharmacogenomics 9, 597-624.

Zhang, X., Shirahatti, N. V, Mahadevan, D., Wright, S.H., 2005. A conserved glutamate residue in transmembrane helix 10 influences substrate specificity of rabbit OCT2 (SLC22A2). J. Biol. Chem. 280, 34813–22.

Zhou, F., Illsley, N.P., You, G., 2006. Functional characterization of a human organic anion transporter hOAT4 in placental BeWo cells. Eur. J. Pharm. Sci. 27, 518–23.

7. Summary

Membrane transporter families SLC21/SLCO and SLC22 are members of the SLC (Solute carriers) protein superfamily and are responsible for the transport of various endo- and xenobiotics across cell membranes. Despite their crucial role in the toxicological response of organisms, their ecotoxicological relevance has not been studied so far. Therefore, the main goal of our study was characterization of SLC21/SLCO and SLC22 transporters in zebrafish (*Danio rerio*) as a highly relevant model organism in biomedical and environmental research. This overall goal was accomplished using phylogenetic analysis and tissue expression profiling, followed by molecular characterization of selected zebrafish SLC transporters of potential (eco)toxicological relevance using transfection in heterologous expression systems and transport activity measurements.

Data obtained from the tissue expression profiling and analysis of phylogenetic relationships with mammalian co-orthologs, implied that following transporters could be crucial for cellular ADME (Absorption, Distribution, Elimination and Excretion) in zebrafish: Oatp1d1 in liver; Oatp2b1 in liver, kidney and gills; Oat3, Oat2c and Oat2e in kidney; Oat2d in intestine; and Oct1 in liver.

We have characterized Oatp1d1 in detail. This is the first characterization of *Slc21* transporter in zebrafish which provides important insights into the functional evolution of OATP1/Oatp1 subfamily. Diversification of the OATP1/Oatp1 subfamily occurred after the emergence of jawed fish; the Oatp1d group emerged in teleosts and is absent in tetrapods, whereas OATP1A/Oatp1a and OATP1B/Oatp1b emerged at the root of tetrapods. Substrate specificity analysis and tissue expression analysis revealed similarities with mammalian OATP1A/Oatp1a and OATP1B/Oatp1b members and differences from mammalian OATP1C/Oatp1c proteins. We suggest an important role of Oatp1d1 in hormonal balance in fish, as well as its involvement in elimination of steroid hormone metabolites and foreign compounds through bile. Based on the results on extracellular and intracellular pH manipulations, we propose that Oatp1d1 transport activity is pH gradient dependant. Analysis of evolutionary conservation and importance of structural properties revealed that: (i) H79 located in the intracellular LP3 is conserved within the OATP1/Oatp1 subfamily and is crucial for transport activity; (ii) N-glycosylation pattern is conserved within OATP1/Oatp1 subfamily and is important for membrane localization with the four N-linked glycosylation sites involved (N122, N133, N499, N512); (iii) evolutionary conserved CRAC motif is important for the membrane localization of Oatp1d1; and finally (iv), our results show that Oatp1d1 is present in the plasma membrane as a dimer and possibly as a higher order oligomer, with highly conserved glycophorin motifs in transmembrane domains 5 and 8 (TMD5 and 8) involved in the oligomer formation. Our results contribute to the better understanding of the OATP/Oatp evolution in vertebrates and offer the first insight into the functional and structural properties of a novel zebrafish Oatp1 ortholog.

In respect to the interaction of SLC transporters with environmental contaminants, zebrafish Oatp1d1 has been selected for further characterization given its dominant expression in liver as a

main excretory organ. We have found that Oatp1d1 is involved in the transport of diverse environmentally relevant compounds, including perfluorooctanesulfonic acid (PFOS), nonylphenol, gemfibrozil, diclofenac, 17α-ethynilestradiol (EE2) and caffeine which are high affinity substrates of Oatp1d1. Other environmental contaminants are potent Oatp1d1 inhibitors at environmentally relevant concentrations, including perfluorooctanoic acid (PFOA) and synthetic estrogens (estrone and estradiol). Although acting differently, both groups of compounds (i.e. substrates and inhibitors) could disrupt normal Oatp1d1 transport function in fish. Most importantly, considering tissue localization of Oatp1d1 and its substrate specificity, we hypothesize that its inhibition could be implicated in:

(1) the inhibition of Oatp1d1-mediated uptake of excess steroid hormone conjugates into hepatocytes, and

(2) the inhibition of DHEAS uptake in the brain and testes, which could in turn cause physiological effects in fish.

Likewise, the inhibition of Oatp1d1 by many environmental contaminants further emphasizes their potential role in modulating the uptake processes. We believe the presented characterization of Oatp1d1 in relation to its interaction with environmentally relevant contaminants will foster better understanding of the mode(s) of action of tested compounds, and enable more accurate predictions of their disposition and possible harmful effects in fish. Finally, considering that zebrafish is recognized as an excellent model in (eco)toxicological research, and a detailed characterization of the uptake processes is a necessary prerequisite for its reliable use, we believe data from this work will significantly contribute to this overall goal.

In addition to the detailed characterization of Oatp1d1, we have performed initial characterization of three zebrafish OATs of potential toxicological relevance. We suggest that Oat3 and potentially Oat2c are important for the elimination of foreign compounds through the kidney, whereas Oat2d could be involved in the elimination of endogenous and xenobiotic compounds through intestine.

In summary, this PhD thesis represents the first comprehensive characterization of membrane proteins from OATP/Oatp and SLC22/Slc22 families in fish and provides important insights into the function of these important cellular determinants of toxicological response.

8. Sažetak

Membranski transporteri obitelji SLC21/SLCO i SLC22 su pripadnici SLC (engl. *Solute Carriers*) proteinske nadobitelji i odgovorni su za transport različitih endo- i ksenobiotika kroz staničnu membranu. Unatoč ključnoj ulozi u toksikološkom odgovoru organizma, njihova ekotoksikološka važnost nije bila razjašnjena do sada. Stoga je glavni cilj našeg istraživanja bila karakterizacija Slc21 i Slc22 transportera kod zebrice (*Danio rerio*) kao važnog modelnog organizma u biomedicinskim i okolišnim istraživanjima. Ovaj sveobuhvatni cilj ostvaren je koristeći filogenetsku i ekspresijsku analizu, nakon kojih je sljedila molekularna karakterizacija odabranih SLC transportera zebrice od potencijalnog ekotokisokološkog značaja, koristeći transfekciju u heterologne ekspresijske sustave te mjerenje transportne aktivnosti. Podaci dobiveni ekspresijskom analizom tkiva zebrice i analizom filogenetskih odnosa sa ortolozima sisavaca ukazali su na potencijalnu važnost slijedećih transportera u staničnom ADME fenomenu (engl. *Absorption, Distribution, Metabolism, Excretion*): Oatp1d1 u jetri, Oatp2b1 u jetri, bubregu i škrgama, Oat3, Oat2c i Oat2e u bubregu, Oat2d u crijevu i Oct1 u jetri.

Detaljnije smo karakterizirali novi Oatp kod zebrice, Oatp1d1. Ovo istraživanje predstavlja prvu karakterizaciju Oatp transportera zebrice te pruža bitan uvid u funkcionalnu evoluciju OATP1/Oatp1 podobitelji. Do diverzifikacije OATP1/Oatp1 podobitelji dolazi nakon razvoja riba čeljusnica; Oatp1d skupina se javlja kod riba koštunjača i nije prisutna kod tetrapodnih kralješnjaka, dok se OATP1A/Oatp1a i OATP1B/Oatp1b pojavljuju kod tetrapodnih kralješnjaka. Analize supstratne specifičnosti i tkivne ekspresije pokazale su sličnosti s OATP1A/Oatp1a i OATP1B/Oatp1b članovima kod sisavaca i različitosti u odnosu na OATP1C/Oatp1c proteine. Na temelju ovih rezultata predlažemo važnu ulogu Oatp1d1 u hormonalnoj ravnoteži riba, odnosno u eliminaciji metabolita steroidnih hormona i stranih tvari putem žuči. Nadalje, rezultati dobiveni manipulacijama unutarstaničnog i izvanstaničnog pH ukazali su da je transportna aktivnost Oatp1d1 ovisna o pH gradijentu. Analiza evolucijske sačuvanosti i važnosti strukturnih obilježja pokazala je da: (i) H79 u trećoj unutarstaničnoj petlji sačuvan je unutar OATP1/Oatp1 podobitelji i bitan je za transportnu aktivnost, (ii) N-glikozilacijski obrazac je sačuvan unutar OATP1/Oatp1 podobitelji i bitan je za membransku lokalizaciju te uključuje četiri N-glikozilacijska mjesta (N122, N133, N499, N512); (iii) evolucijski sačuvan CRAC motiv bitan je za membransku lokalizaciju Oatp1d1, i naposljetku, (iv), Oatp1d1 je prisutan u staničnoj membrani u formi dimera te potencijalno oligomera višeg reda, dok su evolucijski sačuvani glikoforinski motivi unutar transmembranske domene 5 i 8 (TMD 5 i 8) odgovorni za formiranje oligomera. Naši rezultati predstavljaju doprinos boljem razumijevanju evolucije OATP/Oatp obitelji u kralješnjaka i daju prvi uvid u funkcionalna i strukturna obilježja novog Oatp1 ortologa zebrice.

Vezano uz interakciju SLC transportera s okolišnim zagađivalima, Oatp1d1 odabrali smo za daljnju karakterizaciju s obzirom na njegovu visoku ekspresiju u jetri kao glavnom ekskretornom organu.

Otkrili smo da je Oatp1d1 uključen u transport raznolikih okolišno relevantnih zagađivala, uključujući perfluorooktan-sulfidnu kiselinu (PFOS), nonilfenol, gemfibrozil, diklofenak, 17α-etinilestradiol (EE2) i kafein, koji su visoko-afinitetni supstrati transportera Oatp1d1. Druga okolišna zagađivala, poput perfluorooktanične kiseline (PFOA) i sintetskih hormona (estron i estradiol), su snažni inhibitori Oatp1d1 transportera, i to pri okolišno relevantnim koncentracijama. Unatoč različitom djelovanju, obje grupe spojeva (tj. supstrati i inhibitori) potencijalno mogu poremetiti normalnu transportnu funkciju Oatp1d1 kod riba. Najbitnije, uzimajući u obzir tkivnu lokalizaciju i supstratnu specifičnost Oatp1d1, pretpostavljamo da njegova inhibicija može utjecati na:

(1) inhibiciju unosa suvišnih konjugata steroidnih hormona u hepatocite putem Oatp1d1, i
(2) inhibiciju unosa DHEAS-a u mozak i testise putem Oatp1d1 što bi moglo uzrokovati fiziološke promjene kod riba.

U skladu s ovim rezultatima i predloženim hipotezama, inhibicija Oatp1d1 putem mnogobrojnih okolišnih zagađivala dodatno naglašava njihovu potencijalnu ulogu u modulaciji procesa unosa. Smatramo da će provedena karakterizacija Oatp1d1 u odnosu na njegovu interakciju s okolišno relevantnim zagađivalima doprinijeti boljem razumijevanju mehanizma djelovanja proučavanih tvari te da će omogućiti točnije predviđanje raspoloživosti navedenih tvari i njihovog potencijalno štetnog djelovanja u riba. Naposljetku, s obzirom da je zebrica prepoznata kao važna modelna vrsta u ekotoksikološkim istraživanjima te da je detaljna karakterizacija procesa unosa potreban alat za njeno pouzdano korištenje, smatramo da će podaci dobiveni ovim istraživanjem značajno doprinijeti ovom sveobuhvatnom cilju.

Uz detaljnu karakterizaciju Oatp1d1, proveli smo i inicijalnu karakterizaciju tri potencijalno važna Organska anionska transportera (Oat-a) kod zebrice. Naši rezultati ukazali su da su Oat3 i potencijalno Oat2c bitni faktori u eliminaciji zagađivala putem bubrega, dok bi Oat2d mogao biti bitan za eliminaciju endogenih tvari i ksenobiotika putem crijeva.

Zaključno, ova disertacija predstavlja prvu sveobuhvatnu karakterizaciju membranskih proteina OATP/Oatp i SLC22/Slc22 obitelji u riba te pruža prvi uvid u funkciju ovih bitnih staničnih odrednica toksikološkog odgovora.

9. Abbreviations

2,4-D	2,4-diphenoxyacetic acid
5CF	5-carboxyfluorescein
6CF	6-carboxyfluorescein
A	Alanine
AEBSF	4-(2-Aminoethyl) benzenesulfonyl fluoride hydrochloride
AHTN	7-acetyl -1,1,3,4,4,6-hexamethyl-1,2,3,4 tetrahydronapthalene
An	Anolis carolinensis
ASF	Amphiphilic solute facilitator
BisA	Bisphenol A
BCECF	2',7'-bis-(2-carboxyethyl)-5-(and-6)-carboxyfluorescein
BCECF-AM	2',7'-bis-(2-carboxyethyl)-5-(and-6)-carboxyfluorescein acetoxymethyl ester
BHT	Butylated hydroxytoluen
BSP	Bromosulfophthalein
C	Cysteine
cAMP	Cyclic adenosine monophosphate
cDNA	complementary Deoxyribonucleic acid
cGMP	Cyclic guanosine monophosphate
CH	Cholate
Ci	Ciona intestinalis
CRAC	Cholesterol Recognition interaction Amino acid Consensus
Cy3	Cyanine 3
CycA	Cyclosporine A
D	Aspartate
DAPI	Diamidino-2-phenylindole
DBP	Dibutyl phthalate
DEET	N,N-diethyl meta-toluamide
DEHP	bis(2-ethylhexyl) phthalate
DEP	Diethyl phthalate
DHEAS	Dehydroepiandrosterone sulphate
dhFL	dihydrofluorescein
DMEM	Dulbecco's modified Eagle medium
DNA	Deoxyribonucleic acid
Dr	Danio rerio
DTT	Dithiothreitol
E1	Estrone
E2	Estradiol
E3S	Estrone-3-sulfate
EDTA	Ethylenediaminetetraacetic acid
EE2	17α-ethynilestradiol
EF1α	Elongation factor 1α

FBS	Fetal Bovine Serum
FITC	Fluorescein isothiocyanate
G	Glycine
Ga	Gastrosteus aculeatus
Gg	Gallus gallus
Gfb	Gemfibrozil
GFP	Green fluorescent protein
Gm	Gadus morhua
H	Histidine
[^{3}H]E3S	[^{3}H]estrone-3-sulfate
HEK293	Human Embryonic Kidney 293
HEPES	Hydroxyethyl piperazineethanesulfonic acid
HKG	Housekeeping gene
[^{3}H]pAH	[3H]p-aminohippurate
Hs	Homo sapiens
I	Inhibitor
IgG	Immunoglobulin G
IgG-HRP	Immunoglobulin G - horseradish peroxidase
K	Lysine
Lc	Latimeria chalumnae
Le	Leucoraja erinacea
LP	Loop
LY	Lucifer Yellow
MES	2- (N morpholino) ethanesulfonic acid
MF	Membrane fraction
MFS	Multifacilitator superfamily
Mm	Mus musculus
MNE	Mean normalized expression
MPF	Mutagenic forward primer
MPR	Mutagenic reverse primer
mRNA	messanger Ribonucleic acid
N	Aparagine
na	not available
nd	not determined
ne	no effect
NH_4Cl	Ammonium chloride
NP-40	Nonidet P-40
OATP/Oatp	Organic anion transporting polypeptide
OAT/Oat	Organic anion transporter
OCT/Oct	Organic cation transporter

OCTN/Octn	Organic carnitine transporter
Ol	Oryzas latipes
ORCTL/Orctl	Organic cation like transporter
pAH	p-aminohippurate
PBS	Phosphate-buffered saline
PCR	Polymerase chain reaction
PEI	Polyethyleneimine
PFOA	Perfluorooctanoic acid
PFOS	Perfluorooctanesulfonic acid
PGE2	Prostaglandine E2
pH_i	intracellular pH
pH_o	extracellular pH
PPCP	Pharmaceuticals and personal care products
R	Arginine
rhB	rhodamineB
Rn	Rattus norvegicus
RNA	Ribonucleic acid
Q	Glutamine
qRT-PCR	Quantitative Real-Time polymerase chain reaction
S	Substrate
SD	Standard deviation
SDS	Sodium dodecyl sulphate
SE	Standard error
SLC	Solute carrier
SPF	Specific F primer
SPR	Specific R prime
syn	synonym
TCDC	Taurochenodeoxycholate
TCL	Total cell lysate
TMD	Transmembrane domain
Tn	Tetraodon nigroviridis
Tris	Tris(hydroxymethyl)aminomethane
Tr	Takifugu rubripes
V	Valine
WGD	Whole genome duplication
wt	wild type
X-gal	5-bromo-4-chloro-3-indolyl-β-D-galactopyranoside
Xl	Xenopus laevis
Xt	Xenopus tropicalis
Y	Tyrosine

10. Supplement

A)

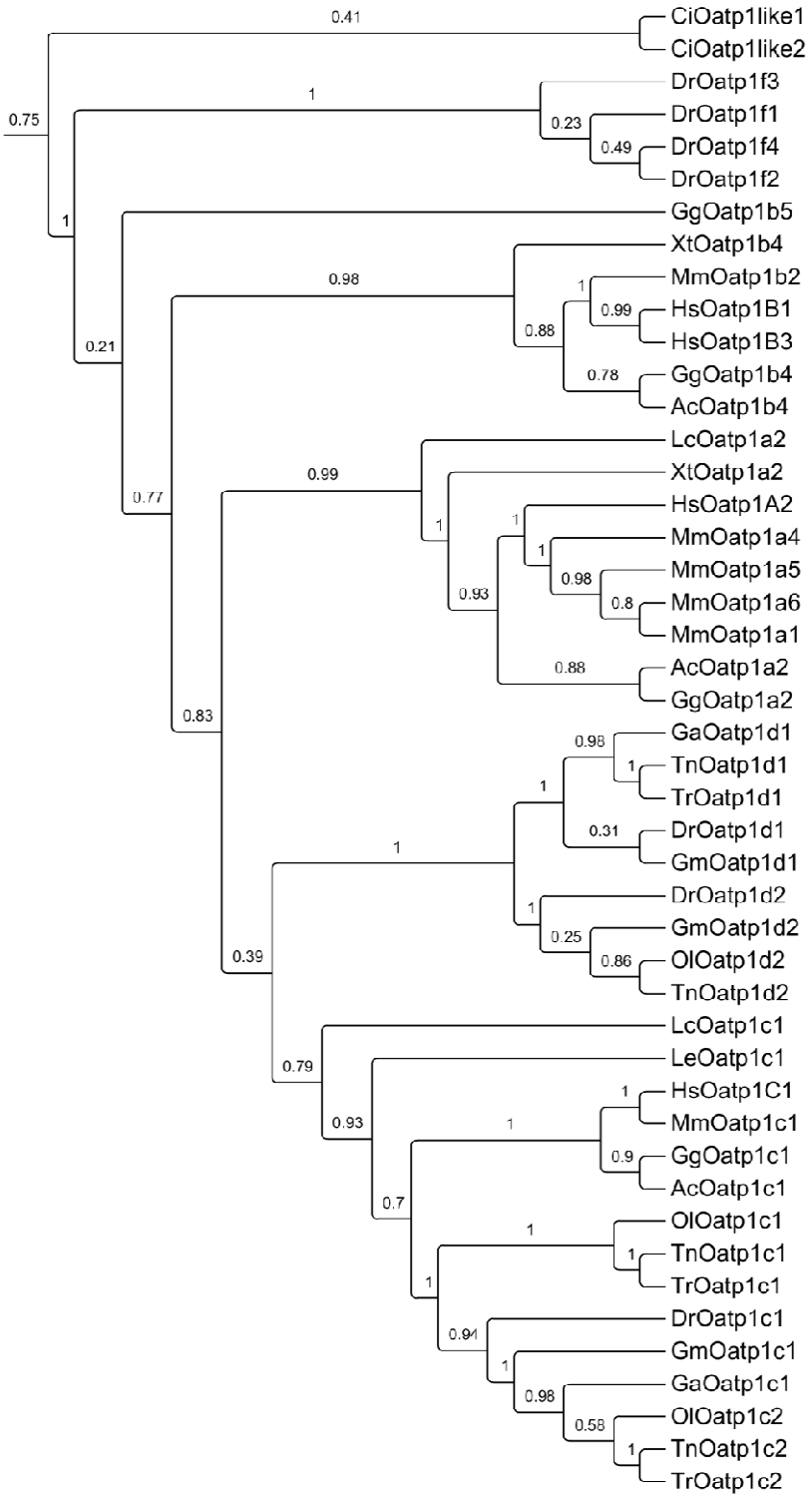
CiOatp1like1
CiOatp1like2
DrOatp1f3
DrOatp1f1
DrOatp1f4
DrOatp1f2
GgOatp1b5
XtOatp1b4
MmOatp1b2
HsOatp1B1
HsOatp1B3
GgOatp1b4
AcOatp1b4
LcOatp1a2
XtOatp1a2
HsOatp1A2
MmOatp1a4
MmOatp1a5
MmOatp1a6
MmOatp1a1
AcOatp1a2
GgOatp1a2
GaOatp1d1
TnOatp1d1
TrOatp1d1
DrOatp1d1
GmOatp1d1
DrOatp1d2
GmOatp1d2
OlOatp1d2
TnOatp1d2
LcOatp1c1
LeOatp1c1
HsOatp1C1
MmOatp1c1
GgOatp1c1
AcOatp1c1
OlOatp1c1
TnOatp1c1
TrOatp1c1
DrOatp1c1
GmOatp1c1
GaOatp1c1
OlOatp1c2
TnOatp1c2
TrOatp1c2

B)

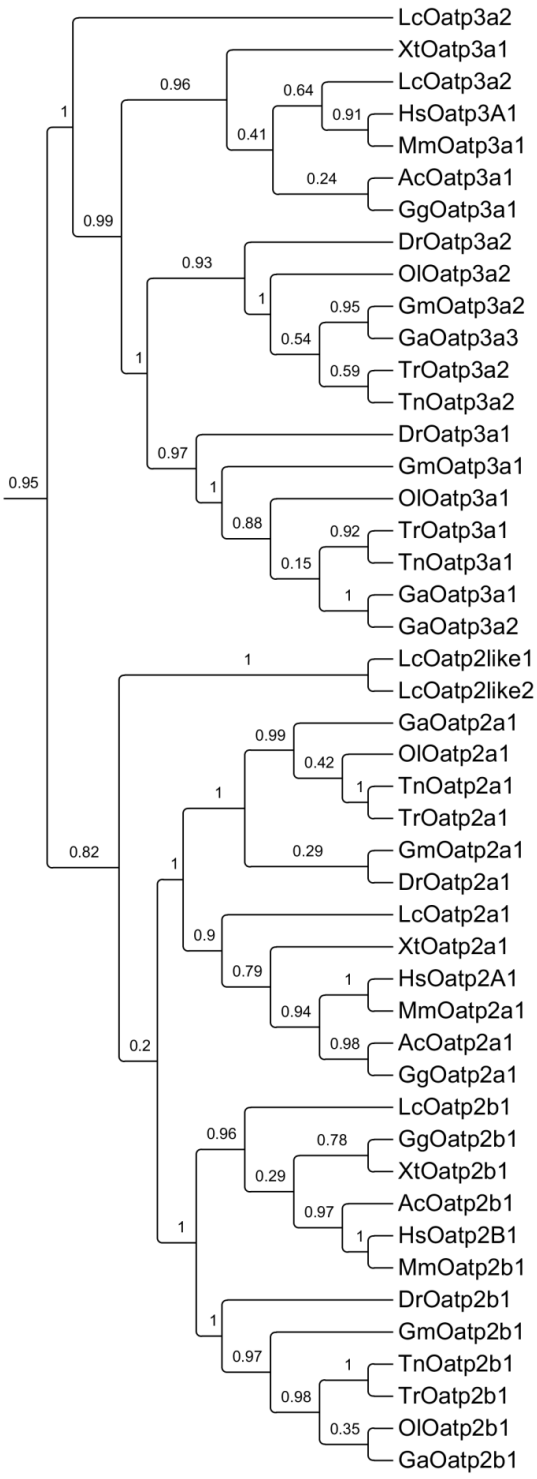
LcOatp3a2
XtOatp3a1
LcOatp3a2
HsOatp3A1
MmOatp3a1
AcOatp3a1
GgOatp3a1
DrOatp3a2
OlOatp3a2
GmOatp3a2
GaOatp3a3
TrOatp3a2
TnOatp3a2
DrOatp3a1
GmOatp3a1
OlOatp3a1
TrOatp3a1
TnOatp3a1
GaOatp3a1
GaOatp3a2
LcOatp2like1
LcOatp2like2
GaOatp2a1
OlOatp2a1
TnOatp2a1
TrOatp2a1
GmOatp2a1
DrOatp2a1
LcOatp2a1
XtOatp2a1
HsOatp2A1
MmOatp2a1
AcOatp2a1
GgOatp2a1
LcOatp2b1
GgOatp2b1
XtOatp2b1
AcOatp2b1
HsOatp2B1
MmOatp2b1
DrOatp2b1
GmOatp2b1
TnOatp2b1
TrOatp2b1
OlOatp2b1
GaOatp2b1

C)

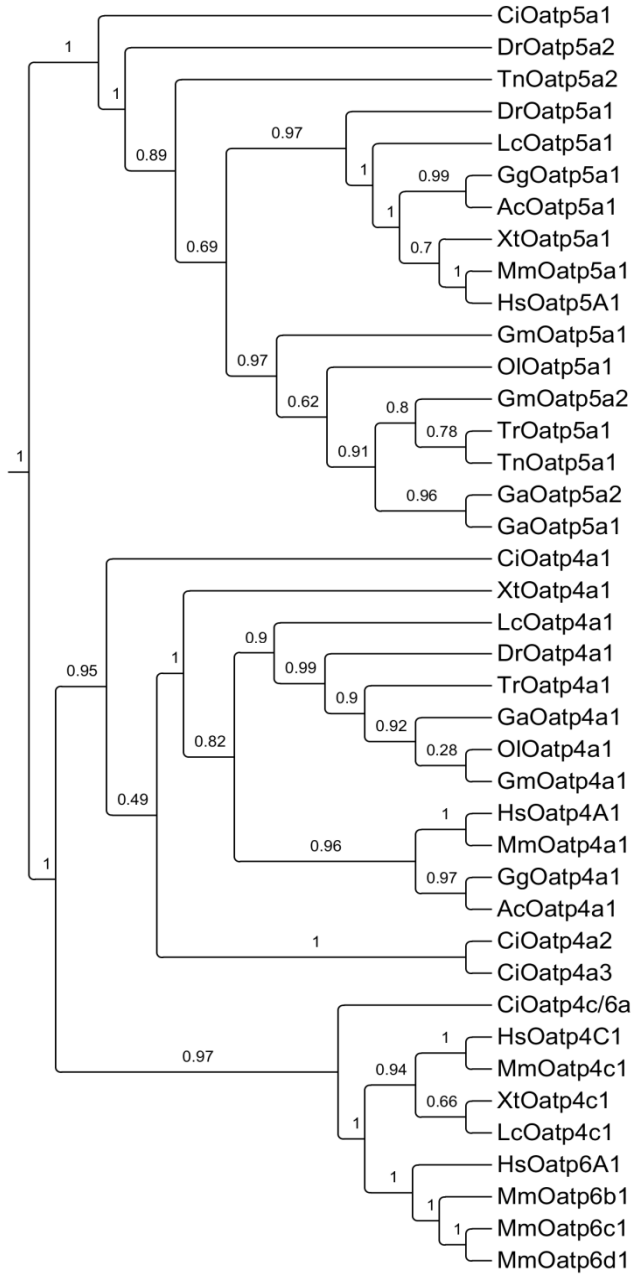

Figure S1. Phylogenetic tree of the OATP/Oatp family (Organic anion transporting polypeptides; gene family name *SLC21* or *SLCO*) in vertebrates. Tree was constructed as a whole, but due to the space constraints the figure is separated into **A**) OATP1/Oatp1 subfamily, **B**) OATP2/Oatp2 and OATP3/Oatp3 subfamilies, and **C**) OATP4-6/Oatp4-6 subfamilies. Species abbreviations: Hs, *Homo sapiens*; Mm, *Mus musculus*; Gg, *Gallus gallus*; Ac, *Anolis carolinensis*; Xt, *Xenopus tropicalis;* Dr, *Danio rerio;* Tn, *Tetraodon nigroviridis*; Tr, *Takifugu rubripes*; Ga, *Gastrosteus aculeatus*; Ol, *Oryzas latipes*; Lc, *Latimeria chalumnae;* Le, *Leucoraja erinacea;* Ci, *Ciona intestinalis*.

A)

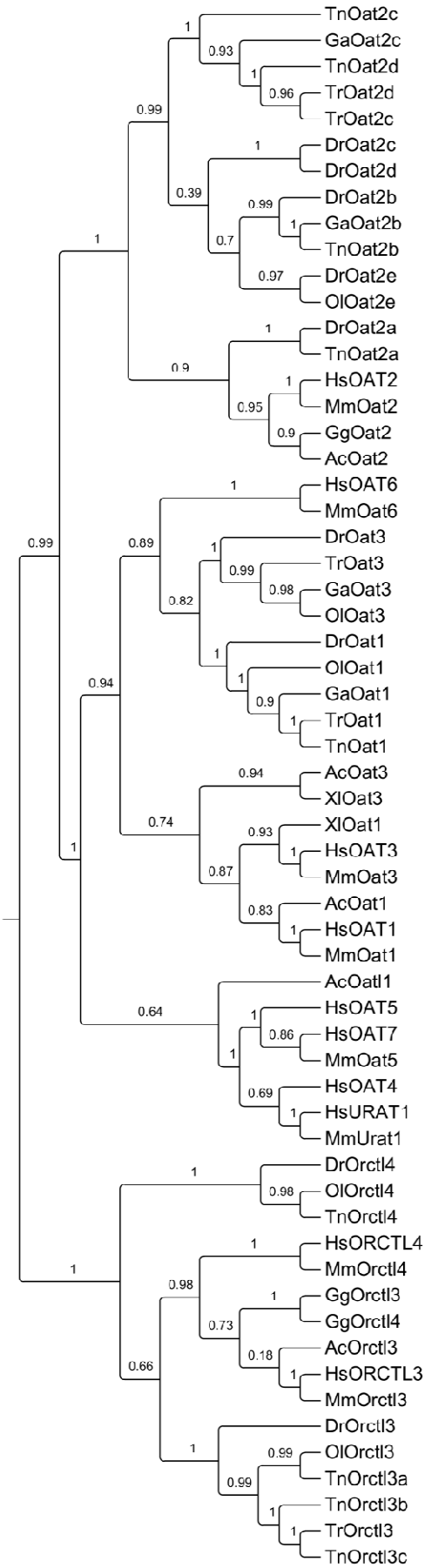
TnOat2c
GaOat2c
TnOat2d
TrOat2d
TrOat2c
DrOat2c
DrOat2d
DrOat2b
GaOat2b
TnOat2b
DrOat2e
OlOat2e
DrOat2a
TnOat2a
HsOAT2
MmOat2
GgOat2
AcOat2
HsOAT6
MmOat6
DrOat3
TrOat3
GaOat3
OlOat3
DrOat1
OlOat1
GaOat1
TrOat1
TnOat1
AcOat3
XlOat3
XlOat1
HsOAT3
MmOat3
AcOat1
HsOAT1
MmOat1
AcOatl1
HsOAT5
HsOAT7
MmOat5
HsOAT4
HsURAT1
MmUrat1
DrOrctl4
OlOrctl4
TnOrctl4
HsORCTL4
MmOrctl4
GgOrctl3
GgOrctl4
AcOrctl3
HsORCTL3
MmOrctl3
DrOrctl3
OlOrctl3
TnOrctl3a
TnOrctl3b
TrOrctl3
TnOrctl3c

B)

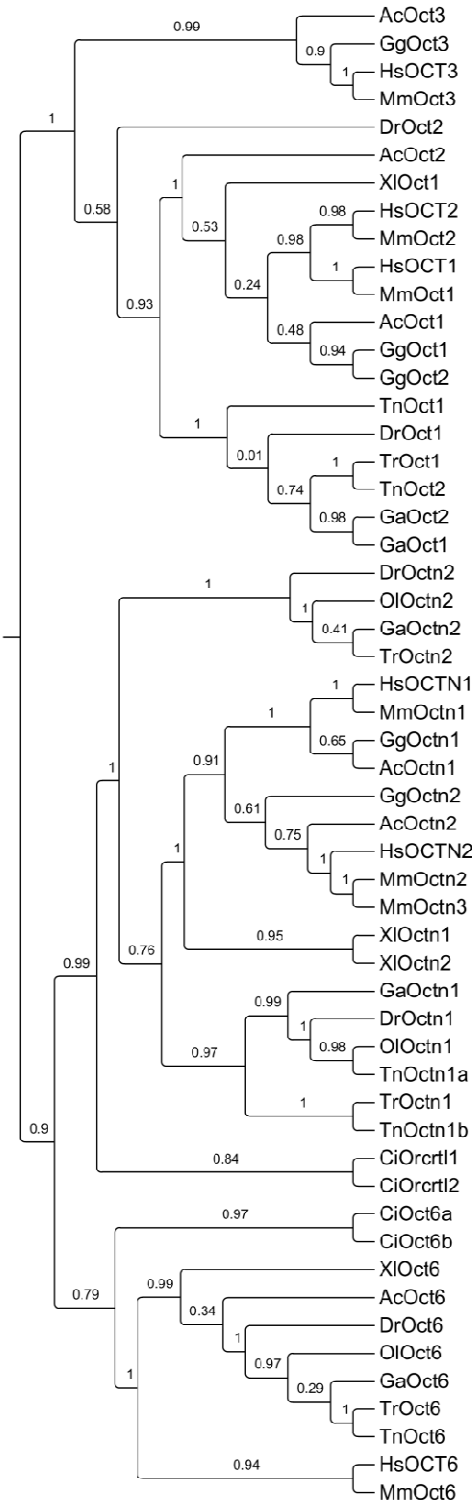

Figure S2. Phylogenetic tree of the SLC22/Slc22 family in vertebrates. Tree was constructed as a whole, but due to the space constraints the figure is separated into **A**) OAT/Oat and ORCTL/Ortcl subgroups, and **B**) OCT/Oct and OCTN/Octn subgroups. Species abbreviations: Hs, *Homo sapiens*; Mm, *Mus musculus*; Gg, *Gallus gallus*; Ac, *Anolis carolinensis*; Xt*, Xenopus tropicalis;* Dr*, Danio rerio;* Lc*, Latimeria chalumnae;* Le*, Leucoraja erinacea;* Ci, *Ciona intestinalis*.

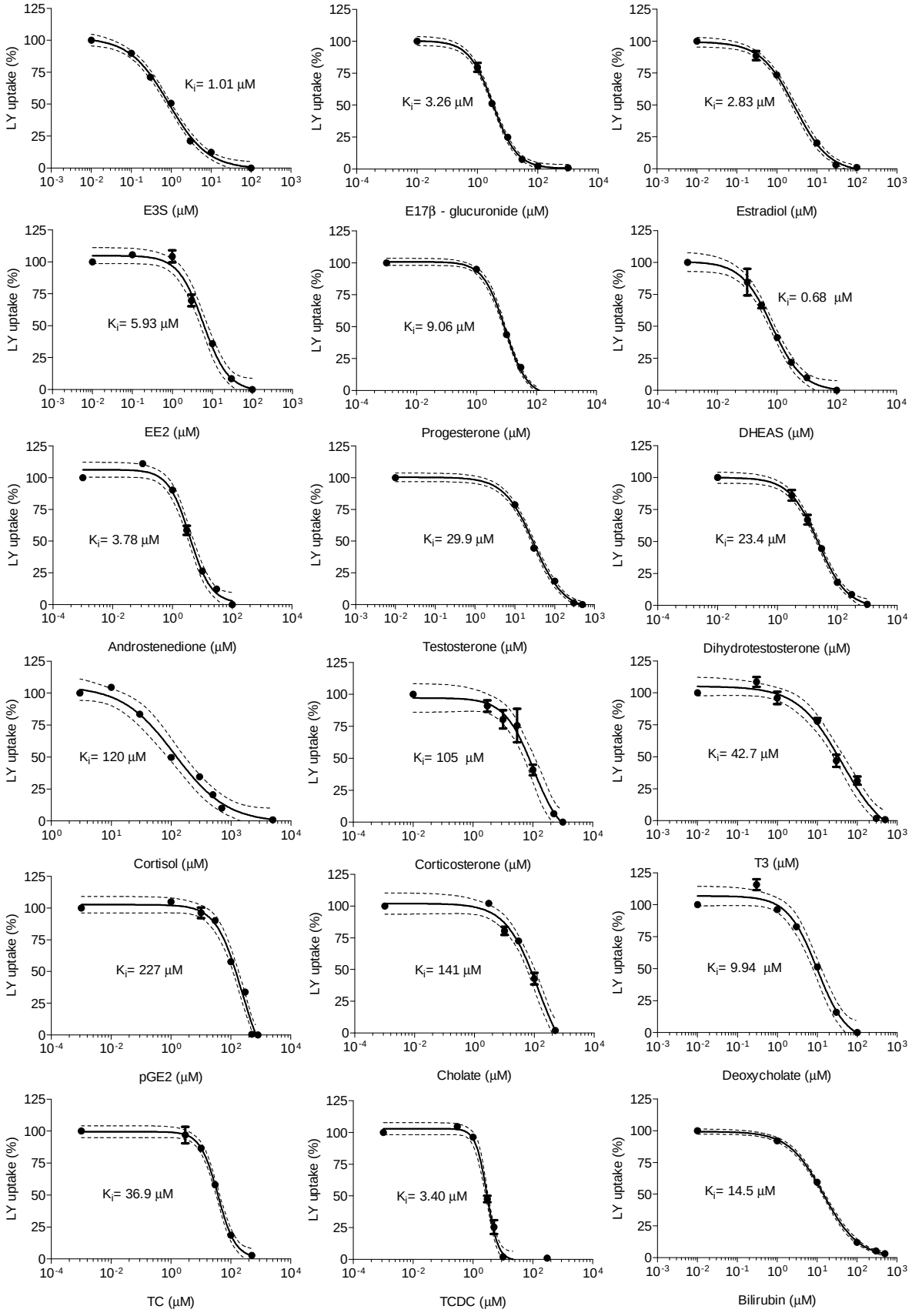

Continuing on the next page

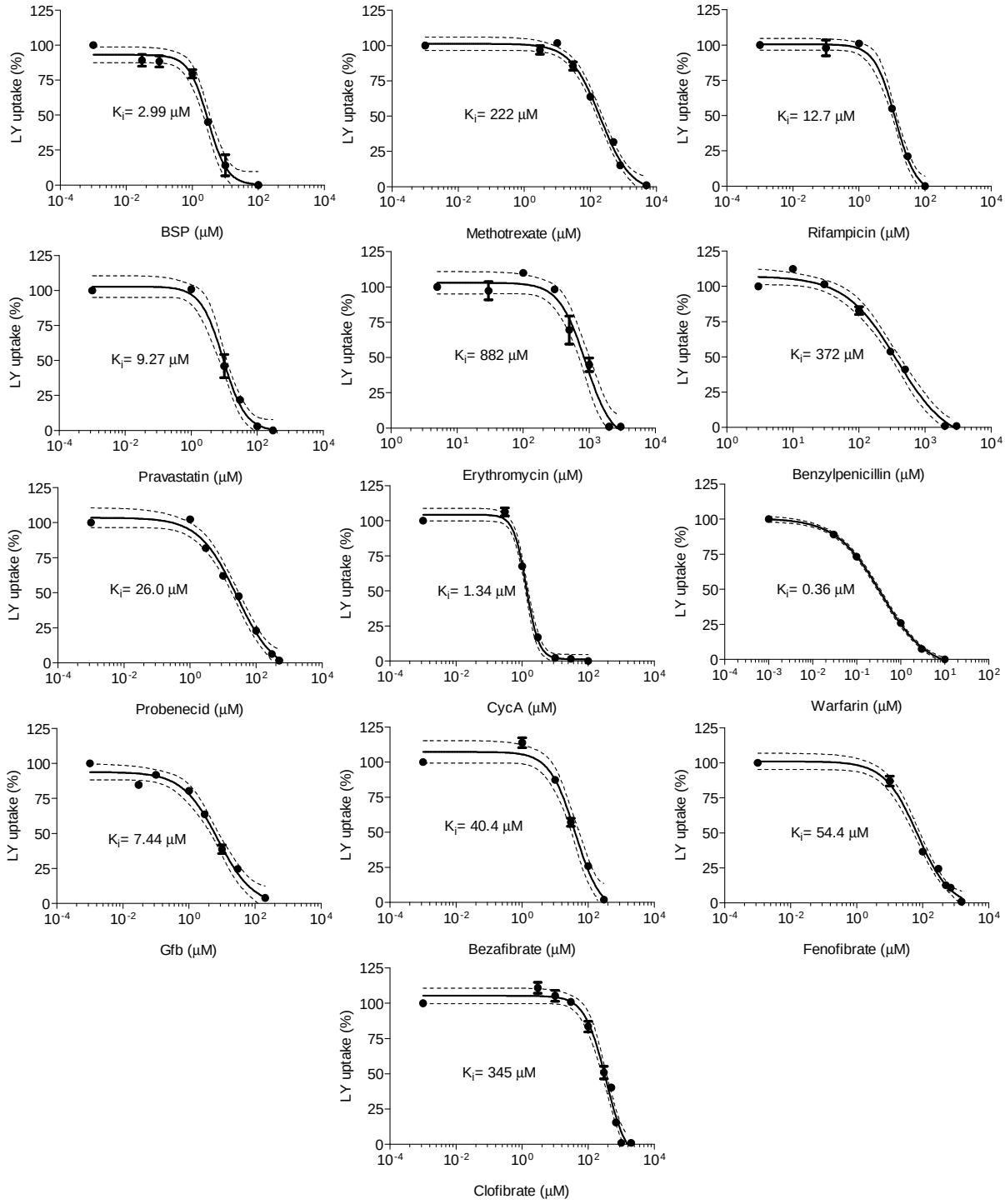

Figure S3. Concentration dependent inhibition of Oatp1d1-mediated Lucifer yellow (LY) uptake by a physiological interactors and pharmaceuticals known to interact with mammalian OATP1A2, OATP1B1, OATP1B3 and OATP1C1. The specific uptake of LY is expressed as percentage relative to the LY uptake in the absence of an interactor (set to 100%). For the purpose of K_i calculations data were fitted to the sigmoidal four parameters dose - response model (variable slope) in the GraphPad Prism 5. Values on X-axis were transformed to logarithmic scale (log X). Abbreviations are listed in the Chapter 9. Each data point represents the mean ± SD from triplicate determinations (note that note that SDs were < 5% when not visible on the charts).

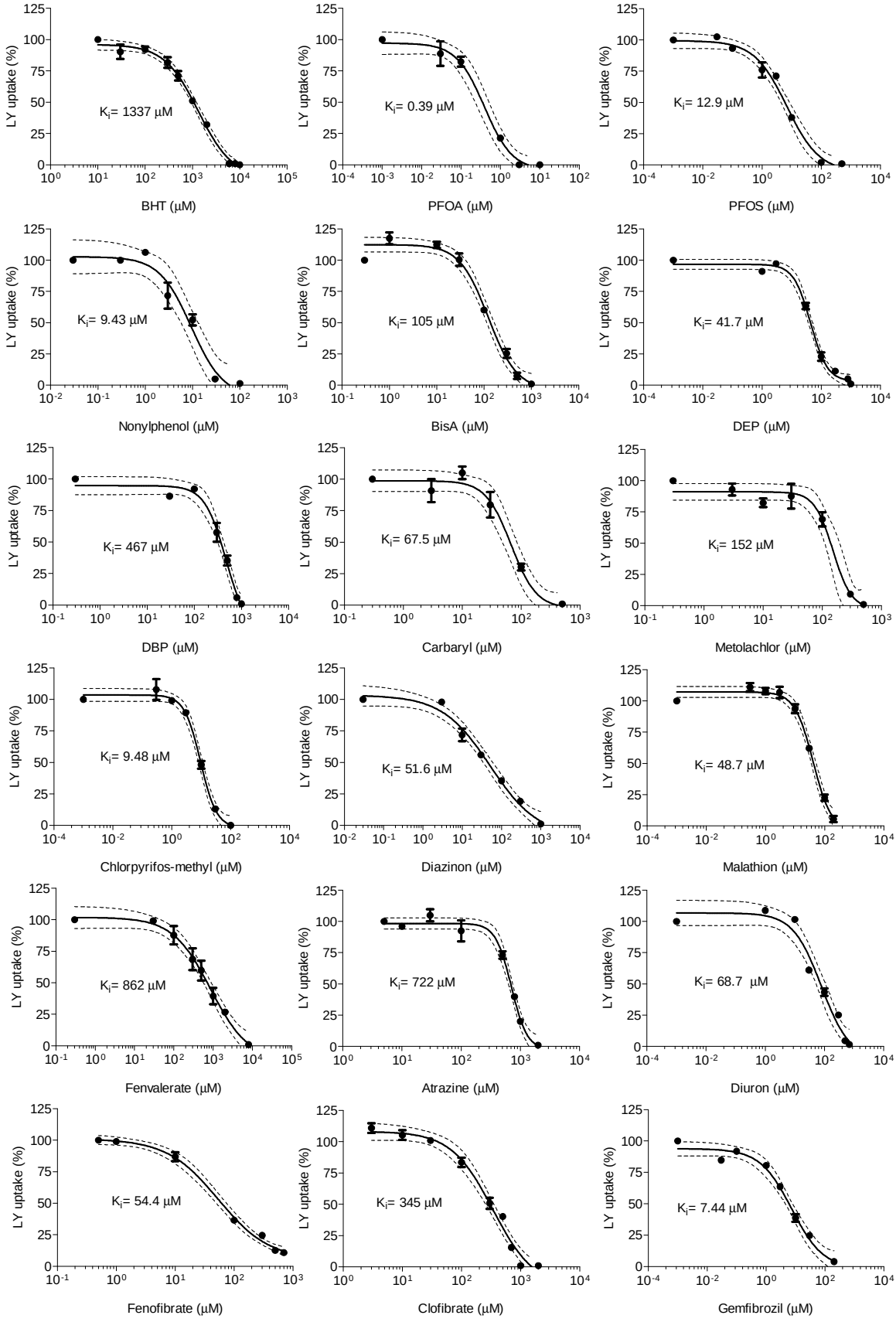

Continuing on the next page

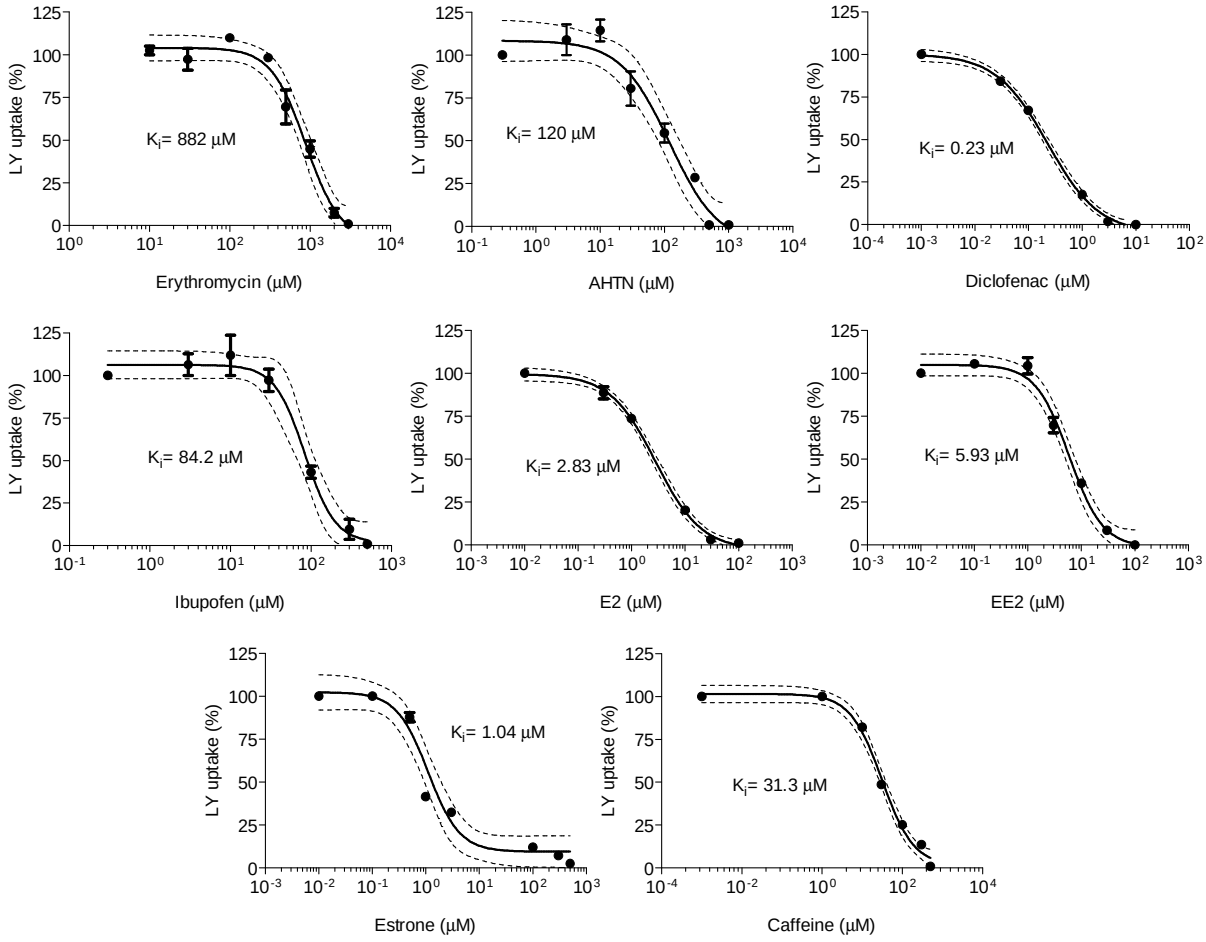

Figure S4. Concentration dependent inhibition of Oatp1d1-mediated Lucifer yellow (LY) uptake by a set of environmental contaminants from three groups of pollutants: industrial compounds: BHT, PFOA, PFOS, nonylphenol, Bis A, DEP and DBP; pesticides: carbaryl, metolachlor, chlorpyrifos methyl, diazinon, malathion, fenvalerate, atrazine and diuron, and pharmaceuticals and personal care products: fenofibrate, clofibrate, gemfibrozil, erythromycin, AHTN, diclofenac, ibuprofen, E2, EE2, E1 and caffeine. The specific uptake of LY is expressed as percentage relative to the LY uptake in the absence of an interactor (set to 100%). Values on X-axis were transformed to logarithmic scale (log X). Abbreviations are listed in the Chapter 9. For the purpose of K_i calculations data were fitted to the sigmoidal four parameters dose - response model (variable slope) in the GraphPad Prism 5. Each data point represents the mean ± SD from triplicate determinations (note that note that SDs were < 5% when not visible on the charts).

Table S1. Protein annotation and accesion numbers of protein sequences used in the phylogentic analysis of OATP/Oatp family (Organic anion transporting polypeptides; gene name *SLC21 or SLCO*) in chordates. Protein sequence accession codes starting with ENS were retrieved from the ENSEMBL database (http://www.ensembl.org/index.html), while the others were retrieved from NCBI database (http://www.ncbi.nlm.nih.gov/). Species abbreviations: Hs, *Homo sapiens*; Mm *Mus musculus*; Gg, *Gallus gallus*; Ac, *Anolis carolinensis*; Xt*, Xenopus tropicalis;* Dr*, Danio rerio;* Gm, *Gadus morhua*; Tn*, Tetraodon nigroviridis;* Tr*, Takifugu rubripes;* Ga*, Gastrosteus aculeatus;* Ol*, Oryzas latipes;* Lc*, Latimeria chalumnae;* Le*, Leucoraja erinacea*; Ci, *Ciona intestinalis*.

Protein annotation	Accession number
HsOatp1A2	NP_066580.1
HsOatp1B1	NP_006437.3
HsOatp1B3	NP_062818.1
HsOatp1C1	NP_059131.1
HsOatp2A1	NP_005621.2
HsOatp2B1	NP_009187.1
HsOatp3A1	NP_037404.2
HsOatp4A1	NP_057438.3
HsOatp4C1	NP_851322.3
HsOatp5A1	NP_112220.2
HsOatp6A1	NP_775759.3
MmOatp1a1	NP_038825.1
MmOatp1a4	NP_109612.1
MmOatp1a5	NP_570931.1
MmOatp1a6	NP_076207.1
MmOatp1b2	NP_065241.1
MmOatp4c1	NP_766246.1
MmOatp6b1	NP_001034564.1
MmOatp6c1	NP_083218.1
MmOatp6d1	NP_081860.1
GgOatp1a2	XP_416421
GgOatp1b4	XP_416418
GgOatp1b5	XP_416420
GgOatp1c1	NP_001034186
GgOatp2a1	XP_422673
GgOatp2b1	XP_417242
GgOatp3a1	XP_413876
GgOatp4a1	NP_001026027
GgOatp5a1	XP_418287
AcOatp1a2	XP_003220807.1
AcOatp1b4	XP_003220808.1
AcOatp1c1	XP_003220826.1
AcOatp2a1	XP_003218457.1
AcOatp2b1	XP_003228194.1
AcOatp3a1	XP_003226621.1
AcOatp4a1	XP_003220718.1
AcOatp5a1	XP_003219683.1

Table continuing on the next page

XtOatp1a2	NP_001096302
XtOatp1b4	NP_001027493
XtOatp2a1	AAI68578
XtOatp2b1	NP_001096429
XtOatp3a1	ENSXETP00000016624
XtOatp4a1	NP_001120155
XtOatp4c1	ENSXETP00000051447
XtOatp5a1	ENSXETP00000033334
DrOatp1c1	AAI63443
DrOatp1d1	NP_001082802
DrOatp1d2	XP_001337850
DrOatp1f1	NP_998082
DrOatp1f2	NP_001121745
DrOatp1f3	NP_001129156
DrOatp1f4	NP_001074135
DrOatp2a1	ENSDARP00000083168
DrOatp2b1	AAI34875
DrOatp3a1	NP_001038653
DrOatp3a2	XP_699020
DrOatp4a1	XP_696263
DrOatp5a1	XP_698555
DrOatp5a2	XP_684701
GmOatp1c1	ENSGMOP00000002723
GmOatp1d1	ENSGMOP00000018404
GmOatp1d2	ENSGMOP00000018423
GmOatp2a1	ENSGMOP00000020421
GmOatp2b1	ENSGMOP00000002967
GmOatp3a2	ENSGMOP00000000909
GmOatp3a1	ENSGMOP00000013936
GmOatp4a1	ENSGMOP00000007474
GmOatp5a2	ENSGMOP00000004438
GmOatp5a1	ENSGMOP00000017847
TnOatp1c1	ENSTNIP00000019119
TnOatp1c2	ENSTNIP00000003444
TnOatp1d2	ENSTNIP00000019119
TnOatp1d1	ENSTNIP00000005303
TnOatp2a1	ENSTNIP00000021848
TnOatp2b1	ENSTNIP00000009641
TnOatp3a2	ENSTNIP00000008546
TnOatp3a1	ENSTNIP00000015669
TnOatp5a2	ENSTNIP00000006884
TnOatp5a1	ENSTNIP00000010818
TrOatp1c1	ENSTRUP00000043527
TrOatp1c2	ENSTRUP00000041455
TrOatp1d1	ENSTRUP00000010101
TrOatp2a1	ENSTRUP00000042419
TrOatp2b1	ENSTRUP00000013822
TrOatp3a1	ENSTRUP00000020057
TrOatp3a2	ENSTRUP00000019060
TrOatp4a1	ENSTRUP00000005498
TrOatp5a1	ENSTRUP00000029129

Table continuing on the next page

GaOatp1c1	ENSGACP00000011556
GaOatp1d1	ENSGACP00000025212
GaOatp2a1	ENSGACP00000004882
GaOatp2b1	ENSGACP00000002446
GaOatp3a1	ENSGACP00000014229
GaOatp3a2	ENSGACP00000014227
GaOatp3a3	ENSGACP00000019600
GaOatp4a1	ENSGACP00000005867
GaOatp5a1	ENSGACP00000003707
GaOatp5a2	ENSGACP00000003712
OlOatp1c1	ENSORLP00000005628
OlOatp1c2	ENSORLP00000010386
OlOatp1d2	ENSORLP00000010971
OlOatp2a1	ENSORLP00000001215
OlOatp2b1	ENSORLP00000016823
OlOatp3a1	ENSORLP00000010494
OlOatp3a2	ENSORLP00000018677
OlOatp4a1	ENSORLP00000002993
OlOatp5a1	ENSORLP00000010182
LcOatp1a2	ENSLACP00000015462
LcOatp1c1	ENSLACP00000014388
LcOatp2a1	ENSLACP00000009326
LcOatp2a2	ENSLACP00000011524
LcOatp2b1	ENSLACP00000007063
LcOatp3a1	ENSLACP00000010258
LcOatp3a2	ENSLACP00000010257
LcOatp3a3	ENSLACP00000011370
LcOatp4a1	ENSLACP00000018696
LcOatp4c1	ENSLACP00000013274
LcOatp5a1	ENSLACP00000018667
LeOatp1c1	AF449798_1
CiOatp1like1	ENSCINP00000024480
CiOatp1like2	ENSCINP00000024369
CiOatp4a1	ENSCINP00000031355
CiOatp4a2	ENSCINP00000008014
CiOatp4a3	ENSCINP00000008014
CiOatp4c/6a	ENSCINP00000019793
CiOatp5a1	ENSCINP00000003289

Table S2. Protein annotation and accesion numbers of protein sequences used in the phylogentic analysis of SLC22/Slc22 family in vertebrate. Species abbreviations: Hs, *Homo sapiens*; Mm *Mus musculus*; Gg, *Gallus gallus*; Ac, *Anolis carolinensis*; Xl*, Xenopus laevis;* Dr*, Danio rerio;* Tn*, Tetraodon nigroviridis;* Tr*, Takifugu rubripes;* Ga*, Gastrosteus aculeatus;* Ol*, Oryzas latipes.*

Protein annotation	Accession number
HsOAT1	NP_004781.2
HsOAT2	NP_006663.2
HsOAT3	NP_004245.2
HsOAT4	NP_060954.1
HsOAT5	NP_001034841.3
HsOAT6	NP_001004326.4
HsOAT7	NP_543142.2
HsURAT1	NP_653186.2
HsORCTL3	NP_004247.2
HsORCTL4	NP_004794.2
HsOCT1	NP_003048.1
HsOCT2	NP_003049.2
HsOCT3	NP_068812.1
HsOCTN1	NP_003050.2
HsOCTN2	NP_003051.1
HsOCT6	NP_149116.2
MmOat1	NP_032792.2
MmOat2	NP_659105.2
MmOat3	NP_112471.3
MmOat5	NP_659034.1
MmOat6	NP_941052.1
MmUrat1	NP_033229.3
MmOrctl3	NP_598741.2
MmOrctl4	NP_001032838.1
MmOct1	NP_033228.2
MmOct2	NP_038695.1
MmOct3	NP_035525.1
MmOctn1	NP_062661.1
MmOctn2	NP_035526.1
MmOctn3	NP_062697.1
MmOct6	NP_081848.1
GgOat2	NP_001186367.1
GgOrctl3	XP_418528.3
GgOrctl4	XP_418529.3
GgOct1	XP_419621.3
GgOct2	XP_419622.2
GgOct3	XP_419620.4
GgOctn1	NP_001139603.1
GgOctn2	NP_001039293.1
AcOat1	ENSACAP00000006348
AcOat2	ENSACAP00000004498
AcOat3	ENSACAP00000013862
AcOrctl3	ENSACAP00000009649
AcOatl1	ENSACAP00000008001
AcOct1	ENSACAP00000003531
AcOct2	ENSACAP00000003545
AcOct3	ENSACAP00000003332
AcOctn1	ENSACAP00000019006
AcOctn2	ENSACAP00000012434
AcOct6	ENSACAP00000010768

Table continuing on the next page

XlOat1	NP_001087663.1
XlOat3	NP_001087661.1
XlOct1	NP_001087673.1
XlOctn1	NP_001088049.1
XlOctn2	NP_001080898.1
XlOct6	AAH80416.1
DrOat1	AAH95733.1
DrOat2a	NP_001077330.1
DrOat2b	XP_001340340.3
DrOat2c	XP_001337343.1
DrOat2d	XP_001337264.3
DrOat2e	NP_956643.1
DrOat3	NP_996960.1
DrOrctl3	NP_001070840.2
DrOrctl4	XP_001346178.2
DrOct1	NP_998315.1
DrOct2	NP_001107932.1
DrOctn1	XP_001340836.1
DrOctn2	NP_957143.1
DrOct6	NP_001020659.1
GaOat1	ENSGACP00000027657
GaOat2b	ENSGACP00000015157
GaOat2c	ENSGACP00000023551
GaOat3	ENSGACP00000027316
GaOct1	ENSGACP00000007873
GaOct2	ENSGACP00000007823
GaOctn1	ENSGACP00000027599
GaOctn2	ENSGACP00000027601
GaOct6	ENSGACP00000015320
OlOat1	ENSORLP00000015952
OlOat2e	ENSORLP00000024217
OlOat3	ENSORLP00000007641
OlOrctl3	ENSORLP00000012386
OlOrctl4	ENSORLP00000014717
OlOctn2	ENSORLP00000001412
OlOctn1	ENSORLP00000001455
OlOct6	ENSORLP00000017631
TrOat1	ENSTRUP00000000970
TrOat2c	ENSTRUP00000035983
TrOat2d	ENSTRUP00000035982
TrOat3	ENSTRUP00000043583
TrOrctl3	ENSTRUP00000044590
TrOct1	ENSTRUP00000022458
TrOctn1	ENSTRUP00000005016
TrOctn2	ENSTRUP00000009792
TrOct6	ENSTRUP00000047083

Table continuing on the next page

TnOat1	ENSTNIP00000010475
TnOat2a	ENSTNIP00000007735
TnOat2b	ENSTNIP00000012754
TnOat2c	ENSTNIP00000015332
TnOat2d	ENSTNIP00000015333
TnOrctl3a	ENSTNIP00000001359
TnOrctl3b	ENSTNIP00000015723
TnOrctl3c	ENSTNIP00000015723
TnOrctl4	ENSTNIP00000010741
TnOct1	ENSTNIP00000000542
TnOct2	ENSTNIP00000001184
TnOctn1a	ENSTNIP00000017277
TnOctn1b	ENSTNIP00000001229
TnOct6	ENSTNIP00000015214
CiOrcrtl1	XP_002132109.1
CiOrcrtl2	XP_004225970.1
CiOct6a	XP_002123867.2
CiOct6b	ENSCINP00000031808

11. Curriculum vitae

Education

MSc Oxford University, Oxford, UK, Oxford University Centre For Environment (OUCE), MSc Environmental Change & Management, 2007.

BSc University of Zagreb, Zagreb, Croatia, Faculty of Science; BSc Biology- Ecology, 2005.

Publications

1. **Popovic, M**., Zaja, R., Fent, K., Smital, T. (2013) Molecular characterization of zebrafish Oatp1d1 (*Slco1d1*), a novel organic anion transporting polypeptide. *Journal of Biological Chemistry*. 288 (47), 33894-33911.

2. Zaja,R., Terzić, S., Senta,I., Lončar J., **Popovic, M**., Ahel, M., Smital, T. (2013) Identification of P-Glycoprotein Inhibitors in Contaminated Freshwater Sediments. *Environmental Science and Technology*, 47 (9), 4813-4821.

3. Smital, T., Terzić, S., Lončar, J., Senta, I., Žaja, R., **Popović, M**., Mikac, I., Tollefsen, K.-E., Thomas, K.V., Ahel, M. (2013) Prioritisation of organic contaminants in a river basin using chemical analyses and bioassays. *Environemntal Science and Pollution Research* 20 (3), 1384-1395.

4. Zaja R, Lončar J, **Popovic M**, Smital T. (2011) First characterization of fish P-glycoprotein (abcb1) substrate specificity using determinations of its ATPase activity and calcein-AM assay with PLHC-1/dox cell line. *Aquatic toxicology* 103 (1-2), pp. 53-62.

5. Smital T, Terzic S, Zaja R, Senta I, Pivcevic B, **Popovic M**, Mikac I, Tolllefsen, KE, Thomas KV, Ahel M. (2011) Assessment of toxicological profiles of the municipal wastewater effluents using chemical analyses and bioassays. *Ecotoxicology and Environmental Safety* 74 (4), pp. 844-851.

6. **Popovic, M**., Zaja, R., Smital, T. (2010) Organic anion transporting polypeptides (OATP) in zebrafish (*Danio rerio*): phylogenetic analysis and tissue distribution. *Comparative Biochemistry and physiology -A: Molecular & Integrative Physiology* 155 (3), pp. 327-335.

7. **Popovic, M**., Zaja, R., Loncar, J., Smital, T. (2010) A novel ABC transporter: The first insight into zebrafish (*Danio rerio*) Abch1. *Marine Environmental Research* 69 (SUPPL. 1), pp. S11-S13.

8. Loncar, J., **Popovic, M**., Zaja, R., , Smital, T. (2010) Gene expression analysis of the efflux transporters in rainbow trout (*Oncorhynchus mykiss*). *Comparative Biochemistry and physiology C-Toxicology & Pharmacology*. 151, 209.

9. **Popović, M**., Gottstein-Matočec S. (2006). Biological aspects of the Spinicaudata (Branchiopoda, Diplostraca) in the largest alluvial wetland in Croatia. *Crustaceana* 79 (4): 423-440**.**

Publications under review/in preparation

1. **Popovic, M**., Žaja, R, Fent, K., Smital, T. (2014). Interaction of environmental contaminants with zebrafish uptake transporter Oatp1d1 (*Slco1d1*). Under review.

2. Glišić, B., Mihaljević, I., Žaja, R., **Popovic, M.***, Lončar, J., Fent, K., Smital, T., Kovačević, R. (2014). Glutathione-S-transferase superfamily in zebrafish (Danio rerio). In preparation (*corresponding author).

3. Krznar, P.*, **Popovic, M**.*, Lončar, J., Zaja, R., Tvrtko Smital (2014) First characterization of MATE (Multidrug and Toxin Extrusion) proteins in zebrafish. In preparation (*equal contribution).

Research experience

2008 - present - pHD student in the Laboratory for Molecular Ecotoxicology, Division for Marine and Environmental Research, Ruđer Bošković Institute, Zagreb, Croatia.

2010 - 5 months stay in the laboratory of prof. dr. Karl Fent, University of Applied Sciences, Basel, Switzerland, collaboration on the joint research project „Establishing and developing of an ecotoxicology platform in Serbia and Croatia: a focus on zebrafish (Danio rerio)“, SCOPES project funded by the Swiss National Science foundation (SNSF) Grant SCOPES-IZ73ZO_128025/1.]

Trainings

2013 - Summer school on ‘Protein interactions, assemblies and human diseases’, Spetses, Greece.

2012 - Education and Training in Basic Radiation Safety for Radiation Workers (to work with radiation sources used in scientific and research laboratories), University of Applied Health Studies, Zagreb, Croatia.

2009 - 10th International Summer School on Biophysics: Supramolecular Structure and Function, Rovinj, Croatia.

Fellowships

2006/2007 **OSI/FCO Chevening Scholarship** (Open Society Institute/Foreign Commonwealth Office): scholarship covered all the costs of one year MSc at the Oxford University Centre for Environment (OUCE).

2002 – 2004 **City of Zagreb scholarship** during the 3th and 4th year of undergraduate studies

Awards and scholarships

2013 – FEBS (Federation of European Biochemical Societies), EMBO (European Molecular Biology Organization) and IUBMB (International Union of Biochemistry and Molecular Biology) joint scholarship for the attendance at Spetsai summer school ‘Protein interactions, assemblies and human disease', Greece.

2012 – Student scholarship given by **FEBS** and Croatian society for biochemistry and molecular biology for the attendance (oral presentation) at the FEBS3+ Meeting – From molecules to life and back, Opatija, Croatia.

2011 – Student scholarship for the attendance (presentation) at the 16th International Symposium on Pollutant Responses in Marine Organisms (PRIMO 16), Long Beach, California.

2010 – FEBS scholarship for the attendance (poster and short presentation) at the 35th Annual meeting of Federation of European Biochemical Societies – ' FEBS - Molecules of Life' and YSF (Young scientist Forum), Goteborg, Sweden.

2009 – Scholarship given by 'European Biophysical Societies' Association (**EBSA)'** for the attendance at 10th International Summer School on Biophysics 'Supramolecular Structure and Function', Rovinj, Croatia.
2009 – **Best presentation award** for young researchers at the 15th International Symposium on Pollutant Responses in Marine Organisms (PRIMO 15), Bordeaux, France.

2009 - Student scholarship for the attendance (presentation) at the 15th International Symposium on Pollutant Responses in Marine Organisms (PRIMO 15), Bordeaux, France.

Conference platform presentations

2012 - 'Gottinger Transporttage', Center of Physiology, Gottingen, Germany. Molecular characterization of a novel Organic Anion Transporting Polypeptide, zebrafish Oatp1d1 (*Slco1d1*).

2012 - FEBS3+ Meeting 'From molecules to life and back', Opatija, Croatia. Molecular characterization of a novel Organic Anion Transporting Polypeptide, zebrafish Oatp1d1 (*Slco1d1*).

2011 - 16th International Symposium on Pollutant Responses in Marine Organisms (PRIMO 16), California, US. First characterization of zebrafish (Danio rerio) uptake transporters (Solute Carrier families SLC21 and SLC22).

2009 - 15th International Symposium on Pollutant Responses in Marine Organisms (PRIMO 15), Bordeaux, France (Best presentation award). A novel ABC transporter: first insight into zebrafish (Danio rerio) Abch1.

Memberships

Croatian society of biochemistry and molecular biology

Co-supervisions

Diploma thesis, Petra Krznar (2012). Gene expression and phylogeny of MATE (Multi Drug and Toxin Extrusion) proteins in zebrafish, *Danio rerio* (Hamilton, 1822.). Faculty of Sciences, University of Zagreb, Croatia.